DET KGL. DANSKE VIDENSKABERNES SELSKAB
MATEMATISK-FYSISKE MEDDELELSER, BIND XXIII, NR. 1

DEDICATED TO PROFESSOR NIELS BOHR ON THE OCCASION OF HIS 60TH BIRTHDAY

GENERAL PROPERTIES OF THE CHARACTERISTIC MATRIX IN THE THEORY OF ELEMENTARY PARTICLES I

BY

C. MØLLER

KØBENHAVN
I KOMMISSION HOS EJNAR MUNKSGAARD
1945

CONTENTS

Printed in Denmark
Bianco Lunos Bogtrykkeri A.S

INTRODUCTION

According to HEISENBERG[1], the well-known convergence difficulties, inherent in all quantum field theories so far developed, are due to the existence of a new universal constant of the dimension of a length. This constant plays the role of a minimal length representing a limit to the application of the ordinary concepts of quantum field theory in a similar way as the existence of Planck's constant limits the unambiguous application of classical mechanical concepts to atomic systems. The correct incorporation of this universal length into the theory is still unknown.

Recently, however, HEISENBERG[2] has taken an important step towards the future theory. In ordinary quantum mechanics an atomic system is completely defined by the Hamiltonian function of the system. Now, the assumption of a Hamiltonian which by means of the Schrödinger differential equation defines a continuous time-displacement of the wave function seems to be in contradiction with the existence of a universal minimal length. HEISENBERG therefore concludes that the Hamiltonian function will lose its predominant importance in the future theory, and that the atomic systems in this theory must be defined by other fundamental functions.

A primary problem will be to determine these functions. This problem is intimately connected with the question which quantities of the current theory will keep their meaning or, in other words, which quantities will still be regarded as 'observable' in the future theory. Although it is difficult to give an exhaustive answer to this question at present, it is natural to assume that any quantity, whose determination is unaffected by the existence of the minimal length, may be considered as 'observable.'

Such quantities are the energy and momentum of a free particle, the cross section of any collision process with or without creation and annihilation of particles, and the discrete energy values of atomic systems in closed stationary states. In quantum mechanics these quantities may be calculated by means of the Schrödinger equation when the Hamiltonian of the system is known. The collision cross sections, however, are given more directly by the matrix elements of a certain unitary matrix S, which in a rather complicated way depends on the Hamiltonian. Therefore HEISENBERG assumes that in the future theory this characteristic matrix S or an Hermitian matrix η connected with S by the relation

$$S = e^{i\eta}$$

will take over the role played by the Hamiltonian in quantum theory, i. e. in future the atomic systems should be defined by giving the matrices S or η.

In quantum mechanics the Hamiltonian of a special system could be obtained by a simple procedure from the classical Hamiltonian of the system. The most urgent, and until now entirely unsolved, problem will now be that of finding the procedure by which the characteristic matrix may be derived in each special case. As a first step towards a solution of this problem we may try to find the general conditions satisfied by the matrix S in any case, and it seems natural to assume that all conditions satisfied by S in quantum mechanics independently of the special form of the Hamiltonian, will hold also in the future theory.

A condition of this kind, stated by HEISENBERG[2] in his first paper, is the equation

$$S^\dagger S = S S^\dagger = 1,$$

expressing that S is a unitary matrix. In section 1 of the present paper, we shall give an alternative, and perhaps a somewhat more rigorous, proof of this equation.

Another important condition stated by HEISENBERG is the invariance of the matrix S under Lorentz transformations. In section 2 we shall prove this property by using the transformation properties of cross sections and the connection between

these quantities and the elements of the matrix S. The invariance of the fundamental matrix S brings about a considerable simplification in the description of atomic systems, as compared with the quantum mechanical description in which the fundamental matrix—the Hamiltonian—has rather complicated transformation properties. In section 3 it is shown how the invariance property of S may be used to find a number of general 'constants of collision', i. e. variables which commute with S and with the total kinetic energy. Such quantities as have the same values or mean values before and after the collision will probably in the future theory play a similar important role as the constants of motion in ordinary quantum mechanics.

When the matrix elements of S are given as functions of the (real) momentum variables of the system, we are thus able to calculate the cross sections for all collision processes, but, as shown in section 1, the discrete energy values in closed stationary states of the system are so far completely undetermined. However, if S is assumed to be an analytic function of the momentum variables now regarded as complex variables, these energy values may, as remarked by KRAMERS and HEISENBERG[3],* be obtained as the energies corresponding to those purely imaginary values of the momentum variables which make S equal to zero. In a sequel to the present paper these problems will be considered in more detail and new general conditions for the matrix elements of S will be derived.

Thus, all the quantities which according to HEISENBERG are to be considered 'observable,' are in this way derivable from the matrix S, which therefore in fact plays a similar role as the Hamiltonian in the old theory. It remains to be seen if the atomic systems are completely defined by a given S, or if the future theory will contain observable quantities which cannot be calculated from the matrix S.

* I am greatly indebted to Professor HEISENBERG for an opportunity of seeing his manuscript before publication.

1. The characteristic matrix S. The unitarity condition. Independence of S of the energy values in closed stationary states.

In this section we shall consider a collision between a certain number of like particles from the point of view of ordinary quantum mechanics. Let $\boldsymbol{k}_i$ be the momentum operator of the i'th particle. If κ is the rest mass of the particle, the corresponding kinetic energy is $W_i = \sqrt{\kappa^2 + k_i^2}$, and the total kinetic energy and the total momentum of the particles are given by

$$\left.\begin{aligned} W &= \sum_i W_i = \sum_i \sqrt{\kappa^2 + k_i^2} \\ \boldsymbol{K} &= \sum_i \boldsymbol{k}_i , \end{aligned}\right\} \qquad (1)$$

respectively.*

If the eigenvalues of $\boldsymbol{k}_i$ are denoted by $\boldsymbol{k}'_i$, the wave function in momentum space will be a function of the vectors $\boldsymbol{k}'_i$. Since we want to treat the general case of a collision in which annihilation and creation processes may take place, the total number n of particles is not a constant of the motion, and we shall have to consider a succession of wave functions[5]

$$\text{const.},\ \psi(\boldsymbol{k}'_1),\ \psi(\boldsymbol{k}'_1, \boldsymbol{k}'_2), \cdots \psi(\boldsymbol{k}'_1, \cdots \boldsymbol{k}'_i, \cdots \boldsymbol{k}'_{n'})$$

corresponding to the different eigenvalues n' of n. For simplicity we shall in what follows treat the different particles as distinguishable, which means neglecting all exchange effects. However, if the particles for instance have Bose statistics, all the wave functions are of course symmetrical in the variables $\boldsymbol{k}'_i$.

In a representation where the $\boldsymbol{k}_i$ are diagonal matrices (a '$\boldsymbol{k}$-representation'), any quantity like the potential energy V will be represented by a matrix $(\boldsymbol{k}'_1 \cdots \boldsymbol{k}'_{n'} \,|\, V \,|\, \boldsymbol{k}''_1 \cdots \boldsymbol{k}''_{n''})$, where n' may be different from n'' corresponding to a transition in which the number of particles is changed. We shall often simply write $(\boldsymbol{k}' \,|\, V \,|\, \boldsymbol{k}'')$ for these general matrix elements.

The representation is not uniquely determined by the condition that the $\boldsymbol{k}_i$ are diagonal, since the phase factors in the

* Throughout this paper are used the same units as in HEISENBERG's paper, where $\boldsymbol{k}$, W, and κ all have the dimensions of a reciprocal length.

representation may be chosen arbitrarily. If $(\boldsymbol{k}'|\,V\,|\boldsymbol{k}'')^{\times}$ denotes the representative of the operator V in an other $\boldsymbol{k}$-representation we have

$$(\boldsymbol{k}'|\,V\,|\boldsymbol{k}'')^{\times} = e^{i\alpha(\boldsymbol{k}')}(\boldsymbol{k}'|\,V\,|\boldsymbol{k}'')\,e^{-i\alpha(\boldsymbol{k}'')}, \tag{2}$$

where $\alpha(\boldsymbol{k}') = \alpha(\boldsymbol{k}'_1, \cdots \boldsymbol{k}'_{n'})$ may be any real function of the variables $(\boldsymbol{k}') = (\boldsymbol{k}'_1, \cdots \boldsymbol{k}'_{n'})$. Similarly, if $(\boldsymbol{k}'|\,)^{\times}$ and $(\boldsymbol{k}'|\,)$ are the representatives of the same state in the two representations, we have

$$(\boldsymbol{k}'|\,)^{\times} = e^{i\alpha(\boldsymbol{k}')}\,(\boldsymbol{k}'|\,). \tag{2'}$$

Let us consider a stationary state of the system with the energy E. The corresponding time independent Schrödinger equations in the different momentum spaces may then be written

$$\left.\begin{gathered}(E-W')\,\Psi(\boldsymbol{k}'_1 \cdots \boldsymbol{k}'_{n'}) = \\ \sum_{n''}\int(\boldsymbol{k}'_1 \cdots \boldsymbol{k}'_{n'}|\,V\,|\boldsymbol{k}''_1 \cdots \boldsymbol{k}''_{n''})\,d\boldsymbol{k}''_1\,d\boldsymbol{k}''_2 \cdots d\boldsymbol{k}''_{n''}\,\Psi(\boldsymbol{k}''_1 \cdots \boldsymbol{k}''_{n''}) \\ n' = 1,\ 2,\ 3 \cdots\end{gathered}\right\} \tag{3}$$

Here W' is the eigenvalue of W corresponding to the values $(\boldsymbol{k}'_1, \cdots \boldsymbol{k}'_{n'})$ of the momentum vectors, and $d\boldsymbol{k}''_i$ is a volume-element in the momentum space of the i'th particle. The integration and summation on the right hand side of (3) is to be extended over all the different momentum spaces. In what follows we shall simply write $\int d\boldsymbol{k}''$ instead of $\sum_{n''}\int d\boldsymbol{k}''_1 \cdots d\boldsymbol{k}''_{n''}$ and (3) will be written

$$(E-W')\,\Psi(\boldsymbol{k}') = \int(\boldsymbol{k}'|\,V\,|\boldsymbol{k}'')\,d\boldsymbol{k}''\,\Psi(\boldsymbol{k}''), \tag{4}$$

where $(\boldsymbol{k}')$ is short for $(\boldsymbol{k}'_1, \cdots \boldsymbol{k}'_{n'})$.

We shall now in particular consider a stationary collision process in which the primary particles have the momentum values $(\boldsymbol{k}^0_1, \cdots \boldsymbol{k}^0_{n^0}) = (\boldsymbol{k}^0)$. Thus, the corresponding wave function being a function of both $(\boldsymbol{k}^0)$ and $(\boldsymbol{k}')$, it will be denoted by

$$(\boldsymbol{k}'_1 \cdots \boldsymbol{k}'_{n'}|\,\Psi\,|\boldsymbol{k}^0_1 \cdots \boldsymbol{k}^0_{n^0}) = (\boldsymbol{k}'|\,\Psi\,|\boldsymbol{k}^0). \tag{5}$$

If we consider all possible collisions with varying initial momentum vectors $(\boldsymbol{k}^0)$, the functions (5) define a matrix Ψ, which may be called the wave matrix.

According to (4) the components of the wave matrix satisfy the equations

$$(W^0 - W')\,(\boldsymbol{k}' \mid \Psi \mid \boldsymbol{k}^0) = \int (\boldsymbol{k}' \mid V \mid \boldsymbol{k}'')\, d\boldsymbol{k}''\, (\boldsymbol{k}'' \mid \Psi \mid \boldsymbol{k}^0), \quad (6)$$

where $E = W^0 = \sum_i \sqrt{\kappa^2 + k_i^{02}}$ is the total energy of the system for the given initial conditions. Using the ordinary rule for matrix multiplication, (6) may be written

$$\Psi W - W\Psi = V\Psi. \quad (7)$$

The wave matrix Ψ is a sum of two parts:

$$\Psi = \Psi^0 + T, \quad (8)$$

where Ψ^0 and T represent the incident and the scattered waves, respectively. In configuration space the function Ψ^0 represents a set of plane waves. In the $\boldsymbol{k}$-representation Ψ^0 is simply

$$\left.\begin{aligned} &(\boldsymbol{k}'_1 \cdots \boldsymbol{k}'_{n'} \mid \Psi^0 \mid \boldsymbol{k}^0_1 \cdots \boldsymbol{k}^0_{n^0}) = \delta(\boldsymbol{k}' - \boldsymbol{k}^0) = \\ &\begin{cases} 0 \text{ for } n' \neq n^0 \\ \delta(\boldsymbol{k}'_1 - \boldsymbol{k}^0_1) \cdots \delta(\boldsymbol{k}'_{n'} - \boldsymbol{k}^0_{n^0}) \text{ for } n' = n^0. \end{cases} \end{aligned}\right\} \quad (9)$$

Thus we get for Ψ

$$\Psi = 1 + T, \quad (10)$$

where 1 denotes the unit matrix.

We shall from now on treat the quantity Ψ as an operator whose representatives in different representations are connected by the ordinary rules of quantum mechanical transformation theory. In particular a change in phase leads to a change in the representatives of Ψ given by (2). Thus Ψ will in any representation have the form (10) with the first term equal to the unit matrix.

If we put

$$U = -2\pi i V\Psi = -2\pi i V - 2\pi i VT, \quad (11)$$

we get, from (6), (10), and (11),

$$(W^0 - W')\,(\boldsymbol{k}' \mid T \mid \boldsymbol{k}^0) = -\frac{1}{2\pi i}(\boldsymbol{k}' \mid U \mid \boldsymbol{k}^0). \quad (12)$$

Solving with respect to T, we obtain the general solution

$$(\boldsymbol{k}' \mid T \mid \boldsymbol{k}^0) = -\frac{1}{2\pi i}(\boldsymbol{k}' \mid U \mid \boldsymbol{k}^0)\left[\frac{1}{W^0 - W'} + \lambda\delta(W^0 - W')\right], \quad (13)$$

where λ is an arbitrary constant. If T is to represent outgoing waves only, λ must, according to DIRAC[6] and HEISENBERG[2], be chosen equal to $-i\pi$. Here it is understood that an integral over W' containing the singular factor $\frac{1}{W^0 - W'}$ must be taken as the Cauchy principle value, defined as the limit for $\varepsilon \to 0$ of the integral when the small domain $W^0 - \varepsilon$ to $W^0 + \varepsilon$ is excluded from the range of integration.

If we introduce the improper functions

$$\delta_{\pm}(W' - W^0) = \frac{\pm 1}{2\pi i (W' - W^0)} + \frac{1}{2}\delta(W' - W^0) \quad (14)$$

(13) may be written

$$(\boldsymbol{k}' \mid T \mid \boldsymbol{k}^0) = \delta_{+}(W' - W^0)\,(\boldsymbol{k}' \mid U \mid \boldsymbol{k}^0). \quad (15)$$

If T is eliminated from (11) by means of (15), we get an integral equation, which completely determines U when the potential V is given.

Since the total momentum is conserved, the elements of the wave matrices Ψ, T, and U must have the form

$$(\boldsymbol{k}' \mid U \mid \boldsymbol{k}^0) = \delta(\boldsymbol{K}' - \boldsymbol{K}^0)\,(\boldsymbol{k}' \mid U_{\boldsymbol{K}^0} \mid \boldsymbol{k}^0), \quad (16)$$

where $(\boldsymbol{k}' \mid U_{\boldsymbol{K}^0} \mid \boldsymbol{k}^0)$ is a submatrix of U corresponding to a fixed value $\boldsymbol{K}' = \boldsymbol{K}^0$ of the total momentum.

If $A^{\dagger}$ is the Hermitian conjugate of a matrix A defined by

$$(\boldsymbol{k}' \mid A^{\dagger} \mid \boldsymbol{k}'') = (\boldsymbol{k}'' \mid A \mid \boldsymbol{k}')^{*}, \quad (17)$$

we get from (11)

$$U^{\dagger} = 2\pi i \Psi^{\dagger} V, \quad (18)$$

since $V^{\dagger} = V$, on account of V being Hermitian. Multiplying (11) by $\Psi^{\dagger}$ on the left, and (18) by Ψ on the right, and adding, we get

$$\Psi^{\dagger} U + U^{\dagger} \Psi = 0, \quad (19)$$

or, using (10),

$$U + U^\dagger + T^\dagger U + U^\dagger T = 0. \tag{20}$$

This equation, in which the potential V has disappeared, represents a general condition for the wave matrices. From (15), (14), and (17) we get

$$(\boldsymbol{k}' \mid T^\dagger \mid \boldsymbol{k}^0) = \delta_+ (W' - W^0)\ (\boldsymbol{k}' \mid U^\dagger \mid \boldsymbol{k}^0), \tag{21}$$

and the matrix equation (20) becomes

$$\left.\begin{aligned} &(\boldsymbol{k}' \mid U + U^\dagger \mid \boldsymbol{k}^0) + \\ &\int (\boldsymbol{k}' \mid U^\dagger \mid \boldsymbol{k}'')\, d\boldsymbol{k}''\, (\boldsymbol{k}'' \mid U \mid \boldsymbol{k}^0)\, [\delta_+ (W' - W'') + \delta_+ (W'' - W^0)] = 0. \end{aligned}\right\} \tag{22}$$

We now define a new matrix R by

$$\left.\begin{aligned} &(\boldsymbol{k}' \mid R \mid \boldsymbol{k}^0) = \delta (W' - W^0)\ (\boldsymbol{k}' \mid U \mid \boldsymbol{k}^0) = \\ &\delta (\boldsymbol{K}' - \boldsymbol{K}^0)\, \delta (W' - W^0)\ (\boldsymbol{k}' \mid U_{\boldsymbol{K}^0 W^0} \mid \boldsymbol{k}^0), \end{aligned}\right\} \tag{23}$$

where $(\boldsymbol{k}' \mid U_{\boldsymbol{K}^0 W^0} \mid \boldsymbol{k}^0)$ is a submatrix corresponding to fixed values $\boldsymbol{K}^0$ and W^0 for the total momentum and energy. When (22) is multiplied by $\delta (W' - W^0)$, the integral in (22) will contain a factor

$$\left.\begin{aligned} &\delta (W' - W^0)\ [\delta_+ (W^0 - W'') + \delta_+ (W'' - W^0)] = \\ &\delta (W' - W^0)\, \delta (W'' - W^0) = \delta (W' - W'')\, \delta (W'' - W^0) \end{aligned}\right\} \tag{24}$$

on account of (14), and by (23) we thus get the simple matrix equation

$$R + R^\dagger + R^\dagger R = 0. \tag{25}$$

Now, if we define HEISENBERG's characteristic matrix S by the equation

$$S = 1 + R, \tag{26}$$

(25) becomes identical with the equation

$$S^\dagger S = 1. \tag{27}$$

This condition alone is not, however, sufficient to make S a unitary matrix. We must also have

$$S S^\dagger = 1. \tag{28}$$

In order to prove this last equation we consider that solution Ψ_- of the Schrödinger equation (6) in which the outgoing waves T in (10) are replaced by ingoing waves. We then have

$$\Psi_- = 1 + T_- \tag{29}$$

with

$$(\boldsymbol{k}' \mid T_- \mid \boldsymbol{k}^0) = \delta_-(W' - W^0)\,(\boldsymbol{k}' \mid U_- \mid \boldsymbol{k}^0), \tag{30}$$

where the function δ_+ in (15) has been replaced by δ_-. Since Ψ_- is a solution of (6) and, by (14),

$$(W^0 - W')\,\delta_-(W' - W^0) = \frac{1}{2\pi i},$$

we have

$$U_- = 2\pi i V \Psi_- \tag{31}$$

on the analogy of (11). From (31) and the Hermitian conjugate equation

$$U_-^\dagger = -2\pi i \Psi_-^\dagger V \tag{32}$$

we get as before

$$\Psi_-^\dagger U_- + U_-^\dagger \Psi_- = 0, \tag{33}$$

or, by (29),

$$U_- + U_-^\dagger + T_-^\dagger U_- + U_-^\dagger T_- = 0 \tag{34}$$

analogously with (20). If this matrix equation is written out, we obviously get an equation obtained from (22) by replacing U and δ_+ by U_- and δ_-, respectively. Therefore, if we define a matrix R_- by

$$(\boldsymbol{k}' \mid R_- \mid \boldsymbol{k}^0) = \delta(W' - W^0)\,(\boldsymbol{k}' \mid U_- \mid \boldsymbol{k}^0), \tag{35}$$

we get from (34) analogously with (25)

$$R_- + R_-^\dagger + R_-^\dagger R_- = 0. \tag{36}$$

Further, multiplying (18) by Ψ_- on the right, and (31) by $\Psi^\dagger$ on the left, and subtracting, we get

$$U^\dagger \Psi_- - \Psi^\dagger U_- = 0, \tag{37}$$

or

$$U^\dagger - U_- + U^\dagger T_- - T^\dagger U_- = 0 \tag{38}$$

by (10) and (29).

Written in terms of representatives this equation reads

$$\left.\begin{aligned}&(\boldsymbol{k}'\,|\,U^{\dagger}-U_{-}\,|\,\boldsymbol{k}^{0})+\\&\int(\boldsymbol{k}'\,|\,U^{\dagger}\,|\,\boldsymbol{k}'')\,d\boldsymbol{k}''\,(\boldsymbol{k}''\,|\,U_{-}\,|\,\boldsymbol{k}^{0})\,[\delta_{-}(W''-W^{0})-\delta_{+}(W'-W'')]=0\end{aligned}\right\}\quad(39)$$

on account of (21) and (30).

Since

$$\delta_{+}(W^{0}-W'')=\delta_{-}(W''-W^{0}),$$

we get by multiplication of (39) with $\delta(W'-W^{0})$ and using (23) and (35)

$$R^{\dagger}=R_{-}. \tag{40}$$

(36) may thus be written

$$R+R^{\dagger}+RR^{\dagger}=0. \tag{41}$$

This equation together with (25) shows that R and $R^{\dagger}$ are commuting:

$$RR^{\dagger}=R^{\dagger}R. \tag{42}$$

Therefore also the matrices S and $S^{\dagger}$ commute, and the equation (28) holds as a consequence of (27). On account of the unitarity conditions (27) and (28) S may now be written in the form

$$S=e^{i\eta}, \tag{43}$$

where η is an Hermitian matrix—HEISENBERG's η-matrix.

In a perturbation theory, where V is considered as small, U, T, R, and η are also small, as is seen from (11), (15), (23), and (43). In the first approximation we get from (11)

$$U=-2\pi iV, \tag{44}$$

and from (26), (43), and (23)

$$\eta=\frac{1}{i}R, \tag{45}$$

and

$$(\boldsymbol{k}'\,|\,\eta\,|\,\boldsymbol{k}^{0})=-2\pi\delta(W'-W^{0})\,(\boldsymbol{k}'\,|\,V\,|\,\boldsymbol{k}^{0}), \tag{46}$$

showing that the η-matrix is essentially equal to the potential energy in this approximation.

Instead of the $3n'$ variables $(\boldsymbol{k}'_1 \cdots \boldsymbol{k}'_{n'})$ we now introduce the total momentum $\boldsymbol{K}'$, the total energy W', and $3n'-4$ other variables $(x') = (x'_1 \cdots x'_{3n'-4})$ as independent variables. When $\Delta' = \dfrac{\partial(\boldsymbol{K}'W'x')}{\partial(\boldsymbol{k}'_1 \cdots \boldsymbol{k}'_{n'})}$ denotes the functional determinant corresponding to this transformation, the connection between the matrix elements of any matrix A in the two representations is given by

$$(\boldsymbol{k}' \,|\, A \,|\, \boldsymbol{k}^0) = \sqrt{\Delta'}\ (\boldsymbol{K}'W'x' \,|\, A \,|\, \boldsymbol{K}^0W^0x^0)\sqrt{\Delta^0}, \tag{47}$$

provided the phase factors are unaffected by the transformation. For the representatives of any state in the two representations we have similarly

$$(\boldsymbol{k}' \,|) = \sqrt{\Delta'}\ (\boldsymbol{K}'W'x' \,|). \tag{47'}$$

In the new representation any of the three matrices R, S, and η have the form

$$(\boldsymbol{K}'W'x' \,|\, R \,|\, \boldsymbol{K}^0W^0x^0) = \delta(\boldsymbol{K}' - \boldsymbol{K}^0)\,\delta(W' - W^0)\ (x' \,|\, R \,|\, x^0). \tag{48}$$

Here

$$(x' \,|\, R \,|\, x^0) = (x' \,|\, U_{\boldsymbol{K}^0W^0} \,|\, x^0) \tag{49}$$

is a submatrix corresponding to fixed values $\boldsymbol{K}' = \boldsymbol{K}^0$ and $W' = W^0$ of the total momentum and energy. For the submatrices an equation like (27) takes the form

$$\int (x' \,|\, S^\dagger \,|\, x'')\, dx'' (x'' \,|\, S \,|\, x^0) = \int (x'' \,|\, S \,|\, x')^*\, dx'' (x'' \,|\, S \,|\, x^0) = \delta(x' - x^0). \tag{50}$$

It should be remembered, however, that $\int dx''$ is an abbreviation for $\sum\limits_{n''} \int dx''_1 \cdots dx''_{3n''-4}$, just like

$$\int d\boldsymbol{k}'' = \sum_{n''} \int d\boldsymbol{k}''_1 \cdots d\boldsymbol{k}''_{n''}. \tag{51}$$

Returning now to the general equation (22) we get in the new representation with $y = (\boldsymbol{K}, x)$

$$\left.\begin{aligned} &(W'y' \,|\, U + U^\dagger \,|\, W^0y^0) + \\ \int (W'y' \,|\, U^\dagger \,|\, W''y'')\, dW''\, dy'' &(W''y'' \,|\, U \,|\, W^0y^0)\ [\delta_+(W' - W'') + \\ &\delta_+(W'' - W^0)] = 0. \end{aligned}\right\} \tag{52}$$

If we multiply this equation by $\frac{1}{W'-W^0}$, or by $\delta_+(W'-W^0)$, a special investigation of the singularity at $W'=W^0$ will be necessary. By (15) and (21) the result of a multiplication with $\delta_+(W'-W^0)$ can be written

$$\left.\begin{aligned} &(W'y'\,|\,T+T^\dagger\,|\,W^0y^0)+\\ \int(W'y'\,|\,U^\dagger\,|\,W''y'')\,dW''\,dy''\,&(W''y''\,|\,U\,|\,W^0y^0)\\ &\delta_+(W'-W^0)\,[\delta_+(W'-W'')+\delta_+(W''-W^0)]=\\ &A(W^0,y',y^0)\,\delta(W'-W^0), \end{aligned}\right\} \tag{53}$$

where A so far is an arbitrary function of W^0, y', and y^0. The right hand side is zero except for $W'=W^0$ and vanishes entirely if multiplied by $W'-W^0$, thus in fact (53) reduces to (52) by multiplication with $W'-W^0$. The function A must be determined in such a way that an integration of the equation (53) with respect to W' over a range containing the value W^0 leads to a correct result. We need only integrate (53) from $W^0-\varepsilon$ to $W^0+\varepsilon$ and afterwards we can let ε go to zero.

Now we get from (14) by a simple calculation

$$\left.\begin{aligned} &\delta_+(W'-W^0)\,[\delta_+(W'-W'')+\delta_+(W''-W^0)]=\\ &\frac{1}{(2\pi i)^2(W'-W'')(W''-W^0)}+\frac{1}{4\pi i}\,\frac{\delta(W''-W')}{W''-W^0}+\frac{1}{4\pi i}\,\frac{\delta(W''-W^0)}{W'-W''}+\\ &\frac{1}{2}\,\delta(W'-W^0)\,\delta(W''-W^0)=\delta_+(W'-W'')\,\delta_+(W''-W^0)+\\ &\frac{1}{4}\,\delta(W'-W^0)\,\delta(W''-W^0). \end{aligned}\right\} \tag{54}$$

Further we have, for any function $f(W')$ which is continuous at $W'=W^0$,

$$\lim_{\varepsilon\to 0}\int_{W^0-\varepsilon}^{W^0+\varepsilon} f(W')\,\delta_+(W'-W^0)\,dW'=f(W^0)\lim_{\varepsilon\to 0}\int_{W^0-\varepsilon}^{W^0+\varepsilon}\delta_+(W'-W^0)\,dW'=\frac{f(W^0)}{2}, \tag{55}$$

and

$$\lim_{\varepsilon\to 0}\int_{W^0-\varepsilon}^{W^0+\varepsilon}\frac{f(W')\,dW'}{(2\pi i)^2\,(W'-W'')\,(W''-W^0)}=\frac{f(W^0)\,\delta(W''-W^0)}{4}. \tag{56}$$

In fact, we have, with $\xi = W'' - W^0$

$$\left.\begin{aligned} \lim_{\varepsilon \to 0} \int_{W^0-\varepsilon}^{W^0+\varepsilon} \frac{dW'}{(2\pi i)^2 (W' - W'')(W'' - W^0)} = \\ \lim_{\varepsilon \to 0} \begin{cases} \frac{1}{4\pi^2 \xi} ln \frac{-\varepsilon - \xi}{\varepsilon - \xi} & \text{for } \xi < -\varepsilon \\ \frac{1}{4\pi^2 \xi} ln \frac{\varepsilon + \xi}{\varepsilon - \xi} & \text{for } -\varepsilon < \xi < \varepsilon \\ \frac{1}{4\pi^2 \xi} ln \frac{\varepsilon + \xi}{\xi - \varepsilon} & \text{for } \xi > \varepsilon, \end{cases} \end{aligned}\right\} \quad (57)$$

and this function is easily shown to be equal to $\frac{1}{4}\delta(\xi) = \frac{1}{4}\delta(W'' - W^0)$ in the limit $\varepsilon \to 0$.

When the operation $\lim_{\varepsilon \to 0} \int_{W^0-\varepsilon}^{W^0+\varepsilon} dW'$ is applied to the equation (53), we thus, using (15), (21), the first equation (54), (55), and (56), get

$$\left.\begin{aligned} A(W^0, y', y^0) = \frac{1}{2}(W^0 y' | U + U^\dagger | W^0 y^0) + \\ \int (W^0 y' | U^\dagger | W'' y'')\, dW''\, dy''\, (W'' y'' | U | W^0 y^0) \\ \left[\frac{1}{4}\delta(W'' - W^0) + \frac{1}{2}\delta(W'' - W^0)\right] = \\ \frac{1}{4}\int (W^0 y' | U^\dagger | W^0 y'')\, dy''\, (W^0 y'' | U | W^0 y^0). \end{aligned}\right\} \quad (58)$$

Here we have also used the equation

$$\left.\begin{aligned} (W^0 y' | U + U^\dagger | W^0 y^0) + \\ \int (W^0 y' | U^\dagger | W^0 y'')\, dy''\, (W^0 y'' | U | W^0 y^0) = 0, \end{aligned}\right\} \quad (59)$$

which follows from (23) and (25) by integration of (25) with respect to W'.

Introducing the expression (58) for A into (53) we get, using the last equation (54),

$$\left.\begin{aligned}(W'y'\,|\,T+T^\dagger\,|\,W^0y^0)+\\ \int (W'y'\,|\,U^\dagger\,|\,W''y'')\,dW''dy''\,(W''y''\,|\,U\,|\,W^0y^0)\\ \delta_+(W'-W'')\,\delta_+(W''-W^0)=0,\end{aligned}\right\}(60$$

or

$$T+T^\dagger+T^\dagger T=0. \tag{61}$$

For the wave matrix Ψ in (10) we have therefore

$$\Psi^\dagger\Psi=1, \tag{62}$$

which shows that the matrix elements $(\boldsymbol{k}'\,|\,\Psi\,|\,\boldsymbol{k}^0)$, considered as functions of $(\boldsymbol{k}')$ with fixed $(\boldsymbol{k}^0)$, are normalized eigenfunctions of the Hamiltonian $H=W+V$ belonging to the continuous eigenvalues $E=W^0=\sum_i \sqrt{\kappa^2+k_i^{02}}$.

The matrix Ψ, however, will not in general be a unitary matrix, since the equation

$$\Psi\Psi^\dagger=1 \tag{63}$$

will hold in special cases only. When (63) holds, the reciprocal of Ψ exists, and $\Psi^{-1}=\Psi^\dagger$. From the Schrödinger equation (7), which may be written

$$\Psi W=H\Psi, \tag{64}$$

we then, by multiplication with Ψ^{-1} on the right, get

$$H=\Psi W\Psi^{-1}, \tag{65}$$

showing that the matrices H and W have the same eigenvalues. (63) can thus only be true for systems which do not have any closed states.

In the general case we may define an Hermitian operator

$$\mathcal{E}=1-\Psi\Psi^\dagger \tag{66}$$

which, on account of (62), satisfies the equation

$$\mathcal{E}^2=1-2\,\Psi\Psi^\dagger+\Psi\Psi^\dagger\Psi\Psi^\dagger=1-\Psi\Psi^\dagger=\mathcal{E}. \tag{67}$$

Hence $\mathcal{E}$ has the eigenvalues 0 and 1.

Further we have

$$H\Psi\Psi^\dagger-\Psi\Psi^\dagger H=0. \tag{68}$$

To prove this equation, multiply (64) by $\psi^\dagger$ on the right and the conjugate equation

$$W\psi^\dagger = \psi^\dagger H \tag{69}$$

by ψ on the left, and subtract.

(68) shows that $\psi\psi^\dagger$ and therefore also $\mathcal{E}$ commute with H. Thus $\mathcal{E}$ and H have a common system of eigenfunctions.

Since

$$\mathcal{E}\,\psi = 0 \tag{70}$$

according to (66) and (62), the functions $(\boldsymbol{k}' \mid \psi \mid \boldsymbol{k}^0)$ belonging to the continuous eigenvalues of H, are also eigenfunctions of $\mathcal{E}$ belonging to the eigenvalue 0. Moreover these functions are the only eigenfunctions of that kind. To prove this, let us assume that $\Phi(\boldsymbol{k}')$ is another independent eigenfunction of $\mathcal{E}$ with the eigenvalue 0, then Φ may be taken orthogonal to all the functions $(\boldsymbol{k}' \mid \psi \mid \boldsymbol{k}^0)$, i. e.

$$\left.\begin{aligned} \psi^\dagger \Phi &= 0 \\ \text{and} \qquad \mathcal{E}\,\Phi &= 0 \end{aligned}\right\} \tag{71}$$

which, by (66), leads to the equation

$$\Phi = 0.$$

The eigenfunctions $\psi_r(\boldsymbol{k}')$ of H belonging to the discrete* eigenvalues are therefore also eigenfunctions of $\mathcal{E}$ with the eigenvalue 1. If $\psi_r(\boldsymbol{k}')$ is considered as a matrix with one column only, while $\psi_r^\dagger(\boldsymbol{k}') = \psi_r(\boldsymbol{k}')^*$ is considered as a matrix with one row only, the orthogonality relations for the discrete eigenstates may be written

$$\left.\begin{aligned} \psi_r^\dagger \psi_s &= \delta_{rs} \\ \psi_r^\dagger \psi &= 0. \end{aligned}\right\} \tag{72}$$

Since the functions $\psi_r(\boldsymbol{k}')$ are the only eigenfunctions of $\mathcal{E}$ belonging to the eigenvalue 1, all other eigenfunctions belonging to the eigenvalue 0, we obviously have

$$(\boldsymbol{k}' \mid \mathcal{E} \mid \boldsymbol{k}'') = \sum_r \psi_r(\boldsymbol{k}')\,\psi_r^\dagger(\boldsymbol{k}''), \tag{73}$$

* The index r numerating the 'discrete' energy values will in general also include continuous variables such as the total momentum $\boldsymbol{K}^0$ of the system.

and the equation (66) may be written

$$(\boldsymbol{k}' \mid \Psi\Psi^{\dagger} \mid \boldsymbol{k}'') + \sum_{r} \Psi_r(\boldsymbol{k}')\, \Psi_r^{\dagger}(\boldsymbol{k}'') = (\boldsymbol{k}' \mid 1 \mid \boldsymbol{k}''), \qquad (74)$$

which in the general case replaces (63).

We shall now discuss the question whether the discrete energy values in the closed stationary states are at least partly determined by the S-matrix, as originally indicated by HEISENBERG[7]. *A priori*, this seems possible, since the asymptotic form of the wave function in great distances which determines the collision cross sections, depends chiefly on the form of the potential function in small distances, which again is essential for the position of the discrete energy levels. From the preceding developments it follows, however, that the discrete energy values are completely independent of the form of the S-matrix. To see this, let us assume that we do not know only the submatrices S and R, but the whole matrices U and Ψ. With given Ψ the operator $\mathfrak{E}$ is given by (66). Determining the eigenfunctions of $\mathfrak{E}$ belonging to the eigenvalue 1, we get simultaneously the eigenfunctions $\Psi_r(\boldsymbol{k}')$ of H belonging to the discrete energy values or at least linear combinations of these functions. The values of the energy in these states, however, are completely undetermined. The energy levels in the closed states may be changed in an arbitrary way without any change in Ψ, i. e. without any effect on the results of collision processes. New fundamental assumptions about the S-matrix will thus be necessary in order to determine the energy values in the closed states. To this question we shall return in the sequel to this paper.

2. General definition of cross sections. Connection between the cross sections and the characteristic matrix S. Proof of the invariance of S.

In order to investigate the transformation properties of the matrix S under Lorentz transformations it seems natural to use the connection between the matrix elements of S and the cross sections. For this purpose we need a general definition of cross sections in an arbitrary Lorentz frame of reference. The current

textbooks give definitions of cross sections only for the special frames of reference, where either the center of gravity or one of the particles are initially at rest. In the general case it will now be most convenient to use a definition which makes the cross sections entirely independent of the frame of reference. This condition, together with the well-known expression for the cross section in the system where the center of gravity is at rest, uniquely determines the definition to be adopted in the general case.

We shall first consider a collision between particles 1 and 2 without creation of new particles. Let ϱ_1^0 and ϱ_2^0 be the densities of particles 1 and 2 in the incident beams and let $\boldsymbol{u}_1^0$ and $\boldsymbol{u}_2^0$ be the corresponding particle velocities. If $dQ = \sigma d\Omega$ denotes the differential cross section for a scattering of particles 2 say into a solid angle $d\Omega$, we have in the center of gravity system

$$dQ = \frac{dN}{\varrho_1^0 \varrho_2^0 |\boldsymbol{u}_1^0 - \boldsymbol{u}_2^0|},$$

where dN is the number of particles 2, which, pr. unit volume and unit time, i. e. pr. unit four-dimensional volume, is scattered into the solid angle $d\Omega$.

Since the four dimensional volume is invariant, the number dN must be independent of the frame of reference. Thus the cross section must in general be given by

$$dQ = \frac{dN}{F^0}, \tag{75}$$

where the factor F^0 is an invariant, which in the center of gravity system reduces to $\varrho_1^0 \varrho_2^0 |\boldsymbol{u}_1^0 - \boldsymbol{u}_2^0|$. As is easily seen, F^0 must then be given by

$$F^0 = \varrho_1^0 \varrho_2^0 \sqrt{|\boldsymbol{u}_1^0 - \boldsymbol{u}_2^0|^2 - |\boldsymbol{u}_1^0 \times \boldsymbol{u}_2^0|^2}. \tag{76}$$

Here $\boldsymbol{u}_1^0 \times \boldsymbol{u}_2^0$ is the vector product of the vectors $\boldsymbol{u}_1^0$ and $\boldsymbol{u}_2^0$, which is zero if $\boldsymbol{u}_1^0$ and $\boldsymbol{u}_2^0$ are parallel, as is the case in the center of gravity system.

To prove the invariance of F^0 we use the fact that the quantities $k_i^\mu = (\boldsymbol{k}_i, W_i)$ and $k_{i\mu} = (\boldsymbol{k}_i, -W_i)$ by any Lorentz transformation transform like the components of a four-vector. The

quantities $k_1^\mu k_2^\nu - k_1^\nu k_2^\mu$ are thus the components of an antisymmetrical tensor and the quantity

$$\left.\begin{aligned} B &= \sqrt{|\boldsymbol{k}_1 W_2 - \boldsymbol{k}_2 W_1|^2 - |\boldsymbol{k}_1 \times \boldsymbol{k}_2|^2} = \\ &= \sqrt{\frac{-1}{2}\left(k_1^\mu k_2^\nu - k_1^\nu k_2^\mu\right)\left(k_{1\mu} k_{2\nu} - k_{1\nu} k_{2\mu}\right)} \end{aligned}\right\} \quad (77)$$

is an invariant.* Further we have for any Lorentz transformation connecting the variables of two frames of reference K and $\bar{K}$.

$$\left.\begin{aligned} \bar{\varrho}_i &= \varrho_i \frac{1 - \boldsymbol{v}\boldsymbol{u}_i}{\sqrt{1-\boldsymbol{v}^2}} \\ \overline{W}_i &= W_i \frac{1 - \boldsymbol{v}\boldsymbol{u}_i}{\sqrt{1-\boldsymbol{v}^2}}, \quad \boldsymbol{u}_i = \frac{\boldsymbol{k}_i}{W_i}, \end{aligned}\right\} \quad (78)$$

where $\boldsymbol{v}$ represents the velocity of $\bar{K}$ relative to K. Hence $\frac{\varrho_1 \varrho_2}{W_1 W_2} = \frac{\bar{\varrho}_1 \bar{\varrho}_2}{\overline{W}_1 \overline{W}_2}$ and the quantity F^0 in (76) may be written as a product of two invariant quantities:

$$F^0 = \frac{\varrho_1^0 \varrho_2^0}{W_1^0 W_2^0} \cdot B^0$$

with B^0 given by (77).

Thus the cross section defined by (75) and (76) is invariant. Further it is symmetrical in the two particles and reduces to the usual definition of cross sections in the center of gravity system. The same holds for that system in which one of the particles, say particle 1, is initially at rest, since in this case F^0 reduces to $F^0 = \varrho_1^0 \varrho_2^0 u_2^0$.

We shall now trace the connection between the scattering cross section dQ and the matrix elements of S. For this purpose we need the Schrödinger function $\Psi(\boldsymbol{x}_1 \boldsymbol{x}_2)$ in configuration space. This function is obtained from the wave matrix $(\boldsymbol{k}_1' \boldsymbol{k}_2' \,|\, \Psi \,|\, \boldsymbol{k}_1^0 \boldsymbol{k}_2^0)$ by means of the equation

$$\Psi(\boldsymbol{x}_1 \boldsymbol{x}_2) = \int (\boldsymbol{x}_1 \boldsymbol{x}_2 \,|\, \boldsymbol{k}_1' \boldsymbol{k}_2')\, d\boldsymbol{k}_1'\, d\boldsymbol{k}_2'\, (\boldsymbol{k}_1' \boldsymbol{k}_2' \,|\, \Psi \,|\, \boldsymbol{k}_1^0 \boldsymbol{k}_2^0) \quad (79)$$

with the transformation function

* Here the usual convention is made regarding the summation from 1 to 4 over dummy indices like μ and ν in (77).

$$(\boldsymbol{x}_1 \boldsymbol{x}_2 \,|\, \boldsymbol{k}'_1 \boldsymbol{k}'_2) = (2\pi)^{-3}\, e^{i(\boldsymbol{k}'_1 \boldsymbol{x}_1 + \boldsymbol{k}'_2 \boldsymbol{x}_2)}\, e^{i\gamma(\boldsymbol{k}'_1 \boldsymbol{k}'_2)}, \tag{80}$$

where $\gamma' = \gamma(\boldsymbol{k}'_1 \boldsymbol{k}'_2)$ is a real function of $\boldsymbol{k}'_1$ and $\boldsymbol{k}'_2$ depending on the phases in the chosen $\boldsymbol{k}$-representation.[8] γ' may also be a function of the time. For the incident waves we get, by (8) and (9),

$$\psi^0(\boldsymbol{x}_1 \boldsymbol{x}_2) = (2\pi)^{-3}\, e^{i(\boldsymbol{k}^0_1 \boldsymbol{x}_1 + \boldsymbol{k}^0_2 \boldsymbol{x}_2)}\, e^{i\gamma^0} = (2\pi)^{-3} e^{i\boldsymbol{K}^0 \boldsymbol{x}_1}\, e^{i\boldsymbol{k}^0_2 (\boldsymbol{x}_2 - \boldsymbol{x}_1)}\, e^{i\gamma^0}, \tag{81}$$

while the scattered waves on account of (8), (15), and (16), are given by

$$\left.\begin{aligned} T(\boldsymbol{x}_1 \boldsymbol{x}_2) &= (2\pi)^{-3} \int e^{i(\boldsymbol{k}'_1 \boldsymbol{x}_1 + \boldsymbol{k}'_2 \boldsymbol{x}_2)}\, e^{i\gamma'}\, \delta(\boldsymbol{K}' - \boldsymbol{K}^0) \\ &\quad \delta_+(W'_1 + W'_2 - W^0)\, (\boldsymbol{k}'_1 \boldsymbol{k}'_2 \,|\, U_{\boldsymbol{K}^0} \,|\, \boldsymbol{k}^0_1 \boldsymbol{k}^0_2)\, d\boldsymbol{k}'_1\, d\boldsymbol{k}'_2 = \\ &= (2\pi)^{-3} e^{i\boldsymbol{K}^0 \boldsymbol{x}_1} \int e^{i\boldsymbol{k}'_2 (\boldsymbol{x}_2 - \boldsymbol{x}_1)}\, e^{i\gamma(\boldsymbol{K}^0 - \boldsymbol{k}'_2, \boldsymbol{k}'_2)} \\ &\quad \delta_+\left(\sqrt{K^2 + |\boldsymbol{K}^0 - \boldsymbol{k}'_2|^2} + \sqrt{K^2 + k'^2_2} - W^0\right) (\boldsymbol{K}^0 - \boldsymbol{k}'_2, \boldsymbol{k}'_2 \,|\, U_{\boldsymbol{K}^0} \,|\, \boldsymbol{k}^0_1 \boldsymbol{k}^0_2)\, d\boldsymbol{k}'_2 . \end{aligned}\right\} \tag{82}$$

Now we are only interested in the asymptotic values of T for $r = |\boldsymbol{x}_2 - \boldsymbol{x}_1| \to \infty$. Introducing polar coordinates in the $\boldsymbol{k}'_2$-space with the direction $\boldsymbol{e}'_2 = \dfrac{\boldsymbol{x}_2 - \boldsymbol{x}_1}{|\boldsymbol{x}_2 - \boldsymbol{x}_1|}$ as polar axis, the integration with respect to the angles in the integral in (82) leads to the expression[9]

$$\left.\begin{aligned} T(\boldsymbol{x}_1 \boldsymbol{x}_2)_{r \to \infty} &= (2\pi)^{-3} e^{i\boldsymbol{K}^0 \boldsymbol{x}_1} \frac{2\pi}{ir} \left\{ \int_0^\infty e^{ik'_2 r}\, (\boldsymbol{K}^0 - k'_2 \boldsymbol{e}'_2, k'_2 \boldsymbol{e}'_2 \,|\, U_{\boldsymbol{K}^0} \,|\, \boldsymbol{k}^0_1, \boldsymbol{k})^0_2 \right. \\ &\quad e^{i\gamma(\boldsymbol{K}^0 - k'_2 \boldsymbol{e}'_2, k'_2 \boldsymbol{e}'_2)}\, \delta_+\left(\sqrt{K^2 + |\boldsymbol{K}^0 - k'_2 \boldsymbol{e}'_2|^2} + \sqrt{K^2 + k'^2_2} - W^0\right) k'_2\, dk'_2 - \\ &\left. \int_0^\infty e^{-ik'_2 r}\, (\boldsymbol{K}^0 + k'_2 \boldsymbol{e}'_2, -k'_2 \boldsymbol{e}'_2 \,|\, U_{\boldsymbol{K}^0} \,|\, \boldsymbol{k}^0_1, \boldsymbol{k}^0_2)\, e^{i\gamma(\boldsymbol{K}^0 + k'_2 \boldsymbol{e}'_2, -k'_2 \boldsymbol{e}'_2)} \right. \\ &\quad \left. \delta_+\left(\sqrt{K^2 + |\boldsymbol{K}^0 + k'_2 \boldsymbol{e}'_2|^2} + \sqrt{K^2 + k'^2_2} - W^0\right) k'_2\, dk'_2, \right\} \end{aligned}\right\} \tag{83}$$

where only terms of the order $\dfrac{1}{r}$ have been retained. When the argument of the δ_+-function is denoted by $A(k'_2)$, and when $f(k'_2)$ is any function of k'_2, we have[9], neglecting terms of the order $\dfrac{1}{r^2}$,

$$\int_0^\infty e^{ik_2' r} f(k_2')\, \delta_+(A)\, k_2'\, dk_2' = \frac{e^{i\bar{k}_2' r}\, \bar{k}_2'}{\left.\frac{\partial A(\bar{k}_2')}{\partial \bar{k}_2'}\right|_{\text{const. } \boldsymbol{e}_2'}} f(\bar{k}_2'), \tag{84}$$

where $\bar{k}_2'$ is the value of k_2' determined by

$$A(k_2') = 0, \tag{85}$$

and the differentiation of $A(k_2')$ with respect to k_2' is to be performed by constant $\boldsymbol{e}_2'$.

In the same approximation we have

$$\int_0^\infty e^{-ik_2' r} f(k_2')\, \delta_+(A)\, k_2'\, dk_2' = 0, \tag{86}$$

so that the second integral in (83) may be neglected.

In the first integral we put

$$\boldsymbol{k}_2' = \bar{k}_2' \boldsymbol{e}_2' \quad \text{and} \quad \boldsymbol{k}_1' = \boldsymbol{K}^0 - \bar{k}_2' \boldsymbol{e}_2'. \tag{87}$$

Thus $\boldsymbol{k}_1'$ and $\boldsymbol{k}_2'$ are now the values of the momentum variables following from the theorems of conservation of momentum and energy. When W_1', W_2', $\boldsymbol{u}_1'$ and $\boldsymbol{u}_2'$ are the corresponding energies and velocities, we get, since the differentiation in $\frac{\partial A}{\partial k_2'}$ is to be performed by constant $\boldsymbol{e}_2'$,

$$\left.\frac{\partial A}{\partial k_2'}\right|_{\text{const. } \boldsymbol{e}_2'} = \left(\frac{\boldsymbol{k}_2'}{W_2'} - \frac{\boldsymbol{k}_1'}{W_1'}\right) \boldsymbol{e}_2' = (\boldsymbol{u}_2' - \boldsymbol{u}_1')\, \boldsymbol{e}_2'. \tag{88}$$

Using (84) and (88) in the calculation of the first integral in (83) we finally get for the total wave function in configuration space the asymptotic expression*

$$\left.\begin{aligned} \Psi(\boldsymbol{x}_1 \boldsymbol{x}_2)_{r\to\infty} &= \Psi^0(\boldsymbol{x}_1 \boldsymbol{x}_2) + T(\boldsymbol{x}_1 \boldsymbol{x}_2)_{r\to\infty} = \\ = (2\pi)^{-3} e^{i\boldsymbol{K}^0 \boldsymbol{x}_1} &\left\{ e^{i\boldsymbol{k}_2^0 (\boldsymbol{x}_2 - \boldsymbol{x}_1)} e^{i\gamma^0} - 2\pi i \frac{e^{ik_2' r} e^{i\gamma'}}{r} \frac{k_2' (\boldsymbol{k}_1' \boldsymbol{k}_2' \mid U_{\boldsymbol{K}^0 W^0} \mid \boldsymbol{k}_1^0 \boldsymbol{k}_2^0)}{(\boldsymbol{u}_2' - \boldsymbol{u}_1')\, \boldsymbol{e}_2'} \right\}. \end{aligned}\right\} \tag{89}$$

The probability of finding the particle 2 in a distance $r = |\boldsymbol{x}_2 - \boldsymbol{x}_1|$ from the particle 1 after the collision is thus proportional to

* This asymptotic expression for Ψ is seen to be correct only if the potential function goes to zero faster than $\frac{1}{r}$ as r tends to infinity. Thus, a slight modification of the theory is necessary in the limiting case of a Coulomb field.

$$\frac{(2\pi)^2}{r^2}\,\frac{k_2'^2\,|(\boldsymbol{k}_1'\boldsymbol{k}_2'\,|\,U_{\boldsymbol{K}^0W^0}|\,\boldsymbol{k}_1^0\boldsymbol{k}_2^0)|^2}{|(\boldsymbol{u}_2'-\boldsymbol{u}_1')\,\boldsymbol{e}_2'|^2}\,. \tag{90}$$

To get the number of particles 2 which pr. unit time are scattered into the solid angle $d\Omega$ in the direction $\boldsymbol{e}_2'$, we have to multiply (90) by the factor $|(\boldsymbol{u}_2'-\boldsymbol{u}_1')\,\boldsymbol{e}_2'|\cdot r^2 d\Omega$, which determines the current through a surface element $r^2 d\Omega$ placed at right angles to the direction $\boldsymbol{e}_2'$ in a constant distance r from the particle 1. Taking account of the particle densities in the incident waves we finally for the scattering cross section get

$$dQ_{\text{scat.}} = 4\pi^2\,\frac{k_2'^2\,|(\boldsymbol{k}_1'\boldsymbol{k}_2'\,|\,U_{\boldsymbol{K}^0W^0}|\,\boldsymbol{k}_1^0\boldsymbol{k}_2^0)|^2}{\sqrt{|\boldsymbol{u}_1^0-\boldsymbol{u}_2^0|^2-|\boldsymbol{u}_1^0\times\boldsymbol{u}_2^0|^2}\cdot|(\boldsymbol{u}_2'-\boldsymbol{u}_1')\,\boldsymbol{e}_2'|}\,d\Omega\,. \tag{91}$$

The matrix $U_{\boldsymbol{K}^0W^0}$ occurring in this expression is, apart from the δ-functions, identical with the matrix R in (23).

If we put

$$I = \sqrt{W_1'W_2'}\,(\boldsymbol{k}_1'\boldsymbol{k}_2'\,|\,U_{\boldsymbol{K}^0W^0}|\,\boldsymbol{k}_1^0\boldsymbol{k}_2^0)\,\sqrt{W_1^0W_2^0} \tag{92}$$

(91) may be written

$$dQ_{\text{scat.}} = 4\pi^2\,\frac{|I|^2}{B^0}\,\frac{k_2'^2\,d\Omega}{|(\boldsymbol{u}_2'-\boldsymbol{u}_1')\,\boldsymbol{e}_2'|\cdot W_1'W_2'}\,, \tag{93}$$

where B^0 is the invariant quantity defined by (77).

Since the vectors $\boldsymbol{k}_1'$ and $\boldsymbol{k}_2'$ are determined by the conservation theorems, we have

$$(\boldsymbol{u}_2'-\boldsymbol{u}_1')\,\boldsymbol{e}_2' = \frac{\partial\,(W_1'+W_2')}{\partial\,k_2'} = \frac{\partial\,W'}{\partial\,k_2'}\,, \tag{94}$$

where $\boldsymbol{k}_1'$ in W_1' is to be put equal to $\boldsymbol{K}^0-k_2'\boldsymbol{e}_2'$ before the differentiation, which then is performed by constant $\boldsymbol{e}_2'$. (93) may therefore also be written

$$dQ_{\text{scat.}} = 4\pi^2\,\frac{|I|^2}{B^0}\iint\delta\,(\boldsymbol{K}'-\boldsymbol{K}^0)\,\delta\,(W'-W^0)\,\frac{d\boldsymbol{k}_1'}{W_1'}\,\frac{k_2'^2\,dk_2'\,d\Omega}{W_2'}\,, \tag{95}$$

where the integration in $\int d\boldsymbol{k}_1'$ is to be extended over the whole $\boldsymbol{k}_1'$-space, while the integration in $\int dk_2'$ ranges from 0 to ∞. For small U and V, where (44) holds, the expression (95) is easily

seen to be identical with the usual quantum mechanical expression for the cross section, derived by a perturbation method in which the potential V is treated as small. The integral in (95) is obviously invariant, $\delta(\boldsymbol{K}'-\boldsymbol{K}^0)\,\delta(W'-W^0)$ and $\frac{d\boldsymbol{k}'_i}{W'_i}$ being invariant quantities (cf. equation (129) section 3). Since the same holds for dQ and B^0, (95) shows that the modulus of the quantity I, defined by (92), must be relativistically invariant.

Let us now consider the case where a new particle 3 is created during the collision. The cross section for a process in which the new particle obtains a momentum between $\boldsymbol{k}'_3$ and $\boldsymbol{k}'_3+d\boldsymbol{k}'_3$, while particle 2 is scattered into a solid angle $d\Omega$ in the direction $\boldsymbol{e}'_2$, may be derived as before. We simply get

$$dQ_{\text{scat.,emis.}} = 4\pi^2 \frac{k'^2_2\,|\,(\boldsymbol{k}'_1\boldsymbol{k}'_2\boldsymbol{k}'_3\,|\,\boldsymbol{U}_{\boldsymbol{K}^0W^0}\,|\,\boldsymbol{k}^0_1\boldsymbol{k}^0_2)\,|^2}{\sqrt{|\,\boldsymbol{u}^0_1-\boldsymbol{u}^0_2\,|^2-|\,\boldsymbol{u}^0_1\times\boldsymbol{u}^0_2\,|^2}\cdot|\,(\boldsymbol{u}'_2-\boldsymbol{u}'_1)\,\boldsymbol{e}'_2\,|}\,d\Omega\,d\boldsymbol{k}'_3 \qquad (96)$$

on a close analogy of (91). By the same arguments as before we find that the modulus of the quantity

$$\sqrt{W'_1W'_2W'_3}\,(\boldsymbol{k}'_1\boldsymbol{k}'_2\boldsymbol{k}'_3\,|\,U_{\boldsymbol{K}^0W^0}\,|\,\boldsymbol{k}^0_1\boldsymbol{k}^0_2)\,\sqrt{W^0_1W^0_2}$$

is a relativistic invariant. The same holds for a general matrix element of $\boldsymbol{U}_{\boldsymbol{K}^0W^0}$ and therefore also for the elements of the matrix R defined by (23).

Let us now consider an arbitrary Lorentz transformation. In the momentum space of the i'th particle, say, this will in general be a non-linear transformation

$$\bar{\boldsymbol{k}}_i = \mathcal{L}(\boldsymbol{k}_i). \qquad (97)$$

If all transformed quantities are distinguished by a bar, the representative of the transformed matrix $\bar{R}$ in a $\bar{\boldsymbol{k}}$-representation will be denoted by $(\bar{\boldsymbol{k}}'\,|\,\bar{R}\,|\,\bar{\boldsymbol{k}}^0)$. Further let $\bar{\boldsymbol{k}}'_i$ and $\bar{\boldsymbol{k}}^0_i$ denote those eigenvalues of $\bar{\boldsymbol{k}}_i$ which are connected with the eigenvalues $\boldsymbol{k}'_i$ and $\boldsymbol{k}^0_i$ by (97), i. e.

$$\bar{\boldsymbol{k}}'_i = \mathcal{L}(\boldsymbol{k}'_i);\quad \bar{\boldsymbol{k}}^0_i = \mathcal{L}(\boldsymbol{k}^0_i). \qquad (98)$$

The result of the preceding investigation may then be written

$$\sqrt{[W'_i]}\,\left|(\boldsymbol{k}'\,|\,R\,|\,\boldsymbol{k}^0)\right|\sqrt{[W^0_i]} = \sqrt{[\bar{W}'_i]}\,\left|(\bar{\boldsymbol{k}}'\,|\,\bar{R}\,|\,\bar{\boldsymbol{k}}^0)\right|\sqrt{[\bar{W}^0_i]}, \qquad (99)$$

where the symbol $[W_i']$ is used for the product of the energies corresponding to the values $(\boldsymbol{k}'_1, \cdots \boldsymbol{k}'_{n'})$ of the momentum variables.

In his papers quoted above HEISENBERG[2] has stated a more general equation viz.

$$\sqrt{[W_i']}\,(\boldsymbol{k}'|R|\boldsymbol{k}^0)\sqrt{[W_i^0]} = \sqrt{[\bar{W}_i']}\,(\bar{\boldsymbol{k}}'|\bar{R}|\bar{\boldsymbol{k}}^0)\sqrt{[\bar{W}_i^0]} \quad (100)$$

where the modulus $|(\boldsymbol{k}'|R|\boldsymbol{k}^0)|$ in (99) is replaced by $(\boldsymbol{k}'|R|\boldsymbol{k}^0)$. In contrast to the equation (99) which holds for any choice of the phases in the $\bar{\boldsymbol{k}}$-representation, the equation (100) cannot be true for all $\bar{\boldsymbol{k}}$-representations, since a change in phase in the $\bar{\boldsymbol{k}}$-representation will change the right hand side of (100) in accordance with (2) while the left hand side remains unchanged. By means of the equation (25) and the corresponding equation

$$\bar{R} + \bar{R}^\dagger + \bar{R}^\dagger \bar{R} = 0 \quad (101)$$

for the transformed matrix $\bar{R}$, it may be shown, however, that it is possible, for given phases of the $\boldsymbol{k}$-representation, to choose the phases in the $\bar{\boldsymbol{k}}$-representation in such a way that (100) is true.

According to the special theory of relativity the momentum and energy variables of a particle transform like the components of a four vector. Hence we find by a simple calculation that the functional determinant Δ', corresponding to the transformation $(\boldsymbol{k}'_1, \cdots \boldsymbol{k}'_{n'}) \rightarrow (\bar{\boldsymbol{k}}'_1, \cdots \bar{\boldsymbol{k}}'_{n'})$ given by (98), is

$$\Delta' = \frac{\partial(\bar{\boldsymbol{k}}'_1 \cdots \bar{\boldsymbol{k}}'_{n'})}{\partial(\boldsymbol{k}'_1 \cdots \boldsymbol{k}'_{n'})} = \frac{[\bar{W}_i']}{[W_i']}. \quad (102)$$

We may now put

$$(\boldsymbol{k}'|R|\boldsymbol{k}^0) = |(\boldsymbol{k}'|R|\boldsymbol{k}^0)|\,e^{ir(\boldsymbol{k}';\boldsymbol{k}^0)} \quad (103)$$

and

$$(\bar{\boldsymbol{k}}'|\bar{R}|\bar{\boldsymbol{k}}^0) = |(\bar{\boldsymbol{k}}'|\bar{R}|\bar{\boldsymbol{k}}^0)|\,e^{i\bar{r}(\bar{\boldsymbol{k}}';\bar{\boldsymbol{k}}^0)}, \quad (104)$$

where the arguments $r(\boldsymbol{k}';\boldsymbol{k}^0)$ and $\bar{r}(\bar{\boldsymbol{k}}';\bar{\boldsymbol{k}}^0)$ are real functions of the variables $(\boldsymbol{k}', \boldsymbol{k}^0)$ and $(\bar{\boldsymbol{k}}', \bar{\boldsymbol{k}}^0)$, respectively.

If we change the phases in the $\boldsymbol{k}$-representation in accordance with (2), the argument $r(\boldsymbol{k}';\boldsymbol{k}^0)^\times$ of the new representative of R, defined by

$$(\boldsymbol{k}' \mid R \mid \boldsymbol{k}^0)^{\times} = |(\boldsymbol{k}' \mid R \mid \boldsymbol{k}^0)|\, e^{i r(\boldsymbol{k}';\boldsymbol{k}^0)^{\times}} \tag{105}$$

is obviously given by

$$r(\boldsymbol{k}';\boldsymbol{k}^0)^{\times} = r(\boldsymbol{k}';\boldsymbol{k}^0) + \alpha(\boldsymbol{k}') - \alpha(\boldsymbol{k}^0). \tag{106}$$

When we use (104) and (17), the equation (101), written in terms of representatives, becomes

$$\left.\begin{aligned} &|(\bar{\boldsymbol{k}}' \mid \bar{R} \mid \bar{\boldsymbol{k}}^0)|\, e^{i\bar{r}(\bar{\boldsymbol{k}}';\bar{\boldsymbol{k}}^0)} + |(\bar{\boldsymbol{k}}^0 \mid \bar{R} \mid \bar{\boldsymbol{k}}')|\, e^{-i\bar{r}(\bar{\boldsymbol{k}}^0;\bar{\boldsymbol{k}}')} + \\ &+\int |(\bar{\boldsymbol{k}}'' \mid \bar{R} \mid \bar{\boldsymbol{k}}')|\, d\bar{\boldsymbol{k}}''\, |(\bar{\boldsymbol{k}}'' \mid \bar{R} \mid \bar{\boldsymbol{k}}^0)|\, e^{i[\bar{r}(\bar{\boldsymbol{k}}'';\bar{\boldsymbol{k}}^0) - \bar{r}(\bar{\boldsymbol{k}}'';\bar{\boldsymbol{k}}')]} = 0, \end{aligned}\right\} \tag{107}$$

where $(\bar{\boldsymbol{k}}'', \bar{\boldsymbol{k}}', \bar{\boldsymbol{k}}^0)$ are connected with $(\boldsymbol{k}'', \boldsymbol{k}', \boldsymbol{k}^0)$ by equations of the form (98). On account of (99) and (102), (107) may be written

$$\begin{aligned} &|(\boldsymbol{k}' \mid R \mid \boldsymbol{k}^0)|\, e^{i\bar{r}(\bar{\boldsymbol{k}}';\bar{\boldsymbol{k}}^0)} + |(\boldsymbol{k}^0 \mid R \mid \boldsymbol{k}')|\, e^{-i\bar{r}(\bar{\boldsymbol{k}}^0;\bar{\boldsymbol{k}}')} + \\ &+\int |(\boldsymbol{k}'' \mid R \mid \boldsymbol{k}')|\, d\boldsymbol{k}''\, |(\boldsymbol{k}'' \mid R \mid \boldsymbol{k}^0)|\, e^{i[\bar{r}(\bar{\boldsymbol{k}}'';\bar{\boldsymbol{k}}^0) - \bar{r}(\bar{\boldsymbol{k}}'';\bar{\boldsymbol{k}}')]} = 0 \end{aligned}$$

or, by means of (103)

$$\left.\begin{aligned} &(\boldsymbol{k}' \mid R \mid \boldsymbol{k}^0)\, e^{i[\bar{r}(\bar{\boldsymbol{k}}';\bar{\boldsymbol{k}}^0) - r(\boldsymbol{k}';\boldsymbol{k}^0)]} + (\boldsymbol{k}' \mid R^{\dagger} \mid \boldsymbol{k}^0)\, e^{-i[\bar{r}(\bar{\boldsymbol{k}}^0;\bar{\boldsymbol{k}}') - r(\boldsymbol{k}^0;\boldsymbol{k}')]} + \\ &\int (\boldsymbol{k}' \mid R^{\dagger} \mid \boldsymbol{k}'')\, d\boldsymbol{k}''\, (\boldsymbol{k}'' \mid R \mid \boldsymbol{k}^0)\, e^{i[\bar{r}(\bar{\boldsymbol{k}}'';\bar{\boldsymbol{k}}^0) - \bar{r}(\bar{\boldsymbol{k}}'';\bar{\boldsymbol{k}}') - r(\boldsymbol{k}'';\boldsymbol{k}^0) + r(\boldsymbol{k}'';\boldsymbol{k}')]} = 0. \end{aligned}\right\} \tag{108}$$

The equation (108) must, for arbitrary $\mathcal{L}$ in (98), be identical with the equation (25), which, in terms of representatives, reads

$$(\boldsymbol{k}' \mid R \mid \boldsymbol{k}^0) + (\boldsymbol{k}' \mid R^{\dagger} \mid \boldsymbol{k}^0) + \int (\boldsymbol{k}' \mid R^{\dagger} \mid \boldsymbol{k}'')\, d\boldsymbol{k}''\, (\boldsymbol{k}'' \mid R \mid \boldsymbol{k}^0) = 0. \tag{109}$$

This is possible only if the three exponential functions in (108) are equal for all values of the momentum variables. Thus we get the following two equations:

$$\bar{r}(\bar{\boldsymbol{k}}';\bar{\boldsymbol{k}}^0) + \bar{r}(\bar{\boldsymbol{k}}^0;\bar{\boldsymbol{k}}') = r(\boldsymbol{k}';\boldsymbol{k}^0) + r(\boldsymbol{k}^0;\boldsymbol{k}') \tag{110}$$

$$\bar{r}(\bar{\boldsymbol{k}}'';\bar{\boldsymbol{k}}') - \bar{r}(\bar{\boldsymbol{k}}'';\bar{\boldsymbol{k}}^0) + \bar{r}(\bar{\boldsymbol{k}}';\bar{\boldsymbol{k}}^0) = r(\boldsymbol{k}'';\boldsymbol{k}') - r(\boldsymbol{k}'';\boldsymbol{k}^0) + r(\boldsymbol{k}';\boldsymbol{k}^0). \tag{111}$$

These equations are not independent, however, since (110) may

be derived from (111) by adding the equation obtained from (111) by interchanging $(\boldsymbol{k}')$ and $(\boldsymbol{k}^0)$.

We can now put

$$r(\boldsymbol{k}';\boldsymbol{k}^0) = \bar{r}(\bar{\boldsymbol{k}}';\bar{\boldsymbol{k}}^0) + \bar{f}(\bar{\boldsymbol{k}}';\bar{\boldsymbol{k}}^0), \tag{112}$$

where the function $\bar{f}$, by means of (98), may be regarded as a function of the transformed variables. If we introduce (112) into (110) we get

$$\bar{f}(\bar{\boldsymbol{k}}^0;\bar{\boldsymbol{k}}') = -\bar{f}(\bar{\boldsymbol{k}}';\bar{\boldsymbol{k}}^0). \tag{113}$$

Similarly we get from (111), (112), and (113)

$$\bar{f}(\bar{\boldsymbol{k}}';\bar{\boldsymbol{k}}'') + \bar{f}(\bar{\boldsymbol{k}}'';\bar{\boldsymbol{k}}^0) = \bar{f}(\bar{\boldsymbol{k}}';\bar{\boldsymbol{k}}^0). \tag{114}$$

This equation must hold for all values of the independent variables $(\bar{\boldsymbol{k}}', \bar{\boldsymbol{k}}'', \bar{\boldsymbol{k}}^0)$ and represents a functional equation for $\bar{f}$. The general solution of (114) is

$$\bar{f}(\bar{\boldsymbol{k}}';\bar{\boldsymbol{k}}^0) = \bar{\alpha}(\bar{\boldsymbol{k}}') - \bar{\alpha}(\boldsymbol{k}^0), \tag{115}$$

where $\bar{\alpha}(\bar{\boldsymbol{k}}')$ is an arbitrary function of the variables $(\bar{\boldsymbol{k}}')$ only.

Thus, (112) takes the form

$$r(\boldsymbol{k}';\boldsymbol{k}^0) = \bar{r}(\bar{\boldsymbol{k}}';\bar{\boldsymbol{k}}^0) + \bar{\alpha}(\bar{\boldsymbol{k}}') - \bar{\alpha}(\bar{\boldsymbol{k}}^0). \tag{116}$$

By a suitable change of the phases in the $\bar{\boldsymbol{k}}$-representation, in accordance with (106), the right hand side of (116) may be made equal to the argument function $\bar{r}(\bar{\boldsymbol{k}}';\bar{\boldsymbol{k}}^0)^\times$ in the new $\bar{\boldsymbol{k}}$-representation. If we afterwards omit the cross by which all functions in the new $\bar{\boldsymbol{k}}$-representation are distinguished, we thus have

$$r(\boldsymbol{k}';\boldsymbol{k}^0) = \bar{r}(\bar{\boldsymbol{k}}';\bar{\boldsymbol{k}}^0), \tag{117}$$

showing that the quantity $r(\boldsymbol{k}';\boldsymbol{k}^0)$ is invariant provided the phases of the $\bar{\boldsymbol{k}}$-representation are suitably chosen. With this choice (100) is seen to be a consequence of (99), (103), (104), and (117). The equation (100) will then hold also for the matrices S and η defined by (26) and (43).

Even on condition that (117) and (100) are to hold, the phases of the $\bar{\boldsymbol{k}}$-representation are not at all uniquely determined by the phases adopted in the $\boldsymbol{k}$-representation, since the representatives of R, on account of the δ-functions in (23) will be invariant under all such transformations of the type (2), where α is an arbitrary function of the total momentum and energy only. In particular we may choose the same phases in the $\bar{\boldsymbol{k}}$-representation as in the $\boldsymbol{k}$-representation, in which case the representatives of a matrix A in the two representations, according to (47) and (102), are connected by the equation

$$(\boldsymbol{k}' \mid A \mid \boldsymbol{k}^0) = \sqrt{\frac{[\overline{W}'_i]}{[W'_i]}}\,(\bar{\boldsymbol{k}}' \mid A \mid \bar{\boldsymbol{k}}^0)\sqrt{\frac{[\overline{W}^0_i]}{[W^0_i]}}. \tag{118}$$

Now the representative of $\bar{S}$ in the $\boldsymbol{k}$-representation is, by (118) and (100) applied to S instead of R, given by

$$(\boldsymbol{k}' \mid \bar{S} \mid \boldsymbol{k}^0) = \sqrt{\frac{[\overline{W}'_i]}{[W'_i]}}\,(\bar{\boldsymbol{k}}' \mid \bar{S} \mid \bar{\boldsymbol{k}}^0)\sqrt{\frac{[\overline{W}^0_i]}{[W^0_i]}} = (\boldsymbol{k}' \mid S \mid \boldsymbol{k}^0), \tag{119}$$

or

$$\bar{S} = S. \tag{120}$$

Thus Heisenberg's characteristic matrix is an invariant matrix, i. e. S and $\bar{S}$ have the same eigenvalues and the same eigenstates.

The matrix S, however, is not only invariant in the sense of equation (100). Since all frames of reference moving with constant velocity, are entirely equivalent as regards the development of the collision process, all functions like $(\boldsymbol{k}' \mid \Psi \mid \boldsymbol{k}^0)$, $(\boldsymbol{k}' \mid U \mid \boldsymbol{k}^0)$, and $(\boldsymbol{k}' \mid S \mid \boldsymbol{k}^0)$ must be what may be called invariant in form, i. e. $(\bar{\boldsymbol{k}}' \mid \bar{S} \mid \bar{\boldsymbol{k}}^0)$ is the same function of the transformed variables $(\bar{\boldsymbol{k}}')$ and $(\bar{\boldsymbol{k}}^0)$ as the function $(\boldsymbol{k}' \mid S \mid \boldsymbol{k}^0)$ of the variables $(\boldsymbol{k}')$ and $(\boldsymbol{k}^0)$. This means that the invariant quantities in (100) must be functions of the four-dimensional scalar products $\boldsymbol{k}'_i \boldsymbol{k}'_l - W'_i W'_l$, $\boldsymbol{k}'_i \boldsymbol{k}^0_l - W'_i W'_l$, or $\boldsymbol{k}^0_i \boldsymbol{k}^0_l - W^0_i W^0_l$, only.

In what follows we shall exclusively have to do with form-invariant matrices. Any such matrix A will obviously have the same eigenvalues as the corresponding transformed matrix $\bar{A}$, but A and $\bar{A}$ will not in general have the same eigenstates. As

an example we may take the magnitude M^2 of the total angular momentum, the total kinetic energy, or the matrix U in (11). Only if A is invariant in the sense of (100) or (120), the eigenvalues and eigenstates of A and $\bar{A}$ will be identical.

3. The eigenvalue problem in the new theory. Constants of collision. Consequences of the invariance of S.

The main problem in the usual quantum mechanics is that of finding the canonical transformation which brings the Hamiltonian on diagonal form, or in other words of determining the eigenvalues and eigenfunctions of the Hamiltonian. This problem is equivalent to the problem of finding a complete set of commuting constants of the motion, i. e. variables which commute with the Hamiltonian and with each other. In the representation where these constants of the motion are represented by diagonal matrices, the Hamiltonian will also be on diagonal form. In some cases it is possible at once to write down a number of constants of the motion. For instance, if the Hamiltonian is a form-invariant under all rotations in ordinary space, the components of the total angular momentum commute with the Hamiltonian, and the magnitude of the angular momentum together with the component in a fixed direction then will form an (incomplete) set of commuting constants of the motion.

In the new theory we are faced with the analogous problem of transforming the characteristic matrix on diagonal form. Since, however, the matrix S is invariant under a larger group of transformations than the Hamiltonian, we are able at once to write down a larger number of quantities, which commute with S. The most important among these quantities are those which also commute with the total kinetic energy W. Such quantities commuting with S and W we may call constants of collision or collision constants, since they have the same values (or mean values) in the initial and final states.[10]

On account of the factor $\delta(\boldsymbol{K}' - \boldsymbol{K}^0)\,\delta(W' - W^0)$ in (23), R and therefore also $S = 1 + R$ commute with the components of the total momentum $\boldsymbol{K}$ and with the total kinetic energy W. The four quantities

$$(K^\mu) = (K_x, K_y, K_z, W) \tag{121}$$

thus represent a set of commuting collision constants. This result is connected with the invariance of S under space-time translations. Similarly the invariance of S under all rotations in four-dimensional space gives us at once six other quantities commuting with S.

Let us for a moment consider a space of m dimensions with coordinates $(x^r) = (x^1, x^2, \cdots, x^m)$. A general infinitesimal transformation of coordinates in this space is then given by

$$\bar{x}^r = x^r + \varepsilon f^r(x^1, \cdots, x^m), \tag{122}$$

where ε is an infinitesimal parameter, while f^r is an arbitrary function of the coordinates. Now, consider a quantity $a = a(x^1, \cdots, x^m)$ depending on the coordinates (x^r). If $\bar{a}$ is the corresponding transformed quantity, the 'substantial' variation of a is defined by

$$\delta a = \bar{a}(\bar{x}) - a(x), \tag{123}$$

while the 'local' variation is given by

$$\delta^* a = \bar{a}(x) - a(x). \tag{124}$$

Neglecting terms of the second order in ε, we obviously have

$$\delta a = \delta^* a + \varepsilon \sum_r f^r \frac{\partial}{\partial x^r} a. \tag{125}$$

If a is a form-invariant quantity, i. e. if $\bar{a}(\bar{x})$ is the same function of the transformed variables $(\bar{x})$ as a of the variables (x), we have $\bar{a}(x) = a(x)$, or

$$\delta^* a = 0. \tag{126}$$

Hence

$$\delta a = \varepsilon \sum_r f^r \frac{\partial}{\partial x^r} a. \tag{127}$$

Now, let the variables (x^r) be identified with the components of the momentum vectors $\{(\boldsymbol{k}'), (\boldsymbol{k}^0)\} = \{\boldsymbol{k}'_1 \cdots \boldsymbol{k}'_{n'}, \boldsymbol{k}^0_1 \cdots \boldsymbol{k}^0_{n^0}\}$ and let a be the function $a(\boldsymbol{k}', \boldsymbol{k}^0) = \delta(\boldsymbol{K}' - \boldsymbol{K}^0)\,\delta(W' - W^0)$. For an infinitesimal Lorentz transformation in the direction of the x-axis we have for all particles, if ε is the infinitesimal relative velocity,

$$\bar{k}'_{ix} = k'_{ix} - \varepsilon W'_i, \quad \bar{k}'_{iy} = k'_{iy}, \quad \bar{k}'_{iz} = k'_{iz} \tag{128}$$

and similar transformation equations for the variables $\boldsymbol{k}_i^0$. By means of (127) we get in this case, since $x\,\delta(x) = 0$,

$$\begin{aligned}\delta a &= \delta(\overline{\boldsymbol{K}}' - \overline{\boldsymbol{K}}^0)\,\delta(\overline{W}' - \overline{W}^0) - \delta(\boldsymbol{K}' - \boldsymbol{K}^0)\,\delta(W' - W^0)\\ &= -\varepsilon \sum_i \left(W_i' \frac{\partial}{\partial k_{ix}'} + W_i^0 \frac{\partial}{\partial k_{ix}^0} \right) \delta(\boldsymbol{K}' - \boldsymbol{K}^0)\,\delta(W' - W^0)\\ &= -\varepsilon \left[\delta'(K_x' - K_x^0)(W' - W^0)\,\delta(W' - W^0) \right.\\ &\qquad \left. + (K_x' - K_x^0)\,\delta(K_x' - K_x^0)\,\delta'(W' - W^0) \right] \delta(K_y' - K_y^0)\,\delta(K_z' - K_z^0)\\ &= 0.\end{aligned}$$

In the same way it is shown that the function

$$\delta(\boldsymbol{K}' - \boldsymbol{K}^0)\,\delta(W' - W^0) = \delta(\overline{\boldsymbol{K}}' - \overline{\boldsymbol{K}}^0)\,\delta(\overline{W}' - \overline{W}^0) \quad (129)$$

is invariant for a general Lorentz transformation, in contrast to the function $\delta(\boldsymbol{K}' - \boldsymbol{K}^0)\,\delta_+(W' - W^0)$, which has more complicated transformation properties.

Now, let a be given by

$$a(\boldsymbol{k}', \boldsymbol{k}^0) = \sqrt{[W_i']}\,(\boldsymbol{k}' \mid A \mid \boldsymbol{k}^0)\,\sqrt{[W_i^0]},$$

where A is any form-invariant matrix. A need not, however, be really invariant in the sense of (100) and (120). For the Lorentz transformation (128) we then by means of (127) get

$$\left.\begin{aligned}\delta a &= \sqrt{[\overline{W}_i']}\,(\overline{\boldsymbol{k}}' \mid \bar{A} \mid \overline{\boldsymbol{k}}^0)\,\sqrt{[\overline{W}_i^0]} - \sqrt{[W_i']}\,(\boldsymbol{k}' \mid A \mid \boldsymbol{k}^0)\,\sqrt{[W_i^0]}\\ &= -\varepsilon \sum_i \left(W_i' \frac{\partial}{\partial k_{ix}'} + W_i^0 \frac{\partial}{\partial k_{ix}^0} \right) \sqrt{[W_i']}\,(\boldsymbol{k}' \mid A \mid \boldsymbol{k}^0)\,\sqrt{[W_i^0]}\\ &= -\varepsilon \sqrt{[W_i'][W_i^0]} \sum_i \left\{ \frac{1}{2} \left(W_i' \frac{\partial}{\partial k_{ix}'} + \frac{\partial}{\partial k_{ix}'} W_i' \right) \right.\\ &\qquad \left. + \frac{1}{2} \left(W_i^0 \frac{\partial}{\partial k_{ix}^0} + \frac{\partial}{\partial k_{ix}^0} W_i^0 \right) \right\} (\boldsymbol{k}' \mid A \mid \boldsymbol{k}^0).\end{aligned}\right\} \quad (130)$$

Here we have used equations of the type

$$W_i' \frac{\partial}{\partial k_{ix}'} \sqrt{[W_i']} = \sqrt{[W_i']}\,\frac{1}{2} \left(W_i' \frac{\partial}{\partial k_{ix}'} + \frac{\partial}{\partial k_{ix}'} W_i' \right), \quad (131)$$

which follow immediately from the definition of $[W_i']$ in (99).

Now, let $\boldsymbol{\xi}_i = (\xi_i, \eta_i, \zeta_i)$ be the vector operator, which, in the $\boldsymbol{k}$-representation, is identical with the operator of differentiation

$$i\frac{\partial}{\partial \boldsymbol{k}'_i} = i\left(\frac{\partial}{\partial k'_{ix}}, \frac{\partial}{\partial k'_{iy}}, \frac{\partial}{\partial k'_{iz}}\right)$$

when operating to the right, and with

$$-i\frac{\partial}{\partial \boldsymbol{k}^0_i} = -i\left(\frac{\partial}{\partial k^0_{ix}}, \frac{\partial}{\partial k^0_{iy}}, \frac{\partial}{\partial k^0_{iz}}\right).$$

when operating to the left. When we define a new vector operator $\boldsymbol{N} = (N_x, N_y, N_z)$ by

$$\boldsymbol{N} = \sum_i \overline{W_i \boldsymbol{\xi}_i} = \frac{1}{2}\sum_i (W_i \boldsymbol{\xi}_i + \boldsymbol{\xi}_i W_i), \tag{132}$$

the equation (130) may, after division with $\sqrt{[W'_i]}\sqrt{[W^0_i]}$, be written

$$(\boldsymbol{k}' \mid \bar{A} \mid \boldsymbol{k}^0) - (\boldsymbol{k}' \mid A \mid \boldsymbol{k}^0) = -\frac{\varepsilon}{i}(\boldsymbol{k}' \mid N_x A - A N_x \mid \boldsymbol{k}^0), \tag{133}$$

where we have made use of (118).

Introducing the quantum Poisson Bracket (P.B.) of two variables A and B by

$$[A, B] = \frac{1}{i}(AB - BA), \tag{134}$$

we may write (133) as

$$\delta A = \bar{A} - A = \varepsilon [A, N_x]. \tag{135}$$

For a finite Lorentz transformation with the relative velocity v we then have

$$\bar{A} = e^{ixN_x} A e^{-ixN_x} \tag{136}$$

with $x = \mathrm{tgh}^{-1} v$. If instead we had considered Lorentz transformations in the directions of the other coordinate axes, we had got similar formulae with N_x replaced by N_y or by N_z.

We shall now consider a rotation through an infinitesimal angle ε in ordinary space around the z-axis. The transformation equations are for each particle

$$\left.\begin{aligned} \bar{k}'_{ix} &= k'_{ix} + \varepsilon k'_{iy} \\ \bar{k}'_{iy} &= k'_{iy} - \varepsilon k'_{ix} \\ \bar{k}'_{iz} &= k'_{iz} \end{aligned}\right\} \quad (137)$$

and similar equations for $\boldsymbol{k}_i^0$.

By means of (127) we get in this case in the same way as before

$$\delta A = \bar{A} - A = \varepsilon [A, M_z]; \quad (138)$$

where M_z is the z-component of the vector operator $\boldsymbol{M}$ defined by

$$\boldsymbol{M} = \sum_i (\boldsymbol{\xi}_i \times \boldsymbol{k}_i). \quad (139)$$

Hence for a finite rotation through an angle θ

$$\bar{A} = e^{i\theta M_z} A e^{-i\theta M_z}. \quad (140)$$

For rotations around the x- and y-axes we have simply to replace M_z in these formulae by M_x and M_y, respectively. The transformations (136) and (140) are contact transformations. Thus any functional relation between (form-invariant) matrices, as for instance commutation relations, will be covariant under Lorentz transformations.

According to its definition the operator $\boldsymbol{\xi}_i$ depends on the phases in the $\boldsymbol{k}$-representation and, by a suitable choice of the phases, $\boldsymbol{\xi}_i$ may be made equal to the coordinate vector $\boldsymbol{x}_i$ of the i'th particle. In this latter case the phase constant γ' in (80) is zero and the vector $\boldsymbol{M}$ is identical with the total angular momentum. In another Lorentz frame of reference we have a similar operator $\bar{\boldsymbol{\xi}}_i$ which in the $\bar{\boldsymbol{k}}$-representation is represented by differentiation operators. Provided the phases in the $\bar{\boldsymbol{k}}$-representation are chosen in accordance with the transformation formula (118), the connection between $\bar{\boldsymbol{\xi}}_i$ and $\boldsymbol{\xi}_i$ is given by (136) and (140).

The variables $\bar{\boldsymbol{\xi}}_i$ defined in this way, however, in general will not be equal to the coordinate vectors $\bar{\boldsymbol{x}}_i$ of the i'th particle in the new Lorentz frame, even if the phases in the $\boldsymbol{k}$-representation are chosen in such a way that $\boldsymbol{\xi}_i$ is equal to $\boldsymbol{x}_i$. This may be simply illustrated by considering the non-relativistic approximation, where the Lorentz transformation takes the simple form of a Galilei transformation

$$\left.\begin{aligned} &\bar{x}_i = x_i - vt, \quad \bar{y}_i = y_i, \quad \bar{z}_i = z_i \\ &\bar{k}_{ix} = k_{ix} - v\kappa, \quad \bar{k}_{iy} = k_{iy}, \quad \bar{k}_{iz} = k_{iz}. \end{aligned}\right\} \quad (141)$$

In this approximation we have

$$\boldsymbol{N} = \sum_i \kappa \boldsymbol{\xi}_i. \tag{142}$$

Thus $\boldsymbol{N}$ commutes with ξ_i, η_i, and ζ_i, and we get from (136)

$$\bar{\xi}_i = \xi_i, \tag{143}$$

so that $\bar{\xi}_i$ will be different from $\bar{x}_i$ defined by (141), even if $\boldsymbol{\xi}_i$ is equal to $\boldsymbol{x}_i$. In this latter case we have $\gamma' = 0$ in (80), but the corresponding phase constant $\bar{\gamma}'$ in the new Lorentz frame will be given by

$$\bar{\gamma}' = vt\bar{K}'_x. \tag{144}$$

When A in (135) and (138) is the matrix S, we have $\delta S = \bar{S} - S = 0$ on account of the invariance of S under all rotations in space-time. Thus S must commute with the components

$$M_x,\ M_y,\ M_z,\ N_x,\ N_y,\ N_z \tag{145}$$

of the vectors $\boldsymbol{M}$ and $\boldsymbol{N}$. The components of the former vector are even constants of collision, since $\boldsymbol{M}$ commutes with W. This follows from (138), remembering that W is invariant under all rotations in ordinary space.

The concept of a constant of collision is obviously more comprehensive than the concept of a constant of motion. The latter quantity can only be defined in cases where a Hamiltonian exists, while a constant of collision for its definition only requires the existence of the characteristic matrix. If a Hamiltonian of the system exists, six of the seven collision constants in (121) and (145), viz. the components of $\boldsymbol{K}$ and $\boldsymbol{M}$, are constants of the motion, while W is a collision constant only. The total kinetic energy of the particles has the same value in the initial and final states and is thus a constant of collision, but it is not, of course, a constant of the motion, since the kinetic energy is partly transformed into potential energy during the collision. In the new theory, which renounces a detailed description of the collision process and considers the results of the collision as observable only, the constants of collision will probably take over the role played by the constants of motion in quantum mechanics.

The quantities (145) are not commuting. Our next problem will be to construct a maximal number of functions of

the variables (121) and (145), which commute with each other and with the variables (121). These functions will then also commute with S and they will together with the variables (121) form a set of commuting constants of collision. Now let (α) denote a complete set of commuting collision constants. In the α-representation the matrix S (or η) will then be diagonal and the eigenvalues of S will be functions of the eigenvalues of (α). Thus S may in any representation be regarded as a function of the α's. Since S is an invariant matrix, it will, however, be a function of invariant combinations of the α's only. Such invariant combinations are also constants of collision and it is convenient from the beginning to choose these invariant collision constants as members of the complete set. We shall therefore begin with an investigation of the transformation properties of the variables (121) and (145). For this purpose we must establish the commutability relations for these variables.

For the variables $\boldsymbol{\xi}_i$ and $\boldsymbol{k}_i$ we have the canonical relations

$$[k_{ix}, k_{jy}] = 0, [\xi_i, \eta_j] = 0, [\xi_i, k_{jx}] = \delta_{ij}, [\xi_i, k_{jy}] = 0, \quad (146)$$

etc. Hence for the components of the vector $\boldsymbol{M}$ in (139) we get the well-known commutation relations for the components of the angular momentum in quantum mechanics

$$[M_x, M_y] = M_z, \cdots \quad (147)$$

Here we have explicitly written down one only of the three equations, following from each other by cyclic permutation of the letters x, y, z. In the same way we get, by (132), (139), and (146),

$$\left.\begin{aligned} &[N_x, M_x] = 0, [N_x, M_y] = N_z, [N_x M_z] = -N_y, \cdots \\ &[N_x, N_y] = -M_z, \cdots\cdots\cdots\cdots\cdots\cdots\cdots\cdots \end{aligned}\right\} (148)$$

where again, as everywhere in what follows, the dots indicate equations, which may be obtained from those explicitly written down by cyclic permutation of the letters x, y, z.

Finally for the P.B.'s of a variable (121) with a variable (145) we get

$$\left.\begin{aligned} &[M_x, K_x] = 0, [M_x, K_y] = K_z, [M_x, K_z] = -K_y, [M_x, W] = 0 \cdots \\ &[\boldsymbol{N}, W] = \boldsymbol{K}, [N_x, K_x] = W, [N_x, K_y] = 0 \cdots\cdots\cdots\cdots \end{aligned}\right\} (149)$$

The commutation relations (149) simply express the four-vector character of $(\boldsymbol{K}^\mu) = (\boldsymbol{K}, W)$. For an infinitesimal Lorentz transformation in the direction of the x-axis, we have, for instance, by (135) and (149)

$$\left.\begin{aligned} &\delta K_x = -\varepsilon W,\ \delta K_y = \delta K_z = 0 \\ &\delta W = -\varepsilon K_x, \end{aligned}\right\} \quad (150)$$

which are the transformation equations of a four-vector.

Thus the P.B.-relations (149) must remain true, if $(\boldsymbol{K}, W)$ is replaced by any other matrix four-vector.

Similarly it follows from (147) and (148) that the quantities

$$(M^{\mu\nu}) = \begin{pmatrix} 0 & M_z & -M_y & N_x \\ -M_z & 0 & M_x & N_y \\ M_y & -M_x & 0 & N_z \\ -N_x & -N_y & -N_z & 0 \end{pmatrix} \quad (151)$$

are the components of an antisymmetrical tensor; in fact we get as before, by (135) and (148), the equations

$$\left.\begin{aligned} &\delta M_x = 0,\ \delta M_y = -\varepsilon N_z,\ \delta M_z = \varepsilon N_y, \\ &\delta N_x = 0,\ \delta N_y = \varepsilon M_z,\ \delta N_z = -\varepsilon M_y, \end{aligned}\right\} \quad (152)$$

which are just the transformation equations for the components of an antisymmetrical tensor. The square of this tensor

$$\frac{1}{4} M^{\mu\nu} M_{\mu\nu} = \frac{1}{2}(|\boldsymbol{M}|^2 - |\boldsymbol{N}|^2)$$

is an invariant scalar, it thus commutes with the components of $\boldsymbol{M}$ and $\boldsymbol{N}$. Further, as a function of the variables (145) it also commutes with S.

The antisymmetrical tensor $M^{\mu\nu}$ has a 'dual' tensor $\check{M}^{\mu\nu}$, which is obtained from (151) by replacing $\boldsymbol{M}$ by $\boldsymbol{N}$ and $\boldsymbol{N}$ by $-\boldsymbol{M}$. The product of the two tensors

$$\frac{1}{4} M^{\mu\nu} \check{M}_{\mu\nu} = \boldsymbol{M}\boldsymbol{N}$$

is a pseudoscalar, i. e. it behaves like a scalar under all rota-

tions in space-time, but changes its sign by spatial reflections at the origin. The quantities

$$\frac{1}{2}\left[|\boldsymbol{M}|^2-|\boldsymbol{N}|^2\right],\ \boldsymbol{M}\boldsymbol{N} \tag{153}$$

thus commute with S and with all the variables (145). Moreover they are the only independent functions of the variables (145) of that kind.

The quantities (153) do not, however, commute with the variables (121). If we construct the P.B.'s of these quantities with the components of the four-vector $K^\mu = (\boldsymbol{K}, W)$, we get a new four-vector

$$G^\mu = (\boldsymbol{G}, G^4) = \frac{1}{2}\left[|\boldsymbol{M}|^2-|\boldsymbol{N}|^2, K^\mu\right] \tag{154}$$

and a pseudo-four-vector

$$\Gamma^\mu = (\boldsymbol{\Gamma}, \Gamma^4) = \left[\boldsymbol{M}\boldsymbol{N}, K^\mu\right]. \tag{155}$$

By means of (149) we get at once the following expressions for G^μ and Γ^μ:

$$G^\mu = \left\{\begin{array}{l} \boldsymbol{G} = -(\overline{\boldsymbol{M}\times\boldsymbol{K}})-\overline{\boldsymbol{N}W} \\ G^4 = -\boldsymbol{N}\boldsymbol{K} \end{array}\right\} \tag{156}$$

and

$$\Gamma^\mu = \left\{\begin{array}{l} \boldsymbol{\Gamma} = -(\boldsymbol{N}\times\boldsymbol{K})+\boldsymbol{M}W \\ \Gamma^4 = \boldsymbol{M}\boldsymbol{K}. \end{array}\right\} \tag{157}$$

On account of the symmetrization bars in (156), which have the same meaning as in (132), all the variables G^μ and Γ^μ are Hermitian. A comparison of (156) and (157) with (151) and with the corresponding expression for $\breve{M}^{\mu\nu}$ shows that

$$\left.\begin{array}{l} G^\mu = \overline{M^{\mu\nu}K_\nu} \\ \Gamma^\mu = \breve{M}^{\mu\nu}K_\nu. \end{array}\right\} \tag{158}$$

From G^μ and Γ^μ we can construct two scalars and one pseudo-scalar:

$$G^\mu G_\mu,\ \Gamma^\mu\Gamma_\mu,\ \overline{G^\mu\Gamma_\mu}. \tag{159}$$

Since the quantities $G^\mu K_\mu$ and $\Gamma^\mu K_\mu$ are identically zero, on account of the antisymmetry of $M^{\mu\nu}$ and $\breve{M}^{\mu\nu}$, the variables (153) and (159) together with

$$K = \sqrt{-K^\mu K_\mu} = \sqrt{W^2 - K^2} \tag{160}$$

are the only independent invariant functions which can be constructed from the quantities (121) and (145). K is the rest mass of the system as a whole.

We are now particularly interested in those of the variables (153)—(160) which commute with the four-vector (K^μ). By means of (149) it is easily seen that only the variables

$$\Gamma^\mu = (\boldsymbol{\Gamma}, \Gamma^4), \quad \Gamma^\mu \Gamma_\mu = |\boldsymbol{\Gamma}|^2 - (\Gamma^4)^2 \tag{161}$$

given by (157), have this property, i. e.

$$\left[\Gamma^\mu, K^\nu\right] = 0, \quad \left[\Gamma^\mu \Gamma_\mu, K^\nu\right] = 0. \tag{162}$$

To prove these equations it is not, however, necessary explicitly to use the relations (149). On account of the covariance of all commutation relations under Lorentz transformations we need only prove (162) for a single component of Γ^μ, say for Γ^4. Now, $\Gamma^4 = \boldsymbol{M}\boldsymbol{K}$ is the component of $\boldsymbol{M}$ in the direction of $\boldsymbol{K}$. Thus, by (138), $[K^\nu, \boldsymbol{M}\boldsymbol{K}]$ determines the variation of the variables $K^\nu = (\boldsymbol{K}, W)$ by a rotation about the direction of $\boldsymbol{K}$, and since both the vector $\boldsymbol{K}$ and W are unchanged by such a rotation, we must have

$$\left[K^\nu, \boldsymbol{M}\boldsymbol{K}\right] = \left[K^\nu, \Gamma^4\right] = 0.$$

The variables Γ^μ do not commute with each other, but they commute with the quantity $\Gamma^\nu \Gamma_\nu$. This statement may be verified by direct calculation, but it also follows from the fact that $\Gamma^\nu \Gamma_\nu$ is invariant, for this means that $\Gamma^\nu \Gamma_\nu$ commutes with $\boldsymbol{M}$ and $\boldsymbol{N}$ besides with K^ν and therefore it also commutes with the Γ^μ, which are functions of $\boldsymbol{M}$, $\boldsymbol{N}$, and K^ν. As a set of commuting constants of collision we may then for instance take the variables (121) together with the two variables

$$\left.\begin{aligned} \Gamma^\mu \Gamma_\mu &= (-\boldsymbol{N}\times\boldsymbol{K} + \boldsymbol{M}W)\,(-\boldsymbol{N}\times\boldsymbol{K} + \boldsymbol{M}W) - (\boldsymbol{M}\boldsymbol{K})\,(\boldsymbol{M}\boldsymbol{K}) \\ \Gamma^3 &= \Gamma_z = -N_x K_y + N_y K_x + M_z W. \end{aligned}\right\} \tag{163}$$

We shall now determine the eigenvalues and eigenfunctions of $\Gamma^\mu \Gamma_\mu$ and Γ_z. These variables both commute with the K^μ and

they must therefore in the $(\boldsymbol{K}, W, x)$-representation, defined by (47), have the form

$$\left.\begin{aligned}(\boldsymbol{K}'W'x' \,|\, \Gamma^\mu \Gamma_\mu \,|\, \boldsymbol{K}^0 W^0 x^0) = \\ = \delta(\boldsymbol{K}' - \boldsymbol{K}^0)\, \delta(W' - W^0)\, (x' \,|\, (\Gamma^\mu \Gamma_\mu)_{\boldsymbol{K}^0 W^0} \,|\, x^0),\end{aligned}\right\} \quad (164)$$

where $(\Gamma^\mu \Gamma_\mu)_{\boldsymbol{K}^0 W^0}$ is a submatrix corresponding to fixed values $\boldsymbol{K}^0$, W^0 of the total momentum and energy. Since $\Gamma^\mu \Gamma_\mu$ is invariant, we have for any Lorentz transformation

$$\Gamma^\mu \Gamma_\mu = \overline{\Gamma}^\mu \overline{\Gamma}_\mu, \quad (165)$$

where all the variables in the new frame of reference are distinguished by a bar. For the functional determinant corresponding to the transformation $(\boldsymbol{K}', W', x') \to (\overline{\boldsymbol{K}}', \overline{W}', \overline{x}')$, we get

$$\left.\begin{aligned}\frac{\partial(\overline{\boldsymbol{K}}', \overline{W}', \overline{x}')}{\partial(\boldsymbol{K}', W', x')} = \frac{\partial(\overline{\boldsymbol{K}}', \overline{W}', \overline{x}')}{\partial(\overline{\boldsymbol{k}}_1 \cdots \overline{\boldsymbol{k}}'_{n'})} \cdot \frac{\partial(\overline{\boldsymbol{k}}'_1 \cdots \overline{\boldsymbol{k}}'_{n'})}{\partial(\boldsymbol{k}'_1 \cdots \boldsymbol{k}'_{n'})} \cdot \frac{\partial(\boldsymbol{k}'_1 \cdots \boldsymbol{k}'_{n'})}{\partial(\boldsymbol{K}', W', x')} = \\ = \overline{\Delta}' \frac{[\overline{W}'_i]}{[W'_i]} \cdot \frac{1}{\Delta'},\end{aligned}\right\} \quad (166)$$

by means of (47) and (102). Here $\overline{\Delta}'$ is the same function of the new variables as the function Δ' of the variables of the original frame of reference. Thus (165) may be written

$$\left.\begin{aligned}(\boldsymbol{K}'W'x' \,|\, \Gamma^\mu \Gamma_\mu \,|\, \boldsymbol{K}^0 W^0 x^0) = \sqrt{\frac{|\overline{\Delta}'|[\overline{W}'_i]}{|\Delta'|[W'_i]}} \\ (\overline{\boldsymbol{K}}' \overline{W}' \overline{x}' \,|\, \overline{\Gamma}^\mu \overline{\Gamma}_\mu \,|\, \overline{\boldsymbol{K}}^0 \overline{W}^0 \overline{x}^0) \sqrt{\frac{|\overline{\Delta}^0|[\overline{W}^0_i]}{|\Delta^0|[W^0_i]}}.\end{aligned}\right\} \quad (167)$$

Now let the new system of reference be chosen in such a way that $\overline{\boldsymbol{K}}^0 = 0$. In this 'center of gravity' system, which of course depends on the value of the vector $\boldsymbol{K}^0$, the matrix elements of $\overline{\Gamma}^\mu \overline{\Gamma}_\mu$ have a particularly simple form. From the definition of $\overline{\Gamma}^\mu \overline{\Gamma}_\mu$ in (163) we simply get

$$(\overline{\boldsymbol{K}}' \overline{W}' \overline{x}' \,|\, \overline{\Gamma}^\mu \overline{\Gamma}_\mu \,|\, \overline{\boldsymbol{K}}^0 \overline{W}^0 \overline{x}^0) = (\overline{\boldsymbol{K}}' \overline{W}' \overline{x}' \,|\, |\overline{M}|^2 \,|\, \overline{\boldsymbol{K}}^0 \overline{W}^0 \overline{x}^0) \cdot \overline{W}^{0^2}. \quad (168)$$

Since the square of the total angular momentum does not commute with the components of $\boldsymbol{K}$, we cannot in general assign

numerical values to $\boldsymbol{M}^2$ and $\boldsymbol{K}$ simultaneously. In the special case, however, where the components of $\boldsymbol{K}$ are all given the value zero, we may also assign a definite numerical value to one of the components of $\boldsymbol{M}$ and to $\boldsymbol{M}^2$, since this will not contradict the commutability relations (149). Thus, in the center of gravity system the matrix elements of $\overline{\boldsymbol{M}}^2$ have the form

$$(\overline{\boldsymbol{K}}'\overline{W}'\overline{x}'\,||\,\overline{M}\,|^2|\,\overline{\boldsymbol{K}}^0\overline{W}^0\overline{x}^0) = \delta(\overline{\boldsymbol{K}}')\,\delta(\overline{W}'-\overline{W}^0)\,(\overline{x}'\,||\,\overline{M}\,|^2_{\overline{\boldsymbol{K}}^0=0,\,\overline{W}^0}|\,\overline{x}^0). \quad (16$$

From (164), (167), 168) and (169) we now get a simple relation between the submatrices $(\Gamma^\mu\Gamma_\mu)_{\boldsymbol{K}^0W}$ and $|\,\overline{\boldsymbol{M}}\,|^2_{\overline{\boldsymbol{K}}^0=0,\,\overline{W}^0}$. Since the factor $\delta(\boldsymbol{K}'-\boldsymbol{K}^0)\,\delta(W'-W^0)$ is invariant (see (129)), and since further $\overline{W}^{0^2} = \overline{W}^{0^2} - |\,\overline{K}^0\,|^2 = \overline{K}^{0^2} = K^{0^2}$ by (160), we get, omitting the indices $(\boldsymbol{K}^0\ W^0)$ and $(\overline{\boldsymbol{K}}^0 = 0,\ \overline{W}^0)$ in the notation of the submatrices,

$$(x'\,|\,\Gamma^\mu\Gamma_\mu\,|\,x^0) = K^{0^2}\sqrt{|D'|}\,(\overline{x}'\,||\,\overline{M}\,|^2\,|\,\overline{x}^0)\sqrt{|D^0|}, \qquad (170)$$

where $D' = D(\boldsymbol{K}^0,\ W^0,\ x')$ is the value of $\sqrt{\dfrac{\overline{\Delta}'\,[\overline{W}'_i]}{\Delta'\,[W'_i]}}$ for $\boldsymbol{K}' = \boldsymbol{K}^0$ and $W' = W^0$. D' is simply the functional determinant corresponding to a Lorentz transformation in the subspace defined by the variables (x) for a fixed energy-momentum four-vector $K^{0\mu}$, i. e.

$$D' = \frac{\partial(\overline{x}')}{\partial(x')}, \qquad (171)$$

and (170) may thus be written

$$\frac{1}{K^{0^2}}\,(\Gamma^\mu\Gamma_\mu)_{\boldsymbol{K}^0W^0} = |\,\overline{\boldsymbol{M}}\,|^2_{\overline{\boldsymbol{K}}^0=0,\,\overline{W}^0}. \qquad (172)$$

From the commutation rules (147) it now follows in the usual way that the eigenvalues of the square of the angular momentum are given by $l^0(l^0+1)$, where l^0 may be any integral positive number or zero. The quantity L defined by

$$L = \frac{\Gamma^\mu\Gamma_\mu}{K^2} \qquad (173)$$

thus has the eigenvalues

$$L^0 = l^0(l^0+1), \quad l^0 = 0, 1, 2 \cdots. \tag{174}$$

Further if

$$(\overline{\boldsymbol{K}}'\ \overline{W}'\ \overline{x}' \mid \overline{\boldsymbol{K}}^0 = 0,\ \overline{W}^0,\ l^0)$$

is the representative of any eigenfunction of $|\overline{M}|^2$, the function

$$(\boldsymbol{K}'W'x' \mid \boldsymbol{K}^0,\ W^0,\ l^0) = \sqrt{|D'|}\,(\overline{\boldsymbol{K}}'\,\overline{W}'\,\overline{x}' \mid \overline{\boldsymbol{K}}^0 = 0, W^0, l^0) \tag{175}$$

will represent an eigenfunction of L with the eigenvalue $L^0 = l^0(l^0+1)$.

The eigenvalues of Γ_z may be obtained in a similar way. Since the Γ^μ transform like a four-vector by Lorentz transformations we have, instead of (165), for the vector $\boldsymbol{\Gamma}$

$$\boldsymbol{\Gamma} = \overline{\boldsymbol{\Gamma}} + \boldsymbol{v}\left\{\frac{\overline{\boldsymbol{\Gamma}}\,\boldsymbol{v}}{v^2}\left(\frac{1}{\sqrt{1-v^2}}-1\right)+\frac{\overline{\Gamma}^4}{\sqrt{1-v^2}}\right\}, \tag{176}$$

where the vector $\boldsymbol{v}$ denotes the velocity of the new system of reference relative to the old system. It is assumed that corresponding coordinate axes in the two systems are parallel. If the new system is the center of gravity system, $\boldsymbol{v}$ is the velocity of the center of gravity, i. e.

$$\boldsymbol{v} = \frac{\boldsymbol{K}^0}{W^0}. \tag{177}$$

In this system we may, according to the definitions (157), simply write

$$\overline{\boldsymbol{\Gamma}} = \overline{\boldsymbol{M}}\,\overline{W}^0, \quad \overline{\Gamma}^4 = 0,$$

and by a simple calculation we get instead of (172)

$$\frac{1}{K^0}(\Gamma_z)_{\boldsymbol{K}^0,\,W^0} = (\overline{a}_x\overline{M}_x + \overline{a}_y\overline{M}_y + \overline{a}_z\overline{M}_z)_{\overline{\boldsymbol{K}}^0=0,\,\overline{W}^0} \tag{178}$$

with

$$\left.\begin{aligned}\overline{\boldsymbol{a}} &= (\overline{a}_x, \overline{a}_y, \overline{a}_z) = \\ &\frac{v_z v_x}{v^2}\left(\frac{1}{\sqrt{1-v^2}}-1\right),\ \frac{v_z v_y}{v^2}\left(\frac{1}{\sqrt{1-v^2}}-1\right),\ 1+\frac{v_z v_z}{v^2}\left(\frac{1}{\sqrt{1-v^2}}-1\right)\Big).\end{aligned}\right\} \tag{179}$$

For the scalar product $\bar{\boldsymbol{a}}\bar{\boldsymbol{M}}$ on the right hand side of (178) we have

$$\bar{\boldsymbol{a}}\bar{\boldsymbol{M}} = |\bar{\boldsymbol{a}}|\,\bar{M}_{\bar{a}}, \tag{180}$$

where $\bar{M}_{\bar{a}}$ is the component of $\bar{\boldsymbol{M}}$ in the direction of the vector $\bar{a}$, while $|\bar{\boldsymbol{a}}|$ is the magnitude of $\bar{\boldsymbol{a}}$. By means of (179), (177), and (160) we get

$$|\bar{\boldsymbol{a}}| = \sqrt{\bar{a}_x^2+\bar{a}_y^2+\bar{a}_z^2} = \sqrt{1+\frac{v_z^2}{1-v^2}} = \sqrt{1+\frac{K_z^{0\,2}}{K^{0\,2}}}. \tag{181}$$

Now, the component of $\bar{\boldsymbol{M}}$ in a given direction has the eigenvalues m^0, where m^0 is an integer ranging from $-l^0$ to $+l^0$. From (178), (180), and (181) it then follows that the submatrix

$$m_{\boldsymbol{K}^0 W^0} = \frac{(\Gamma_z)_{\boldsymbol{K}^0 W^0}}{\sqrt{K^{0\,2}+K_z^{0\,2}}} \tag{182}$$

has the eigenvalues m^0 with $-l^0 \leq m^0 \leq l^0$, and the full matrix

$$m = \frac{\Gamma_z}{\sqrt{K^2+K_z^2}} \tag{183}$$

therefore will also have the eigenvalues m^0 with $-l^0 \leq m^0 \leq l^0$.

Instead of the quantities (163) it will now be convenient to take the six variables

$$K^\mu = K_x, K_y, K_z, W, L, m, \tag{184}$$

defined by (121), (173), (183), and (163), as a set of commuting constants of collision. The total number of particles n commutes with the variables (184), but n does not in general commute with S. n will be a constant of collision in the special case, only, where annihilation and creation processes are excluded. In this case n will have a definite numerical value. For $n = 2$ the variables (184) will form a complete set of collision constants. The matrices S and η then will be functions of K and L, only since these last variables are the only invariant combinations of the variables (184). Thus, the eigenvalues η^0 of η will only depend on the eigenvalues K^0 and L^0 of K and L, i. e.

$$\eta^0 = \eta\,(K^0, l^0). \tag{185}$$

These eigenvalues of η are obtained automatically if we introduce that representation in which the quantities (184) are diagonal, thus the complete solution of the eigenvalue problem in this case follows from the invariance of S and η under Lorentz transformations.

For $n > 2$ or in the more general case where n is not a constant of collision, a complete set of collision constants (α) will of course contain other variables besides the variables (184), and η will be a function of other invariant collision constants besides K and L. If S and η are invariant under other groups of transformations besides the Lorentz transformations, for instance the group of permutation of variables, this property may in a similar way be utilized in the derivation of new constants of collision.

As an application of the general theory developed in this section we shall now express the total cross section for the collision between two particles 1 and 2 as a function of invariant quantities. By means of (47), (49) and the generalized equation (96) we have for the differential cross section in which new particles with the momenta $\boldsymbol{k}'_3, \boldsymbol{k}'_4 \cdots \boldsymbol{k}'_{n'}$ are created

$$dQ_{\text{scat. emis.}} = 4\pi^2 \frac{|\mathcal{A}^0| \cdot |\mathcal{A}'| \cdot |(x'|R|x^0)|^2 k'^2_2}{\sqrt{|\boldsymbol{u}^0_1 - \boldsymbol{u}^0_2|^2 - |\boldsymbol{u}^0_1 \times \boldsymbol{u}^0_2|^2} \cdot |(\boldsymbol{u}'_1 - \boldsymbol{u}'_2)\,\boldsymbol{e}'_2|}\, d\Omega\, d\boldsymbol{k}'_3 \cdots d\boldsymbol{k}'_{n'} \tag{186}$$

with

$$(x'|R|x^0) = (x'|U_{\boldsymbol{K}^0 W^0}|x^0) = (x'|e^{i\eta} - 1|x^0)$$

on account of (26) and (43). Since we are now constantly working in the subspace corresponding to fixed values $\boldsymbol{K}^0, W^0$ of the total momentum and energy, we may from now on omit the indices $\boldsymbol{K}^0, W^0$ in submatrices like $(x'|R|x^0)$.

It is now convenient to choose the variables (x) in the following way:

$$\left.\begin{aligned} (x') &= (\zeta', \varphi', \boldsymbol{k}'_3, \cdots \boldsymbol{k}'_{n'}) \\ \zeta' &= \cos\theta' = \frac{k'_{2z}}{k'_2}, \quad \varphi' = \operatorname{arctg} \frac{k'_{2y}}{k'_{2x}}, \end{aligned}\right\} \tag{187}$$

i. e. θ', φ' are the polar angles of the direction $\boldsymbol{e}'_2 = \frac{\boldsymbol{k}'_2}{k'_2}$. For the functional determinant a simple calculation gives

$$\Delta' = \frac{(\boldsymbol{u}'_1 - \boldsymbol{u}'_2)\,\boldsymbol{e}'_2}{k'^2_2}. \tag{188}$$

Further we have

$$d\Omega\, d\boldsymbol{k}'_3 \cdots d\boldsymbol{k}'_{n'} = d\zeta'\, d\varphi'\, d\boldsymbol{k}'_3 \cdots d\boldsymbol{k}'_{n'} = dx',$$

so the total cross section is given by

$$Q = C^0 \int |(x'|R|x^0)|^2\, dx' \tag{189}$$

with

$$C^0 = \frac{4\pi^2 |\Delta^0|}{\sqrt{|\boldsymbol{u}^0_1 - \boldsymbol{u}^0_2|^2 - |\boldsymbol{u}^0_1 \times \boldsymbol{u}^0_2|^2}} \tag{190}$$

and

$$\int dx' = \sum_{n'=2}^{\infty} \int d\zeta'\, d\varphi'\, d\boldsymbol{k}'_3 \cdots d\boldsymbol{k}'_{n'}.$$

Now, let $(\alpha) = (\boldsymbol{K}, W, \beta)$ be a complete set of collision constants and let $(x'|\beta^0)_{\boldsymbol{K}^0, W^0} = (x'|\beta^0)$ be the transformation functions connecting the (x)-representation with the (β)-representation. Since

$$\int |(x'|R|x^0)|^2\, dx' = (x^0|R^\dagger R|x^0)$$

and by (25) and (26) and (43)

$$R^\dagger R = -R - R^\dagger = 1 - e^{i\eta} + 1 - e^{-i\eta}$$

$$= 2(1 - \cos\eta) = 4\sin^2\frac{\eta}{2},$$

we get

$$\int |(x'|R|x^0)|^2\, dx' = 4\left(x^0\left|\sin^2\frac{\eta}{2}\right|x^0\right) = 4\int \sin^2\frac{\eta(\beta')}{2}\, d\beta'\, |(x^0|\beta')|^2. \tag{191}$$

Thus,

$$Q = 4C^0\left(x^0\left|\sin^2\frac{\eta}{2}\right|x^0\right) = 4C^0 \int \sin^2\frac{\eta(\beta')}{2}\, d\beta'\, |(x^0|\beta')|^2, \tag{192}$$

where of course $\int d\beta'$ is to be replaced by a sum in the case of discrete eigenvalues of β.

The variables (β) may be divided into two groups $(\beta) = (\iota, \gamma)$, where (ι) contains all the invariant collision constants, while (γ) contains only non-invariant quantities. Thus L, defined by (173), will be a member of (ι), while the quantity m, defined by (183), is contained in (γ). η then will be a function of K and (ι), only, and (192) may be written

$$Q = 4\,C^0 \int \sin^2 \frac{\eta\,(K^0, \iota')}{2}\, d\iota'\, f(x^0, \iota') \tag{193}$$

with

$$f(x^0, \iota') = \int |(x^0 \,|\, \iota'\,\gamma')|^2\, d\gamma'. \tag{194}$$

Let us now consider an arbitrary Lorentz transformation, and let

$$\bar{\beta} = (\bar{\iota}, \bar{\gamma}) = U \beta\, U^{-1} \tag{195}$$

be the collision constants in the new frame of reference, connected with the old collision constants $\beta = (\iota, \gamma)$ by a contact transformation. The unitary matrix U is given by (136) and (140). Since the (ι) are invariants, we have

$$\bar{\iota} = \iota. \tag{196}$$

The transformation function connecting the β-representation with the $\bar{\beta}$-representation thus has the form

$$(\beta^0 \,|\, \bar{\beta}') = \delta(\iota^0 - \bar{\iota}')\,(\gamma^0 \,|\, \bar{\gamma}')$$

and since

$$(x^0 \,|\, \bar{\beta}') = \int (x^0 \,|\, \beta^0)\, d\beta^0\, (\beta^0 \,|\, \bar{\beta}'),$$

we get

$$(x^0 \,|\, \bar{\iota}' = \iota', \bar{\gamma}') = \sqrt{|D^0|}\; (\bar{x}^0 \,|\, \bar{\iota}' = \iota', \bar{\gamma}') = \int (x^0 \,|\, \iota'\,\gamma^0)\, d\gamma^0\, (\gamma^0 \,|\, \bar{\gamma}'), \tag{197}$$

where the functional determinant D^0 is given by

$$D^0 = \frac{\partial\,(\bar{x}^0)}{\partial\,(x^0)} = \frac{\Delta^0\,[\bar{W}_i^0]}{\Delta^0\,[W_i^0]}. \tag{198}$$

On account of the fundamental relation

$$\int (\gamma^0 \,|\, \bar{\gamma}')\, d\bar{\gamma}'\, (\gamma'' \,|\, \bar{\gamma}')^* = \int (\gamma^0 \,|\, \bar{\gamma}')\, d\bar{\gamma}'\, (\bar{\gamma}' \,|\, \gamma'') = \delta(\gamma^0 - \gamma'')$$

holding for any transformation function, we then from (197) get

$$\int d\bar{\gamma}' \,|(x^0|\bar{\iota}'=\iota', \bar{\gamma}')|^2 = \int |(x^0|\iota'\gamma^0)|^2 \, d\gamma^0, \tag{199}$$

or

$$f(x^0, \iota') = |D^0| \bar{f}(\bar{x}^0, \bar{\iota}'=\iota'), \tag{200}$$

where

$$\bar{f}(\bar{x}^0, \bar{\iota}') = \int |(\bar{x}^0|\bar{\iota}'\bar{\gamma}')|^2 \, d\bar{\gamma}' \tag{201}$$

is the function corresponding to (194) in the transformed system. By integration over all values of (x^0) for $n^0 = 2$ we get from (200) and (198)

$$\int_{n^0=2} f(x^0, \iota') \, dx^0 = \int_{n^0=2} \bar{f}(\bar{x}^0, \bar{\iota}'=\iota') \left| \frac{\partial(\bar{x}^0)}{\partial(x^0)} \right| dx^0 = \int_{n^0=2} \bar{f}(\bar{x}^0, \bar{\iota}'=\iota') \, d\bar{x}^0, \tag{202}$$

which shows that the function

$$g(\iota') = \int_{n^0=2} f(x^0, \iota') \, dx^0 \tag{203}$$

is an invariant function of the eigenvalues of the invariants (ι).

Now, let the new system of reference be a 'center of gravity' system in which $\bar{\boldsymbol{K}}^0 = 0$. Then the function $\bar{f}$ defined by (201) will be constant for all values of $(\bar{x}^0)$, i. e. $\bar{f}$ is independent of the direction of $\bar{\boldsymbol{k}}_2^0$. This follows from the fact that $\bar{f}(\bar{x}^0)$ as a function of the variables $(\bar{x}^0)$ is invariant and form-invariant under all rotations in ordinary space. So we have

$$\bar{f}(\bar{x}^0, \bar{\iota}'=\iota') = \frac{1}{4\pi} \int_{n^0=2} \bar{f}(\bar{x}^0, \bar{\iota}'=\iota') \, d\bar{x}^0 = \frac{g(\iota')}{4\pi} \tag{204}$$

by (202) and (203). In an arbitrary frame of reference, where $\boldsymbol{K}^0 \neq 0$, we then by (200) and (204) get

$$f(x^0, \iota') = |D^0| \frac{g(\iota')}{4\pi} \tag{205}$$

and for the total cross section (193)

$$Q = G^0 \int g(\iota') \sin^2 \frac{\eta(\iota')}{2} \, d\iota', \tag{206}$$

where

$$G^0 = \frac{4 C^0 |D^0|}{4\pi} = \frac{4\pi}{B^0} |\bar{\Delta}^0| \, \bar{W}_1^0 \, \bar{W}_2^0 \tag{207}$$

on account of (190), (198), and (77).

Since $\bar{\boldsymbol{k}}_1^0 = -\bar{\boldsymbol{k}}_2^0$, we further, by means of (188), (77), and (160), get

$$\left.\begin{aligned} |\bar{\mathcal{I}}^0|\,\overline{W}_1^0\,\overline{W}_2^0 &= \frac{|(\bar{\boldsymbol{k}}_2^0\,\overline{W}_1^0 - \bar{\boldsymbol{k}}_1^0\,\overline{W}_2^0)\,\bar{\boldsymbol{e}}_2^0|}{\bar{k}_2^{02}} = \frac{\overline{W}_1^0 + \overline{W}_2^0}{\bar{k}_2^0} \\ &= \frac{(\overline{W}_1^0 + \overline{W}_2^0)^2 - |\bar{\boldsymbol{k}}_1^0 + \bar{\boldsymbol{k}}_2^0|^2}{\sqrt{|\bar{\boldsymbol{k}}_1^0\,\overline{W}_2^0 - \bar{\boldsymbol{k}}_2^0\,\overline{W}_1^0|^2 - |\bar{\boldsymbol{k}}_1^0 \times \bar{\boldsymbol{k}}_2^0|^2}} = \frac{K^{02}}{B^0}. \end{aligned}\right\} \quad (208)$$

Thus we get the general formula

$$Q = \frac{4\pi K^{02}}{B^{02}} \int g(\iota') \sin^2 \frac{\eta(K^0, \iota')}{2}\, d\iota', \quad (209)$$

by which the total cross section is given as a function of invariant quantities.

In the special case where the total number of particles n is a constant of collision, we have $(\iota) = L$ and $(\gamma) = m$, and by (203) and (194) we get

$$g(l') = \int f(x^0, l')\, dx^0 = \sum_{m'=-l'}^{l'} \int |(x^0 \,|\, l'm')|^2\, dx^0 = 2l' + 1 \quad (210)$$

on account of the normalization condition for the eigenfunctions $(x^0 \,|\, l'm')$. Thus in this case $g(l')$ is simply equal to the number of eigenstates corresponding to a definite value $L' = l'(l'+1)$ of the variable L and the total cross section is

$$Q = \frac{4\pi K^{02}}{B^{02}} \sum_{l'=0}^{\infty} (2l'+1) \sin^2 \frac{\eta(K^0, l')}{2}. \quad (211)$$

In a system where the center of gravity is at rest, i. e. $\boldsymbol{K}^0 = 0$, (211) reduces further to the well-known formula

$$Q = \frac{4\pi}{k_2^{02}} \sum_{l'=0}^{\infty} (2l'+1) \sin^2 \frac{\eta'}{2}, \quad (212)$$

and in this special case the numbers l' and m' may be interpreted as the quantum numbers determining the magnitude and the component of the angular momentum in a definite direction.

References.

1) W. HEISENBERG, Ann. d. Phys. **32**, 20, 1938. See also N. BOHR, Conference on Nuclear Physics in Rome 1931, p. 119; V. WEISSKOPF, Zs. f. Phys. **89**, 27, 1934; A. MARCH, *ibid.* **104**, 93, 161, 1936; **105**, 620, 1937; G. WATAGHIN, ibid. **88**, 92; **92**, 547, 1934.
2) W. HEISENBERG, Die "beobachtbaren Grössen" in der Theorie der Elementarteilchen I, Zs. f. Phys. **120**, 513, 1943; II, *ibid.* **120**, 673, 1943.
3) W. HEISENBERG, Die "beobachtbaren Grössen" in der Theorie der Elementarteilchen III, in preparation.
4) C. MØLLER, General Properties of the Characteristic Matrix in the Theory of Elementary Particles II, in preparation.
5) See e. g. V. FOCK, Zs. f. Phys. **75**, 622, 1932.
6) P. A. M. DIRAC, Quantum Mechanics 2. edition, Oxford 1935, p. 199.
7) W. HEISENBERG, *loc. cit.* 2), I, 515.
8) *loc. cit.* 6) p. 102.
9) See e. g. P. A. M. DIRAC, *loc. cit.* 6), p. 198.
10) cf. a fortcoming paper "On the Correspondence Principle in the Theory of Elementary Particles".

Indleveret til Selskabet den 1. December 1944.
Færdig fra Trykkeriet den 16. Juli 1945.

DET KGL. DANSKE VIDENSKABERNES SELSKAB
MATEMATISK-FYSISKE MEDDELELSER, BIND XXIII, NR. 2

DEDICATED TO PROFESSOR NIELS BOHR ON THE OCCASION OF HIS 60TH BIRTHDAY

ON THE EFFECTIVE CHARGE OF FISSION FRAGMENTS

BY

N. O. LASSEN

KØBENHAVN
I KOMMISSION HOS EJNAR MUNKSGAARD
1945

Printed in Denmark.
Bianco Lunos Bogtrykkeri A/S

(1) Introduction.

Since the discovery of the fission phenomenon by HAHN and STRASSMANN[1] in 1938 the properties of the fission fragments have been investigated in many ways. At an early stage it was suggested that the fission particles are thrown apart with very high kinetic energies, and this was experimentally established by FRISCH[2] and many others. Later on, the masses, energies, and ranges of the fission particles have been more closely studied by means of ionization chambers. The atomic numbers of several fission products have been determined by chemical means and in this way information about the charges of the fission nuclei has been obtained.

The charge of the fission nucleus is not the same as the effective charge of the fission fragment, because the fission nucleus does not travel alone but is accompanied by a number of the electrons from the original atom. As a result of the large energy and rather short range the specific ionization of the fragments is very great as compared with that of α-particles, which also was found by investigators using a cloud chamber, for instance BØGGILD, BROSTRØM, and LAURITZEN;[3] therefore the particles may be supposed to have a rather high charge, i. e. only a fraction of the electrons from the original atom accompany the nucleus. The magnitude of the effective charge was early assumed to be about $15—20\,\varepsilon$, where ε is the electronic charge, this being the result obtained by using Bethe's relation for energy loss per cm. range of heavy particles,[4] although, as we have not to do with a single heavy particle, but with a nucleus and a cluster of electrons, the use of this relation may be somewhat problematic; the rate of energy loss along range indicates that the effective charge in the beginning decreases rapidly because of capture of electrons.[3 and 5]

Unpublished calculations by Prof. BOHR based upon the assumption that those electrons in the uranium atom which have velocities smaller than the initial velocities of the fission fragments are left back while the others follow the fragments show that the initial effective charge of the particles has a value of about $20\,\varepsilon$; further calculations indicate that the charge decreases rapidly along the first part of the path and then is rather low, about unity along the rest of the path.[5]

The experiments to be described in the present paper give some information about the initial effective charge. Fission fragments from a thin layer of uranium were deflected in a magnetic field and the values of $H\varrho$ were determined. An experimental determination of the initial effective charge of the fission particles has previously been made by PERFILOV,[6] who also measured the deflection of the fragments in a magnetic field and in close agreement with the above mentioned estimates found a value of $20\,\varepsilon$. However, as the result was rather uncertain, the estimated error being 20 per cent. and the paths of only 7 particles being determined, it was found desirable to repeat the experiments.

(2) Experimental Arrangement.

The target of uranium was placed in the cyclotron about 6 mm. behind a target of beryllium, which was bombarded with 6 *MeV* deuterons, thus being a strong source of neutrons. The magnetic field of the cyclo ron was used to deflect the fission particles and the paths of these were determined by means of the arrangement shown in fig. 1. In this is seen the brass ring (1) of the cyclotron chamber; (2) is a stud on this consisting of a 3-inch copper tube and a flange, (3) is a cylindrical chamber made of a piece of a 5-inch copper tube and a brass flange, which fits to the stud; the chamber is closed by the brass disk (4), in which is cut a slit. Inside the chamber there is the same pressure as in the cyclotron, the slit being covered with a window of mica and the connections (5) being made tight by means of rubber rings and glyptal. (6) is a second chamber, a $4\frac{1}{2}$ inch brass tube with a bottom and a flange; the space inside this chamber is filled with nitrogen taken from a steel tank with commercial nitrogen carefully cleared of oxygen by means of red-hot copper

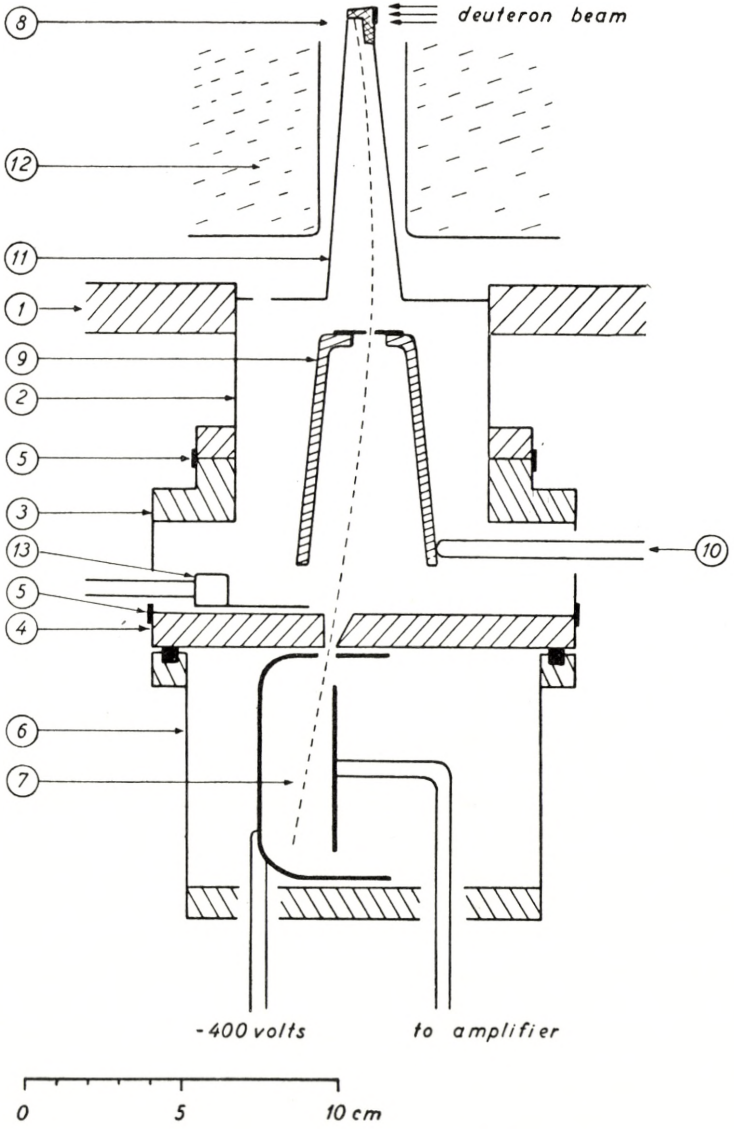

Fig. 1. Experimental arrangement. Horizontal section.

and of water by means of sulphuric acid. A slow stream of nitrogen through the chamber was maintained during the experiments. (7) is the ionization chamber. The beryllium and uranium targets are placed on a water-cooled copper block (8). Before entering the ionization chamber the fission particles must pass

through the mica window and through a second slit—which in what follows is referred to as the slit—made from two knives supported by the brass plate (9), which is fastened on a movable slide (not shown in the figure) and can be operated from outside by means of the brass rod (10), against which it is pressed by a spring. The position of the brass rod and therefore of the slit can be read on a scale with an accuracy of 0.1 mm. (11) is a shield, which prevents scattered deuterons from entering the ionization chamber, (12) denotes the dees of the cyclotron and (13) is a combined diaphragm and holder, which can be operated from outside and put in five positions with the following consequences: In the first position the window is entirely free, in the second the free length of the window is reduced to one half, the other half being covered by the diaphragm, and in the third position the window is entirely closed; in the fourth position a rather large target of uranium is placed just outside the window, and finally in the fifth position this target is replaced by an α-gun to be described later.

The beryllium target was prepared from metallic beryllium, which was available as a crystalline powder. The powder was placed in a cylinder of iron closed with a piston and in an atmosphere of hydrogen heated to a temperature of about 800° C. and then forged to a pill, which was ground off and soldered to the copper block, ammonium chloride being used as a flux.[7] Several other methods of preparing the target was tried, but with no success, and though this procedure is rather tricky, it was found possible to get good targets in this way. The target must be rather thin, about 0.5 mm., so that the heat may be easily transmitted; it is very difficult to melt the beryllium outside the cyclotron, but very easy to do so inside it. For the same reason the copper block must be very effectively cooled; in the arrangement used this requirement was not perhaps entirely fulfilled, as it was supposed to be of more importance that the distance between the beryllium target and the uranium one was kept short and that the direction between the two targets did not diverge too much from the direction of the deuterons; as a consequence it was necessary to keep the energy input of the cyclotron oscillator rather low in order to avoid destroying the beryllium target by melting or evaporation.

The uranium target was made by evaporation *in vacuo* of uranium powder, which was placed on a tungsten band with a width of 5 mm. and the temperature of which was slowly raised to incandescence; the target plate was held at a distance of 5 cm. and in the beginning protected by a screen, which was removed by means of a magnet when the temperature had reached its final value; in this way most of the impurities of the uranium powder—12 per cent.—were prevented from reaching the target. Two targets were used, target I on a support of copper sheet, target II on a support of mica sheet. The dimensions were for I 20×1.3 mm.^{2} and for II 20×0.7 mm.^{2}; the thicknesses of the two layers were nearly the same, about 0.35 mg. per cm.^{2}, as determined by a counting of the α-particles.

The width of the slit, which can be varied from 0 to 8 mm., will be mentioned in each case.

Two brass disks (4) were made. In one of them (I) the window had a width of 4.0 mm. and a length of 66 mm. with three 2 mm. cross bars, the effective opening thus being 4.0 by 60 mm.^{2}. In the second (II), the window had a width af 2.0 mm. and an effective length of 56 mm. The mica was placed between the brass disk, which was carefully polished, and a frame of 0,5 mm. copper, piceïn being used for fastening and tightening. Several windows were used, in the beginning with thicknesses of about 1.5 mg. per cm.^{2}; although the splitting of this rather large mica sheet is a tedious process, it was soon found desirable to use thinner windows. Precautions then had to be taken to keep the difference of pressure on the two sides of the window below some 20 cm. of *Hg* during the evacuation of the cyclotron after the apparatus had been put in place; except when used the windows were submitted to a pressure difference of about one cm. of mercury, of course always in the same direction. The results mentioned in what follows were obtained with a window of type I with a thickness of 0.93 mg. per cm.^{2} and a window of type II with a thickness of 0.73 mg. per cm.^{2}

The amplifier contained three stages, the two last of which for convenience were placed at some distance from the cyclotron, the first being placed in a tube stiffly connected with the ionization chamber. As in the actual ionization chamber nothing could be changed without filling the whole cyclotron with air, a second cham-

ber was used for testing, while the amplifier was built, and for some measurements, e. g. the determination of the thicknesses of uranium targets. The amplifier could be connected with a thyratron and a mechanical counter; however, in the experiments to be mentioned it was connected with a cathode ray oscillograph through an extra auxiliary amplifier; by varying the amplification of this extra amplifier it was possible to record both α-particles and fission particles without touching the actual amplifier. Some trouble was caused by electrical disturbances, the amplifier being placed in the same room as the 50 kW short wave oscillator of the cyclotron. Finally, all voltages were taken from batteries and the heating current from an accumulator, all shielded in metal boxes. The pulses on the oscillograph were recorded by a camera with a moving film. The developed films were put into a small diascope and the measuring carried out on the picture, this being in a standard position.

(3). Adjustment of the Amplifier.

The first thing to be done was to test the linearity of the amplifier and to adjust the arrangement. This was done by means of artificial pulses taken from a small machine, the diagram of which is given in fig. 2; C_2 is continuously charged

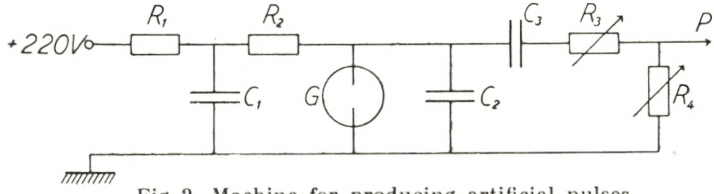

Fig. 2. Machine for producing artificial pulses.

R_1: $10^6\,\Omega$ R_2: $10^7\,\Omega$ R_3: $10^6 - 10^7\,\Omega$ R_4: 10^3—$10^5\,\Omega$
C_1: $4\,\mu F$ C_2: $0.25\,\mu F$ C_3: $50\,pF$ G a glim lamp.

through R_2, but when the potential reaches the critical value of the glim lamp G, it suddenly drops down again; part of the pulse is carried from the point P to a little condenser, which is in stiff connection with the grid of the first valve of the amplifier; the size of the transmitted pulse can be varied in steps from 1 to 100 in arbitrary units by varying R_4; the size of the units can be varied by means of R_3.

The adjustment was now carried out in the following way: An α-gun was made; the source of α-particles was *RaD* on a small piece of a mica window from an old radon source. By a diaphragm a narrow beam of α-particles was selected, which was allowed to enter the ionization chamber through the window in such a direction that none of the α-particles would hit the walls of the chamber; the range of the particles was reduced by means of an absorber of mica placed on the diaphragm of the gun.

In the case of window I the following data were obtained: Thickness of absorber and window $2.6 + 0.9 = 3.5$ mg. per cm.^{2} equal to $3.5/1.45 = 2.4$ cm. of air; the figure 1.45 as well as many other figures in what follows is found in a paper by LIVINGSTON and BETHE[8]. The range of the α-particle in the ionization chamber is found to be $3.8 - 2.4 = 1.4$ cm. of air, which is to be corrected to 1.35 cm., because the particles travel 0.2 cm. behind the window before entering the actual chamber, the pressure of which being 19 cm. Hg. Thus each of the particles delivers an energy of 2.5 *MeV* within the chamber, and this is found to correspond to pulses of 21.5 mm. as measured in the standard way previously described. The arbitrary unit of artificial pulses used being denoted with k, the following figures were found: 7, 14.4, 21.7, 27.6, and 34.6 mm. corresponding to $1k$, $2k$, $3k$, $4k$, and $5k$, respectively. The spreading about these values according to the background noise of the amplifier was the same, about ± 2 mm., whether the pulses were due to α-particles or were artificial. As a result of the adjustment we thus find that $1k$ corresponds to 0.84 ± 0.05 *MeV*, which of course is independent of the amplification. For larger values of the artificial pulses we get a little correction because in the machine R_3 is not infinitely large as compared with R_4.

This result could be reproduced, while it was found that the amplification was not entirely constant and the amplifier therefore had to be adjusted by artificial pulses rather often.

(4). Experiments with Geometry I.

The width of target and window are 1.3 and 4.0 mm., respectively. When the width of the slit is 1.3 mm., it is seen that a beam of particles travelling in straight lines and defined

by the target and the slit will just fill the window; as the fission particles travel in lines with rather small curvatures nearly the same will apply to particles with the same $H\varrho$. In the experiments for determination of $H\varrho$ the slit therefore was 1.3 mm., and its position was changed in steps of 1.3 mm., ranging between -10.4 and $+22.1$, where 0 denotes the position in which the middle lines of target, slit, and window are in the same plane and the sign is chosen in such a way that positive particles are deflected against positive figures.

It was then found that for all positions of the slit the oscillograph showed a large number of pulses corresponding to energies up to about 10 *MeV*; these are ascribed to nitrogen atoms in the ionization chamber recoiling after collision with fast neutrons, or, more strictly speaking, to coincidences between several such recoil atoms. Only for a few positions of the slit essentially larger pulses were obtained, in magnitudes up to about 50 *MeV*, and these must be ascribed to fission particles from the uranium target entering the ionization chamber along the paths indicated in fig. 1, as was asserted in the following way:

(1) By means of the diaphragm (13) (fig. 1) it was immediately established that the pulses are due to particles entering through the window.
(2) Next, it was shown, by means of an arrangement (not shown in the figure) which permitted closing of the slit by turning the rod (10), that the particles pass through the slit.
(3) A test run without uranium target showed no such pulses, although the recording system surely was in proper order, as fission particles from the control uranium target on (13) could be recorded. Consequently the particles are coming from the uranium target.
(4) The pulses cannot be due to coincidences between α-particles as the number of those amonts to 0.05 per min. only, while the number of the large pulses are about 10 per min. Further the pulses are only observed when the cyclotron is running.

Thus the pulses corresponding to energies essentially higher than 10 *MeV* are undoubtedly due to fission fragments; however, as will be seen below, the lower energy limit of the fission

pulses is probably smaller than the upper energy limit of the recoil pulses, and hence it is impossible to distinguish between the two sorts of pulses in the region from about 10 *MeV* and downwards.

Fig. 3 shows a copy of one of the recording films; several fission pulses are seen, both the actual primary pulses (upwards) and the secondary pulses after the return of the amplifier. When viewed visually on the oscillograph, the recoiling atoms are

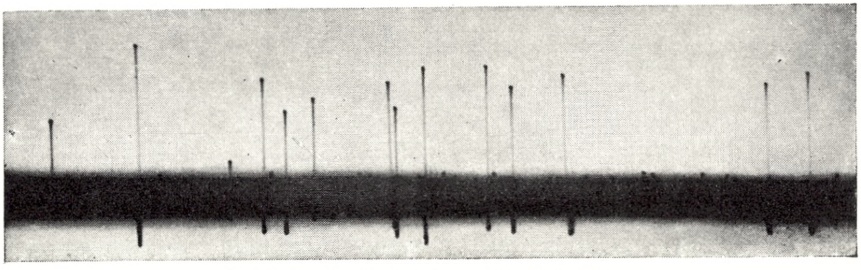

Fig. 3. A piece of a recording film.
The largest fission pulses correspond to about 50 *MeV*. The horizontal line is due to recoil atoms; its width corresponds to about 10 *MeV*, which does not determine the uncertainty of energy measurements (see text).

seen as a lot of pulses, but they appear in so large a number, that on the rather slowly moving film they cannot be separated, but produce the broad horizontal line, which, of course, does not determine the uncertainty of the energy measurements.

In fig. 4 are plotted the number of pulses larger than 12 *MeV* against the displacement of the slit, the number of course being referred to the same dose of neutrons; as regards the scale of $H\varrho$, see below. The neutron dose was measured by an instrument also used for managing the cyclotron; it consisted of an ionization chamber with boron layers on the plates, which was surrounded by paraffine and was connected with a galvanometer and with a recorder registering the electrical charge passing through the boron chamber, thus giving a measure of the number of neutrons in relative units (denoted in what follows as n. u.).

Fig. 5 shows the energy distribution obtained for the five positions of the slit giving reasonable yields, the numbers being referred to the same neutron dose of 1,000 n. u., which was

about the dose used. The hatching to the left of the 12 *MeV* line indicates the pulses due to recoil atoms; as in the abscence of fission particles very few pulses a little larger than 10 *MeV* were recorded, most of the pulses in the region 12—16 *MeV* and all larger pulses are due to fission fragments. On the other hand some of the fission particles may have energies less than 12 *MeV*; nevertheless, as indicated by fig. 5, it seems permis-

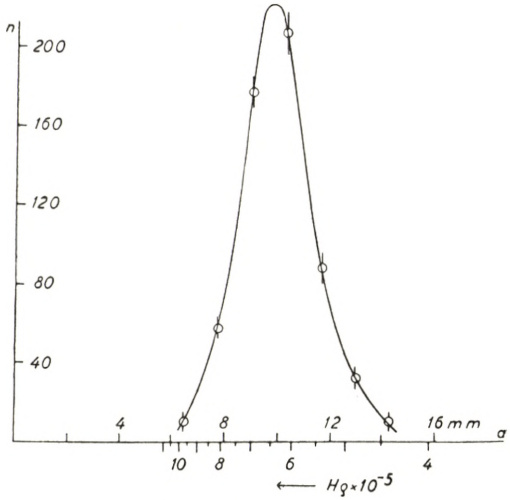

Fig. 4. Deflection curve for fission fragments obtained with geometry I.
Abscissa a: displacement of slit.
Ordinate n: number of fragments per 1,000 n. u.
Scale of $H\varrho$ in units of 10^5 oersted × cm.

sible to assume that this is only a small part of the total number, so that the correction which ought to be added to the numbers in fig. 4 may be omitted.

As is known from many previous investigations, two groups of fission particles exist, with different masses, energies, and ranges. Now, in fig. 4 only one peak is found, and therefore it might be suspected that only one of the two groups has been found and that a second group was lying outside the region which could be investigated by the apparatus, or that the second group had too little energy to be recorded after passing through the window. The former of these possibilities would involve an effective charge higher than 40 elementary units, which, from a theoretical point of view, would, indeed, be very surprising;

the latter would also be very astonishing, and in fact fig. 5 indicates that both groups of fission fragments are represented, the energy distribution curves clearly showing two peaks. The two groups have very nearly the same $H\varrho$ and therefore we get only one peak in fig. 4; still, it will be noticed that the

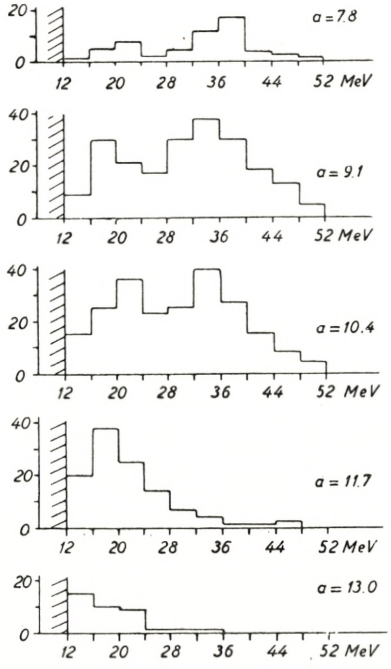

Fig. 5. Energy distribution of fission fragments for various positions of the slit (geometry I).
Ordinate: number of fragments per 1,000 n. u.
a: displacement of the slit in mm.

relative abundance of the two groups is not the same for the different positions of the slit, but that the most energetic is found to be predominant for the largest values of $H\varrho$. Since in the two groups corresponding particles have the same momentum, this means that in general the particles with the smallest masses have also the smallest effective charges; from an experimental point of view it may, of course, be an open question, whether this rule holds for each single fission process or not, but it certainly does so for some fissions, as the particles for $a = 11.7$ and 13.0 belong almost entirely to the heavy group,

and they must have corresponding particles in the light group with the same mv and smaller values of a, i. e. smaller values of e. This seems to be in contradiction to the theory outlined by Prof. BOHR in the above-mentioned paper,[5] in which the formula for the effective charge is given as

$$Z^{\text{eff}} = Z^{\frac{1}{3}} \cdot \frac{V}{V_0},$$

Z and V being the nuclear charge and the velocity of the fragment, $V_0 = 2.2 \times 10^8$ cm. per sec. The light and the heavy fragment being denoted with indices 1 and 2, we get

$$\frac{Z_1^{\text{eff}}}{Z_2^{\text{eff}}} = \left(\frac{Z_1}{Z_2}\right)^{\frac{1}{3}} \cdot \frac{V_1}{V_2} \backsim \left(\frac{m_1}{m_2}\right)^{\frac{1}{3}} \cdot \frac{V_1}{V_2}$$

and since $m_1 V_1 = m_2 V_2$

$$\frac{Z_1^{\text{eff}}}{Z_2^{\text{eff}}} \backsim \left(\frac{m_2}{m_1}\right)^{\frac{2}{3}}.$$

Thus, a consequence of the theory is that the light particle has the higher effective charge; as now the theory was in good agreement with the experiments of BØGGILD, RROSTRØM and LAURITZEN, the present results at a first sight seem to be disagreeing not only with the theory, but also with the experiments mentioned. However, as already pointed out by Prof. BOHR in the paper, Z^{eff}, the charge effective in electronic interactions, may be different from the total charge of the fragment, e. In the deflection experiments we have to do with the total charge e, while the theory deals with the quantity Z^{eff}; therefore, strictly speaking we have no discrepancy, but we find that the two quantities behave inversely, as we have $e_1 < e_2$ and $Z_1^{\text{eff}} > Z_2^{\text{eff}}$.

The energy distribution for the total number of fission fragments of all $H\varrho$-values might be obtained by adding up the five curves of fig. 5; however, it was obtained in a more direct way by changing the width of the slit from 1.3 to 6.5 mm. and placing it in such a position that it covered the whole

region through which the fission particles were passing. This arrangement was also used for some test experiments:

Firstly, the voltage of the ionization chamber was varied and energy distribution curves were determined for values of 200, 300, and 400 volts; the three curves were identical within the limits of statistical errors, this indicating that a voltage of 400 is enough to ensure saturation and a sufficiently short time of

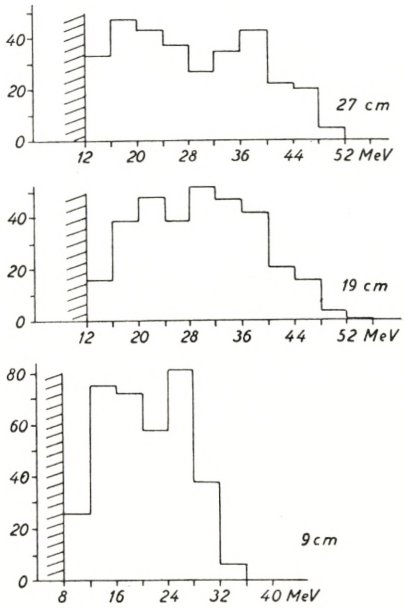

Fig. 6. Energy distribution obtained with various pressures in the ionization chamber.

collecting the ions as compared with the resolving time of the amplifier, which had to be rather small (10^{-4} sec.) in order to diminish the pulses due to coincidences between recoil atoms.

Secondly, the pressure in the ionization chamber was varied; the pressure generally used was 19 cm. *Hg*, but now energy distribution curves were determined for pressures of resp. 27, 19, and 9 cm. *Hg*. The result is shown in fig. 6; while the first two curves are almost identical, the last one deviates considerably, the maximum energy being decreased from 52 *MeV* to 36 *MeV*; this is in agreement with the expected residual range of about 1.5 cm. of normal air.

Fig. 7 gives the sum of all measurements of the energy distribution curve carried out with nitrogen pressure 19 cm. *Hg* and the one carried out with 27 cm. *Hg*. The two groups are clearly seen, although the valley between the two peaks is rather small as compared with the distribution obtained when the total energy of the fission particles is measured (see e. g. fig. 11 in the paper by FLAMMERSFELD, JENSEN, and GENTNER[9]). Of course this is at least partly due to the way in which the histogram is drawn with the rather large energy intervals of

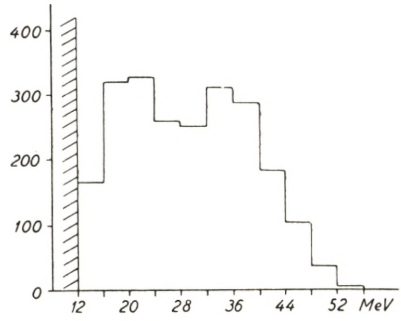

Fig. 7. Energy distribution of fission fragments having traversed 0.93 mg. per cm^2. of mica.

4 *MeV*; these were chosen because a test run with artificial pulses showed that the spreading of such pulses was less than ± 0.5 *MeV* with the cyclotron stopped, but increased to about ± 2 *MeV* with the cyclotron running. FLAMMERSFELD, JENSEN, and GENTNER find the maximum energy to be 106 *MeV*; now BÖGGILD, BROSTRØM, and LAURITZEN[3] give velocity-range curves for fission fragments, and a calculation on this base gives for the maximum energy of the particles having traversed 0.9 mg. per cm.^{2} of mica a value of about 55 *MeV* in good agreement with the value measured. The minimum energy cannot be calculated in the same way, as the result greatly depends upon the range, and this is not known with sufficient accuracy; however, the calculation gives a value between 10 and 20 *MeV* which is also in agreement with fig. 7 and which justifies the omission of the correction to the curve in fig. 4.

(5) Experiments with Geometry II.

Of course every geometrical arrangement with finite dimensions will tend to make the peak in fig. 4 broader and to conceal possible details. As the observed peak only extends over five positions of the slit, it was desirable to repeat the experiments with a geometry giving a higher resolution. This was performed with geometry II, in which each of the three significant dimensions, the widths of the uranium layer, the window, and the slit, determining respectively the amount of uranium, the solid angle, and the size of the $H\varrho$-intervals, was reduced to about half of the previous values, the yield of fission for each single position of the slit consequently being reduced to one eighth. The time and the costs are in this way increased by a factor of sixteen as the number of positions of the slit to be investigated is twice as large as before; therefore, it was not found possible to improve the geometry further.

The widths of the uranium layer and the slit were 0.7 mm. and the slit was moved in steps of 0.7 mm. The width of the window was intended to be 2.0 mm., this being the width of the slit cut in the brass disk (4) (fig. 1), but some of the piceïn used for fastening the mica foil happened to cover about 0.5—0.8 mm. along one of the edges, the actual width thus being about 1.4 mm.

It is important, when studying the initial effective charge, to get a thin target of uranium, but in order not to decrease the yield further, the new uranium layer was made of the same thickness as the first one, this being considered as a rather thin target. However, it was to be feared that, because of possible irregularities of the copper support, the effective stopping power of the layer might differ from the value determined from the amount of uranium; to avoid this the new target was made on a support of mica as already mentioned.

The result of the experiments is given in fig. 8 by the open circles and the curve. The region outside the peak on both sides was investigated with a slit of 6.5 mm.; nothing was found. The full circles in the figure are the circles from fig. 4 (geometry I), the ordinates having been reduced by a suitable factor, so that the total yield of fission particles of all values of $H\varrho$ is the

same for each set of circles. The agreement between the two experiments is satisfactory. It is evident that when we use geometry I with the broad slit, etc., the curve must be broader, i. e. the full circles must lie outside the curve on both sides as is seen to be the case; hence it follows, from the way in which the ordinates of the full circles were reduced, that they must lie inside the curve for the middle α-values.

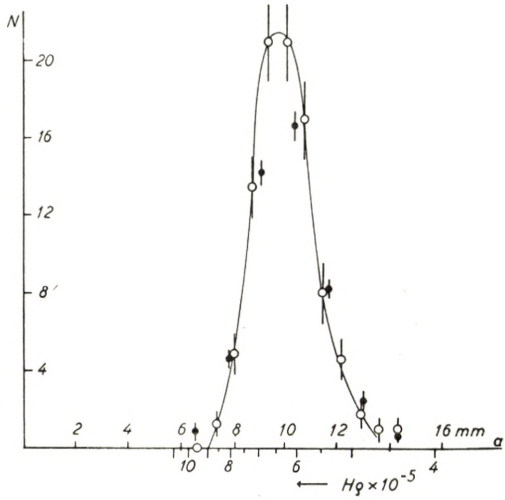

Fig. 8. Deflection curve for fission fragments obtained with geometry II (open circles).
Abscissa α: displacement of slit.
Ordinate: number of fragments per 1,000 n. u.
Scale of $H\varrho$ in units of 10^5 oersted × cm.
Full circles, see text.

By the determination of the curve on fig. 8 any uncertainty caused by an unknown correction was avoided as the pressure in the ionization chamber was kept at 9 cm. *Hg*, which reduced the background due to recoil atoms to 6—8 *MeV*, while, as the thickness of the window was now only 0.73 mg. per $cm.^2$, the smallest energies of the fission particles were about 10 *MeV*, a free space thus remaining between the two sorts of pulses.

The energy distribution curve in fig. 9 was determined in the same way as before, the pressure in the ionization chamber now being 23 cm. *Hg*. As before the two groups of fission fragments are clearly visible, and a comparison with fig. 7 shows

that the energies are increased in accordance with the use of a thinner window.

As indicated by fig. 8, the two groups of fission fragments have so nearly equal $H\varrho$-values that they are not separated

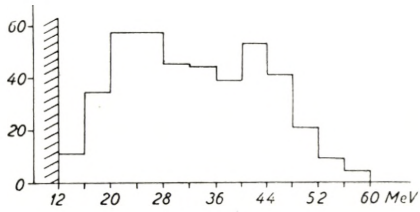

Fig. 9. Energy distribution of fission fragments having traversed 0.73 mg. per cm.^{2} of mica.

even with this better geometry. It was found desirable to investigate the energy distribution for the various positions of the slit corresponding to the experiments of fig. 5, but on account of the rather small yield this was only performed for two positions, which were chosen one on each side of the peak and so

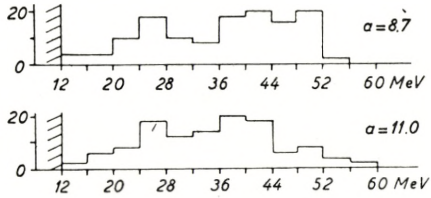

Fig. 10. Energy distribution of fission fragments for two positions of the slit (geometry II).
Ordinate: number of fragments per 6,000 n. u.
a: displacement of the slit in mm.

that the yield was about half the maximum yield. The distance a of the slit from zero position was resp. 8.4 and 10.7 mm., the width of the slit 0.7 mm. and the pressure in the ionization chamber 23 mm. Hg; the result is seen in fig. 10. The two curves are very nearly equal; still, if we divide the numbers into two portions with energies resp. lower and higher than 36 *MeV*, we find for the first curve ($a = 8.4$) resp. 27 and 38, and for the second curve ($a = 10.7$) resp. 30 and 29. Thus the difference between the two energy distributions, if any, is that in the first case, i. e. for the largest $H\varrho$, the most energetic group of fission fragments is more strongly represented than in the second case.

This is in agreement with the result found with geometry I; nevertheless, the difference between the two curves is scarcely greater than could be explained by statistical fluctuations, the material being much too small, and the only certain conclusion which can be drawn from fig. 10 is that both groups of fission particles are represented for both positions of the slit and in ratios not differing very much. This seems to indicate that we cannot expect to get a curve with two peaks even when the $H\varrho$-distribution curve was determined with a much better geometry.

(6) The Scale of $H\varrho$.

By the calculation of the scale of $H\varrho$ previous measurements of the magnetic field of the cyclotron magnet were used. At the starting-point of the fission fragments the field was very nearly the same as in the centre of the cyclotron, about 15,000 oersted, while at the end of the paths it had decreased to about 45 per cent of this value. Now the path of a particle with a fixed value of $H\varrho$ and starting along the radius of the cyclotron was calculated by means of analytical methods, the path being divided into a number of smaller portions with increasing values of ϱ corresponding to the decreasing H. The curve thus found was drawn to the scale of 3/1 on a piece of transparent paper, which was placed upon a drawing of the apparatus and rotated about the starting-point of the particles, until the curve passed through the central-point of the window; the intersection between the curve and the plane of the slit indicates the position of the latter corresponding to the value of $H\varrho$ concerned. This procedure was carried out for three values of ϱ and the result is shown in Table 1. The last column shows that the product $a \times H\varrho$ is a constant within the limits of error, as indeed was to be expected from simple geometrical considerations. As a mean value we get $a \times H\varrho = 63.0 \cdot 10^5$ and this is used to define the scale.

Table 1.

Initial ϱ	$H\varrho$	a	$a \times H\varrho$
50 cm	$7.40 \cdot 10^5$ oersted × cm.	8.4 mm.	62.2×10^5
35 -	5.18 -	12.1 -	62.7×10^5
25 -	3.70 -	17.3 -	64.0×10^5

In order to check the scale an experiment was made in which α-particles from *ThC'* were deflected in the apparatus. The uranium layer was replaced by a metal wire 0.7 mm. in diameter, which for some hours had been activated in an atmosphere of thoron, and measurements were performed in the usual way, the result being illustrated by the two curves in fig. 11. The α-particles from *ThC'* have an energy of 8.77 *MeV*; the relation $H\varrho = \frac{\sqrt{2\,mE}}{e}$ gives $H\varrho = 4.27 \cdot 10^5$ oersted cm. The displacement a as calculated by use of the scale is 14.8 mm., and the agreement between the scale and the experiment is seen to be rather good.

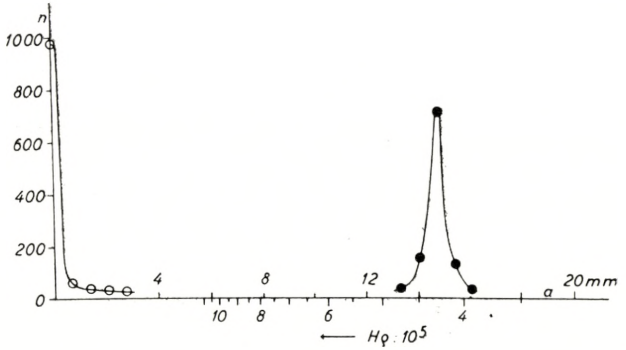

Fig. 11. Deflection of *Th C'* α-particles measured by geometry II.
Abcissa a: displacement of slit.
Ordinate n: number of particles per min.
Open circles without magnetic field.
Full circles with magnetic field 14,800 oersted.

The areas beneath the two curves of fig. 11 of course are equal. In the case of the open circles we have to do with particles travelling in straight lines; the shape of this curve thus gives information about the resolving power of the geometry. The ordinate for $a = 0.7$ is about 7 per cent. of the peak value, which is exactly what can be calculated for geometry II, the width of the window being 1.4 mm.; for larger values of a we ought to get zero, while in the experiment a background was found of about 2 per cent. of the peak value. In the case of the full circles of fig. 11, the shape of the curve shows that the particles have not exactly the same $H\varrho$.

(7) The Value of the Initial Effective Charge *e*.

Fig. 12 gives the $H\varrho$-distribution curve as obtained by means of geometry II, considering the correction due to the fact that in the experiment da was constant, not $d(H\varrho)$. By using the relation $e = \frac{\sqrt{2\,mE}}{H\varrho}$ we could calculate e, if only we knew mE. This quantity may be calculated e. g. from the data of FLAMMERSFELD, GENTNER, and JENSEN; fig. 13 shows the curve thus found

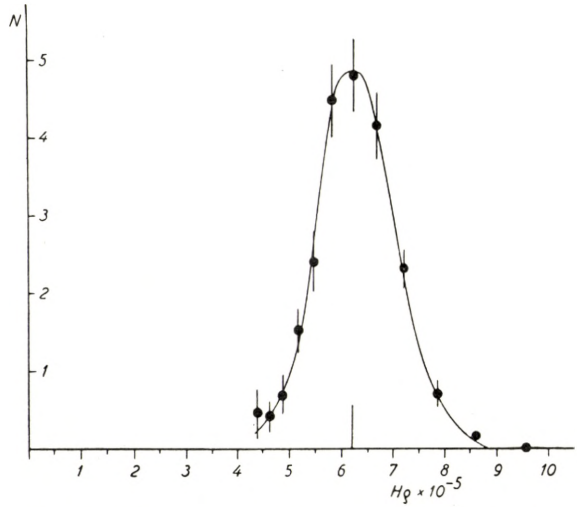

Fig. 12. Distribution of $H\varrho$ for fission fragments.

for the distribution of mE. Now we do not know exactly corresponding values of $H\varrho$ and mE; but combining the most frequent values $H\varrho = 6.2 \cdot 10^5$ oersted × cm. and $mE = 8.5 \cdot 10^3$ mass units × *MeV* we get $e = 21\,\varepsilon$ and putting the limits of mE at 6.5 and 10.5×10^3 we find that the particles having $H\varrho = 6.2 \cdot 10^5$ have effective charges between 19 and 24 ε. Combining the limits of $H\varrho$, 4.5 and $8.5 \cdot 10^5$ with the limits of mE we find:

(1) e lies between 13 ε and 33 ε except for a very few particles, and
(2) There exist particles corresponding to every e-value, of course only full numbers, between 18 ε and 26 ε.

Roughly spoken fig. 8 may be said to give a picture of the distribution of e, as we may write $mE = 8.5 \cdot 10^3 \pm 25$ per cent.,

that is to say $e = \frac{\text{constant}}{H\varrho} \pm 13$ per cent, or $e = 2.1 \cdot a \pm 13$ per cent.

FLAMMERSFELD and co-workers used slow neutrons to produce fission, while in the present experiments the neutrons were rather fast, and therefore it is not, of course, quite permissible to combine the values of $H\varrho$ and mE in the way shown; nevertheless it is known[10] that the energy distribution of the fission particles does not vary much with the energy of

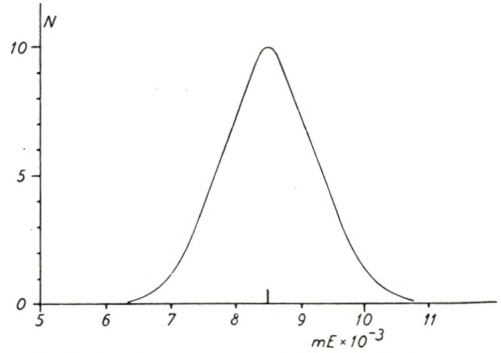

Fig. 13. Distribution of mE for fission fragments.

the neutrons, so that we may expect the calculated e-values to be rather good.

(8) Summary.

By means of the cyclotron magnet fission fragments from a thin layer of uranium were deflected; the deflection curve consisted of one single peak and energy distribution curves showed that both groups of fission particles were present, i. e. the two groups have nearly the same $H\varrho$. The experiments further showed that the two groups have not exactly the same $H\varrho$, the most energetic group being predominant for the highest $H\varrho$-values, i. e. the fragment with the smallest mass generally has also the smallest effective charge. By the aid of a better resolving geometry an attempt was made to separate the two groups, but in vain; the two experiments agreed well with each other. From the $H\varrho$-distribution thus determined and the distribution of mE as derived from the paper of FLAMMERSFELD, GENTNER, and JENSEN, the value of the charge e was calculated.

The result of the experiments, an effective charge of about 21 ε, is in good agreement with the calculation by Prof. BOHR mentioned in the introduction. Still, the theory gives a higher effective charge for the lighter fragment than for the heavier, while the opposite was found in the experiments; nevertheless, this is no actual discrepancy, as the theory deals with Z^{eff}, the charge effective in electronic interactions, while the experiments give the total charge e.

The present work was carried out at the Institute of Theoretical Physics in Copenhagen, and the author wishes to express his best thanks to the Director of the Institute, Professor N. BOHR as well as to Professor J. C. JACOBSEN for their interest in the experiments and their great encouragement, the latter also for active help in the design of the apparatus and on many other occasions. My thanks are also due to BØRGE MADSEN, M. Sc., for help in solving some mechanical problems and TORBEN HUUS, M. Sc., for valuable discussions.

Institute of Theoretical Physics,
University of Copenhagen.

Note added in proof.

A small improvement of the ionization chamber together with the use of argon instead of nitrogen in the chamber has made it possible in later experiments to distinguish clearly between the two groups of fission fragments and to determine the $H\varrho$-distribution curves for each of the two groups. In agreement with the previous results it was found that the two $H\varrho$-curves do not coincide, but that the abscissae of the curve for the light fragment are slightly, about 0.5×10^5 oersted $\times$ cm., higher than those of the curve for the heavy group. The most frequent values of $H\varrho$ for the light and heavy groups are found to be 6.7 and $6.0 \cdot 10^5$ oersted $\times$ cm., corresponding to e-values of $20\,\varepsilon$ and $22\,\varepsilon$, respectively.

References.

1. Hahn und Strassmann: Naturwiss. 27. 11. 1939.
2. O. R. Frisch: Nature 143, 276, 1939.
3. Bøggild, Brostrøm, and Lauritzen: D. Kgl. Danske Vidensk. Selskab, Math.-fys. Medd. XVIII, 4, 1940.
4. Bethe: Ann. d. Phys. 1930, Bd. 5, 375.
5. N. Bohr: Phys.-Rev. 59, 270, 1941.
6. Perfilov: Comptes rendus Acad. Sci. U. R. S. S. 28, 5, 1940.
7. H. R. Crane: Rev. Sc. Instr. 9, 428, 1938.
8. Livingstone and Bethe: Rev. Mod. Phys. Vol. 9, Nr. 3, p. 245, 1937.
9. Flammersfeld, Jensen, and Gentner: Zs. f. Phys. 120, 450, 1943.
10. Jentschke and Prankl: Phys. Zs. XL, 706, 1939.

Indleveret til Selskabet den 17. November 1944.
Færdig fra Trykkeriet den 6. September 1945.

DET KGL. DANSKE VIDENSKABERNES SELSKAB
MATEMATISK-FYSISKE MEDDELELSER, BIND XXIII, NR. 3

DEDICATED TO PROFESSOR NIELS BOHR ON THE OCCASION OF HIS 60TH BIRTHDAY

ON THE PLANENESS OF INTERFEROMETER PLATES

BY

EBBE RASMUSSEN

KØBENHAVN
I KOMMISSION HOS EJNAR MUNKSGAARD
1945

Printed in Denmark
Bianco Lunos Bogtrykkeri

Introduction.

Highest precision is claimed by those optical surfaces which are used for producing interference fringes in different kinds of interferometers. While ordinary optical surfaces are regarded as being satisfactory when the deviations from the wanted form (spherical, plane etc.) are smaller than $^1/_4$—$^1/_5$ of the wavelength of the light to be used, it is generally expected that the deviations from planeness of good interferometer plates may not exceed $^1/_{40}$—$^1/_{50}$ wavelength, *i. e.* the plates should be ground to a precision of 10^{-5} mm. This is particularly the case when the plates are destined to the use in an interference spectroscope for separating very close spectrum lines as, for example, in investigations of hyperfine structure by means of the Fabry-Perot étalon. The resolving power of this instrument depends, by a given plate distance, on three factors, *viz.* the planeness of the surfaces, the reflecting power of the silver film, and the precision of the adjustment to parallelism. Usually, the resolving power will be a result of all three factors acting together.

Most experimenters working with the Fabry-Perot étalon may be satisfied with obtaining the required resolving power by varying the distance of the plates and the thickness of the silver film, realizing neither how good the plates are nor to what degree the deviation from exact planeness may influence the resolving power. This standpoint is probably due to the facts that no simple methods of examination of the plates have so far been available and, primarily, that the physicist is unable to improve his plates by grinding.

In this paper simple methods will be described for testing of interferometer plates and for separately examining the different factors on which the resolving power depends.

Methods for Testing of Interferometer Plates.

For examining the planeness of interferometer plates only methods of highest sensitivity are available, *i. e.* methods depending just on interference. It should be expected, therefore, that an examination of the interference fringes produced by the interferometer itself could give some information. The testing of the planeness of a surface is carried out by using the Fizeau fringes of equal thickness formed in a thin wedge-shaped air interspace between the surface and a standard flat, when illuminated by monochromatic light. As the interval e between two consecutive fringes corresponds to a variation of $\frac{\lambda}{2}$ of the thickness of the air interspace, a deviation ε of a fringe from a straight line implies that the surface in the point concerned deviates from planeness with $\frac{\varepsilon}{e} \cdot \frac{\lambda}{2}$. In measuring the deviations of the fringes from linearity and equidistance it is possible thus to give a quantitative statement of local deviations from planeness as used in optical workshops and often mentioned in the literature[1].

Such an examination could of course conveniently be carried out by means of the great technical interferometers which were recently built for this purpose[2]; these instruments, however, are too expensive for ordinary physical laboratories. It is possible, nevertheless, by simple means to improvise an instrument allowing us to make measurements with the same accuracy as with the said great interferometers, if only a pair of suitable lenses is available. Such an arrangement, which has been used in this laboratory for a preliminary testing of unsilvered interferometer plates, is to be described in the following.

In the left part of Fig. 1 is shown a schematic design of the apparatus. The light from the light source L (an Osram spectral lamp) is concentrated upon the diaphragm B_1 by means of the condensor C and is then made parallel by the objective O_1. After passing a half-silvered glass plate G making an angle of 45°, the

[1] F. Kohlrausch, Praktische Physik. 17. Aufl. p. 408, 1935.
E. Einsporn, ZS. f. Instrkd. **57**, 265, 1937.
C. G. Peters and H. S. Boyd, Journ. opt. Soc. **IV**, 407, 1920.
[2] R. Landwehr, ZS. f. Instrkd. **62**, 73, 1942.
O. Schönrock, ZS. f. Instrkd. **62**, 357, 1942.

beam will hit perpendicularly upon the thin air layer between the two unsilvered interferometer plates F—P. The reflected beam will then be reflected at a right angle by the plate G, passing through a second objective O_2, in the focal plane of which the diaphragm B_2 is placed, through which the interference fringes can be observed. As objectives O_1 and O_2 were applied two achromatic lenses with an aperture of 65 mm. and with the focal lengths 700 and 400 mm., respectively, belonging to the Steinheil

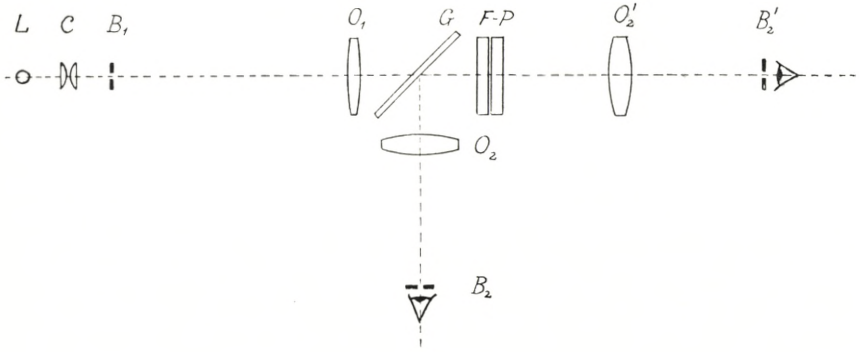

Fig. 1.

glass spectrograph GH. The circular diaphragm B_1 could be diminished to 0.5 mm. in diameter, giving a sufficient parallelism of the beam also at greater thickness of the air interspace. The diaphragm B_2, having a diameter of 2 mm., served only for fixing the eye position and for removing the light reflected from the front and back of the pair of plates. B_2 could be replaced by a camera in order to photograph the fringes. This arrangement was easily constructed by means of two optical benches, placed perpendicular to each other.

As a holder for the interferometer plates served the Fabry-Perot étalon itself with a distance ring of 1 mm. thickness. The étalon was of the same type as the construction by Carl Zeiss, as developed by G. Hansen. The plates were delivered by Bernhard Halle, Berlin. The use of the Fabry-Perot étalon as a holder for the plates involves a very easy adjustment of the air layer perpendicular to the beam by means of the adjusting screws of the instrument and, moreover, a convenient adjustment of the

wedge angle of the air layer by means of the three screws working upon elastic tongues. A rapid setting of the wished fringe distance is obtained, and the interference pattern is widely insensitive against vibrations.

Fig. 2. Fizeau fringes by unsilvered plates. d = 1 mm. Cd 6438.

Fig. 2 is a reproduction of a photographic negative of the interference fringes from a pair of fairly good quartz plates taken with the light of the red *Cd*-line 6438 A.U. As there was no standard flat in this arrangement, only relative measurements could be obtained. The accuracy in the determination of planeness by means of this method does not exceed 10^{-5} mm., or $^1/_{50}$ wavelength, being limited by the diffuseness of the fringes, which does not permit to measure them more accurately than $^1/_{25}$ of the interval of the fringes.

The accuracy obtained is thus limited due to the fact that the fringes are produced only by two reflected beams giving very diffuse fringes. It is therefore tempting to test the planeness with silvered plates in order to profit by the highly increased sharpness of the fringes caused by the great number of cooperating reflected beams. Actually, one cannot anticipate whether the silvering will change the form of the surface. However, in the case of the Fabry-Perot plates, this procedure may be justified since they are employed only after coating with silver and, therefore, only the optical planeness of the silver film is of interest.

At the degree of silvering (reflecting power about 90 %) generally applied to the Fabry-Perot plates, it appears inconvenient to observe the fringes produced by reflected light, since the beam reflected from the first surface is much stronger than the following reflected beams. Therefore, sharp dark fringes are obtained against a bright background, the contrast being rather insufficient. On the other hand, when the light passes through the plates, disturbances caused by reflected light are avoided, and an

image appears, complementary to the first, consisting of sharp bright lines against a dark background. This image is very suitable for the purpose in question.

An arrangement for qualitative testing of silvered interferometer plates based on this principle has been proposed by M. DUFFIEUX[1] and could easily be improved in such a way as to allow quantitative measurements.

The above described apparatus for testing the unsilvered plates could easily be extended to test the silvered plates[2], as indicated in the right part of Fig. 1. As the interference fringes should be observed by transmitted light, it was found convenient to arrange the optical parts simply along an optical bench of a length of 2 m. The glass plate G was removed, and the Fabry-Perot étalon with an 1 mm. distance ring between the silvered plates was placed in the parallel beam from the collimator B_1O_1. The objective O_2 was then moved to O_2', and the diaphragm B_2 to B_2', as shown in the figure. The interference fringes were observed through B_2', using O_2' as a magnifier in order to obtain a sufficient field of view. B_2' was placed in the focus of O_2', and in order to secure that the image was formed in infinity, the étalon was placed in the second focal plane of O_2'. B_2' could again be replaced by a camera adjusted to infinity (a 9×12 cm. plate camera with 13.5 cm. focal length). The aperture of the camera lens had to be made so small that false reflexions were avoided.

The adjustment of the light beam to parallelism and of the air layer perpendicular to the beam was carried out by autocollimation, using the light reflected from the interferometer plates. This could be done very accurately both with unsilvered and silvered plates. In order to facilitate this adjustment the diaphragm B_1 was covered with white painting on its back side. A number of diaphragms with fixed diameters 0.5 — 1.0 — 1.5 — 2.0 mm. were used.

Fig. 3 shows a photographic negative of the fringes from strongly silvered plates taken with the 1 mm. distance ring and by the light from the *Cd*-line 6438 A.U. A comparison of this

[1] M. DUFFIEUX, Revue d'Optique **11**, 159, 1932.

[2] The silvering was carried out by evaporation in high vacuum according to R. RITSCHL's method. ZS. f. Phys. **69**, 578, 1931.

picture with Fig. 2, taken with the same plates, indicates clearly the great improvement and the increased possibility of recognizing very small defects on the surface. Small irregularities in the fringes, which correspond to deviations of about $^1/_{50}$ wavelength and which could not be detected on Fig. 2, appear very clearly.

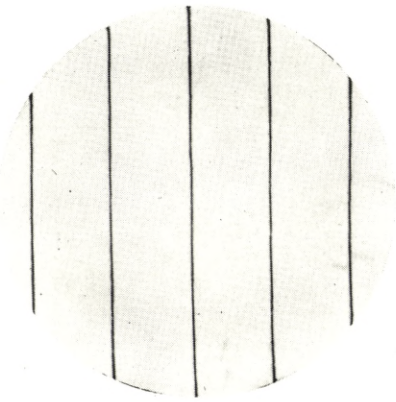

Fig. 3. Fizeau fringes by silvered plates. d = 1 mm. Cd 6438.

The determination of the errors of the plates was carried out by measuring the photographic exposures by means of a measuring microscope. Such measurements on repeatedly silvered plates led to the result that the errors of a given surface were not modified by the coating with silver, provided that a distance of at least 15 cm. was used during the evaporation of silver. For the best surfaces examined the greatest deviations from planeness were about $^1/_{50}$ wavelength.

The Accuracy in Determinations of Planeness.

Accuracy and sensitivity of the described measuring method for silvered surfaces depends primarily on the breadth of the interference fringes and, consequently, on the reflecting power of the silver film.

The intensity distribution within an interference fringe produced by an infinite number of reflected beams of monochromatic light is given by AIRY's formula

$$I = \frac{I_0}{1 + \frac{4\varrho}{(1-\varrho)^2} \cdot \sin^2 \frac{\alpha}{2}}. \qquad (1)$$

where I_0 is the maximum intensity, ϱ the reflecting power, and α the phase angle. This formula is, strictly speaking, valid only for HAIDINGER's interference rings formed in an exactly plane parallel air layer. However, it could also be used in the case of

FIZEAU's fringes produced in a wedge-shaped air layer, when the wedge angle is very small and therefore a sufficient number of beams are contributed.

In order to employ the Airy formula to a calculation of the intensity distribution in the neighbourhood of the maximum intensity of the fringe, it is convenient to replace the sine with the angle itself, which is a sufficient approximation[1]. Setting, at the same time, $I_0 = 1$, the formula is reduced to

$$I = \frac{(1-\varrho)^2}{(1-\varrho)^2 + \varrho \cdot \alpha^2}. \tag{2}$$

The half intensity breadth (instrument breadth) of the fringes could then be calculated by putting $I = {}^1/_2$, giving in angle units

$$2\,\alpha_{0.5} = 2 \cdot \frac{1-\varrho}{\sqrt{\varrho}}. \tag{3}$$

In estimating the accuracy of the measurement of planeness it is appropriate to introduce the relation half intensity breadth/fringe interval, which may be denoted as the relative half intensity breadth γ.

As one fringe interval corresponds to $\alpha = 2\pi$, we get for γ

$$\gamma = \frac{2\,\alpha_{0.5}}{2\pi} = \frac{1-\varrho}{\pi\sqrt{\varrho}}. \tag{4}$$

This quantity obviously depends only on the reflecting power ϱ of the silver film. For values of ϱ from 0.85 to 0.95, the reciprocal value of γ is calculated in the following table.

ϱ	${}^1/\gamma$	ϱ	${}^1/\gamma$
0.85	19.3	0.91	33.3
0.86	20.8	0.92	37.7
0.87	22.5	0.93	43.3
0.88	24.6	0.94	50.8
0.89	26.9	0.95	61.2
0.90	29.8		

On the assumption that the accuracy in setting the cross-wires of the measuring microscope upon the fringes amounts to ${}^1/_{10}$ of the half intensity breadth, it will be possible to measure deviations

[1] Cf. H. C. BURGER and P. H. VAN CITTERT, ZS. f. Phys. **44**, 58, 1927. H. KOPFERMANN, Kernmomente, Leipzig 1940, p. 82.

from a straight line with an accuracy of $^1/_{10}\,\gamma$, *i. e.* if $\varrho = 0.9$, about $^1/_{300}$ of the fringe interval. As this interval corresponds to $\frac{\lambda}{2}$, an accuracy of $^1/_{600}$ wavelength or about 10^{-6} mm. can be obtained.

For the interference fringes formed by unsilvered plates the relative half intensity breadth is $^1/_2$, since the intensity distribution follows a pure sine curve. If the setting again can be done accurately to $^1/_{10}$ of the half intensity breadth, an accuracy of $^1/_{20}$ fringe interval or $^1/_{40}$ wavelength should be obtained in the determination of planeness. This is in accordance with the usual experience. When using silvered plates, the accuracy is thus increased 10 to 20 times.

The preceding considerations are only valid if the interference fringes really can be regarded as curves of equal thickness, *i. e.* if the angle of incidence is exactly constant. Although the measurements were performed at normal incidence, the finite area of the diaphragm of the collimator might cause a failure in the parallelism of the light beam[1]. If the beam contains all angles of incidence ranging from 0 to a small value β, it follows from the interference condition that the number of order must vary slightly. For a beam exactly normal to the air layer, the order of interference is $m_1 = \frac{2\,d}{\lambda}$ and, for a beam with the angle of incidence β, $m_2 = \frac{2\,d\cos\beta}{\lambda}$.

Then,

$$\Delta m = m_1 - m_2 = \frac{2\,d}{\lambda}(1-\cos\beta) \text{ or, as } \cos\beta = 1-\frac{\beta^2}{2},$$

$$\Delta m = d\cdot\frac{\beta^2}{\lambda} \text{ or } \beta = \sqrt{\frac{\lambda\cdot\Delta m}{d}}.$$

In order to avoid unsharpness caused by lack of parallelism of the light beam, Δm should be negligible as compared with the relative half intensity breadth γ. For $\varrho = 0.9$, we have $\gamma = {}^1/_{30}$. If we permit $\Delta m = {}^1/_{100}$, we get for $\lambda = 5.10^{-5}$ cm. and $d = 0.1$ cm. that $\beta = 2.10^{-3}$. This condition is easily fulfilled at the applied focal length (700 mm.) of the collimator, if the diameter of the diaphragm does not exceed 2.8 mm.

[1] Ch. Fabry, Revue d'Optique, **1**, 445, 1922.

It should further be emphasized that, in the calculation of the half intensity breadth, it was assumed that the employed spectrum line was strictly monochromatic, while the real measurements are to be made with a line of finite breadth. If this natural line breadth is known, it is easy to estimate its influence upon the accuracy of the measurements. By differentiating the interference condition $m\lambda = 2d\cos i$ we get

$$\frac{\lambda}{\Delta\lambda} = -\frac{m}{\Delta m} \text{ or } |\Delta m| = m \cdot \frac{\Delta\lambda}{\lambda} = 2d \cdot \frac{\Delta\lambda}{\lambda^2}$$

for normal incidence. Δm must also here be small compared with the instrument breadth γ. Using the red *Cd*-line 6438 A.U., for which the natural half intensity breadth was measured to about 0.02 A.U., we get for $d = 0.1$ cm.

$$\Delta m = 2 \cdot 10^{-7} \cdot \frac{0.02}{6438^2} = \frac{1}{100},$$

which could be neglected compared with $\gamma = {}^1/_{30}$.

In order to be quite sure that the natural line breadth does not influence the measurements a distance ring as thin as possible should consequently be used; simultaneously, this involves a reduction in unsharpness which is due to the lack of parallelism of the light, as mentioned above. A distance ring of 0.5—1.0 mm. will be sufficient for this purpose[1]. Three strips of metal foils, 0.1 mm. thick, might also be applied, but they are not so easy to manage.

When using very thin metal sheets as distance spacers another source of error must be taken into account, *viz.* an increased danger of deformation of the interferometer plates due to unequal forces from the three adjustment screws. Such a deformation appears in the interference fringes which then lose their straight lined form and instead assume a characteristic fan-shaped appearance. With greater thickness the elasticity of the material will easier prevent great forces to arise.

Under proper conditions, however, it should be possible to obtain an accuracy in the measurements of planeness of at least

[1] See P. P. Koch, Ann. d. Phys. **42**, 1, 1913.

$^1/_{600}$ wavelength or 10^{-6} mm. This accuracy was actually attained by repeated measurements of small deviations from planeness.

The same accuracy should also be obtainable from all measurements based upon interference, when silvered plates are used.

The Dependence of the Resolving Power on the Planeness.

In order to estimate the influence of the errors in the surfaces on the resolving power of the Fabry-Perot plane parallel étalon it appears reasonable first to calculate the maximum resolving power, *i. e.* the resolving power obtained from ideal, faultless plates by collaboration of an infinite number of rays. The above derived expression (3) for the half intensity breadth (instrument breadth), which holds both for the Fizeau fringes and the Haidinger rings formed in the plane parallel layer, could be expressed in wave-numbers (cm.$^{-1}$) rather than in angle units, remembering that $\alpha = 2\pi$ corresponds to $\Delta\nu = \frac{1}{2d}$ cm^{-1}. We get for the half intensity breadth

$$\Delta\nu_{0.5} = \frac{1-\varrho}{2\pi d\sqrt{\varrho}} \text{ cm}^{-1}.^1$$

A preliminary value for the resolving power R is then obtained, assuming that two spectrum lines can just be separated, if their distance is equal or greater than the half intensity breadth.

$$R = \frac{\lambda}{\Delta\lambda_{0.5}} = \frac{\nu}{\Delta\nu_{0.5}} = \frac{2\pi d\sqrt{\varrho}}{\lambda(1-\varrho)}.$$

As is well-known, the half intensity breadth is unfit for this calculation, but, as shown by Lord Rayleigh, the line breadth should be used, for which $I = 0.4$, corresponding to a minimum in the resulting intensity curve of about 20 % of the maximum intensity[2]. For this line breadth we find, using Airy's formula (2), that $2\alpha_{0.4} = 2 \cdot \sqrt{1.5} \cdot \frac{1-\varrho}{\sqrt{\varrho}}$

[1] H. Kopfermann, Kernmomente. Leipzig 1940, p. 82.
[2] W. H. J. Childs, Journ. scient. Instr. **3**, 97, 1926.

or, converted into wave-numbers, $\Delta\nu_{0.4} = \frac{(1-\varrho)\sqrt{1.5}}{2\pi d\sqrt{\varrho}}$ cm^{-1}, *i. e.* $\sqrt{1.5}$ times greater than the half intensity breadth $\Delta\nu_{0.5}$. The real maximum resolving power will then be $\sqrt{1.5}$ times smaller than calculated by means of $\Delta\nu_{0.5}$.

$$R = \frac{2\pi d\sqrt{\varrho}}{\lambda(1-\varrho)\sqrt{1.5}} \qquad (5)$$

From this formula we get *e. g.* for $d = 0.5$ cm., $\lambda = 5.10^{-5}$ cm. and $\varrho = 0.9$ that $R = 500\,000$.

In order to estimate the smallest errors in planeness allowed, the interference equation $m\lambda = 2d\cos i$ should be differentiated, keeping m and i constant. We then find

$$\frac{\lambda}{\Delta\lambda} = \frac{d}{\Delta d} \text{ or } \Delta d = d \cdot \frac{\Delta\lambda}{\lambda} = \frac{d}{R}.$$

Replacing R by (5), we obtain $\Delta d = \frac{\lambda \cdot (1-\varrho)\sqrt{1.5}}{2\pi\sqrt{\varrho}}$.

This expression gives the error in planeness Δd which would cause a change in wavelength $\Delta\lambda$ corresponding to the maximum resolving power. The permissible errors should then be essentially smaller than the value Δd. The claims in planeness of the surface depend only on the reflecting power ϱ and increase strongly with ϱ. Thus, for $\varrho = 0.9$ and $\lambda = 5.10^{-5}$ cm. we get $\Delta d = 10^{-5}$ mm. $= {}^1/_{50}\,\lambda$ and for $\varrho = 0.95$ $\Delta d = {}^1/_{100}\,\lambda$.

In order to utilize fully such high reflecting powers, the deviations from planeness should consequently not exceed ${}^1/_{100}$—${}^1/_{200}$ wavelength. Also the adjustment of the étalon to parallelism should be carried out with the same precision.

Determination of the Maximum Resolving Power.

The maximum resolving power of the Fabry-Perot parallel plate étalon was determined experimentally in different spectrum regions. By the arrangement described for silvered plates in

Fig. 1, first an exposure of the Fizeau fringes was made by illumination with a spectrum line in the spectrum region in question, using so small a thickness of the air layer (f. ex. 0.1 mm.) that neither the natural line breadth nor the deficiency in parallelism of the light could play any part. Subsequently, a second exposure was made on the same plate under unaltered conditions and with the same time of exposure, but with only half the intensity of illumination, attained by means of a rotating sector placed in the parallel beam, between O_1 and F—P in Fig. 1. These two exposures were then measured by means of a Zeiss registrating micro-photometer, giving directly the relative half intensity breadth γ of the fringe.

The measurements gave values for γ constant for a given silver coating and independent of the thickness of the air layer, provided that it was smaller than a given value. The measured values for strong silverings were ranging from $^1/_{30}$ to $^1/_{50}$, as was to be expected for reflecting powers of about 0.9. The reflecting power of the surface was not measured, as the necessary equipment is unavailable at the present time.

By combining formulae (4) and (5), we get

$$R = \frac{2\,d}{\lambda \cdot \gamma \cdot \sqrt{1.5}}$$

by means of which the maximum resolving power R could be determined for every thickness d, using the measured value of γ.

For $\gamma = {}^1/_{50}$, $d = 0{,}5$ cm, and $\lambda = 5.10^{-5}$ cm, $R = 800\,000$ is found.

The Use of Fizeau Fringes in Spectroscopy.

The present interference spectroscopy is based upon the application of Haidinger interference rings for equal inclination, which are formed by plane parallel layers and are located in infinity. In the general interference condition $m \cdot \lambda = 2\,d \cos i$ this corresponds to a constant thickness of the air layer d, while the angle of incidence i is variable.

It seems not to be generally known that even the Fizeau

fringes for equal thickness principally can also be used in investigations of the structure of spectrum lines. These fringes are located in the wedge-shaped layer itself and correspond to a constant angle of incidence $i = 0$, while the thickness d is variable.

It may be supposed that these two extreme cases of all possible interference phenomena under ideal conditions are identical with respect to the breadth of the fringes and, consequently, also to the resolving power. The correctness of this assumption depends on the applicability of the Airy formula in both cases.

One may, however, be convinced of the correctness of these considerations after observing the Fizeau fringes at greater thickness of the air interspace, using light from a spectrum line of a known hyperfine structure. Fig. 4 shows an exposure of two fringes of the *Hg I*-line 5461 A.U., taken with a distance ring, 5 mm. thick. All the familiar components of this line could easily be seen, except for the components of the central line, which were not sufficiently separated by the light source (a low pressure mercury arc lamp run with 1 Amp.). Fig. 5 exhibits a similar photograph taken with the green *Tl I*-line 5351 A.U. in two orders with a 5 mm. ring. The source was an Osram Thallium lamp run with 0.6 Amp. The clear separation of the narrow components indicates that the resolving power is in the neighbourhood of half a million.

This manner of using a Fabry-Perot étalon is rather attractive, because the spectrum lines appear really as lines and not as circles. The determination of the intervals of a line structure by such an exposure has to be carried out in the usual manner by measuring the intervals in relation to the distance between consecutive orders, which is $\Delta\nu = \frac{1}{2d}$ cm.$^{-1}$. The method has the advantage that linear interpolation can be used, as the fringes are equally spaced, and the dispersion is constant.

A further advantage of this procedure is that the resolving power is independent of the deviations from planeness of the plates, because every surface element forms its own part of the fringe, irrespective of the other surface elements. At a given plate distance the resolving power of such a "wedge étalon" depends therefore only on the reflecting power of the silver film, unlike

the usual interference spectroscope applying Haidinger rings, for which both the planeness of the surfaces and the accuracy of the adjustment to parallelism greatly influence the resolving power. For a wedge étalon the resolving power is then fundamentally greater than for a parallel plate étalon and is really equal to the maximum resolving power mentioned above. Only with very good plates and an ideal adjustment may the parallel plate étalon give a resolving power approaching that of a wedge étalon.

Fig. 4. Hyperfine structure of Hg 5461. 5 mm. wedge étalon.

Fig. 5. Hyperfine structure of Tl 5351. 5 mm. wedge étalon.

Unfortunately, the wedge étalon can only be used as interference spectroscope in very few cases, because the intensity is too small. The advantages of the wedge étalon only appear when the fringes are pure Fizeau fringes, *i. e.*, when the angle of incidence is really constant. Consequently, the hole in the collimator must be very small, especially at thicker air layers, and therefore the interference fringes become rather faint. In fact, the photographs (Figs. 4 and 5) were exposed for $^1/_2$—1 hour, while for the photographing of the Haidinger rings with the same light sources an exposure of $^1/_4$—$^1/_2$ minute was sufficient. Owing to their weakness the Fizeau fringes can therefore only be used in the study of fine structure, if the spectrum line is very intense.

In order to obtain good results with the wedge étalon, the adjustments of the air layer perpendicular to the beam and of the light beam to parallelism should be carried out very carefully, especially at thicker étalon rings. If the layer is not strictly per-

pendicular to the beam, the fringes will lose their sharpness, and if the beam is convergent or divergent instead of quite parallel, the fringes will be curved instead of being straight lines. However, when using the method of autocollimation mentioned on p. 7, these adjustments could be carried out with sufficient accuracy.

For investigations of natural line breadth of spectrum lines, the wedge étalon method has the advantage of giving straight lines which are better suited for microphotometer work than the Haidinger rings. By this method the natural line breadth of the *Cd*-line 6438 A.U. was measured for the used light source by means of a 10 mm. ring. The result was corrected for the instrument breadth which was measured at very small thickness. A value of 0.05 $cm.^{-1}$, or 0.02 A.U. was found, but this value holds only if the current in the spectral lamp does not exceed 1 Amp.

Although the application of the wedge étalon to investigations of hyperfine structure is thus in most cases impracticable for intensity reasons, it is advisable to employ the method visually for estimating the quality of the silver coating of the plates. By observation of the green *Hg*-line at an étalon thickness of 5—10 mm. one can immediately ascertain whether the silver film gives the wished resolving power, as this inspection does not depend upon the adjusting of the étalon.

The application of a wedge-shaped plate as interference spectroscope is mentioned in a paper by GEHRCKE and JANICKI[1], who used the interference fringes formed by a wedge-shaped glass plate with silvered surfaces illuminated under different angles of incidence. In that case, however, the fringes were located at different distances from the wedge, depending on the angle of incidence, and therefore were not pure Fizeau fringes. The advantage of using pure Fizeau fringes, as done in this work, is based on the fact that cos i better can be held constant by normal incidence where cos i varies as slowly as possible.

[1] E. GEHRCKE and L. JANICKI, Ann. d. Phys. **39**, 431, 1912.

Summary.

Various methods for examining the planeness of interferometer plates have been investigated, and a simple arrangement has been described for such investigations both with unsilvered and silvered plates. The different sources of error were discussed, and an accuracy of the measurements of at least 10^{-6} mm. was obtained.

The influence of deviations from planeness upon the resolving power of a Fabry-Perot étalon was examined and a method was described for the determination of the maximum resolving power for ideal plates.

It has been shown that under certain conditions Fizeau fringes could be used in spectroscopy, and that maximum resolving power could be reached independent of the plate errors.

Acknowledgements.

The author wishes to express his gratitude to Professor NIELS BOHR for putting interferometers and the microphotometer at his disposal. Furthermore, I am very grateful to the CARLSBERG FOUNDATION and to the THOMAS B. THRIGE FOUNDATION for donations given for spectroscopical work in this laboratory. Finally, I wish to thank cand. mag. A. HERMANSEN for his assistance with the measurements, and Mr. P. W. STREANDER for the construction of the apparatus.

Physical Laboratory.
Royal Veterinary and Agricultural College.
Copenhagen, Denmark.

Indleveret til Selskabet den 31. Maj 1945.
Færdig fra Trykkeriet den 21. September 1945.

DET KGL. DANSKE VIDENSKABERNES SELSKAB
MATEMATISK-FYSISKE MEDDELELSER, BIND XXIII, NR. 4

DEDICATED TO PROFESSOR NIELS BOHR ON THE OCCASION OF HIS 60TH BIRTHDAY

DISINTEGRATION OF BORON BY SLOW NEUTRONS

BY

J. K. BØGGILD

KØBENHAVN
I KOMMISSION HOS EJNAR MUNKSGAARD
1945

CONTENTS.

Printed in Danmark.
Bianco Lunos Bogtrykkeri A/S

§ 1. Introduction.

The disintegration of boron by slow neutrons has been investigated by numerous authors using quite different techniques. Since the reaction is exotherm and sensitive to slow neutrons, it is rather appropriate to investigation, the energy release being well defined and the cross section being very large. That the reaction resulted in the formation of ^{7}Li and ^{4}He

$$^{10}_{5}\mathrm{B} + ^{1}_{0}\mathrm{n} \rightarrow ^{4}_{2}\mathrm{He} + ^{7}_{3}\mathrm{Li}$$

was shown by CHADWICK and GOLDHABER (1), TAYLOR and GOLDHABER (2), and by AMALDI, D'AGOSTINO, FERMI, PONTECORVO, RASETTI and SEGRÈ (3). However, a determination of the ranges of the ^{4}He and ^{7}Li particles is rather difficult in view of the shortness of the ranges. The determination of the total energy released in the reaction depends furthermore on the knowledge of the energy range relation for α-particles; unfortunately, this relation is not very reliable for α-particles of short range. Therefore it is not surprising that the various results do not agree too well.

The investigations of the reaction can be arranged in 3 groups, *viz*, A: Methods by which the ranges of the He and Li particles are investigated. WALEN (4), ROTBLAT (5), FÜNFER (6), HAXEL (7), LIVINGSTONE and HOFFMANN (8), and O'CEALLAIGH and DAVIES (9). It is a weak point in these investigations that the boron film is applied as a "thick" layer, which complicates the resolving of probably closely situated groups.

B: Determination of the total length of pared tracks of He and Li particles. TAYLOR and DABHOLKAR (10) (using boron impregnated photographic emulsion), ROAF (11), BOWER, BRETSCHER and GILBERT (12), KURTSCHATOV, MOROZOV, SCHEP-

KIN and KOROTKEVICH (13) (using cloud chambers filled with a gas rich in boron).

C: Determination of the reaction energy. FÜNFER (6) (measuring the size of kicks in a boron coated ionization chamber). MAURER and FISK (14) and WILSON (15) (measuring the size of kicks in a ionization chamber filled with a gas rich in boron).

The results of these investigations are shown in Table I, where the first part gives the range values and the second part the reaction energy.

Table I.

Authors	Range in mm. of air			Reaction energy			
	He-range		Total range	calculated by He-range*		measured by kick size	
	normal level	excited level		normal level	excited level	normal level	excited level
WALEN	8.5	..	..	2.87	..	..	..
ROTBLAT	8.2	..	..	2.78	..	..	..
FÜNFER	8.6	..	..	2.90	..	2.52	..
HAXEL	9.4	6.4	..	3.11	2.19	..	..
LIVINGSTONE, HOFFMANN	8.0	6.6	..	2.72	2.26	..	..
O'CEILLAIGH, DAVIES	8.9	7.15	..	3.00	2.45	..	..
TAYLOR	..	..	11.4	..	..	..	..
ROAF	..	..	11.5	..	..	..	..
BOWER, BRETSCHER, GILBERT	..	7.0	11.3	..	2.40	..	..
KURTSCHATOV, MOROZOV, SCHEPKIN, KOROTKEVICH	(8.8)	(7.4)	11.3 9.4	(2.96)	(2.53)	..	..
MAURER, FISK	..	..	..	..	..	2.80	2.70 2.40 2.26
WILSON	..	..	..	..	..	2.88**	2.46

* The energy values are recalculated, using the energy-range relation of BLEWETT and BLEWETT. Proc. Roy. Soc. A. The publication is not at the author's disposal, and the partly extrapolated data are taken from the work of O'CEALLAIGH and DAVIES.

** Relative measurement, arbitrarily identified with the reaction energy to be expected from the masses (MATTAUCH and FLÜGGE).

It seems rather reasonable for the present to place the He ranges in two groups, *viz.* a main group corresponding to a reaction where the ^{7}Li atom is left in an excited level, and a

weaker long range group leaving the ^{7}Li nucleus in the normal state.

The energy release to be expected from the masses is 2.99 MeV., according to the nuclear masses reported by LIVINGSTONE and BETHE (16), and 2.88 MeV., according to MATTAUCH and FLÜGGE's (17) statements.

The second part of Table I gives the values of the reaction energy calculated from the He ranges and from the size of kicks. When taking into consideration the energy release to be expected, the energy values of Table I seem to indicate that the main group corresponds to a reaction leaving the Li nucleus in an excited level with an energy of 0.4—0.7 MeV. The energy values given for the long range group appear to be fairly consistent with the expected energy; but, after all, the data of Table I concerning the long range group are rather conflicting. The three workers stating to have found both groups give a relative intensity quotient of the long range group to the main group of 1:3 or 1:4. On the other hand, the authors who investigated the total range, using cloud chambers, did not find any long range group, and BOWER, BRETSCHER and GILBERT estimated the intensity of the long range group, if existing, to be less than 1:10. The four groups given by MAURER and FISK agree neither with the cloud chamber reports nor with a similar investigation by WILSON, leading to a main group and a much weaker high energy group (relative intensity 1:15). KURTSCHATOV, MOROZOV, SCHEPKIN and KOROTKEVICH, using a not too convincing estimation of the partition ratio, attribute the main group (total range 11.3 mm.) to the normal state reaction and report in addition the finding of a short range group (total range 9.4 mm.) which corresponds to a reaction leaving the Li nucleus in an excited level.

Evidence of disintegration of boron by slow neutrons following the equation

$$^{10}_{5}\mathrm{B} + ^{1}_{0}\mathrm{n} \rightarrow ^{1}_{1}\mathrm{H} + ^{10}_{4}\mathrm{Be}$$

is given by MAURER and FISK and by KURTSCHATOV, MOROZOV, SCHEPKIN and KOROTKEVICH.

§ 2. Experimental Method.

In preliminary investigations, a 24 cm. cloud chamber was filled with helium and equal parts of liquid $B(O\,CH_3)_3$ and methyl alcohol, the total pressure being about 30 cm. Hg. The high stopping power of the boron ester, however, caused the length of the tracks to be smaller than planned. Better conditions were obtained by using the ethyl ester of boron, $B(O\,C_2H_5)_3$, mixed with equal parts of methyl alcohol. When adding helium to a total pressure of about 30 cm. Hg, the tracks of boron disintegration appeared with a length of about 50 mm. in the chamber. The diaphragm made from commercial rubber was slightly attacked by the boron gas, and frequent refilling with boron ester was necessary.

The neutrons were produced by the high tension apparatus in this institute by bombarding beryllium with deuterons. The target and the chamber were surrounded by paraffin. The emission of neutrons was synchronized to the expansion by a switch in the high tension power supply of the ion source. Stereoscopic photographs were taken with an optical system containing a Contax camera and a mirror placed vertically on one side of the cloud chamber and giving complete direct and mirror images of the chamber. The film plane of the camera was corrected in order to match the oblique projection.

Measurements of the films were carried out by means of the same arrangement, using the same camera and mirror as in the original photograph. The natural size images of the tracks were examined in space, employing the method described by NUTTAL and WILLIAMS (18) which, with some modification, has been used in this institute (19). The method was found to be both convenient and accurate and to yield the additional advantage that the observer, simultaneously with the measurement, is able to control the shape and the position of the tracks. In view of the appreciable change in stopping power of the gas with changing room temperature, the stopping power of the gas was frequently controlled (at about every 40 picture) with Po-α particles. The α-source was placed inside the chamber in a small brass holder which was kept on a slightly higher temperature in order to

prevent vapour condensation. The α-particles were synchronized to the expansion by an electromagnetic shutter. The range r_n of the tracks in standard air was calculated according to the equation

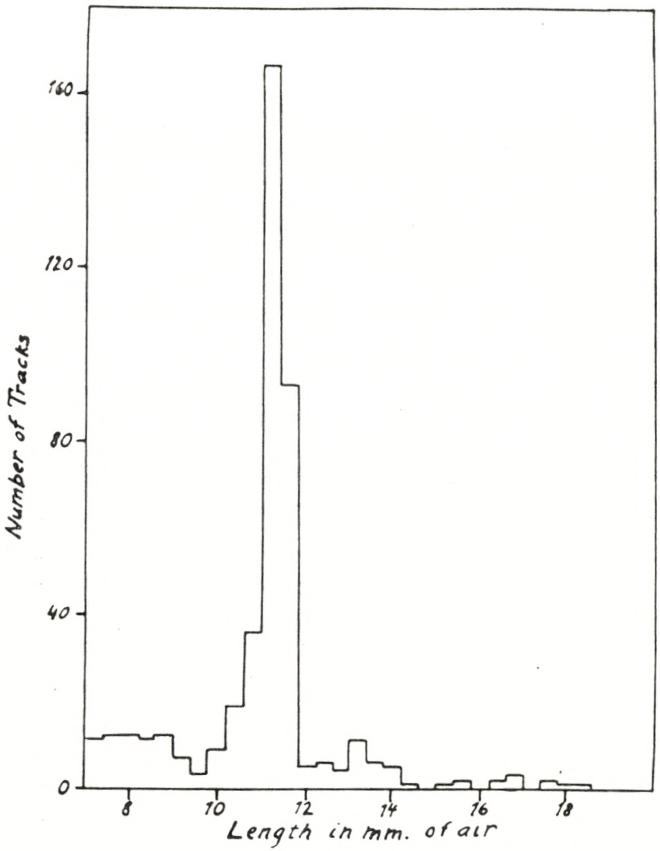

Fig. 1. Statistics of tracks produced by boron disintegrations and recoiling atoms.

$$r_n = 39.0 \frac{r}{r_\alpha} \text{ mm.},$$

where r is the measured length of the tracks and r_α the length of the α-tracks, the range of Po-α particles being 39.0 mm. at 760 mm. Hg. and 15° C.

A histogram of about 450 tracks is shown in Fig. 1. In agreement with most previous investigations performed with the same method, only a single group with a range of 11.2—11.4 mm.

appears above the background of recoil tracks. In accordance with BOWER, BRETSCHER and GILBERT it was found reasonable to estimate a possible long range group to be at least 10 times weaker. A faint trace of a group is visible in the neighbourhood of $13^1/_2$ mm. A definite conclusion, however, is impossible for statistical reasons.

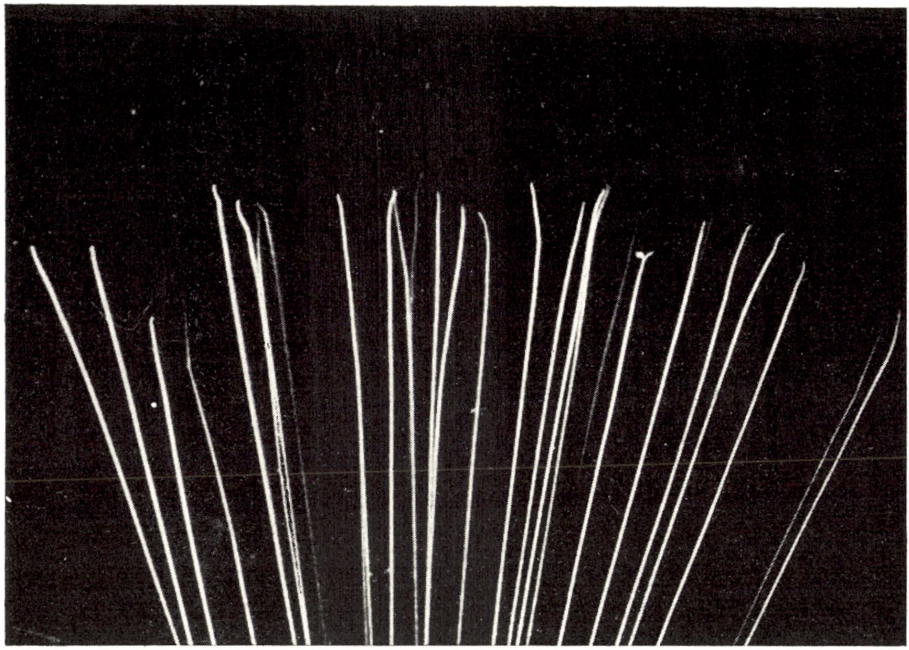

Fig. 2. Later part of the tracks of a beam of α-particles. Demonstrates the tendency to fortuitous bending and curvature close to the very end of the tracks.

A closer examination of the tracks yielded a new method which makes it possible among all tracks in the chamber to pick out those of the boron disintegration. The method is based on the fact that the very ends of the tracks of nuclear particles tend both to fortuitous bending and curvature and to a more frequent branching due to nuclear collisions. Hence, it follows that the tracks of the boron disintegration may be expected to show these characteristic features of low velocity in both ends of the tracks, while the recoil tracks, having high velocities in the first traversed part of the track, will only appear with bending in one end.

Fig. 2 is a reproduction of the later part of a beam of α tracks from the control study, and Fig. 3 reproduces the tracks of a boron disintegration showing fortuitous bending in both ends[1].

A selection embracing only those tracks which show for-

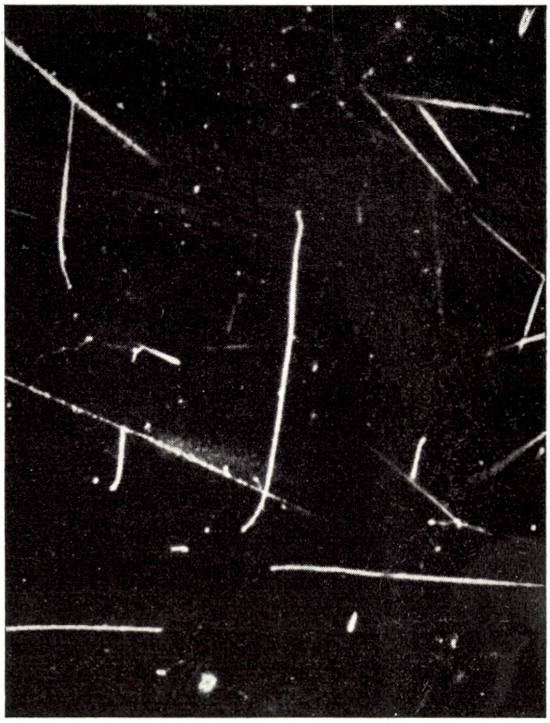

Fig. 3. Track of boron disintegration. The type of track is established by means of the characteristic feature, i. e., the fortuitous bending of both ends of the track demonstrates that the velocity is small in both ends. The track is thus produced by two ionizing particles originating somewhere in the track and moving in opposite directions.

tuitous bending or branching in both ends will rather certainly include a great deal of the boron disintegration. The excluded part without traceable bending in both ends must comprise all the tracks of recoil atoms and some of the boron disintegrations.

[1]) The optical examination makes it possible to detect deformities of the end parts of the tracks considerably less pronounced than by the obvious specimen reproduced here in order to illustrate the method. Fig. 2 demonstrates further the fact that fortuitous bending and curvature are more useful indications of low velocity than branching due to nuclear collision.

The examination of the tracks is facilitated when the neutron source is relatively weak and hence the chamber less occupied of tracks.

A histogram including about 400 selected tracks of a length

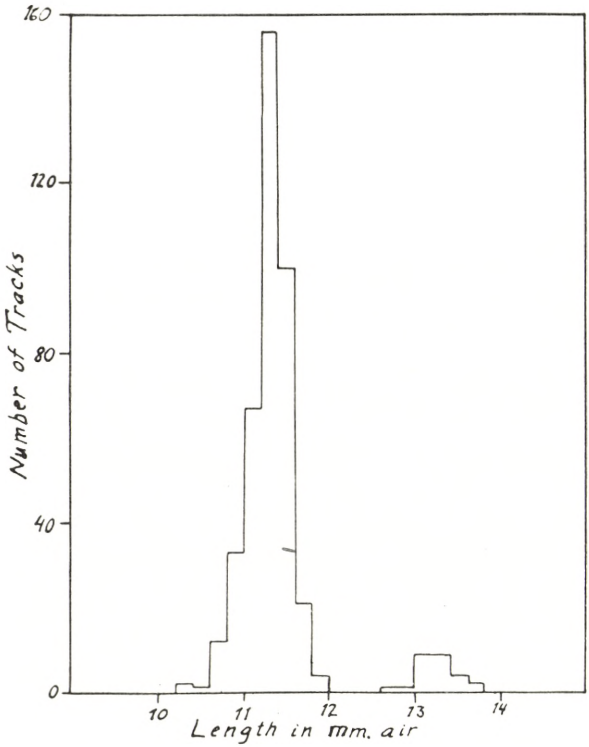

Fig. 4. Statistics of selected tracks. The selection includes only the type of tracks showing fortuitous bending in both ends and involves a complete removing of the background of recoil tracks. In addition to the main group a 15 times weaker long range group is found, the mean range of the two groups being 11.3 and 13.2 mm., respectively.

between 7 and 19 mm. is reproduced in Fig. 4. It demonstrates that the method succeeded in a complete removal of the background. The histogram further shows clearly a very weak group of long range. The total mean ranges of the two groups are found to be 11.3 and 13.2 mm., and the relative intensity 1:15. The long range tracks of the weak group appear to be very similar to the tracks of the main group, indicating that the reaction is

of the same type—$^{10}B(n,\alpha)^{7}Li$—only leaving the ^{7}Li-nucleus in the normal state or in a level of lower excitation. Fig. 5 is a reproduction of a long range track of the weak group. That an identification of the long range group with the boron disinte-

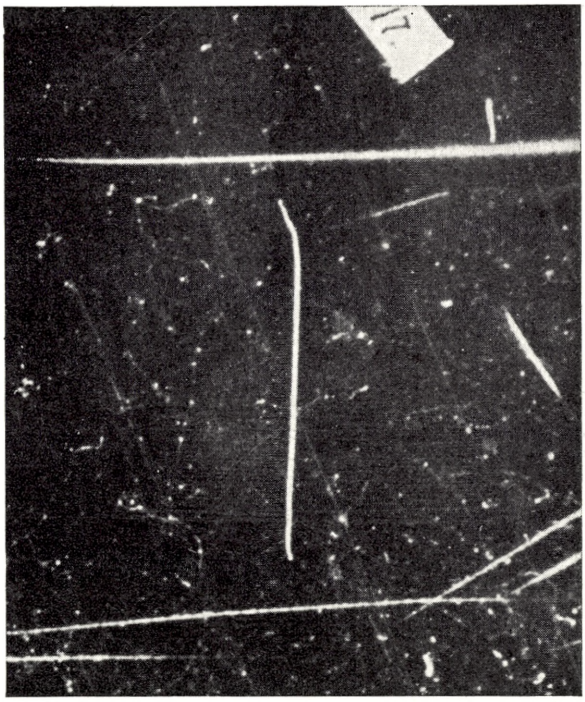

Fig. 5. Track of the long range group. Shows the characteristic bending in both ends.

gration—$^{10}B(n,p)^{10}Be$— is excluded is established in the following part of this work.

§ 3. Examination of Track Types.

It has been demonstrated that the selection of tracks showing fortuitous bending in both ends makes it possible to remove completely the background of recoil atoms. The selected part of the tracks is found to include a great deal of the boron disintegration, but any disintegration in two heavy particles of atoms in the gas by slow neutrons might show tracks of similar features.

The gas in the cloud chamber is known to contain H, He, B, C, N, and O (nitrogen as an impurity in the helium gas). Taking this into account, it might be possible that the weak long range group is produced not by the reaction—$^{10}B(n,\alpha)^{7}Li$—, but by one of the following reactions—$^{10}B(n,p)^{10}Be$—or—$^{14}N(n,p)^{14}C$—. The

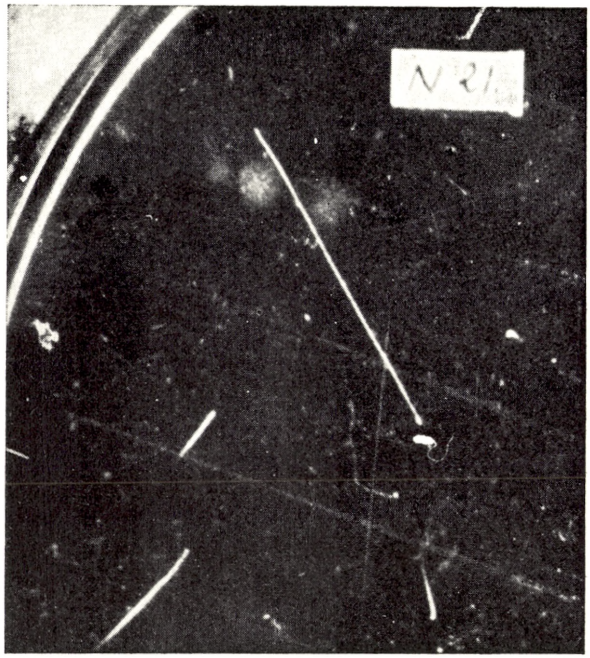

Fig. 6. Track of a nitrogen disintegration. The small lump in the lower end of the track is produced by the recoiling ^{14}C-nucleus.

disintegration of nitrogen by slow neutrons has been studied by CHADWICK and GOLDHABER (20), BONNER and BRUBAKER (21), and BURCHAM and GOLDHABER (22) who have finally identified it with the reaction—$^{14}N(n,p)^{14}C$—. BONNER and BRUBAKER, using cloud chambers, observed a total range of 10.6 mm. This range is so much smaller than the observed range of 13.2 mm. of the long range group of Fig. 4 that it is difficult to attribute this group to nitrogen disintegration. In order to settle the question it was decided to study selected tracks in a gaseous mixture fairly rich in nitrogen and poor in boron ester. The cloud chamber was

filled with air and methyl alcohol to a total pressure of about 18 cm. Hg. Though the piston and the rubber diaphragm were exchanged with new parts never exposed to boron ester, many boron disintegrations were found to occur (due to boron ester dissolved in the rubber gaskets), and both the main group and

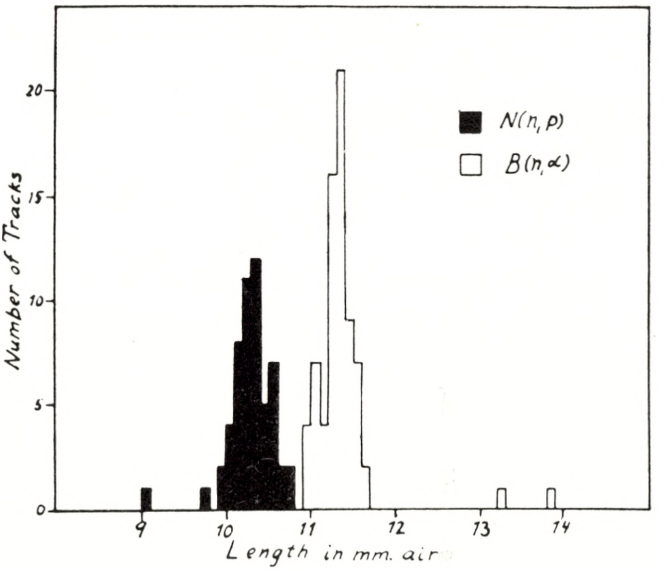

Fig. 7. Statistics of selected tracks of boron and nitrogen disintegration. The mean range of the tracks of nitrogen disintegration is found to be 10.3 mm. and for the main group of boron disintegrations 11.3 mm. The long range group is weakened following the main group and unaffected by the presence of nitrogen.

a few tracks of the long range group appeared, while the nitrogen disintegrations failed to appear. Rather close to the range value given by BONNER and BRUBAKER for the tracks of the nitrogen disintegration, a group of tracks appeared in the excluded part of the tracks, and many of these tracks stood out with a small lump in one end. The feature of the tracks makes it possible to select those of nitrogen disintegration by picking out the tracks showing fortuitous bending in one end and equipped with a small lump in the other end, the part of the track close to the lump being rather straight due to the corresponding high velocity of

the proton[1]. The length of the lump is usually about 1—1 1/2 mm. in the chamber. Fig. 6 is a reproduction of the tracks of a nitrogen disintegration showing the small lump in the lower end of the track. A histogram of about 70 selected boron disintegrations and 55 selected nitrogen disintegrations is shown in Fig. 7. The mean range of the nitrogen disintegration is found to be 10.3 mm., and for the main group of boron disintegration 11.3 mm., in accordance with the value obtained from Fig. 4. The long range group is weakened following the main group, and is unaffected by the presence of nitrogen. Besides, the features of the tracks state that the long range group belongs to the same type of disintegration as the main group and can neither be ascribed to the reaction—$^{14}N(n,p)^{14}C$—nor to the reaction—$^{10}B(n,p)^{10}Be$—, since the features of the tracks of the latter reaction are expected to be similar to the features of the tracks of nitrogen disintegration.

§ 4. Search for Tracks of the Reaction $^{10}B(n, p)^{10}Be$.

A study of the features of the tracks in a gaseous mixture containing nitrogen and boron ester has demonstrated the possibility of distinguishing between tracks produced by the two types of disintegration (n,α) and (n,p), and the weak long range group of Fig. 4 is established as produced by the reaction—$^{10}B(n,\alpha)^{7}Li$—. More extensive experiments were carried out in order to examine possible tracks produced by the boron disintegration—$^{10}B(n,p)^{10}Be$—by slow neutrons. The chamber was filled with helium and equal parts of liquid $B(O\,C_2\,H_5)_3$ and ethyl alcohol to a pressure of about 50 cm. Hg. Two types of tracks were selected separately, one of them being the boron disintegration—$^{10}B(n,\alpha)^{7}Li$—showing fortuitous bending in both ends, and the other one the tracks only bended in one end and lumpy in the other.

A histogram of about 1000 selected tracks is given in Fig. 8, showing the main group and the long range group of ranges 11.4 and 13.4 mm., respectively. The relative intensity of the two groups is 1:15 in agreement with the ratio given in § 2 (Fig. 4).

[1] The selection of tracks of this type is less certain than the selection of the tracks of the boron disintegration. Difficulties in recognizing the lump cause a somewhat larger part of the tracks to escape the selection.

Tracks of the type (n,p) were found as a very weak group with a range of about 10 mm. This is so close to the range (10.3 mm.) of the nitrogen disintegration given in Fig. 7 that it is most reason-

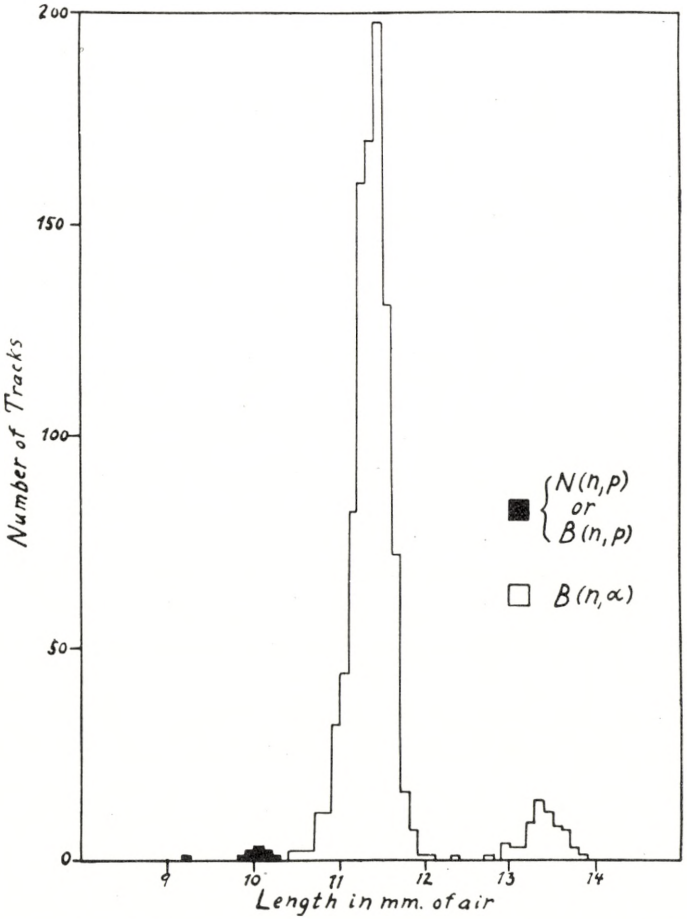

Fig. 8. Statistics of selected tracks of the two types of disintegration (n, α) and (n, p). The mean range of the two groups of boron disintegration is found to be 11.4 and 13.4 mm., respectively. The small group of tracks of the type (n, p) having a range of about 10.0 mm. is attributed to the reaction ^{14}N (n, p) ^{14}C. No trace of the disintegration ^{10}B (n, p) ^{10}Be appears in the figure.

able to assume the nitrogen disintegration—$^{14}N(n,p)^{14}C$—to be responsible for the group. No trace of the enquired boron disintegration—$^{10}B(n,p)^{10}Be$—has been found, though the selection method stands a good chance of finding the group even if the

range happens to be rather close to the range of the main group or the long range group. Evidently, the boron disintegration— $^{10}B(n,p)^{10}Be$—by slow neutrons is pretty rare (somewhat less than 1 % of all disintegrations) or the total range is so small that it is impossible to detect the lump.

§ 5. Preliminary Discussion.

The disintegration of boron (and nitrogen) by slow neutrons has been studied in the following gaseous mixtures: (1) helium and the vapours of equal parts of CH_3OH and $B(OC_2H_5)_3$, total pressure about 30 cm. Hg. (2) air and the vapours of CH_3OH and an unknown small amount of $B(OC_2H_5)_3$, total pressure about 18 cm. Hg, and (3) helium and the vapours of equal parts of C_2H_5OH and $B(OC_2H_5)_3$, total pressure about 50 cm. Hg. The values of the mean total ranges of the tracks are given in Table II.

Table II. Total range in mm. of air.

Gas mixture	$^{14}N(n,p)^{14}C$	$^{10}B(n,\alpha)^{7}Li$	
(1)	..	11.3	13.2
(2)	10.3	11.3	..
(3)	(10.0)	11.4	13.4
Average mean range..	10.3	11.35	13.3

The stopping power of the gaseous mixtures was controlled with Po-α particles (range 39 mm. of air) instead of α-particles of the same short range as the disintegration particles. This might lead to a systematic error in the performed reduction of the ranges to normal air conditions. On the other hand, it has been demonstrated by GURNEY (23) that the stopping power of helium for α-particles is rather independent of the particle range. Since a considerable amount of helium does not influence the reduction, and since, moreover, the measured range of the main group using the gaseous mixtures rich in He (1) and (3) lead to nearly the same value as the gas mixture (2) containing air, it was found reasonable to use the average of the range values given in Table II as mean total range reduced to normal air conditions.

The results of our experiments are given in Table III together with corresponding information from other workers using similar techniques.

Table III. Total range in mm. of air.

Author	$^{10}B(n,\alpha)^{7}Li$			$^{10}B(n,p)^{10}Be$
	Long range group	Main group	Short range group	
TAYLOR, DABHOLKAR	..	11.4	..	..
ROAF	..	11.5	..	..
BOWER, BRETSCHER, GILBERT	no or < 1:10*	11.3	..	..
KURTSCHETOV, MOROZOV, SCHEPKIN, KOROTKEVICH	..	11.3	9.4	5.7
This work	13.3 (1:15)*	11.35	no or < 1:100*	no or < 1:100* or very short

* Intensity estimation relative to the main group.

It will be seen that the range determinations of the main group agree surprisingly well and that only the method of track selection has been able to state the existence of the long range group and to point out the absence or weakness of other groups.

§ 6. Examination of the Partition Ratio.

The total range of the tracks is inappropriate for the determination of the reaction energy. For this purpose, the range of the He-particle must be known either from direct measurements or from determinations of the partition ratio of the two particle ranges together with the total range. BOWER, BRETSCHER and GILBERT succeeded in detecting the common point of origin of the He- and Li-particles by a special technique for measuring the track density along the photographic image of a cloud track; they report that on many tracks the discontinuity in density could easily be seen by eye. The latter technique has not been useful in this work. A discontinuity in density was never observed by eye, not even in the tracks of a short run with a still smaller stopping power, giving a total range in the chamber of about

100 mm. No photometrical measurements were carried out. An examination of the partition ratio was performed by studying the boron disintegrations from a very thin layer of boron evapo-

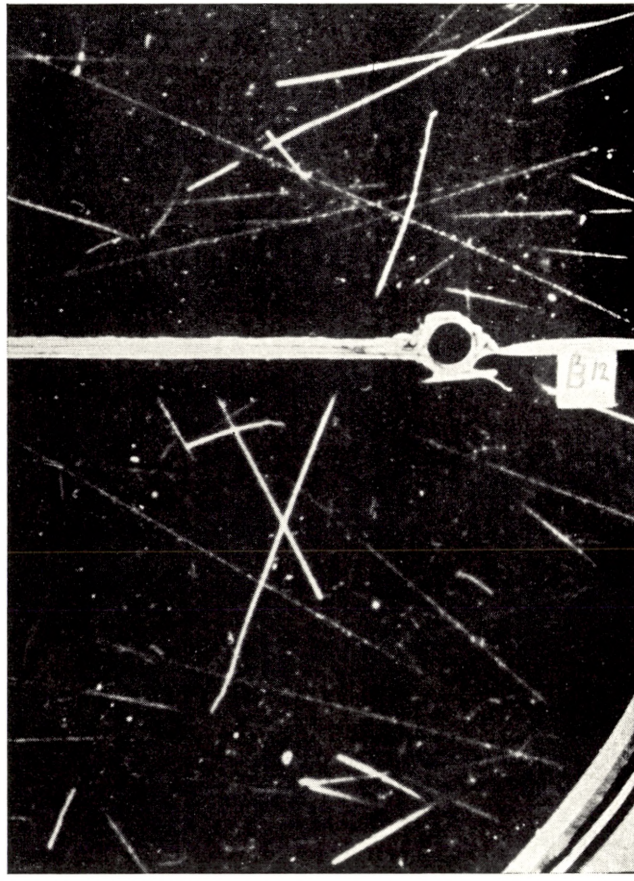

Fig. 9. Pared tracks of a boron disintegration. The boron is evaporated as a very thin layer (0.04 mg/cm^2) on a gold leaf. The white band in the middle of the photo is the frame supporting the gold and boron foils. The short range Li-atom goes upwards and the He-atom downwards through the gold foil. It will be noticed that the tracks are not visible right up to their common point of origin, but that the foil on both sides is surrounded by a condensation-free space.

rated on a gold leaf and supported by a frame in the middle of the chamber. The thickness of the boron film was 0.04 mg/cm^2 and that of the gold leaf 0.16 mg/cm^2, corresponding to about

0.4 and 0.2 mm. of air, respectively. The chamber was filled with helium and ethyl alcohol to a pressure of about 15 cm. Hg.

The number of boron disintegrations from the thin foil is extremely small compared with the number of recoil tracks in the chamber, but it is still possible to recognize the tracks of boron disintegration and to remove to a large extent the background of recoil tracks. The selection has to contain pared tracks starting from the boron foil in opposite directions and showing the characteristic features of low velocity in the ends. Fig. 9 is a reproduction of the pared tracks of a boron disintegration showing fortuitous bending in the ends. The white band in the middle of the photo is the frame supporting the gold and boron foils. The short range Li-atom goes upwards and the He-atom goes downwards through the gold foil.

The result of the measurements is given in Table IV[1]. The Table contains 6 pared tracks, the first 5 of which are estimated to be reliable. The total length of track No. 6 points to a boron disintegration, but the partition ratio diverges so much that the track is supposed to be due to a sporadic contamination with boron ester. The point of origin is then not in the foil, but somewhere in the track.

Table IV.

Track No.	Partition ratio
1	1.64
2	1.52
3	1.68
4	1.64
5	1.50
6	(1.18)

Mean partition ratio 1.60.

This supposition is supported by the fact that a few boron disintegrations originating in the gas of the chamber are found in this part of the investigation despite all possible care, such as

[1] More extensive experiments were planned, but restrictions in the power supply have prevented their performance.

application of new rubber parts, new velvet and daily renovation of the gas and alcohol filling in the chamber.

The mean partition ratio was found to be 1.60 in reasonable accordance with the value 1.62 given by BOWER, BRETSCHER and GILBERT. Combining the average 1.61 of these determinations and the value 11.35 mm. for the total range, the mean range in standard air was found to be 7.0 mm. for the He-atom and 4.35 mm. for the Li-atom.

§ 7. Discussion.

The final problem of the investigation is the determination of the energy released by a reaction leaving the Li-nucleus in the normal state; unfortunately, the examination of the partition ratio of the long range groups has failed, and even a considerably more extensive examination, using the method described in § 6, is hardly able to give an exact measurement of the ratio due to the weakness of the group.

The partition ratio could be determined by means of velocity-range relations for He- and Li-particles combined with the known total range. Though this relation is somewhat questionable for α-particles of short range and unknown for Li-atoms, it was found worth examining a semi-theoretical solution. The velocity range relation for α-particles to be used is based on the Cornell University energy range curves. The velocity range relation for Li-particles is produced from the He-relation by means of BLACKETT's (24) semi-empirical formula

$$R = \text{const} \cdot m \cdot z^{-\frac{1}{2}} \cdot f(v),$$

where R is the range, m the mass, z the atomic number, and v the velocity; the function f(v) is independent of the kind of nucleus. Using these relations, two sets of ranges and velocities R_{He}, v_{He} and R_{Li}, v_{Li} are chosen, satisfying the two conditions: $R_{He} + R_{Li} = R_T$ (R_T = 11.35 mm. and 13.3 mm. for the main group and the long range group, respectively) and $\frac{v_{He}}{v_{Li}} = \frac{7}{4}$. Table V shows the semi-empirical range values and the ex-

perimental results given in § 6 of this work and by BOWER, BRETSCHER and GILBERT. A comparison between the semi-empirical and the experimental range values of the main group indicates the usefulness of the method, especially by extrapolation to the rather closely situated long range group. The calculated partition ratios are therefore supposed to be about 3—4 % too high in both groups and the value to be used for the long range group turns out to be 1.68, giving a He range of 8.35 mm. of air.

According to the Cornell University curves, the energy of a 7.0 mm. and a 8.35 mm. α-particle is 1.32 MeV. and 1.59 MeV., respectively. The energy of the He-particle being $\frac{7}{11}$ of the energy released by the disintegration of boron, the main group and the long range group correspond to reaction energies of $\frac{11}{7} \cdot 1.32 =$ 2.07 MeV. and $\frac{11}{7} \cdot 1.59 = 2.50$ MeV., respectively. The measurements of BLEWETT and BLEWETT indicate an energy some 15 % higher for a given α-range, and lead to a reaction energy of

Table V.

	Semi-empirical			BOWER, BRETSCHER, GILBERT			Our work		
	R_{He}	R_{Li}	$R_{He}:R_{Li}$	R_{He}	R_{Li}	$R_{He}:R_{Li}$	R_{He}	R_{Li}	$R_{He}:R_{Li}$
Main group..	7.1	4.25	1.67	7.0	4.3	1.62	7.0	4.35	1.60
Long range group.....	8.45	4.85	1.74	..	..	..	8.35*	4.95*	1.68*

* Corrected semi-empirical values.

2.40 MeV. for the main group and 2.82 MeV. for the long range group. Considering a reaction energy of 2.88 MeV. to be expected from the masses given by MATTAUCH and FLÜGGE, the experiments tend to confirm the measurements of BLEWETT and BLEWETT, and it was found reasonable to conclude that the long range group corresponds to a reaction leaving the Li-nucleus in the normal state, and that the Li-nucleus has an excited level at 2.82 — 2.40 = 0.42 MeV. The relative intensity of the two

groups indicates that about 93 % of all boron disintegrations by slow neutrons lead to the excited level.

Further evidence about excited states in the ^{7}Li-nucleus obtained from the results of other workers studying the same or other reactions are given in Table VI, and will be seen to

Table VI.

Author	Reaction	Measured object	Excitation energy in MeV.
MAURER, FISK	^{10}B(n,α)^{7}Li	α-groups	0.2 0.41 0.64 0.84?
WILSON	^{10}B(n,α)^{7}Li	α-groups	0.42
This work	^{10}B(n,α)^{7}Li	α-groups	0.42
BOTHE (25)	^{7}Li(α,α)^{7}Li	γ-rays	0.2 0.39 0.59 0.85
FOWLER, LAURITSEN (26)	^{7}Li(p,p)^{7}Li	γ-ray	0.495
Several workers (27)	^{6}Li(d,p)^{7}Li	p-groups	0.445
WILLIAMS, SHEPHERD, HAXBY (28)	^{6}Li(d,p)^{7}Li	γ-rays	0.40
GRAVES (29)	^{9}Be(d,α)^{7}Li	α-groups	0.494
ROBERTS, HEYDENBURG, LOCKER (30)	^{7}Be + e$^-$ ^{7}Li + K	γ-rays	0.425
MAIER-LEIBNITZ (31), RUBIN (32)	^{7}Be + e$^-$ ^{7}Li + K	γ-rays	0.465

confirm the existence of a single excited level with an excitation energy of 0.4—0.5 MeV. BOTHE's results indicating the existence of more than a single excited level is, though doubtful, not out of question, but the results of MAURER and FISK are inconsistent with the work of WILLIAMS and the results of this work, and are most likely due to some uncertainty in the physical conditions of the experiments. Similar circumstances are probably responsible for the registration reported by the same authors of the boron disintegration ^{10}B(n,p)^{10}Be, since this reaction according to § 5 Table III is rather infrequent or the tracks are very short.

§ 8. Disintegration of Nitrogen by Slow Neutrons.

Tracks of the nitrogen disintegration have been studied in § 3 and the tracks are found to consist of a proton track and a

small lump corresponding to the recoiling ^{14}C-nucleus. The length of the lump is usually about $1—1\,^1/_2$ mm. in the chamber, corresponding to 0.3 mm. of air. The total track length being 10.3 mm., the track of the proton was found to be 10.0 mm. of air. According to the range velocity relation for protons given by LIVINGSTONE and BETHE, a 10.0 mm. proton corresponds to an energy of 0.56 MeV. and gives a reaction energy of $\frac{15}{14} \cdot 0.56 =$ 0.60 MeV., which is slightly lower than the value of 0.62 MeV. used for determinations of the mass of the ^{14}C-nucleus.

Summary.

The disintegration of boron by slow neutrons has been studied in a cloud chamber filled with boron ester.

A selection method based on the difference in feature of the tracks of boron disintegration and the tracks of recoiling atoms has made a complete removal of the background possible. A main group and a 15 times weaker long range group have been found, the total length being 11.35 and 13.3 mm. of air, respectively, the former in agreement with several authors. The long range group has been demonstrated to belong to the same type of disintegration as the main group—$^{10}B(n,\alpha)^7Li$—. The absence or weakness of the boron disintegration—$^{10}B(n,p)^{10}Be$—has been demonstrated by a search for tracks similar to those of the nitrogen disintegration—$^{14}N(n,p)^{14}C$—also studied by a selection method. An examination of the tracks going out from a very thin boron foil placed in the chamber has enabled a rough determination of the partition ratio (1.60) of the main group in reasonable agreement with BOWERS, BRETSCHER and GILBERT. A semi-empirical extrapolation leads to a determination of the partition ratio (1.68) of the long range group. Hence, the He-particles have ranges of 7.0 mm. for the main group, and 8.35 mm. for the long range group, and the reaction energies deduced by means of the energy-range relation of BLEWETT and BLEWETT were found to be 2.40 and 2.82 MeV. Consequently, about 93 % of all boron disintegrations by slow neutrons lead to an excited state with an energy of 0.42 MeV. and, in agreement with

several workers, no other excited level in the ^{7}Li-nucleus is found to appear in this or other reactions leading to the same nucleus.

The author wishes to express great appreciation to cand. mag. K. Lindberg Nielsen for his continued assistance during the experiments and to Mr. S. Holm, whose help in the laboratory work has been of great value.

Institute of Theoretical Physics,
University of Copenhagen.

References.

1) C. CHADWICK and M. GOLDHABER, Nature **135**, 65 (1935). Proc. Cambridge Phil. Soc. **31**, 612 (1935).
2) H. J. TAYLOR and M. GOLDHABER, Nature **135**, 341 (1935).
3) E. AMALDI, O. D'AGOSTINO, E. FERMI, B. PONTECORVO, F. RASETTI and E. SEGRÈ, Proc. Roy. Soc. London (A) **149**, 522 (1935).
4) R. J. WALEN, C. R. **202**, 1500 (1936).
5) J. ROTBLAT, Nature **138**, 202 (1936).
6) E. FÜNFER, Ann. d. Phys. **29**, 1 (1937).
7) O. HAXEL, ZS. f. Phys, **104**, 540 (1937).
8) M. S. LIVINGSTONE and J. G. HOFFMANN, Phys. Rev. **53**, 227 (1938).
9) C. O'CEALLAIGH and W. T. DAVIES, Proc. Roy. Soc. London (A) **167**, 81 (1938).
10) A. H. TAYLOR and V. D. DABHOLKAR, Proc. Roy. Soc. London (A) **48**, 285 (1936).
11) D. ROAF, Proc. Roy. Soc. London (A) **153**, 568 (1936).
12) I. C. BOWER, E. BRETSCHER and C. W. GILBERT, Proc. Cambridge Phil. Soc. **34**, 290 (1938).
13) I. KURTSCHATOV, A. MOROZOV, G. SCHEPKIN and P. KOROTKEVICH, Journ. exp. theoret. Phys. (russ.) **8**, 885 (1938).
14) W. MAURER and J. B. FISK, ZS. f. Phys. **112**, 436 (1939).
15) R. S. WILSON, Proc. Roy. Soc. London (A) **177**, 382 (1941).
16) M. S. LIVINGSTONE and H. A. BETHE, Rev. Mod. Phys. **9**, 373 (1937).
17) J. MATTAUCH and S. FLÜGGE, Kernphysikalische Tabellen, Springer, Berlin (1942).
18) J. M. NUTTAL and E. J. WILLIAMS, Proc. Phys. Soc. London **42**, 212 (1930).
19) J. K. BØGGILD, K. J. BROSTRØM and T. LAURITSEN, D. Kgl. Danske Vid. Selskab, mat.-fys. Medd. (Math.-phys. Comm. Acad. Sci. Copenhagen) **18**, 4 (1940).
20) C. CHADWICK and M. GOLDHABER, l. c.
21) T. W. BONNER and W. M. BRUBAKER, Phys. Rev. **48**, 469 (1935). Phys. Rev. **49**, 778 (1936).
22) W. E. BURCHAM and M. GOLDHABER, Proc. Cambridge Phil. Soc. **32**, 632 (1936).
23) R. W. GURNEY, Proc. Roy. Soc. London (A) **107**, 340 (1925).
24) P. M. S. BLACKETT, Proc. Roy. Soc. London (A) **107**, 349 (1925).

25) W. Bothe, ZS. f. Phys. **100**, 273 (1936).
26) W. A. Fowler and C. C. Lauritsen, Phys. Rev. **56**, 840 (1939).
27) L. H. Rumbaugh and L. R. Havstad, Phys. Rev. **50**, 681 (1936). L. H. Rumbaugh, R. B. Roberts and L. H. Havstad, Phys. Rev. **54**, 657 (1938). J. H. Williams, W. G. Shepherd and O. R. Haxby, Phys. Rev. **52**, 390 (1937), H. Neuert, Ann. d. Phys. **36**, 437 (1939).
28) J. H. Williams, W. G. Shepherd and O. R. Haxby, l. c.
29) E. R. Graves, Phys. Rev. **57**, 855 (1940).
30) R. B. Roberts, N. P. Heydenburg and G. L. Locker, Phys. Rev. **53**, 1016 (1938).
31) H. Meier-Leibnitz, Naturwiss. **26**, 614 (1938). ZS. f. Phys. **112**, 569 (1939).
32) S. Rubin, Phys. Rev. **59**, 216 (1941).

Indleveret til Selskabet den 4. Juni 1945.
Færdig fra Trykkeriet den 22. September 1945.

DET KGL. DANSKE VIDENSKABERNES SELSKAB
MATEMATISK-FYSISKE MEDDELELSER, BIND XXIII, NR. 5

DEDICATED TO PROFESSOR NIELS BOHR ON THE OCCASION OF HIS 60TH BIRTHDAY

AN INTEGRATING BEAM METER FOR HIGH TENSION WORK

BY

SVEN WERNER

KØBENHAVN
I KOMMISSION HOS EJNAR MUNKSGAARD
1945

Printed in Denmark.
Bianco Lunos Bogtrykkeri A/S

When observing the output of nuclear disintegrating processes in high tension plants it is often desirable to know the amount of protons etc. which hit the target on the cathode. Data regarding this magnitude can be provided by measurements of current and time; it is difficult, however, to keep the current constant during the time of observation and, frequently, a simple instrument directly indicating the quantity of electricity is needed. In the following, it will be shown that a galvanometer of the moving coil reflecting type is applicable to this purpose, provided that certain conditions are fullfilled.

The equation of motion of the system in an ordinary galvanometer is

$$K\frac{d^2\varphi}{dt^2} + n\frac{d\varphi}{dt} + D\varphi - \frac{1}{10}HsI = 0, \qquad (1)$$

where φ is the angle of rotation, t the time, K the moment of inertia, n the damping coefficient, and D the torsional moment of the suspension. If the strength of the magnetic field is denoted by H and the total area of windings by s, the total flux through the coil will be $Hs\varphi$. When the system moves, an e. m. f. of $10^{-8}Hs\frac{d\varphi}{dt}$ volts is produced, and the induced current will accordingly be $10^{-8}\frac{Hs}{R}\frac{d\varphi}{dt}$ amperes; R being the total resistance (in ohms) of the circuit, $R = r_g + r_e$, where r_g is the resistance of the galvanometer itself, and r_e the resistance of the rest of the circuit. The retarding moment due to this induced current will be $\frac{1}{10}Hs \cdot 10^{-8}\frac{Hs}{R}\frac{d\varphi}{dt} = 10^{-9}\frac{(Hs)^2}{R}\frac{d\varphi}{dt} = n\frac{d\varphi}{dt}$. The current to be measured is denoted by I (amperes) and will produce an angular momentum $\frac{1}{10}HsI$.

In the present case, it was desired that the angular deflection of the galvanometer should be proportional to the quantity of electricity Q ($= \int I dt$) which, during a comparatively long time, e. g. 100 sec., passes through the instrument. The movement of the coil must therefore be extremely slow, and the term $K \frac{d^2\varphi}{dt^2}$ in (1) will be negligible, provided that K is small. The equation of motion will thus be

$$n \frac{d\varphi}{dt} + D\varphi - \frac{1}{10} HsI = 0 \tag{2}$$

and, if the system moves from φ_0 to φ_1 during the time t,

$$(\varphi_1 - \varphi_0) = \frac{1}{10} \frac{Hs}{n} Q - \frac{D}{n} \int_0^t \varphi \, dt. \tag{3}$$

The first term on the right side of this equation is the deflection proportional to Q, and the last term is the error which, for an arbitrarily varying, direct current, will not exceed $-\frac{D}{n}(\varphi_1 - \varphi_0) t$; if the current is almost constant, the error is only half this value. The relative error, which corresponds to the present application, will accordingly be

$$F = -\frac{D}{2n} \frac{(\varphi_1 - \varphi_0)}{(\varphi_1 - \varphi_0)} t \, 100\,\% = -50 \frac{D}{n} t\,\%. \tag{4}$$

The claims, which should be fulfilled by such an instrument, are therefore: 1) a very small torsional moment D and, furthermore, a large damping coefficient $n \left(= 10^{-9} \frac{(Hs)^2}{R} \right)$, which means 2) a large value of Hs and 3) a small value of R.

Condition 1) means that the instrument must be of a similar type as the fluxmeter with its suspension of unspun silk. According to condition 2), the magnetic field H has to be very strong and, if possible, the coil should have a large cross section and many turns. As the moment of inertia of the coil is of minor importance the cross section may, within certain limits, be rather large and of the shape of a square. Many turns, however, will disaccord with claim 3), viz. low resistance. A closer examination reveals that, for a given mass of the coil, the number of turns is insignificant.

The external resistance r_e must be low, so as to get a large damping, and thus the instrument has to be shunted by a small resistance. Generally the galvanometer, when used to indicate the proton current (i) to the target, is coupled with a very large resistance. We have in this case (cf. the figure), $(i-I)\, r_e = I\, r_g$ or $i = \frac{r_g + r_e}{r_e} I = \frac{R}{r_e} I$, where r_e is the resistance

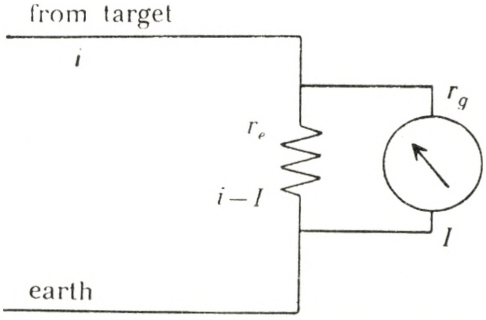

Fig. 1.

of the shunt. If q denotes the quantity of electricity from the target, we get

$$q = \int i dt = \frac{R}{r_e} \int I dt = \frac{R}{r_e} Q.$$

From (3) follows

$$(\varphi_1 - \varphi_0) = \frac{1}{10} \frac{Hs}{n} Q = 10^8 \frac{R}{Hs} Q = 10^8 \frac{r_e}{Hs} q, \qquad (5)$$

which means that the deflection is proportional to q and r_e, so that the sensitivity may easily be varied by changing the shunt. The error may be estimated from (4).

Whether a given instrument is suited to the present purpose can be tested in the following manner. The sensitivity f is determined. As this is the current, which causes a deflection of the light spot of 1 mm on the scale at 1000 mm distance, it corresponds to a rotation of the coil of $(\varphi_1 - \varphi_0) = \frac{1}{2000}$. From equation (2) we find

$$D(\varphi_1 - \varphi_0) = \frac{1}{10} HsI \quad \text{or} \quad D \frac{1}{2000} = \frac{1}{10} Hsf$$

and

$$f = \frac{1}{200}\frac{D}{Hs}. \tag{6}$$

The damping of the instrument may be observed, e.g. by determining the time $t_{\frac{1}{2}}$, in which a given deflection is reduced to half its value. With $I = 0$ and the shunt r_e it follows from (2) that

$$n = D\frac{t_{\frac{1}{2}}}{ln\,2} \text{ or } t_{\frac{1}{2}} = 0.694 \cdot 10^{-9}\frac{(Hs)^2}{DR}. \tag{7}$$

If R is measured, D and Hs may be found and introduced into the expressions

$$(\alpha_1 - \alpha_0) = 2.10^{10}\frac{r_e}{Hs}q \text{ and } F = -5 \cdot 10^{10}\frac{DR}{(Hs)^2} \cdot t\,{}^0\!/_0 \tag{8}$$

derived from (5) and (4), respectively, and where α_0 and α_1 denote the positions of the light spot on the scale (in mm/m) before and after the passage of the quantity q coulombs.

An instrument, corresponding to the results of the present considerations, was constructed. The moving coil had 400 turns 0.10 mm wire, the cross section of the coil was 2×2 cm, $r_g = 100$ ohms (including the connecting ligaments). The suspension was 15 μ Vistra silk, 15 cm. long. The connecting ligaments were made of silver, 4 by 150 μ. The sensitivity was found to be $5.9 \cdot 10^{-10}$ amp/mm/m. The damping coefficient n was found from the time $t_{\frac{1}{2}} = 280$ sec. ($r_e = 0.9$ ohms). We obtained $n = 225$, $(Hs) = 4.7 \cdot 10^6$ and the torsional moment $D = 0.55$. The greater part of D is due to magnetic impurities in the copper coil, the present circumstances making it impossible to obtain unmagnetic material. Better material or a compensation of the induced magnetic moment would give a far smaller D (< 0.1). The error F amounted to 7.5 % during an observation period of 60 sec.; smaller D will result in a correspondingly smaller error.

Examples of some tests performed with this instrument:

1) Sensitivity proportional to the shunt r_e. $t = 60$ sec.

i	r_e	$\alpha_1 - \alpha_0$
6.0 μA	8.0 ohms	106.0 mm/m.
12.0 -	4.0 -	106.0 -
24.0 -	2.0 -	106 -
40.0 -	1.2 -	106 -
200 -	0.24 -	106 -

2) Deflection proportional to the quantity of electricity q, with corrections according to (4). Constant current $i = 24\,\mu$A, and different periods of observation t.

t	$\alpha_1 - \alpha_0$	$\alpha_1 - \alpha_0/t$	$\alpha_1 - \alpha_0/t$ corr.
10 sec.	9.3 mm/m.	0.93	0.94
20 -	18.9 -	0.95	0.97
40 -	36.6 -	0.92	0.96
60 -	53.4 -	0.89	0.96
120 -	100.0 -	0.83	0.96

3) Deflection proportional to q. Constant period of observation and different currents. (No correction needed). ($r_e = 4{,}0$ ohms $t = 60$ sec.

i	$\alpha_1 - \alpha_0$	$\alpha_1 - \alpha_0/i$
3.0 μA	26.7 mm/m.	8.9
6.0 -	53.3 -	8.9
12.0 -	105 -	8.8
24.0 -	209 -	8.7

It was the aim with this note to show that small amounts of electricity (0.1 — 10 milli-coulombs) due to proton currents (from a few to several hundred micro-amperes) conveniently can be measured with a reflecting galvanometer of the fluxmeter type, shunted with a low resistance.

Det Fysiske Institut.
Aarhus Universitet.

Indlevering til Selskabet den 4. Juni 1945.
Færdig fra Trykkeriet den 17. September 1945.

DET KGL. DANSKE VIDENSKABERNES SELSKAB
MATEMATISK-FYSISKE MEDDELELSER, BIND XXIII, NR. 6

DEDICATED TO PROFESSOR NIELS BOHR ON THE OCCASION OF HIS 60TH BIRTHDAY

CONSTRUCTION AND CALCULATION OF A VARIABLE ACOUSTIC IMPEDANCE

BY

V. THORSEN

KØBENHAVN
I KOMMISSION HOS EJNAR MUNKSGAARD
1945

Printed in Denmark.
Bianco Lunos Bogtrykkeri A/S.

Introduction.

In the field of electricity, pure ohmic, inductive and capacitive resistances can rather easily be constructed; similar possibilities are, however, absent within acoustics. Here, the acoustic values corresponding to ohmic resistance, inductance and capacity rarely occur alone, *i. e.* independently of one another, but mostly interdependent, *viz.* the change of one of them involves changes of one or all others. The need of an acoustic standard became a claim after SCHUSTER's construction of an acoustic Wheatstone bridge[1]. Also at Breslau, in WAETZMANN's laboratory, a variable acoustic impedance[2] seems to have been constructed which, however, was troublesome to handle and which, moreover, was only approximately correct; its description never was published. The impedance used by SCHUSTER in his bridge is continuously variable; however, its calculation is rather complicated[3] and it is difficult to make it comprise both the small absorption coefficients from 0 to 10 $^0/_0$ and the great ones exceeding 90 $^0/_0$; finally, its reactive part (the felt tube) and its ohmic part (the piston tube) do not work quite independently of one another. A variable, radiation-damped acoustic impedance including the impedance values which probably exist for the human ear was earlier suggested by THORSEN[4].

In the following, the writer wishes to account in detail for the construction of a variable acoustic impedance which is relatively simple both in its mode of action and its manipulation and

1) K. SCHUSTER: Phys. Zt. **35**, 408, 1934.
2) K. SCHUSTER: E. N. T. **13**, 164, 1936.
3) K. SCHUSTER and W. STÖHR: Akust. Ztschr. **4**, 253, 1939.
4) V. THORSEN: D. Kgl. Danske Vidensk. Selskab, Mat.-fys. Medd. XX, 9, 1943, (in the following denoted as Essay I).

which, furthermore, covers a large range of absorption, *viz.* that from practically 100 % nearly down to 0 %. Besides, it is almost purely radiation-damped, whence its damping is easily measurable, for example, with a condenser microphone. This is of importance not only when its calculations are to be controlled, but it will likewise increase its range of applicability.

1. The Tube as Acoustic Impedance.

According to the theory of the acoustic tube-line, every smooth tube without dissipation represents an acoustic impedance of the magnitude

$$\frac{Z_i}{\varrho c} = \frac{\frac{Z_u}{\varrho c}\cos kl + i \sin kl}{\cos kl + i \frac{Z_u}{\varrho c}\sin kl}. \quad (1)$$ [1)]

Here, $\frac{Z_i}{\varrho c}$ is the inlet impedance, *i. e.* the impedance at the mouth of a tube of length l, which at the other end is terminated by the impedance $\frac{Z_u}{\varrho c}$ (the outlet impedance). When introducing the amplitude reflection coefficient r of the outlet impedance, which is determined by

$$re^{i\vartheta} = \frac{\frac{Z_u}{\varrho c} - 1}{\frac{Z_u}{\varrho c} + 1},$$

and its phase change ϑ, (1) may also be written

$$\frac{Z_i}{\varrho c} = \frac{1 - r^2 - i\,2\,r \sin(2\,kl - \vartheta)}{1 + r^2 - 2\,r\cos(2\,kl - \vartheta)}. \quad (2)$$

1) Cf. V. Thorsen: D. Kgl. Danske Vidensk. Selskab, Mat.-fys. Medd. XX, 10, 1943 (in the following denoted as Essay II).

$\frac{Z_u}{\varrho c}$ then being written in the form $w_0 + iq_0$, (1) passes into

$$\frac{Z_i}{\varrho c} = \frac{w_0 + i\left(q_0 \cos 2kl - \frac{1}{2}[w_0^2 + q_0^2 - 1] \sin 2kl\right)}{(\cos kl - q_0 \sin kl)^2 + w_0^2 \sin^2 kl}. \quad (3)$$

Thus, we have

$$\frac{Z_i}{\varrho c} = w + iq,$$

where

$$\left.\begin{aligned} w &= \frac{w_0}{(\cos kl - q_0 \sin kl)^2 + w_0^2 \sin^2 kl}, \\ q &= \frac{q_0 \cos 2kl - \frac{1}{2}[w_0^2 + q_0^2 - 1] \sin 2kl}{(\cos kl - q_0 \sin kl)^2 + w_0^2 \sin^2 kl}. \end{aligned}\right\} \quad (4)$$

Finally, when introducing the energy absorption coefficient a, we find

$$a = \frac{4w}{(w+1)^2 + q^2} \quad \text{and} \quad \operatorname{tg}\vartheta = \frac{2q}{w^2 + q^2 - 1}.^{1)} \quad (5)$$

The equations (5) in a (w, q) coordinate system with a and $\operatorname{tg}\vartheta$ as parameters represent the known system of circles intersecting one another at right angles, as shown in Fig. 1.

We shall now look at some simple cases. For the absolutely rigid, perfectly reflecting wall, we have

$$a = 0,$$

i. e. the very q axis and, therefore, $w = 0$. Further, $\vartheta = 0$, *i. e.* an infinite large phase circle, whence $q = \infty$. For the absolutely compliant wall, we again have

$$a = 0,$$

1) Cf. Essay I, p. 5, and Essay II, p. 9.

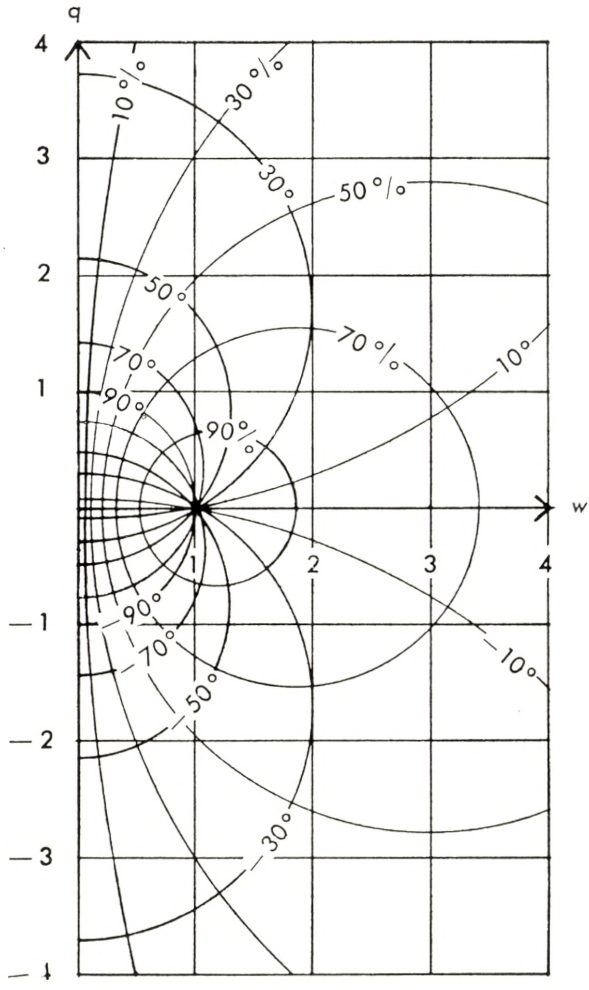

Fig. 1.

hence, also $w = 0$, but in this case $\vartheta = \pm\pi$, *i. e.* $q = 0$. The point (1.0) corresponds to a substance of the same acoustic resistance as the air.

Summarizing, we thus have,

for the rigid wall: $w = 0, \quad q = \infty,$

for the compliant wall: $w = 0, \quad q = 0.$

For the perfectly absorbing substance: $w = 1, \quad q = 0.$

Now, in a tube, we have a combination of acoustic elements, generally both phase change and absorption. If the tube is closed at one end (Fig. 2) with a rigid 100 % reflecting plate,

$$\frac{Z_u}{\varrho c} = w + iq,$$

where

$$w = 0, \quad q = \infty.$$

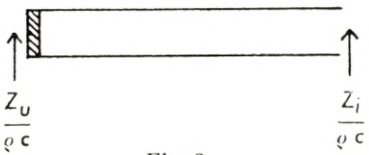

Fig. 2.

The inlet impedance Z_i then, according to (1), becomes

$$\frac{Z_i}{\varrho c} = \frac{\cos kl + i \dfrac{1}{\dfrac{Z_u}{\varrho c}} \sin kl}{\dfrac{1}{\dfrac{Z_u}{\varrho c}} \cos kl + i \sin kl} = -i \cot kl. \tag{6}$$

If $l = 0$, we find $\frac{Z_i}{\varrho c} = \infty$, which result is obvious. If $l = \frac{\lambda}{4}$, $Z_i = 0$, a result which also should be evident, since the tube now is a closed organ pipe measuring $^1/_4$ wave-length. The tube thus represents a pure reactive acoustic resistance which, if l varies from 0 to $\frac{\lambda}{4}$, itself varies from 0 to ∞.

In the same way, the open tube (Fig. 3) can be treated as an acoustic resistance. If we primarily suppose that the mouth represents an entirely compliant wall, we find for $\frac{Z_u}{\varrho c}$

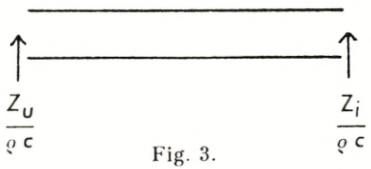

Fig. 3.

$\frac{Z_u}{\varrho c} = w + iq$, where $w = 0$, $q = 0$, which, inserted in (1), gives

$$\frac{Z_i}{\varrho c} = \frac{i \sin kl}{\cos kl} = i \operatorname{tg} kl. \tag{7}$$

For $l = 0$ and $l = \frac{\lambda}{2}$ become $\frac{Z_i}{\varrho c} = 0$, which is also quite obvious. In the latter case, the tube is an open organ pipe measuring $^1/_2$ wave-length. For $l = \frac{\lambda}{4}$, $\frac{Z_i}{\varrho c} = \infty$, whence this acoustic impedance too is purely reactive, varying between 0 and ∞.

In electric analogy, the tube thus in an acoustical conduit acts as a pure reactance (Fig. 4), and the electric generator from the field of electricity may thus be an acoustic generator, for example a telephone or another sound source sending its sound

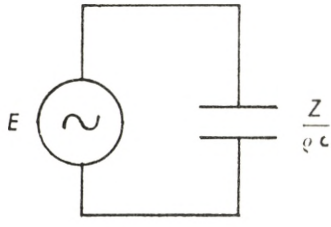

Fig. 4.

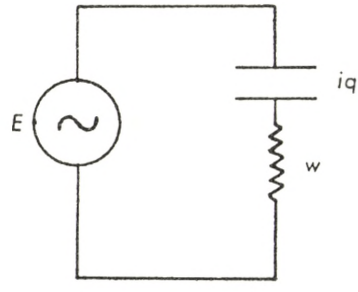

Fig. 5.

energy into the tube. In reality, however, the mouth of an open tube will not be a perfectly compliant wall, so that we have a w of a given, though small, value; q, consequently, is not either quite equal to zero. Thus, neither the real nor the imaginary part of $\frac{Z_i}{\varrho c}$ becomes equal to zero, if $l = \frac{\lambda}{2}$ and the electric comparison picture appears as in Fig. 5. If the tube length varies, w changes along an iso-absorption circle in Fig. 1, and from (4) it is seen that the impedance becomes real, if

$$q_0 \cos 2\,kl - \frac{1}{2}\left[w_0^2 + q_0^2 - 1\right] \sin 2\,kl = 0,$$

or

$$\operatorname{tg} 2\,kl = \frac{2\,q_0}{w_0^2 + q_0^2 - 1} \quad \text{(cf. the 2nd equation (5))}.$$

The corresponding values of w (w_1 and w_2), if $q = 0$, thus become the two values where the iso-absorption circle intersects

the w axis. For these values it holds that $w_1 w_2 = 1$. Thus, the tube as an acoustic impedance is likewise arranged so that, with varying lengths, both the real and the imaginary parts change, however, in such a way that the tube has the same absorption coefficient for all values of l. Hence, w and q change simultaneously so that

$$a = \frac{4\,w}{(w+1)^2 + q^2} = \text{const.}$$

Therefore it may be used as absorption standard, although the values of w are different for each tube length.

A presupposition for the correctness of the above statement is that no other ohmic resistances occur than the radiation resistance. If the tube is so narrow or so long that further dissipation resistance is found in the form of friction, the relations become different. This possibility is treated in detail elsewhere[1].

2. Other Combinations of Tube Impedances.

If we have a combined system of tubes, as shown in Fig. 6, it must obviously have certain peculiar properties. It consists chiefly of a tube which, for theoretical reasons, we imagine to be divided into two parts, l_1 and l_3, and in whose joining-plane (A) is placed a side-branch which, with the help of a tight-fitting metal piston, may be given different lengths (l_2). A sound-wave which enters from the right will divide into two parts at A. That part which enters the side-branch is entirely reflected from the piston and returns to A with a phase difference relative to that passing on through l_3. If l_2 is exactly equal to $\frac{\lambda}{4}$, the wave reflected from the piston will, when reaching A, be exactly in the phase opposite to that which passes

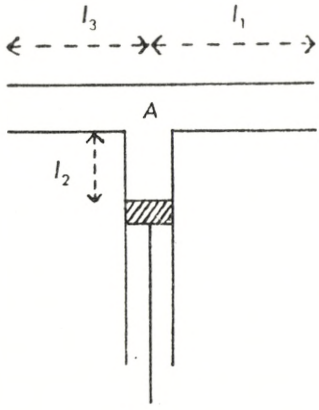

Fig. 6.

[1] Essay I, p. 8 *et seq.*, and Essay II, p. 13 *et seq.*

along l_3, and will thus completely extinguish this wave. In this case, the impedance of the side-branch will short-circuit the impedance of l_3. If the piston is pushed up to A, no effect of the side-branch is observed. Its impedance is infinitely great and connected in parallel to the impedance of l_3. Other peculiar relations should be found if either $l_2 + l_3$ or $l_1 + l_3$ are multiples of half wave-lengths. This side-branch principle was set up by QUINCKE[1].

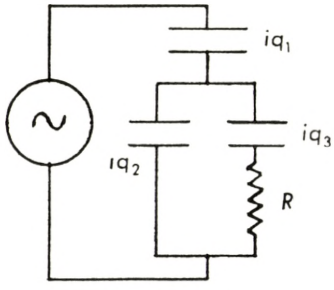

Fig. 7.

The electric equivalent is shown in Fig. 7. R is the radiation at the open (left) end of l_3. If q_2 is equal to ∞, q_1 and q_3 are connected in series; if $q_2 = 0$, R and q_3 are short-circuited and the impedance is equal to iq_1. Roughly spoken, this manner of connecting seems thus to satisfy the above stated demands; yet there are some difficulties which will appear from the following calculation of the impedance.

We find

$$\left.\begin{aligned} Z &= iq_1 + \frac{iq_2\,(R + iq_3)}{iq_2 + R + iq_3} \\ &= \frac{Rq_2^2}{R^2 + (q_2 + q_3)^2} + i\,\frac{R^2\,(q_1 + q_2) + (q_2 + q_3)\,(\Sigma q)}{R^2 + (q_2 + q_3)^2}, \end{aligned}\right\} \quad (8)$$

putting as a simplification

$$q_1 q_2 + q_1 q_3 + q_2 q_3 = (\Sigma q).$$

Further, we find

$$|Z|^2 = \frac{R^2\,(q_1 + q_2)^2 + (\Sigma q)^2}{R^2 + (q_2 + q_3)^2}.$$

From (8) it is evident that Z is not far from being real, if

$$q_2 + q_3 = 0.$$

Therefore it is worth while examining this case somewhat more closely. We find

[1] G. H. QUINCKE: Pogg. Ann. **128**, 177, 1866.

$$Z = \frac{q_2^2}{R} + i(q_1 + q_2). \tag{9}$$

This simplified impedance according to (5) has the absorption coefficient

$$a = \frac{4\,\frac{q_2^2}{R}}{\left(\frac{q_2^2}{R} + 1\right)^2 + (q_1 + q_2)^2} = \frac{4\,Rq_2^2}{(R + q_2^2)^2 + R^2(q_1 + q_2)^2}.$$

If R is small, and particularly if $q_1 + q_2$ moreover is small, this latter expression becomes

$$a = \frac{4\,Rq_2^2}{(R + q_2^2)^2}. \tag{10}$$

Under these presuppositions, *i. e.* $q_2 + q_3 = 0$ and R small, (9) represents a pure ohmic acoustic resistance with an absorption coefficient given in (10). Forming $\frac{da}{dq_2}$, we find

$$\frac{da}{dq_2} = 4\,R\,\frac{(R + q_2^2)^2 \cdot 2\,q_2 - q_2^2\,(R + q_2^2) \cdot 2\,q_2}{(R + q_2^2)^4}, \tag{11}$$

which, put equal to zero, besides $q_2 = 0$ gives

$$R = q_2^2. \tag{12}$$

If this condition is fulfilled, we find

$$a = 1,$$

i. e. 100 % absorption. Now, if q_2 varies so that $q_2 + q_3$ still is equal to zero (q_3 must thus likewise be changed), a varies in accordance with (10). Then it depends to some degree on the rate at which a varies with q_2 for according to (9), Z is no longer purely ohmic if $q_1 + q_2$ deviates considerably from 0. This question, however, will be easiest to elucidate on the basis of experiments, and experiments show that Z within fairly wide absorption limits may be regarded as purely ohmic. This is supported if Z in its tube lengths is arranged so that, at 100 % absorption where $l_2 + l_3 = \frac{\lambda}{4}$, $l_1 + l_2$ is somewhat greater than $\frac{\lambda}{4}$.

When q_2 increases, *i. e.* l_2 decreases $\left(\text{however, } l_2 + l_3 = \frac{\lambda}{4}\right)$, $q_1 + q_2$ will pass from a small positive value through 0 to a small negative value. In this way the range of absorption of the impedance is increased essentially. How far we may go can be decided with the aid of experiments.

We can also see theoretically that the imaginary part of Z is of minor importance. Since, from (9), we find

$$\operatorname{tg} \vartheta = \frac{(q_1 + q_2) R}{q_2^2}, \tag{13}$$

and, if $\frac{d(\operatorname{tg}\vartheta)}{dq_2}$ is formed, we find

$$\frac{d(\operatorname{tg}\vartheta)}{dq_2} = R \frac{q_2^2 \cdot 1 - (q_1 + q_2) \cdot 2\, q_2}{q_2^4} = -Rq_2 \frac{2\, q_1 + q_2}{q_2^4},$$

which, besides $q_2 = 0$, gives

$$q_2 = -2\, q_1. \tag{14}$$

If q_1 is not chosen too small, this value for q_2 brings (12) to a fairly flat minimum of a shape represented in Fig. 8. Experiments also

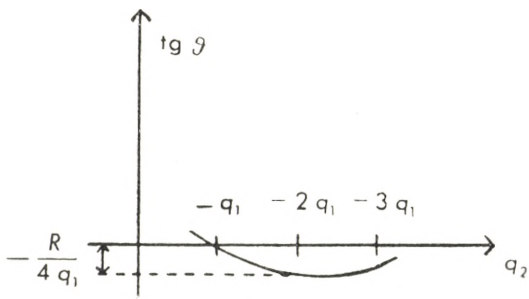

Fig. 8.

prove this to be correct. Evidently, the value (12) gives a maximum for (10)—which should indeed be obvious—since, if q_2 increases from a value smaller than R through R and to a value greater than R, $\frac{da}{dq_2}$ passes from plus through 0 to minus. It appears from (9) that, with decreasing q_2, the ohmic resistance $\frac{q_2^2}{R}$, from being greater than 1, becomes equal to 1 (*viz.*, for $R = q_2^2$) and

finally assumes values below 1. Since two values of $\frac{q_2^2}{R}$, the product of which is equal to 1, lead to the same absorption coefficient, the absorption coefficient as a function of l_2 must become a somewhat symmetrical curve with a maximum for $q_2^2 = R$. It must commence in the vicinity of zero, if l_2 is very small, and again approximate zero, if l_2 approximates $\frac{\lambda}{4}$. It is also important to note that it is possible to get all resistance values, both those greater than 1 and those smaller than 1; however, the greater an absorption coefficient we want to obtain at the maximum, the shorter is the range over which q_2 varies, if resistance values smaller than 1 are wanted, since R is a small magnitude, and the resistance is equal to $\frac{q_2^2}{R}$. The falling branch of the absorption coefficient curve as a function of l_2 therefore becomes very steep. If it is unnecessary to obtain as much as 100 % absorption, the falling branch may be made less steep, the adjustment thus becoming less critical. These relations are also substantiated by the measurements.

The impedance determined by (9) we may call the central point impedance of the combined tube-system.

If we look for inlet and outlet impedances in the two tubes l_1 and l_3, respectively, the former is identical with the inlet impedance in an open tube of length l_3. The inlet impedance is thus determined by the tube which is situated to the left of the central point impedance, the outlet impedance by the tube which is situated to the right of the central point impedance (Fig. 9). The impedance at a given value of the absorption coefficient varies as a function of the tube lengths l_1 and l_3 along the absorption circle determined by $\frac{q_2^2}{R}$, and the w and q values of the inlet impedance are found by intersection of this absorption circle with the line $q = \operatorname{tg} kl_3$; in the same way the w and q values of the outlet impedance are found as the intersection of the absorption circle with the line $q = \operatorname{tg} kl_1$. The q values of the inlet and the outlet impedances naturally become q_3 and q_1. The shorter the tube lengths l_1 and l_3, the more the two impedances approximate one another and, at the same time, the central point

impedance. If $l_1 = l_3$, the inlet and the outlet impedances are equal. However, not before both are equal to zero does the impedance become reactance-free and thus purely ohmic. This is not quite realizable in practice, but if the pipes l_1 and l_3 are

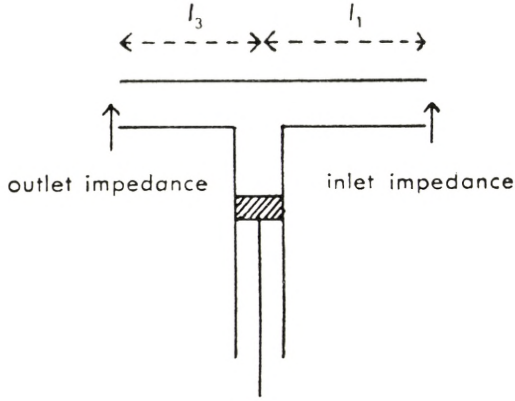

Fig. 9.

short[1], it can approximately be realized, the approximation being best at low frequencies.

We can also get an idea of the highest absorption coefficient to be obtained with given tube lengths. Suppose, for example, that the longest side-branch has the length l, *i. e.* the q value

$$q_A = \operatorname{tg} kl.$$

If this straight line, which runs parallel with the w axis, is brought to intersect the absorption circle system whose equation with the absorption coefficient a as parameter may be written

$$w^2 + q^2 - 2\,w\,\frac{2-a}{a} + 1 = 0,$$

we find

$$w = \frac{2-a}{a} \pm \sqrt{\left(\frac{2-a}{a}\right)^2 - 1 - q_A^2}\,.$$

Real intersection thus is conditioned by

$$\left(\frac{2-a}{a}\right)^2 - 1 + q_A^2 \geqq 0$$

1) Here as well as elsewhere 'short tube lengths' means short in proportion to the wave-lengths or, in other words, kl is a small angle.

or by

$$a \leqq \frac{2}{1+\sqrt{1+q_A^2}}.$$

Accordingly, the sign of equation leads to the highest a-value which the impedance can attain at a given tube length and which thus corresponds to the line $q_A = \operatorname{tg} kl$ just touching the absorption circle.

3. The Influence of Dissipation Damping.

Since it is impossible to keep all the tube lengths short, it is necessary to examine what damping due to friction in the tubes means. This examination claims a picture of comparison

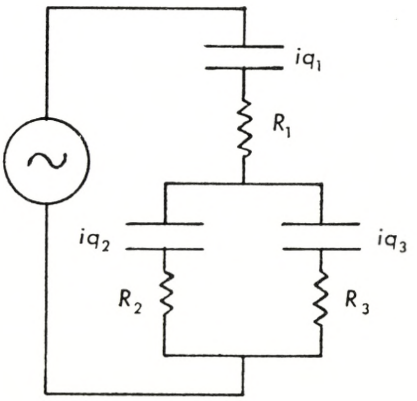

Fig. 10.

as shown in Fig. 10. For the impedance of this system we find

$$Z = R_1 + iq_1 + \frac{(R_2+iq_2)(R_3+iq_3)}{R_2+R_3+i(q_2+q_3)}$$

$$= \frac{R_2R_3-(\Sigma q)+R_1(R_2+R_3)+i[(R_2+R_3)q_1+R_3q_2+R_2q_3+R_1(q_2+q_3)]}{R_2+R_3+i(q_2+q_3)}$$

and, after multiplication of the numerator and the denominator with

$$R_2+R_3-i(q_2+q_3)$$

and some reduction

$$Z = w + iq,$$

where

$$\left.\begin{aligned} w &= \frac{R_2 R_3 (R_2 + R_3) + R_2 q_3^2 + R_3 q_2^2 + R_1 (R_2 + R_3)^2}{(R_2 + R_3)^2 + (q_2 + q_3)^2} \\ q &= \frac{(R_2 + R_3)^2 q_1 + R_2^2 q_3 + R_3^2 q_2 + (q_2 + q_3)(\Sigma q) - R_1 (R_2 + R_3)(q_2 + q_3)}{(R_2 + R_3)^2 + (q_2 + q_3)^2}. \end{aligned}\right\} (15)$$

In case $q_2 + q_3 = 0$, Z assumes the form

$$Z = \frac{R_2 R_3 + q_2^2}{R_2 + R_3} + R_1 + i\left(q_1 + \frac{R_3 - R_2}{R_2 + R_3} q_2\right) \qquad (16)$$

and the absorption coefficient in the first approximation becomes

$$a = \frac{4[(R_2 R_3 + q_2^2)(R_2 + R_3) + R_1 (R_2 + R_3)^2]}{(R_2 R_3 + q_2^2 + R_1 (R_2 + R_3) + R_2 + R_3)^2}. \qquad (17)$$

Just as in the simpler case, where R_1 and R_2 were assumed to be equal to zero, we shall find the maximum for a, when a is regarded as a function of q_2. Thereby we find

$$\frac{da}{dq_2} = 4 \cdot \frac{(R_2 R_3 + q_2^2 + R_1 (R_2 + R_3) + R_2 + R_3) 2 q_2}{N^2}$$

$$- 4 \cdot \frac{[R_2 R_3 + q_2^2 + R_1 (R_2 + R_3)] \cdot 2 [R_2 R_3 + q_2^2 + R_1 (R_2 + R_3) + R_2 + R_3] \cdot 2 q_2 (R_2 + R$$

which, put equal to zero, besides $q_2 = 0$ gives

$$q_2^2 = R_2 + R_3 - R_1 R_2 - R_2 R_3 - R_1 R_3 = R_2 + R_3 - (\Sigma R); \qquad (18)$$

for the sake of simplicity, we put

$$R_1 R_2 + R_2 R_3 + R_1 R_3 = (\Sigma R),$$

i. e. an expression corresponding to (12). If (18) is inserted in (17), we also find $a = 1$, just as before.

R_2 and R_3 being small, (ΣR) is a small magnitude in proportion to R_2 and R_3, whence (17) in good approximation reaches a maximum for

$$q_2^2 = R_2 + R_3.$$

In other words this means that, in (16), R_2R_3 and R_1 may be disregarded so that (16) assumes the following form:

$$Z = \frac{q_2^2}{R_2 + R_3} + i\left(q_1 + \frac{R_3 - R_2}{R_2 + R_3} q_2\right). \tag{19}$$

4. Experimental Results.

In order to test the correctness of the formulae developed in the preceding sections, the writer has performed a series of experiments with an impedance of the form shown in Fig. 6. The impedance was made from brass tubes with a lumen measuring 6 mm. in diameter. The tube length l_1 was 2.9 cm., the shortest tube length l_3 being 1.1 cm. The latter could be lengthened with additional tubes of known lengths. The length of l_2 was varied with a piston which, in order to ensure tightness, was supplied with a piston ring consisting of a piano string. The impedance was connected to a calibrated Schuster bridge. Absorption and phase of the inlet impedance were measured for altogether 14 different lengths of l_3, absorption and phase for each value of l_3 were determined as a function of l_2. The frequency applied was 768 Hz, $\lambda = 44.3$ cm. For the determination of every single absorption and phase curve, measurements were performed for about 30 different values of l_2, particularly close around the maximum. Fig. 11 represents an example of the results obtained in a series of measurements of an absorption curve, and Fig. 12 shows a similar measurement for the corresponding phase curve. The accuracy is extraordinarily satisfactory, c. $^1/_2$ % for the absorption coefficients, and a few degrees for the corresponding phases.

Total results for the maximum absorption coefficients and the corresponding phases are recorded in Table 1; the head lines of the columns are supplied with easily comprehensible symbols referring to those used above. The calculations of a and ϑ are based upon the formulae (5). Finally, the calculations are illustrated by Figs. 13 and 14.

Fig. 13 is very instructive, showing that, for $l_3 = 1.4$ cm., $l_2 = 9.35$ cm., with approximation $R_2 = q_2^2$ so that we here have

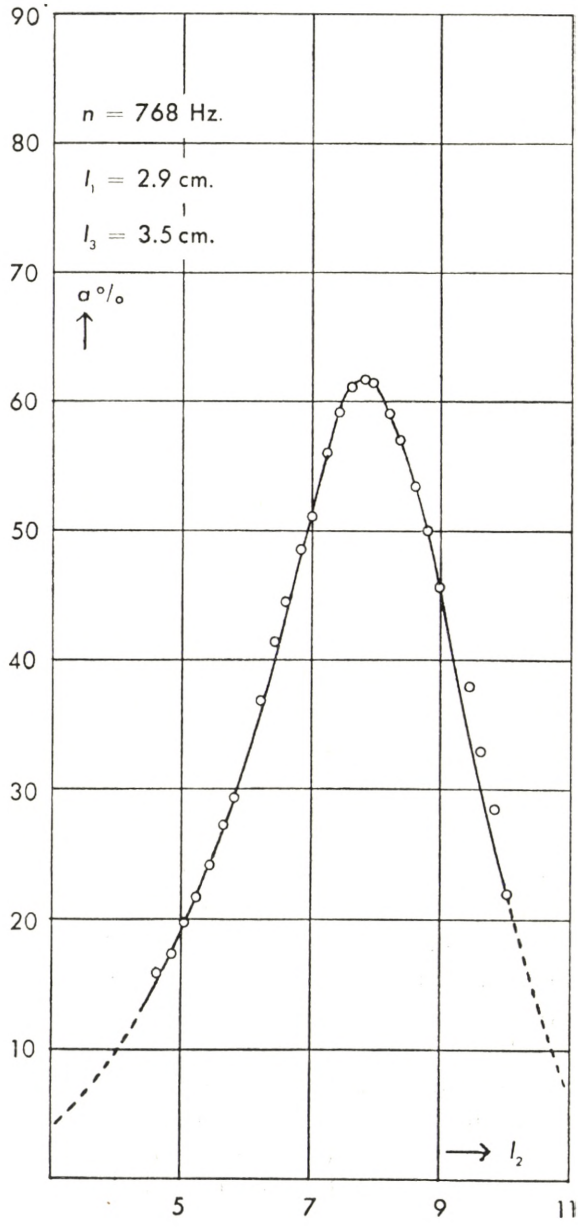

Fig. 11.

Table 1.

l_3	l_2	q_3	q_2	$\frac{q_2^2}{R}$	$\frac{R}{q_2^2}$	α % Calculated	α % Observed	ϑ^0 Calculated	ϑ^0 Observed
5.5	6.8	1.00	0.695	7.91	0.127	39.5	40.5	ca.–90	–90
4.5	7.4	0.740	0.575	5.41	0.184	52.0	52.7	–74.3	–80
3.5	7.8	0,542	0.505	4.16	0.240	61.7	61.5	–59.1	–60
2.9	8.15	0.440	0.445	3.22	0.310	72.0	73.0	–51.0	–53
2.5	8.5	0.375	0.384	2.41	0.415	82.0	83.5	–47.5	–53
2.0	8.85	0.300	0.327	1.74	0.575	92.5	94.5	–41.2	–40
1.8	9.0	0.265	0.300	1.47	0.680	96.0	96.0	–44.0	–35
1.7	9.1	0.250	0.290	1.36	0.736	97.4	97.5	–50.0	–55
1.6	9.2	0.235	0.275	1.23	0.815	98.5	98.0	–58.0	–60
1.5	9.3	0.220	0.260	1.10	0.91	98.5	98.5	–76.6	—
1.4	9.35	0.200	0.250	1.03	0.97	99.5	99.0	ca.–90	—
1.3	9.45	0.190	0.235	0.90	1.11	98.8	99.0	+	+
1.2	9.5	0.175	0.230	0.85	1.18	98.0	97.5	+	+
1.1	9.65	0.160	0.205	0.69	1.45	95.5	97.0	+	+

Hence, a value must be found for l_2, where $q_3^2 + \left(\frac{R}{q_2^2}\right)^2 = 1$, and the denominator therefore is equal to 0, $\operatorname{tg}\vartheta = -\infty$, $\vartheta = -90°$. This point was fortuitously found for $l_3 = 5.5$ cm., $l_2 = 6.8$ cm. If l_2 increases, q_3^2 decreases, while $\frac{R}{q_2^2}$ increases slowly. Here we have

$$q_3^2 + \left(\frac{R}{q_2^2}\right)^2 < 1,$$

whence ϑ becomes negative. For a given value of l_2, we now find on account of the increase in $\frac{R}{q_2^2}$

$$q_3^2 + \left(\frac{R}{q_2^2}\right)^2 = 1,$$

and ϑ again becomes $-90°$. This holds for $l_3 = 1.5$ cm., $l_2 = 9.3$ cm. Hence, in the interval ϑ must have had a (numerical) minimum, *viz.*, for $l_3 = 2.0$ cm., $l_2 = 8.8$ cm. At still higher values for l_2, $\operatorname{tg}\vartheta$ becomes positive, *viz.*, if

$$q_3^2 + \left(\frac{R}{q_2^2}\right)^2 > 1.$$

This is indicated by the dotted branch of the phase curve in the lower part of Fig. 14. The curve presents, however, a very sharp bend, and the accuracy is but small. Actually the experiments only show that the phase becomes positive. Thus a discontinuity in the phase curve occurs. A closer examination of this relation, which could only be found within the very greatest absorption range between 99 to 100 %, is in progress.

It is clear from the preceding account that it will be possible to produce an impedance which can be brought to assume all possible values of absorption and phase. It is a characteristic feature of this impedance that its damping is a pure radiation damping. This means that we might be able to measure the exact effect, emitted from a telephone, on the human ear. If this impedance is known, and measured for example by means of a Schuster bridge, the variable impedance is adjusted to the value and placed before the telephone. Then the radiation of this telephone through the impedance is equal to the effect produced on the ear. A solution of this problem was suggested before[1], and the program of an investigation was briefly as follows.

(1) The radiation curve of a telephone is measured for a series of frequencies.
(2) The impedance of the ear for the same frequencies is measured with a Schuster bridge.
(3) The variable impedance is adjusted for each frequency as equal to the impedance of the ear.
(4) The impedance is placed before the telephone and, subsequently, the radiation is re-measured.

If the distance between telephone and measuring apparatus (condenser microphone) in case 1 and case 4 is the same, information is obtained as to how great a fraction of the effect, which the telephone is able to emit, is absorbed by the ear. Such an impedance will be much easier to handle than the previously suggested one, and it will moreover be possible to make it cover a far greater range. It must, of course, be adjusted to different standard frequencies, and therefore we possibly may be compelled to make a compromise between the lowest frequency to

[1] Essay I, p. 18.

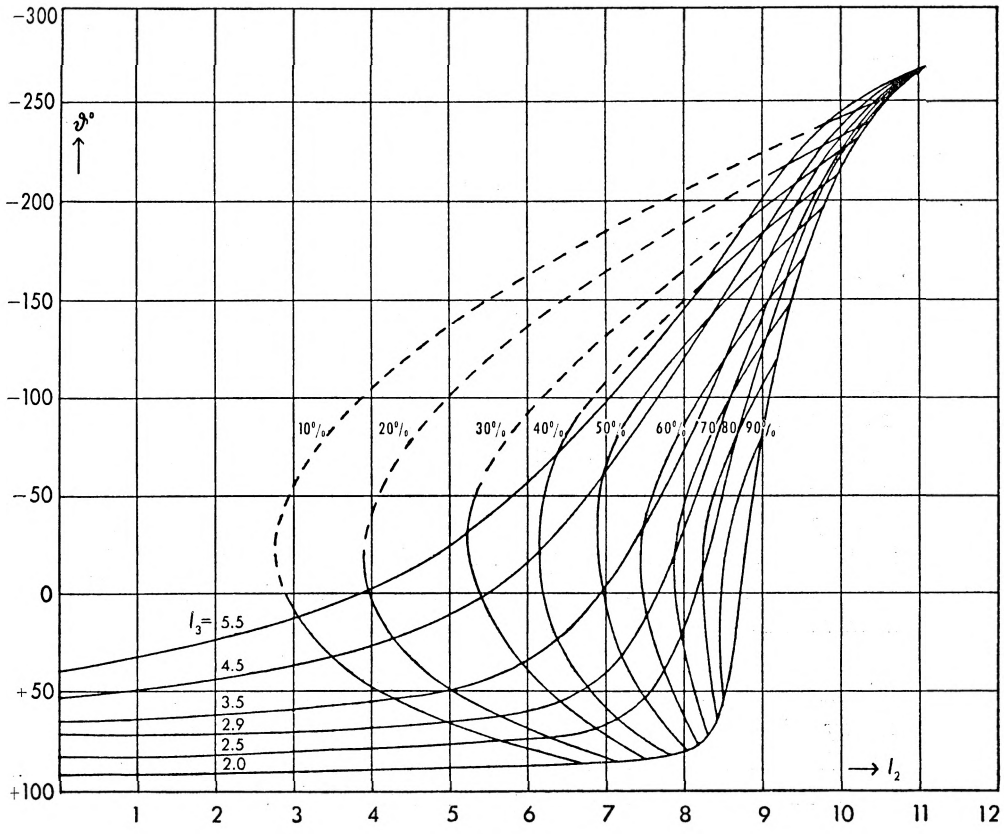

Fig. 15.

be used and the greatest geometric range of the impedance to be allowed.

Fig. 15 was plotted on the basis of all measurements performed. On a series of curves representing the phase as a function of l_2 for different values of l_3 iso-absorption curves for 10, 20, 30, ... 90 % of absorption are inserted. From these multitudes of curves we may infer, possibly by interpolation, which values l_2 and l_3 must obtain in order to yield a given absorption coefficient and a given phase angle. If we want, for example, $a = 25$ %, $\vartheta = 60°$, we evidently need (about) $l_2 = 5.2$ cm. and $l_3 = 3.3$ cm. In the impedance to be constructed both l_2 and l_3 must be continuously variable. Such an impedance has already been produced, and it has proved to comply with our expectations.

As soon as some still unexplained, however less important details are elucidated, an examination of patients is planned.

Summary.

With the aid of a system of acoustic tube impedances a variable acoustic impedance which covers a rather large range of absorption coefficients and phase changes could be constructed and partly calculated. In order to support the theory, numerous measurements of the values of the inlet impedance of the variable impedances were performed. Particularly good agreement with the theoretical expectance was obtained and it also appears from the measurements that the accuracy is significant. The calculations were performed for tubes both with and without dissipation. It is intended to apply the impedance, *inter alia*, to an objective determination of the effect emitted from a telephone on the human ear.

The present work was performed at the Biophysical Laboratory of the University of Copenhagen. To its head, professor Dr. H. M. HANSEN, the author wishes to express his gratitude for the good working conditions put at his disposal.

Indleveret til Selskabet den 2. Juni 1945.
Færdig fra Trykkeriet den 22. September 1945.

DET KGL. DANSKE VIDENSKABERNES SELSKAB
MATEMATISK-FYSISKE MEDDELELSER, BIND XXIII, NR. 7

DEDICATED TO PROFESSOR NIELS BOHR ON THE OCCASION OF HIS 60TH BIRTHDAY

COSMIC RADIATION AND NEGATIVE PROTONS

BY

NIELS ARLEY

KØBENHAVN
I KOMMISSION HOS EJNAR MUNKSGAARD
1945

CONTENTS

Printed in Denmark
Bianco Lunos Bogtrykkeri A/S

Introduction.

The three main problems, still unsolved, in the domain of cosmic ray physics are at present the following:

(a) What is the origin of the enormous energies revealed experimentally in cosmic radiation?

(b) Of what particles does the primary component hitting the top of the atmosphere consist?

(c) How is the genesis of the various components observed in the atmosphere, at sea level and at great depths?

Although much thought has been devoted to the first problem, its final solution has not yet been definitely found. We shall return to it at the end of this discussion. Regarding the second question, it was until recently generally assumed[1] that the primary radiation consists exclusively of electrons,[2] the positons being slightly more numerous than the negatons. The third question was answered by assuming the soft component, known experimentally to consist of electrons and photons, to be produced directly by cascade multiplication from the primary electrons. Next, the hard component, known experimentally to consist of mesons, was assumed to be produced as a secondary radiation by the photons of the soft component in the upper part of the atmosphere. On the other hand, the hard component also gives rise to a secondary soft component, constituting most of the soft component found at sea level, partly by the radioactive decay of the mesons into electrons and neutrinos, partly by their electromagnetic interaction with the atoms in the atmosphere giving rise to knock-on electrons and brems-

[1] Cf. e. g. the survey in EULER and HEISENBERG (1938).

[2] This term we shall use as a generic term for both the positive and the negative particles, which we shall denote as positons and negatons, respectively. (The terms positrons and negatrons often used are incorrect, as the r belongs to the Greek word for amber and not to the ending -on).

strahlung. Besides the mesons the hard component is known experimentally to contain a very small fraction of protons and neutrons, which are assumed to be produced as secondaries from the stars of BLAU and WAMBACHER. These stars are assumed to be nuclear explosion or evaporation processes produced by the absorption of the photons of the soft component. Finally, it has been suggested that the effects at great depths below the surface of the earth may perhaps be interpreted as being due to the hypothetical neutrinos.[1]

In view of the experimental evidence of recent years, however, this picture of the genesis of the various components now seems to be untenable. We shall here first (part 1) try to give a survey of the experimental facts bearing upon our questions (b) and (c). Next, we shall discuss the various possibilities of giving a picture of the genesis compatible with all these data (part 2), thereby discussing (part 3) some arguments in favour of quite a new hypothesis on the existence of *negative protons* in the primary cosmic radiation, which has been put forward independently in two papers by KLEIN and the author.[2] In the discussion of KLEIN's paper (part 4) we shall return to the question of the origin of cosmic radiation.

Part 1. Survey of the present experimental data.

Let us briefly summarize what seems to be known at present of experimental facts bearing upon our questions (b) and (c).

(I) *Intensities at sea level.*

First of all, the experimental intensities at sea level:

soft component = electrons + photons (i. e. that part which is absorbed in 10 cm Pb) $\sim 23\,\%$ of the total intensity;[3]

hard component = mesons (i. e. that part which is not absorbed in 10 cm Pb) $\sim 77\,\%$ of the total intensity;

total intensity $\sim$ 1-2 particles per cm^2 per min;

[1] HEISENBERG (1943) p. 10.

[2] KLEIN (1945), ARLEY (1944).

[3] HEISENBERG (1934) p. 90: soft component $= Z + W + R \sim 29\,\%$ of hard component, i. e. soft $\sim 23\,\%$ of total (cf. [1] p. 30).
JOHNSON (1938) p. 208.

protons ~ fast neutrons ~ $\frac{1}{10}$ particle per cm^2 per day[1] ~ 0·01% of the total intensity;

neutrinos: both existence and, therefore, also intensity quite unknown.

(II) *Latitude effect at sea level.*

Next, we give the experimental data of the geomagnetic effects showing that the primary component consists, at any rate to a certain part, of *charged* particles. The cause of these effects is that the paths of charged particles are bent in the magnetic field of the earth. In order to pass through this field the particles must have a certain minimum energy depending on latitude, incident direction and, to a smaller extent, on longitude due to the magnetic dipole representing the magnetic field of the earth being placed excentrically inside the earth. The theory of these effects has been given by STØRMER, LEMAÎTRE, VALLARTA, and others.[2] The most important of these effects is the *latitude effect* defined as

$$l = \frac{I_{50} - I_0}{I_{50}}, \qquad (1)$$

in which I_{50} and I_0 are the intensities at 50° and 0° geomagnetic latitude (the total intensity being constant at all altitudes above 50° N or below 50° S[3]). The latitude effect depends on the altitude and may be measured for the total radiation or for the hard and the soft components separately. It is, of course, the two last mentioned effects which are of greatest interest. For the *soft component* it is measured by means of G-M-counters, e.g. 3 counters in triangular position covered with 1-2 cm Pb, thus giving the intensity for showers only. The values found by various authors at sea level lie between $l = 0\%$ and $l = 6\%$[4] as compared with values from 14 to 20% for the vertical total.

[1] For the protons: STETTER and WAMBACHER (1939) (quoted in HEISENBERG (1943) p. 121). For the neutrons: FÜNFER (1937), (1938), KORFF (1939), SCHOPPER (1939) (quoted in HEISENBERG (1943) p. 121 and 130).

[2] Cf. e. g. the review of this theory (together with the literature in question) in JOHNSON (1938), BRADDICK (1939) or HEISENBERG (1943).

[3] COSYNS (1936), CARMICHAEL and DYMOND (1937), COMPTON and TURNER (1937).

[4] JOHNSON (1935), PICKERING (1936), JOHNSON and READ (1937), NEHER and PICKERING (1938). (Also quoted in JOHNSON (1938) p. 226).

radiation at sea level measured with the same counters placed in line. If the latitude effect of the total radiation is measured not by counters, but by ionization chambers, the effect turns out somewhat smaller, viz. 8-12 % depending on the longitude;[1] for the chambers measure the intensity from all directions, the counters only the vertical intensity. Taking the rather large statistical fluctuations into account, we conclude with JOHNSON (1938) that

the soft component, = shower producing radiation, shows practically no latitude effect at sea level.

We note that, firstly, it is not quite certain whether the intensity of the shower producing radiation may be put proportional to the intensity of the soft component itself, as this component may also contain some slow electrons which are unable to produce showers in the 1-2 cm Pb placed above the counters. Secondly, also some mesons of the hard component may produce showers. It seems, however, generally agreed in the literature that neither of these two objections need be considered.

In spite of the above mentioned experiments it is stated by HEISENBERG[2] that the soft and the total radiation at sea level, i. e. practically the soft and the hard component, have the same latitude effect ~ 10 %. The reason for this false statement is certainly, as we have already previously pointed out,[3] that HEISENBERG bases his conclusion only on the experiment of AUGER.[4] From this experiment it is, however, impossible to draw any positive conclusions as to the latitude effect of the *soft* component, partly because of the very large fluctuations, partly because the effect for the soft component is here measured by a difference method (vertical intensity in 3 G-M-counters placed in line with and without 20 cm Pb in between). Due to the soft component at sea level contributing only a small fraction of the total intensity (~ 23 %), its contribution to the latitude effect is also small compared with that of the hard component: from (1) we have

[1] COMPTON and TURNER (1937).

[2] Both in the reports of EULER and HEISENBERG (1938) p. 38 and of HEISENBERG (1943) p. 87.

[3] ARLEY and ERIKSEN (1940) p. 20.

[4] AUGER and LEPRINCE-RINGUET (1934). As a curiosity we may mention that HEITLER (1937) draws exactly the opposite conclusion from this same experiment, viz. that the latitude effect of the soft component is 0!

in fact, denoting by indices h and s the quantities referring to the hard and the soft components, respectively,

$$l = \frac{I_{50} - I_0}{I_{50}} = \frac{I^h_{50} - I^h_0}{I^h_{50}} \frac{I^h_{50}}{I_{50}} + \frac{I^s_{50} - I^s_0}{I^s_{50}} \frac{I^s_{50}}{I_{50}} = 0{\cdot}77\, l^h + 0{\cdot}23\, l^s . \qquad (2)$$

Thus, due to the large statistical errors we cannot obtain l^s by such a difference method, but have to measure l^s directly by means of the shower intensities as in the experiments mentioned above ([4] p. 5).

As a result, we conclude with JOHNSON (1938) that

most if not all of the latitude effect at sea level, amounting to 10-20 %, *is due to the hard component.*

This conclusion is also supported by the experiments of JESSE and GILL[1] showing a latitude effect of about 30 % at sea level for large bursts (containing more than 280 particles) in ionization chambers shielded by 12 cm Pb, the effect thus being due to the hard component. The figure 30 % is, however, surprisingly high, but, as the authors point out themselves, it may not be quite certain due to the large statistical uncertainties of the experimental data.

The latitude effect of the total and the soft radiation at high altitudes has been investigated by several authors, but only little material seems to be available concerning the hard component. From the balloon flights with ionization chambers of BOWEN, MILLIKAN and NEHER[2] at the geomagnetic latitudes 60° N, 51° N, 38° N, and 3° N it follows that the *total* radiation shows a very considerable latitude effect between 60° N and 3° N at great altitude, amounting to the following values

m H_2O	6	1	0·5
$l \sim$	23 %	70 %	76 %.

For the soft component (showers in 3 G-M-counters in triangular position, covered with 1·2 cm Pb) JOHNSON[3] finds a

[1] JESSE and GILL (1939).
[2] BOWEN, MILLIKAN and NEHER (1938).
[3] JOHNSON (1935a).

latitude effect of 24 % between 50° N and 28° N geomagnetic latitude at an altitude of 4300 m ~ 46 cm Hg ~ 6 m H_2O. Since experiments with ionization chambers measure the radiation from all directions and therefore give somewhat smaller latitude effects, JOHNSON's figure agrees very well with BOWEN, MILLIKAN and NEHER's value of 23 % between 60° N and 3° N given above; for at this altitude the soft intensity amounts already to about $\frac{2}{3}$ of the total intensity. Although a systematic investigation of the latitude effect of the soft component as a function of the altitude is still lacking, we think it may be concluded that

the latitude effect of the soft component increases highly with increasing altitude.

Regarding the latitude effect of the hard component at great altitudes we have found one experiment only, viz. that of JESSE, WOLLAN and SCHEIN,[1] giving the vertical intensity of 4 G-M-counters with 8 and 10 cm Pb absorbers in between. At an altitude of 3 cm Hg = 0·4 m H_2O they find a latitude effect of 15 % between the geomagnetic latitudes 51° N and 40° N. Consequently, the total latitude effect of the hard component, viz. between 50° and 0°, is much larger than 15 %, and *it would be interesting to obtain experimental determinations of it.* At any rate we conclude that

the latitude effect of the hard component increases with increasing altitudes, although it does not seem to assume such high values as the latitude effect of the soft component.

(III) *East-west asymmetry.*

The second important geomagnetic effect is the east-west asymmetry effect defined as

$$a = \frac{I_{\text{west}} - I_{\text{east}}}{\frac{1}{2}(I_{\text{west}} + I_{\text{east}})}, \tag{3}$$

in which I_{west} and I_{east} are the intensities from a western and an eastern zenith angle z, respectively. This asymmetry depends

[1] JESSE, WOLLAN and SCHEIN (1941).

on z, the geomagnetic latitude λ and the altitude. As the latitude effect, it may be measured for the total radiation (by means of G-M-counter telescopes), for the soft component alone (by means of 3 or more G-M-counters placed in triangular position with small bases and covered with 1-2 cm Pb, thus measuring the intensity of showers,[1] or for the hard component alone (G-M-counters placed in line with about 10 cm Pb absorber in between). Also here it is, of course, the two separate effects which are of greatest interest. At sea level the east-west asymmetry for the total radiation has been investigated by JOHNSON, ROSSI and others.[2] It is found that the effect increases with increasing values of z and decreasing values of λ, amounting at most to about $+15\,\%$ at $z = 45°$ and $\lambda = 0°$. (At $z = 30°$ and $\lambda = 0°$ it is about $+10\,\%$). This variation with z follows from the corresponding variation of the difference between the minimum energies for the western and the eastern direction.[3]

For the soft component, i. e. the showers, JOHNSON[4] finds at sea level for $z = 30°$ $a \sim +5\,\%$ in Peru, i. e. at $\lambda = 0°$. Just as was the case for the latitude effect at sea level, we may thus conclude that

the east-west asymmetry at sea level is much smaller for the soft component than for the total radiation.

For the east-west asymmetry of the hard component at sea level we have been unable to find any suitable experiments.

The variation of the east-west asymmetry with increasing altitude has been investigated by several authors. For the total radiation JOHNSON[2] finds (by means of G-M-counters in line) at $\lambda = 0°$ the following values of a

cm Hg	76	52	46
$z = 30°$ $a \sim$	$+10\,\%$	$+12\,\%$	$+13\,\%$
$z = 45°$ $a \sim$	$+15\,\%$	$+14\,\%$	$+14\,\%$.

[1] Cf. the objections to this procedure mentioned p. 6. Also the asymmetry effect for the soft component must, at any rate at sea level, be determined directly and not by a difference method, cf. p. 6.

[2] JOHNSON (1935 b), (1938). In these papers all the literature in question is quoted.

[3] LEMAÎTRE and VALLARTA (1936); also quoted in HEISENBERG (1943), fig. 9 p. 162.

[4] JOHNSON (1934).

At an altitude of 3 cm Hg, JOHNSON and BARRY[1] at the geomagnetic latitude 20°N find that for $z = 60°$ $a \sim +7\,\%$ for the total radiation as compared with $a \sim +4\,\%$ for $\lambda = 20°\,\mathrm{N}$, $z = 60°$ and at sea level ([2] p. 9).

For the soft component JOHNSON,[2] by means of 3 G-M-counters in triangular arrangement covered with 1·2 cm Pb (i. e. showers), finds that

$a \sim +1{\cdot}2\,\%\,(\pm 1\,\%)$ $z = 35°$ $\lambda = 29°\,\mathrm{N}$ 4300 m above sea level ~ 46 cm
$a \sim +1{\cdot}8\,\%\,(\pm 1\,\%)$ $z = 49°$ — — —

(With the same counters placed in line, but without Pb, i. e. total radiation, he finds at the same place $a \sim +10\,\%$ for $z = 35°$ and $a \sim +13\,\%$ for $z = 49°$.) We note that these figures cannot be compared with the corresponding value $a \sim +5\,\%$ mentioned above for the same experimental arrangement at sea level, because that figure referred to the geomagnetic equator, whereas the figures given here refer to $\lambda = 29°\,\mathrm{N}$. Somewhat larger values are, however, obtained for the total radiation at sea level at the same geomagnetic latitude 29°N, viz. $a \sim +5\,\%$ for $z = 30°$ and $a \sim +3\,\%$ for $z = 45°$ ([2] p. 9).

For the east-west asymmetry of the hard component, measured by means of G-M-counters placed in line with 8·6 cm Pb absorber in between, JOHNSON ([2] p. 9) finds

$a \sim +8\,\%$ $z = 30°$ $\lambda = 29°\,\mathrm{N}$ 46·2 cm Hg
$a \sim +9\,\%$ $z = 45°$ — —

These values are of the same order of magnitude as those found for the same λ, z and altitude for the total radiation, and somewhat larger than the corresponding values for the same λ and z at sea level, viz. $a \sim +3\text{-}5\,\%$ ([2] p. 9).

Finally, SCHEIN and collaborators[3] report having found a "very high positive value" for the east-west asymmetry of the hard component at the top of the atmosphere.

If we try to summarize, we see that the experimental data are rather incomplete. *What is still needed is a more syste-*

[1] JOHNSON and BARRY (1939).
[2] JOHNSON (1935a).
[3] Private letter to prof. HEISENBERG, quoted in HEISENBERG (1943) p. 46.

matic investigation of the east-west asymmetry of the soft and the hard component separately, as a function of each of the three quantities geomagnetic latitude, zenith angle, and altitude. We think, however, that it may be concluded from the experimental data available at present that,

in contrast to the latitude effect, the east-west asymmetry of the total radiation is practically constant or rather decreasing with increasing altitude.

Remembering that most of the radiation found at sea level belongs to the hard component and that the showers show little asymmetry at sea level, we next conclude that

just as was the case for the latitude effect, most if not all of the east-west asymmetry at sea level is due to the hard component.

We may here mention that JOHNSON[1] concludes that the east-west asymmetry is a property of the hard component also in the lower part of the atmosphere, viz. up to about 46 cm Hg, from the fact that it shows approximately a mass-equivalent absorption (when increasing Pb absorbers are interposed between the counters), whereas the soft component shows a Z^2 absorption. The latter statement, although often encountered in literature, is nevertheless false, *the soft component, both experimentally and theoretically, showing an absorption which is also approximately mass-proportional*; for the intensity is not only determined by the shower unit, given essentially by Z^2, but also by the critical energy, which is inversely proportional to Z (being defined as that energy at which the electrons lose just as much energy by bremsstrahlung as by ionization).[2] As a consequence we can only say that the experimental fact just mentioned *agrees* with the hypothesis that the asymmetry in the lower part of the atmosphere belongs to the hard component, but it does not *exclude* the other possibility that part of it belongs to the soft component, too. We think, however, that this last possibility is excluded by another experimental fact stated above, namely that the east-west asymmetry *increases* with increasing zenith.

[1] JOHNSON (1938) p. 228.
[2] HEITLER (1937), ARLEY (1938).

angle. Two factors here pull in opposite directions, the increasing difference between the minimum energies ([3] p. 9) trying to increase the effect, the increasing absorption due to the increased length of the inclined paths traversed trying to decrease the effect. Now, the absorption plays only a small part for the hard component, but a dominating one for the soft component (cf. p. 21). For this component the east-west asymmetry must, therefore, be expected to be practically constant or rather decreasing with increasing values of zenith angle (except, of course, for the very smallest values for which the asymmetry equals zero) in contrast to the increase found experimentally for the total radiation and in agreement with the experimental findings for the soft component, as stated above (p. 9-10).

(IV) *Variation of the intensity with altitude.*

The investigation of the geomagnetic effects is closely connected with that of the variation of the intensity with increasing altitude above sea level. Such experiments were already carried out by HESS in order to prove that the radiation really comes from outside the earth and is not simply due to radioactive contaminations in the earth itself or its atmosphere. Later experiments, especially those by MILLIKAN and his collaborators ([2] p. 7), showed that at the highest altitudes the intensity passes through a maximum and then decreases strongly with increasing altitude. These experiments, which were performed with ionization chambers, however give the intensity of the total radiation and from all directions, and counters are thus to be preferred, giving only the vertical intensity, although results obtained in this way exhibit larger statistical fluctuations than those obtained with chambers. The latest counter measurements for the total radiation are those performed by PFOTZER[1] at Stuttgart, i. e. geomagnetic latitude 50°N. They may thus be directly compared with the corresponding counter measurements for the hard component of SCHEIN, JESSE and WOLLAN[2] (5 counter systems in line with from 4 to 18 cm Pb absorbers in between). PFOTZER's results show that

[1] PFOTZER (1936); also quoted in HEISENBERG (1943) fig. 2 p. 41.
[2] SCHEIN, JESSE and WOLLAN (1941 a); also quoted ibid.

to be vector-mesons, i. e. having spin 1, because the long-living mesons found at sea level must be assumed to be pseudoscalar mesons, i. e. having spin 0. The latter conclusion follows from the discussion of CHRISTY and KUSAKA,[1] who compared the predictions of the meson theory with the sea level observations of SCHEIN and GILL[2] on burst frequency versus burst energy. The comparison shows that at present the most plausible hypothesis is that the large bursts are due mainly to cascade showers produced by the bremsstrahlung emitted by the passage of pseudoscalar mesons, i. e. mesons of spin 0, through the 11 cm Pb absorber placed above the ionization chamber of SCHEIN and GILL. We must, however, object to this conclusion that it is based essentially on the application of the FURRY formula for the fluctuation of the number of electrons in a shower about the mean number. As has been shown by the author,[3] the fluctuation is, however, of varying size and as a rule much greater than that given by the FURRY formula, and these effects will presumably just be of special importance in the large showers met with in bursts.[4]

Apart from the cascade showers of the soft component also 'hard' showers have been found in which several penetrating particles are emitted in a single process.[5] These showers have been observed on Wilson chamber photographs,[6] by G-M-counters,[7] and as the photographic BLAU-WAMBACHER stars.[8] All three effects become much more frequent at high altitudes, the frequency being roughly proportional to the intensity of the soft component. We must therefore conclude that

all these effects are, directly or indirectly, produced by the photons of the soft component

(or perhaps by its electrons, but at present no processes of electrons producing either mesons or protons are known theoretically).

[1] CHRISTY and KUSAKA (1941).
[2] SCHEIN and GILL (1939).
[3] ARLEY (1943).
[4] We intend to investigate this point more closely.
[5] Cf. e. g. the review in HEISENBERG (1943), chaps. 5, 12 and 13.
[6] FUSSELL (1936) and others.
[7] JÁNOSSY and INGLEBY (1940), (1941), and others.
[8] BLAU and WAMBACHER (1937), STETTER and WAMBACHER (1939).

stead of balloons. The highest altitude attained therefore is much smaller, viz. 23 cm Hg. SCHEIN and col. find that at most 5% of the total number of mesons present at this altitude can be produced in this way. Furthermore, they show that these neutral particles cannot be neutrons and, as photons are excluded because of the upper 6 cm Pb,[1] they conclude that the particles are neutral mesons.[2] An important feature also revealed in these experiments is that about 33% of all the mesons at this altitude have energies below 5×10^8 e.v., while at sea level only a very small fraction of the mesons have energies within this range. The same conclusion follows from Wilson chamber photographs obtained by HERZOG and BOSTICK[3] in an airplane at the same altitude. These photographs furthermore indicate that the slow mesons are doubtless produced in multiple processes probably occurring in the neighbourhood of the chamber.

(V) *Various other experiments of importance for our problems.*

Finally, we shall state the results of various other experiments bearing upon our problems.

From several experiments it follows that the mesons are unstable with a mean lifetime of the order of magnitude 10^{-6} sec (mesons at rest).[4] From the YUKAWA theory of β-decay values are, however, deduced which are 10-100 times smaller. Hence we must assume two different kinds of mesons having different lifetimes (and spins).[5] It is therefore of great interest that JUILFS[6] has been able to give arguments for concluding from the variation of the intensity of the hard component with zenith angle that at high altitudes mesons may exist which have much smaller lifetimes. These short-living mesons must be assumed

[1] This, however, may not be true, since also here the photons may pass outside the upper 6 cm Pb and then produce one or several mesons giving coincidence in the 4 lower counters, as also remarked by HEISENBERG (1943) p. 51. Furthermore, a meson may be slightly scattered in the Pb above counter 2 so as to give coincidence between counters 2-5, but not in 1.

[2] Cf. also ROSSI and REGENER (1940), who give experimental evidence of the same conclusion, and ARLEY and HEITLER (1938), who draw the same conclusion from the experiment of MAASS (1936).

[3] HERZOG and BOSTICK (1941).

[4] Cf. e.g. the review in HEISENBERG (1943) p. 78 ff.

[5] ROZENTAL (1941).

[6] JUILFS (1942).

applies to the counts of the side counters measuring the showers. Finally, we should like to know whether the side counters marked 6, measuring the showers, are placed so as to measure showers with small or only those with large angle spread. In the latter case, the negative result *may* be due to the fact that the very energetic showers are very narrow, so that perhaps they may pass more or less undetected *between* the side counters without activating them. We hope that the proposed controls of this extremely important experiment will be carried out in a near future. It would also be interesting to know the intensity of photons at the top of the atmosphere, which may be measured by an anticoincidence method.

Previous to the investigation just mentioned, SCHEIN, JESSE and WOLLAN[1] have carried out another experiment in order to find out whether mesons may also be created by a non-ionizing radiation. For this purpose they measured the difference between the number of coincidences 1-2-3 and 2-3-4, the counters 1 to 4 being placed in line with in all 8 cm Pb between both groups of counters. They interpreted this difference as being due to mesons produced in 2 cm Pb placed between counters 1 and 2 by a radiation which did not produce coincidences in counter 1, i.e. a non-ionizing radiation. They found that up to 6·6 cm Hg this difference increased roughly proportionally to the intensity of the total radiation, i.e. practically proportionally to the soft radiation, which indicates that the non-ionizing radiation in question was the photons of the soft component. This conclusion, however, is not quite unambiguous as the difference may also be partly due to mesons passing outside of the counter 1 and being very slightly scattered in the 2 cm Pb between counters 1 and 2.[2]

The same objection applies to the experiment of SCHEIN, WOLLAN and GROETZINGER.[3] They use an experimental arrangement similar to that of SCHEIN, JESSE and WOLLAN,[1] except that now 6 cm Pb is placed above all the counters to exclude photons, and that the experiments are performed in an airplane in-

[1] SCHEIN, JESSE and WOLLAN (1939), (1940).

[2] If the diagram of the experimental arrangement given in the paper is in true scale, it is even possible to draw a *straight* line through counters 2, 3 and 4 which does not pass through counter 1!

[3] SCHEIN, WOLLAN and GROETZINGER (1940).

the intensity of the total radiation increases steadily up to a maximum at about 8 cm Hg,

at which altitude the intensity is approximately 50 times that at sea level, and then falls off rapidly at higher altitudes. Next, SCHEIN, JESSE and WOLLAN's results show, firstly, that

the hard component does not pass through any maximum, but increases up to the very greatest heights attained,

viz. 2 cm Hg. Secondly, that

all the points for the 4, 6, 8, 10, 12, and 18 cm Pb absorbers lie on the same curve.

In the experiments of SCHEIN, JESSE and WOLLAN, two side counters were, furthermore, operating in order to detect also showers (containing at least 2 particles) produced in 4 and in 6 cm Pb. The result was negative, in that

only a few per cent of the particles traversing 4 and 6 cm Pb were accompanied by showers.

This important experiment is interpreted by the authors as proving that at the top of the atmosphere practically no electrons with energies able to penetrate the 4 cm Pb, i. e. 10^9-10^{12} e.v., can be present, because (a) the penetrating power of the particles measured is constant, (b) they are non-shower-producing. Since the magnetic field of the earth at 56°N cuts off all electrons below 3×10^9 e. v., and since the measurements were carried out up to 2 cm Hg, which is within one shower unit (= 2·6 cm Hg), they furthermore conclude that

in the energy region 10^9-10^{12} e.v. the primary cosmic radiation can contain only a few per cent primary electrons.

As SCHEIN, JESSE and WOLLAN point out themselves, it is, however, necessary to perform control experiments with 2, 1, and 0 cm Pb between the counters in order to obtain the transition to the PFOTZER curve mentioned above. Moreover, it should be emphasized that the thicknesses which are of most interest in this connection, viz. 4 and 6 cm Pb, are represented by only one point each at about 3 cm Hg, but not in the other parts of the curve, especially not at the maximum of the PFOTZER curve. The same

As to the nature of these hard showers it is experimentally found that the showers observed on Wilson photographs consist mainly of mesons together with a few protons. The same is probably true for the hard showers measured by JÁNOSSY and INGLEBY, whereas the photographi stars are known to consist of protons and neutrons (together perhaps with a few mesons). The single protons and neutrons also found in cosmic radiation (cf. p. 5) can probably be fully accounted for as resulting from the explosions observed as the stars.[1] We must thus at present conclude that

there are two different types of non-cascade showers, the explosion showers and the evaporation showers.

The explosion showers consist of mesons produced by multiple processes in which presumably a primary, very energetic photon is absorbed. The protons which may accompany these processes arise from a transfer of a certain part of the energy to the nuclei at which the mesons are produced, thus giving rise to a more or less local heating up and a subsequent evaporation of nucleons. The energies of both the incident particle and the mesons produced as a rule being relativistic in these processes, we must expect the angular dispersion to be rather small, but we are unable to judge whether this agrees with experiments or not. In the evaporation showers the processes are presumably the same, except that the primary photons are less energetic than in the explosion showers so that the binding of the nucleons plays a more dominant rôle. Consequently, most of the energy is transferred to the nucleus in the form of greater heating up. As a result, most of the particles emitted are protons and neutrons and only a few particles are mesons. Both the primary particle and the evaporation particles produced having non-relativistic energies, we must in this case expect a more uniform distribution in space of the particles emitted, as is just found experimentally in the BLAU-WAMBACHER stars.

So far as we can judge, only Wilson chamber photographs have been found showing the direct creation of mesons or protons from primary photons, but not from primary mesons, protons, or electrons. Theoretically, the evaporation showers

[1] Cf. the discussion in HEISENBERG (1943) p. 124 ff.

may also be produced by primary protons and neutrons by 'nuclear ionization',[1] in which the incident particle gives off part of its energy by inelastic collisions, thereby heating up the nucleus, which then evaporates. This process, however, does not seem to have been directly observed. Also such showers may theoretically be produced by the absorption of slow negative mesons[2] (the slow positive mesons being repulsed by the Coulomb forces); for this process will take place long before the radioactive decay. Although this effect seems indirectly verified by the fact that at sea level more positive mesons are found than negative mesons, and next by the experiment of RASETTI[3] who finds that roughly only half of all mesons decay radioactively, the rest being absorbed without decay, no direct evidence seems to have been found, i. e. a Wilson photograph showing a slow meson being absorbed under the emission of several protons.

Finally, the extended showers found by AUGER and collaborators[4] should be mentioned. They measured coincidences between G-M-counters placed up to several 100 meters apart. It has been discussed whether these AUGER showers consist of electrons or of mesons. From absorption measurements AUGER and KOLHÖRSTER assumed them to consist mainly of electrons together with a few mesons, because the number of coincidences was only reduced to about 25% behind 15 cm Pb. At any rate, from Wilson chamber photographs it follows that most of the particles are very energetic electrons.[5] Assuming the AUGER showers to be cascade showers formed at the top of the atmosphere and reaching their maximum at about sea level, it follows that such cascades are not absorbed even in 15 cm Pb. As shown by MOLIÈRE,[6] the cascade theory can actually account for *all* the particles being electrons. Such showers representing at sea level energies up to 10^{15} e. v., they must have been produced by primary particles of energies even up to 10^{18} e. v.

[1] HEISENBERG (1937).
[2] TOMONAGA and ARAKI (1940).
[3] RASETTI (1941).
[4] AUGER and col. (1938), KOLHÖRSTER and col. (1938).
[5] JÁNOSSY and LOVELL (1938), AUGER and col. (1939).
[6] HEISENBERG (1943) p. 35 ff.

Part 2. The various possible hypotheses regarding the primary component.

Having reviewed the main experimental facts of importance for our fundamental problems, (b) and (c) p. 3, we now turn to the next question: by what hypotheses regarding the primary component can we correlate and explain this vast experimental material? We have the following possibilities regarding the primary constituents:

photons, electrons, neutrons, protons, mesons, and neutrinos,

together with combinations of all these particles.

First of all we can exclude the neutrons and the charged mesons, as these particles are unstable with mean lifetimes of the order of magnitude one hour and 10^{-6} sec, respectively. The latter result is deduced experimentally, the former theoretically, but without being verified experimentally. This verification is presumably also impossible because the neutrons are slowed down and absorbed by the various nuclei even in the atmosphere long before they would have time to decay.[1] Furthermore, we shall at once exclude the hypothetical neutrinos from our considerations, as their existence has not yet been directly demonstrated (cf. however the remark on p. 4).

From the geomagnetic effects it follows that at any rate a certain fraction of the primary particles are charged particles. (We note that these effects obviously operate *outside* the atmosphere, the thickness of which is only of the order of magnitude $\frac{1}{10} - \frac{1}{100}$ of the radius of the earth). From the very high values, viz. 70-80%, for the latitude effect of the total radiation at great altitudes, i.e. practically the soft component, it follows that most of the primary particles of the soft component must be charged particles. MILLIKAN and col.[2] estimate that

the energy brought into the atmosphere by non-charged particles can at most amount to 20% of that brought by charged particles.

To obtain as simple a description as possible we shall, therefore, also exclude photons and neutral mesons as primary particles of the soft component. Of course, Nature need not at

[1] HEISENBERG (1943) p. 141.
[2] BOWEN, MILLIKAN and NEHER (1938).

all be simple, and in fact cosmic rays have proved to be far more complicated than anybody has at first imagined. Nevertheless it is generally agreed that to begin with we should try the simplest hypotheses before having recourse to the more complicated ones.

For the hard component the latitude effect as a function of altitude, as mentioned above p. 8, has not yet been fully investigated. Thus, we cannot at present exclude the possibility that a more considerable fraction of the hard component is due to non-ionizing primary particles than the soft one. We shall, however, also here, for the sake of simplicity, assume that *the whole* of the hard component is due to primary charged particles. Consequently in both cases only electrons alone, protons alone, or a combination of these particles remain.

(I) *The electron hypothesis.*

According to this hypothesis[1] the soft component mainly consists of cascade showers from the primary electrons, the integral energy spectrum of which must be assumed to be of the form

$$F(E) = \text{const } E^{-\gamma} \qquad \text{for } E > 1\text{-}2\times 10^9 \text{ e. v.}, \qquad (4)$$

in which we must insert $\gamma \sim 1{\cdot}8$ in order to fit the experiments.[1] Next, the hard component is assumed to consist of secondary mesons produced by the photons of the soft component. Hence the intensity of the hard component must pass through a maximum and approach zero at the top of the atmosphere. As regards the proportion between positons and negatons, JOHNSON[2] has concluded from the very small east-west asymmetry of the soft component at sea level and at 4300 m altitude that there must be practically the same number of positons and negatons (cf. p. 10). This conclusion does not, however, follow unambiguously from the experiments mentioned. From the cascade theory it follows, firstly, that at sea level a soft component produced as cascade showers from either photons, positons, or negatons can show a latitude effect of at most a few per cent and the

[1] This hypothesis forms the basis of the surveys of EULER and HEISENBERG (1938), HEITLER (1938), and ARLEY (1940).

[2] JOHNSON (1935 a).

same, therefore, applies to the east-west asymmetry.[1] At 4300 m altitude, HEITLER[1] estimates the latitude effect at 17%. The corresponding east-west asymmetry has not been worked out, but as a zenith angle z at this altitude increases the layer of air traversed by the shower from $l = 17$ to $l = \frac{17}{\cos z} \sim 20$ and 24 (l measured in shower units) for $z = 30°$ and $z = 45°$, respectively, the primary energies necessary to penetrate this distance will certainly be such as to reduce the east-west asymmetry to at most a few per cent (cf. the discussion on p. 12). *Consequently, we can draw no conclusions as to the sign of the primaries of the soft component from its east-west asymmetry in the lower part of the atmosphere.*

From the east-west asymmetry of the hard component it follows, on the other hand, due to its small absorption (the mesons only losing about 2×10^9 e.v. during their passage through the whole atmosphere) that its primaries must consist of more positive than negative particles. If SCHEIN's experiment mentioned above ([3] p. 10) turns out to be reliable, we must even conclude that

all the primary particles of the hard component are positively charged,

as first concluded by JOHNSON.[2]

Thus we must assume either that the primary radiation mainly consists of positons, or that the mesons can only be produced by the primary positons, but not by the primary negatons. The latter possibility must be rejected at once, because the showers produced by primary electrons of either sign are after some distance practically identical in the number of photons, positons, and negatons, respectively, and it is impossible to imagine processes by which the mesons of the hard component should be produced only by the primary, but not by the secondary electrons. Furthermore, we must at present assume that the mesons are produced only by the photons and not directly by the electrons of the soft component.

We are thus forced to assume the primary electrons to be

[1] HEITLER (1937), ARLEY and ERIKSEN (1940).
[2] JOHNSON (1938), (1939a), (1939c). Cf. also ALFVÉN (1939b).

mainly positive. But this conclusion involves some difficulties. Firstly, both the soft, the hard and thus the total radiation should in this case show a very large positive east-west asymmetry at great altitudes in contrast to the above discussed experiment of JOHNSON and BARRY ([1] p. 10) finding only $a \sim +7\%$ for the total radiation against an expected value $\sim +60\%$ on the hypothesis that the primary radiation consists only of positive particles. *We think this experiment is already a crucial one, which alone is enough to reject the electron hypothesis.* It has, however, been objected to this conclusion that the negative result of the experiment may also be explained by assuming that the direction of the primary particles is not conserved, but is quite blurred by the processes producing the secondary particles.[1] Against this argument it must first of all be pointed out that it seems difficult to understand why this effect should be more pronounced in the upper than in the lower atmosphere or at sea level, where the total radiation shows a considerable east-west asymmetry. If the particles are cascade electrons, most of them will have energies about or rather above the critical energy of air, viz. $1{\cdot}5\times10^8$ e.v., which is much higher than the rest energy of the electrons, and both from the cascade theory of showers and directly from Wilson chamber photographs it then follows that the angular dispersion is very small. Next, by whatever processes particles are created from primary particles of relativistic energies, it follows simply from the Lorentz transformation from the center of gravity coordinate system to that in which the process is observed, that all the particles emitted have very nearly the same direction as the primary particle.[2]

We cannot either agree with the conclusion drawn by JOHNSON[2] from the experiment of JOHNSON and BARRY just discussed, that the primary particles of the soft component are equally positively and negatively charged. We must remember that at the altitude at which this experiment is carried out, viz. 3 cm Hg, the total radiation consists of about 57% mesons and only 43% electrons (as judged from the curves of PFOTZER and of SCHEIN,

[1] HEISENBERG (1943) p. 45.

[2] Cf. also JOHNSON (1939a), (1939b), who reaches the same conclusion from other arguments.

JESSE and WOLLAN[1]); together with SCHEIN's result mentioned above ([3] p. 10) that the east-west asymmetry of the hard component is very considerable, we can thus only conclude from JOHNSON and BARRY's experiment showing a very small east-west asymmetry of the total radiation at great altitude, that *the soft component shows a negative east-west asymmetry at great altitude. This result should, of course, be verified directly.*

A second difficulty in assuming the primary radiation to consist of considerably more positive than negative particles is that it becomes difficult to understand the propagation of the radiation in interstellar space. As pointed out by SWANN,[2] any difference in the space charge of positive and negative particles of any kind would give rise to potential differences quite irreconcilable with the further passage of charged particles through space. (Furthermore ALFVÉN[3] has pointed out that such a difference would also give rise to large magnetic fields. The effect of these fields seems, however, only to be that they make the radiation *isotropic*). Consequently, it is necessary that *in distances far away from the sources of the radiation it must consist of the same number of positive and negative particles.*

Thirdly, the SCHEIN-JESSE-WOLLAN experiment ([2] p. 12) is probably the most crucial experiment which makes the electron hypothesis irreconcilable with experimental facts, quite apart from what detailed picture we may accept of the genesis of the various components. If this experiment is reliable (in spite of the minor objections which, as we have pointed out, may be raised against it (p. 13)), it means partly that the hard component does not pass through any maximum but increases steadily, partly that the primary radiation can at most contain a few per cent electrons, both facts strongly disagreeing with the electron hypothesis.

(II) *The proton hypothesis.*

According to this hypothesis both the soft and the hard component are secondary radiations produced by protons having the same integral energy spectrum (4) as the electrons had previously.

[1] Fig. 1 in SCHEIN, JESSE and WOLLAN (1941), reproduced as fig. 2 in HEISENBERG (1943) p. 41.

[2] SWANN (1933). Cf. also JOHNSON (1939 a).

[3] ALFVÉN (1938), (1939 a).

The intensity of the soft component must, therefore, approach zero at the top of the atmosphere, whereas the hard component must increase steadily since very energetic protons also behave like penetrating particles. As just discussed it is, however, on this hypothesis quite impossible to understand the small east-west asymmetry of the total radiation at great altitude. Next, as also just discussed, it makes the propagation of the radiation in interstellar space impossible. Finally, it makes it quite impossible to understand the latitude effect of the soft component amounting to 70-80% at great altitude; for the electrons could only be produced by processes in which they obtain only a fraction of the primary energy. This primary energy must, therefore, be much higher than if the primary particles were electrons. But when the main contribution to the intensity of the soft component comes from the higher part of the energy spectrum (4), the variation of the minimum energy with geomagnetic latitude will be of little importance. Consequently, the latitude effect becomes much smaller, at most a few per cent, as also emphasized by HEISENBERG.[1] That the secondary electrons can in fact obtain only a fraction of the primary energy is clearly seen by considering those processes by which protons could produce soft showers: by knock-on electrons, by bremsstrahlung and through intermediate mesons. In the latter case, it might be suggested that the soft component in the upper atmosphere is mainly due to the radioactive decay of the very short-living vector-mesons with spin 1, the hard component consisting of the longer living pseudoscalar mesons with spin 0 (cf. p. 15). Now it follows both theoretically[2] and experimentally[3] that the mesons are mainly produced in multiple processes, each meson thus obtaining on the average only a fraction of the primary energy. Furthermore, on an average half the energy of each meson is carried away by the neutrinos. As a result most of the shower intensity would be produced by primary protons with energies beyond the field sensitive region, viz. about $2\text{-}15\times10^9$ e.v., and the soft component could show practically no latitude effect even at very high altitudes.

[1] HEISENBERG (1943) p. 5.
[2] Cf. e.g. HEISENBERG (1943), SWANN (1941), and others.
[3] Cf. e.g. SCHEIN, JESSE and WOLLAN (1941b).

The proton hypothesis must, consequently, also be regarded as irreconcilable with the experimental facts.

(III) *The combined electron-proton hypothesis.*

According to this hypothesis[1] the soft component in the upper atmosphere is produced as cascade showers from primary electrons, whereas the hard component is mainly produced from primary protons. From the above discussion of the very small east-west asymmetry of the total radiation together with SWANN's neutrality argument regarding the number of positive and negative particles in the radiation in interstellar space, it follows that the primary *electron* component must consist practically of only *negatons* in a number equivalent to that of the protons. The only crucial experiment which forces us to reject this in all other respects excellent hypothesis is thus the experiment of SCHEIN, JESSE and WOLLAN (² p. 12), which shows that there can only be at most a few per cent electrons present at the top of the atmosphere.

Summarizing our discussion, we must thus conclude that *the total present experimental evidence is irreconcilable with any of the hypotheses theoretically possible using the particles known at present.* For this negative result the crucial experiments are those of JOHNSON and BARRY (¹ p. 10), SCHEIN, JESSE and WOLLAN (² p. 12), and the latitude effect of the soft component at great altitude. Also the neutrality argument of SWANN (² p. 23), necessary for the propagation of a charged radiation in interstellar space, leads to the same conclusion. We may thus say that

there is at present indirect experimental evidence for the existence of a new and hitherto unknown particle in the primary cosmic radiation,

and we think that the most plausible hypothesis which may be set up as to the nature of this new particle is to assume it to be a *negative proton.*

[1] This hypothesis has been favoured by JOHNSON (1938), (1939 a).

Part 3. The hypothesis of the existence of negative protons in the primary cosmic radiation.

As mentioned in the introduction, this hypothesis has been put forward by the author from the arguments discussed above, and by KLEIN from arguments regarding the origin of cosmic rays.[1] In this part, the consequences of this hypothesis, and in the last part KLEIN's theory will be discussed.

We assume on this hypothesis that

the primary cosmic radiation consists of positive and negative protons with the integral energy spectrum given in (4), *p.* 20,

previously assumed to belong to electrons. From SWANN's neutrality argument we assume that

the numbers of positive and negative protons are practically equal.

Next, we assume that most negative protons will be absorbed by the positive protons at the top of the atmosphere or in the very upper part of it, their total kinetic plus rest energy thereby being transformed into 2 annihilation photons which, due to the conservation of energy and momentum, obtain the same energy and equal, but opposite momenta, uniformly distributed in space in the center of gravity coordinate system. (A *one*-quantum annihilation process is impossible for free protons, and less probable for bound protons than the *two*-quantum process). Due to the Lorentz transformation they will then, as discussed above on p. 22, in the coordinate system in which we observe the process, have practically the same direction as the incident negative proton and energies practically uniformly distributed up to $2Mc^2$ + kinetic energy of the negative proton. These photons then immediately give birth to cascade showers which at higher altitudes constitute most of the soft component. The most energetic of these showers constitute the large AUGER showers, which extend even down to sea level, together with some of the large bursts. Some of the photons may also be absorbed under the emission of mesons, especially more slow mesons.[2]

[1] ARLEY (1944), KLEIN (1945).

[2] This last process seems, however, to occur very seldom as compared with the absorption of photons leading to pair production. This is shown by the fact that the cascade theoretical ROSSI curves fit the experimental curves of

These slow mesons may then be absorbed, if they are negatively charged (cf. p. 18), giving rise to nuclear-evaporation processes in the form of BLAU-WAMBACHER stars, most of which, however, are probably produced directly by the absorption of photons.

As the kinetic energy of the incident negative proton is large as compared with the binding energy of the positive protons and the neutrons in the nuclei they meet in the atmosphere, we may neglect this binding and regard the nucleons as being free. By these annihilation processes we therefore assume that no or little heating up of the rest of the nuclei takes place, and therefore presumably few evaporation nucleons will be emitted. The single protons and neutrons found experimentally we assume to be the result of the stars (cf. the discussion on p. 17).

It may also be possible that some of the negative protons are annihilated in other processes by which mesons are created. In such cases, it is most probable from current theoretical ideas (cf. p. 24) that these processes are multiple, whereby several mesons are created in one elementary act. In order not to complicate the theory more than necessarily, and also because of the above discussion of the latitude effect of electrons produced from the mesons of these processes (p. 24), *we shall, however, tentatively assume that only the photon annihilation is of importance.*

Although most negative protons should on our hypothesis be annihilated in the upper part of the atmosphere, some of them might of course happen to penetrate to the lower parts of the atmosphere. *It is, therefore, possible to obtain direct experimental evidence on our hypothesis by looking for negative protons on Wilson chamber photographs from high altitudes such as mountains or airplanes.*

As for the *positive protons* of the primary radiation we set up the same hypothesis as e. g. JOHNSON in the previous proton or electron-proton hypothesis, viz. that in the upper atmosphere they are momentarily or gradually transformed into mesons (which are presumably only pseudoscalar mesons, as discussed

ROSSI and JÁNOSSY (1939), TRUMPY (1943), NEREson (1942), and others, even up to the highest thicknesses of absorbers employed in these experiments (cf. the theoretical calculation and the comparison with these experiments in ARLEY (1943) chap. 6). On the other hand, the experiments of SCHEIN and col. ([1] and [3] p. 14) seem to show that such processes do occur in the atmosphere.

below p. 29). It may also, of course, be possible that very energetic protons emit bremsstrahlung and knock-on electrons, thereby producing cascade showers which form part of the soft component, but these effects may presumably be entirely neglected. On the other hand, the hard component produces a considerable soft secondary radiation by the radioactive decay electrons of the mesons, and by the knock-on electrons and bremsstrahlung also produced by the mesons, giving at once rise to cascade showers denoted as decay and interaction showers, respectively. These showers presumably form most of the soft component found at sea level.

We shall now discuss the consequences of our hypothesis and the above mentioned assumptions and compare them with the experimental evidence given in part 1.

First, by its very construction our hypothesis is seen to agree with SWANN's neutrality argument. Secondly, the soft component is seen to pass through a maximum, approaching zero at the top of the atmosphere as was found experimentally by PFOTZER and by SCHEIN, JESSE and WOLLAN ([1] and [2] p. 12). Thirdly, the *total* energy of the negative protons is transferred to the soft component produced, and next nearly the same fraction of the negative protons as of the electrons, previously assumed to be the particles having the energy spectrum (4) p. 20, have now energies in the field-sensitive region, viz. about $2\text{-}15\times10^9$ e.v. for electrons; for this energy region is practically the same also for high speed protons (although somewhat lower).[1] Consequently, our hypothesis also leads to the same high values of the latitude effect of the soft component at great altitude as did the electron hypothesis, and as is found experimentally. That part of this soft component which reaches sea-level would, however, just as was the case in the electron hypothesis, now be produced mostly by protons in the non-field-sensitive region and would, consequently, show a latitude effect and an east-west asymmetry (although negative) of at most a few per cent at sea level. Both these effects would, on the other hand, increase very much with increasing altitude. On our hypothesis the soft component should thus at high altitude, where the

[1] Cf. e. g. JOHNSON (1938) table II p. 219, also quoted in HEISENBERG (1943) table 1 p. 152.

contribution to the soft component from the hard component is only small, show a considerable east-west asymmetry in the *opposite* direction of the hard component, i. e. a preponderance of negative primaries, or greater intensity from the east. It should, however, here be noted that this conclusion is based on the assumption that the mesons produced by the positive protons mostly are long-living pseudoscalar mesons. If also a considerable number of short-living vector mesons were produced in these processes, they would already at high altitudes decay into electrons at once giving birth to cascade showers. As a result, the east-west asymmetry of the soft component at great altitude would in this case be less negative or even practically zero. *The direct experimental determination of the east-west asymmetry of the soft component at great altitude is thus of fundamental importance*, although JOHNSON and BARRY'S experiment already gives strong evidence of a considerable *negative* east-west asymmetry of the soft component at great altitude, as discussed above (p. 23). Furthermore, this east-west asymmetry of the soft component should be practically non-increasing with increasing zenith angle (cf. p. 12).

As for the hard component, it is firstly seen that on our hypothesis it does *not* pass through any maximum, but increases steadily up to the very greatest heights. As already stated, the primary protons, having relativistic energies, will behave as a hard component whether they are transformed immediately or gradually into mesons. Next, the hard component now shows the same geomagnetic effects as in the previous proton hypothesis, viz. a latitude effect at sea level of the order of magnitude 10-20 %, which increases with increasing altitude, but less strongly than that of the soft component, because the mesons only lose about 2×10^9 e. v. by their passage through the whole atmosphere. We think that also this statement is in agreement with the experiments although the data are here rather scanty, as discussed on p. 8. Finally, for the same reasons our hypothesis leads to a positive east-west asymmetry already at sea level. Furthermore, this positive east-west asymmetry must increase with increasing altitudes and with increasing zenith angle (cf. p. 12), which statements are both in agreement with the experimental findings.

Combining the latter result with the result of the negative east-west asymmetry of the soft component, we thus see that our hypothesis leads to an east-west asymmetry for the total radiation which decreases with increasing altitude, as is just found experimentally by JOHNSON and BARRY ([1] p. 10; cf. also the discussion on p. 22). *We think that this crucial experiment is a strong argument in favour of our hypothesis.*

We note that it might be thought possible to test experimentally, if our hypothesis is at all accepted, whether the soft component in the upper atmosphere is produced through intermediate vector mesons (cf. above p. 24). For the lifetime of these particles we must presumably assume values of the order of magnitude 10^{-8} sec. In that time, they would on an average move a distance of $10^{-8}.3.10^{10}.\frac{E}{\mu c^2}$ cm $\sim$ 100 m (the velocity being relativistic, and the factor $\frac{E}{\mu c^2} \sim 40$ being the relativistic time factor). Thus, those vector mesons produced in the neighbourhood of the measuring apparatus would pass through it as a hard radiation, but as one showing a *negative* east-west effect. At that altitude at which the hypothetical transformation, negative protons to vector mesons, should take place, we thus might observe a temporary decrease in the east-west asymmetry of the hard component. We think, however, that in view of the fact that such vector mesons must be created in multiple processes, if at all created, this eventual decrease could only amount to a few per cent and thus presumably only be within the measuring errors.

At sea level most of the soft component is presumably due to the decay and interaction showers mentioned above (p. 28),[1] and it could therefore only show a latitude effect of at most a few per cent, these showers representing only a fraction of the energy of the primary particles from which they have been produced. As the same applied to the cascade showers produced from the negative protons, the total soft component at sea level should show a latitude effect of at most a few per cent, as just found experimentally.

As regards the east-west asymmetry of the soft component produced from the hard one, it could also for the same reasons

[1] In HEISENBERG (1943) p. 90, it is estimated that at sea level the soft component is composed of about 62 % decay showers (Z), 17 % interaction showers (W) and 21 % cascade showers (R) (the last originating according to our hypothesis from the negative protons).

as for the latitude effect amount to at most a few per cent, but in the *opposite* direction of the east-west asymmetry of the part of the soft component produced by the negative protons. Consequently, the east-west asymmetry of the total soft component at sea level must be practically zero, as is just found experimentally. With increasing altitude the cascade part of the soft component becomes more and more dominating, and the east-west asymmetry of the soft component should thus on our hypothesis decrease with increasing altitudes, becoming more and more negative, as is indirectly verified by the experiment of JOHNSON and BARRY (cf. the discussion on p. 22).

As for the meson showers and the nuclear stars, i. e. the explosion and the evaporation showers, respectively (cf. p. 16 ff.), it follows from our hypothesis (p. 27) that their frequency should increase roughly proportionally to the intensity of the soft component, as just found experimentally. KLEIN,[1] however, has also suggested the possibility that the stars may be due to the absorption of slowed down negative protons. As here the binding of the nucleons must come into play, such an absorption would lead to a strong heating up of the nucleus and a subsequent evaporation in contrast to the case of very fast protons (cf. p. 27). Also this process would explain that the frequency of the stars increases very strongly with increasing altitude. Although, as we have seen, it is unnecessary to have recourse to this explanation of the stars, because they are equally well explained as the result of the direct absorption of photons (or perhaps of slow negative mesons), we would not exclude the possibility of the existence of such processes.

KLEIN[1] has also suggested another explanation of the very large AUGER showers in order to account for the occurrence of the enormous energies, viz. 10^{15}-10^{18} e.v., necessary if they are to be explained as cascade showers produced at the top of the atmosphere and penetrating down through the whole of the atmosphere to sea level. KLEIN suggests as another explanation that there may also in the primary radiation exist whole grains or dust particles consisting of reversed matter, i. e. matter the atoms of which consist of negative protons, 'antineutrons' and positons (cf. the last part of the present paper). When these grains

[1] KLEIN (1945).

of reversed matter hit the atmosphere, all their constituents are annihilated successively during a very short time by a chain of annihilation processes so that a very large number of very energetic particles are produced within a very narrow space. If it is possible that the particles resulting from these annihilations are mostly photons or electrons, or are immediately transformed into such by cascade multiplication of photons or of the electrons from the radioactive decay of intermediate mesons, we think this to be a most promising explanation of the extremely high total energies revealed in the AUGER showers, these energies now resulting from many primary particles which are transformed practically simultaneously, instead of from one single parent particle as in the previous explanation. The result must, however, on whatever explanation given be electrons, as the AUGER showers are experimentally known to consist mostly, if not exclusively, of electrons (cf. the discussion on p. 18).

Summarizing, we think it may be said that *our hypothesis is able to explain, at any rate qualitatively, all the present experimental evidence.* In fact we have not found any experiment directly contradicting it, but we stress that, of course, *only further experiments can show whether our purely tentative hypothesis contains part of the truth or perhaps even the whole truth of the genesis of cosmic rays.*

Regarding the more quantitative side of the hypothesis it is, due to the very incomplete state of the present quantum theory within these high energy regions, premature to try to deduce any numerical results e.g. for the various intensities and the geomagnetic effects. As discussed by the author,[1] our hypothesis demands a cross section of the order of magnitude 10^{-25} cm^2, i. e. nuclear dimensions, for the fundamental process of the two-quantum annihilation of a negative and a positive proton. Against this, the present DIRAC equation, *which, applied to protons, just demands the existence of negative protons,* gives only a cross section of the order of magnitude 10^{-32} cm^2, i. e. smaller by a factor 10^7. Since we are in these processes far beyond the limits of validity of the

[1] ARLEY (1944).

present quantum theory, as estimated by HEISENBERG ([1] p. 32), this discrepancy may not be so serious, especially when we also keep in mind that the negative protons may certainly participate in quite different processes, the calculation of which is beyond the capacity of the present quantum theory.

Part 4. On the origin of cosmic radiation.

As mentioned in the introduction, the idea of assuming the existence of negative protons in the primary cosmic radiation has also been put forward in a paper by KLEIN.[1] The purpose of this paper, however, is not that of explaining the present experimental data on the behaviour of the radiation in the atmosphere of the earth, but to answer our question (a) p. 3, i. e. to explain the origin of the enormous energies of the cosmic rays. As already pointed out by MILLIKAN and his collaborators,[2] the average energy of the primary energy spectrum (4) p. 20, viz. about 4×10^9 e.v., is just of the same order of magnitude as the rest energy of those nuclei which, from astronomical observations, are known to occur most frequently in interstellar space, namely H, He, C, N, O, and Si. MILLIKAN and his coworkers therefore suggested that the source of the cosmic radiation is simply to be sought in nuclear processes in which these nuclei are annihilated, the rest energy being given off in the form of two electrons. (At least *two* electrons in order to obey the conservation laws for energy and momentum). Due to these conservation laws, the electrons carry each half the energy and have equal, but opposite momenta which are uniformly distributed in space. From this hypothesis we should expect the primary energy spectrum to be not continuous, as assumed in formula (4), but *discrete*, having only the energies corresponding to half the rest energies of the nuclei mentioned, viz.[3]

[1] KLEIN (1945).
[2] BOWEN, MILLIKAN and NEHER (1938).
[3] 1 atomic unit is the rest energy Mc^2 of $\frac{1}{16}$ of O^{16}, i.e. $931{\cdot}05\times10^6$ e.v (cf. e.g. BETHE (1936) p. 86). The atomic weight of the proton being 1·00813, the rest-energy of H^1 is $0{\cdot}9386\times10^9$ e.v., etc.

	H^1	min. en.	He^4	C^{12}	N^{14}	O^{16}	Si^{28}	max. en.
Energy in atomic units	0·5	..	2	6	7	8	14	..
Energy in 10^9 e.v.	0·47	1·4	1·9	5·6	6·6	7·5	13·2	16·5
Corresponding geomagnetic latitude		60°N U.S.A.	56°N U.S.A.	42°N U.S.A.	40°N U.S.A.	33°N U.S.A.	20°N India	0° India

In this table we have also given the geomagnetic latitudes at which these energies represent the minimum energy (for electrons) for the direction of easiest access, which is smaller than the minimum energy for the vertical direction.[1] Since the magnetic dipole of the earth is situated excentrically, these minimum energies vary slightly with longitude.[2] For protons the minimum energies are somewhat smaller for the same latitude.[3] The column denoted by min.en. in the table gives the minimum energy found in the primary spectrum for easiest access, which is generally ascribed to the blocking effect of the sun. The column denoted as max. en. gives the largest minimum energy for vertical incidence at the equator.

On MILLIKAN's hypothesis we should thus expect the intensity of cosmic radiation in the stratosphere to have a banded structure, being constant between the geomagnetic latitudes corresponding to these energies and increasing each time such a latitude is passed from north to south. This effect MILLIKAN and collaborators[4] in fact claim to have observed. Their observations are, however, carried out with ionization chambers and the measurements, therefore, give the total effect of both the soft and the hard component and from all directions. *So it would be more adequate to use G-M-counters and thus try to ascertain whether the effect, if real, exists for the soft, the hard, or both components. Furthermore, the east-west asymmetry should then also show a banded structure*, an effect which does not yet seem to have been observed.

[1] Cf. e.g. JOHNSON (1938) fig. 14 p. 219.
[2] Cf. e.g. JOHNSON (1938) fig. 16 p. 222.
[3] Cf. e.g. JOHNSON (1938) table II p. 219.
[4] MILLIKAN, NEHER and PICKERING (1942), (1943).

However, from a theoretical point of view a process in which nuclei are annihilated, just two electrons thereby being emitted, is quite an unknown process. Furthermore it is irreconcilable with the conservation of charge, and in general also of spin and statistics, which conservation laws are just as fundamental as those for energy and momentum. In order to overcome these theoretical difficulties and yet to be in agreement with the banded structure postulated by MILLIKAN and col., KLEIN has put forward the following hypothesis.

From general theoretical considerations one would expect a perfect symmetry between the positive and negative electricity in the world, a symmetry which was much emphasized by DIRAC's electron theory and the subsequent experimental discovery of the positon. Thus, there ought also to exist what KLEIN calls reversed matter, in which all electric signs are reversed, i.e. which consists of negative protons, 'antiprotons, positons and antineutrons, the magnetic moment of which has a direction with respect to the spin momentum opposite to that of ordinary neutrons. Applying the DIRAC equation also to the nucleons, a positive and a negative proton, as well as a neutron and an antineutron, should be able to annihilate each other just as a positon and a negaton can annihilate each other under the emission of two photons (which process is more probable than the one-quantum annihilation process being possible for bound particles), whereby the photons become equal energies and equal but opposite momenta. The annihilation can perhaps also take place under the emission of two or more mesons.

Since the spectra emitted by ordinary and by reversed matter would be identical, it would be impossible to ascertain whether a given star consists of one or the other form of matter. Assuming the stars of each galactic system to have a common origin, KLEIN now also assumes that all the stars of one galactic system consist of the same kind of matter, but of matter different from one galactic system to another. In the intergalactic space nuclei of both kinds may exist together, due to the extremely small density of matter present there. KLEIN next assumes that these nuclei move about with thermal velocities and by their collisions are at once annihilated as soon as different kinds of matter come into contact with each other, thus giving birth

to the cosmic rays. Now, as mentioned above, the most frequent nuclei are H, He and then C, N, O and Si, which occur in the approximate ratio 100:10:1:1:1:1.[1] Collisions between *like* nuclei will lead to total annihilation, the energy being given off either (a) as two photons, or (b) as two or more mesons. KLEIN assumes that (b) is the dominating process and that just *two* mesons are formed. These mesons will next decay, emitting an electron and a neutrino. KLEIN now argues that, as the nuclei are assumed to move with thermal velocities, each meson will get exactly the rest energy of one nucleus and the electrons therefore practically half that energy, thus just leading to the same discrete energies as postulated by MILLIKAN and collaborators. *This argument is, however, erroneous.* First, it is unlikely that just *two* mesons will be created, because, as discussed by HEISENBERG,[2] the processes with higher multiplicity must be expected to be practically just as probable as the two-meson process. Secondly, whether this is true or not, the mesons will at any rate obtain relativistic velocities and in that case the electrons emitted by the radioactive decay in our coordinate system, due to the Lorentz transformation, will have energies nearly uniformly distributed between 0 and the *whole* meson energy, as previously stated (p. 22),[3] but overlooked by KLEIN. Any such process will thus lead to *continuously* distributed electron energies and not to the band structure postulated by MILLIKAN and col.

Next, as regards collisions between *unlike* nuclei with x ordinary and y reversed nucleons respectively ($x < y$), or vice versa, KLEIN assumes that $2x$ of the nucleons are completely annihilated and that, due to the thermal energies of the colliding particles being small compared with the binding energies of the nuclei, this annihilation energy will, by a sort of internal conversion of either the photons or the mesons produced, be transferred to the remaining $y - x$ nucleons rather than be given off. KLEIN next assumes this heating up to be so violent that all the $y - x$ nucleons are emitted with *equal* energy.

[1] We only wonder whether these figures may be extrapolated to be valid for the inter*galactic* space, as they have, so far as we know, only been deduced experimentally in the inter*stellar* space.

[2] HEISENBERG 1943 p. 115.

[3] Cf. the detailed calculation in EULER and HEISENBERG (1938) § 14.

Just as was the case for the collisions between like nuclei, KLEIN thus assumes the collisions between unlike nuclei to lead to discrete energies. *This last assumption is, however, certainly just as erroneous as the first one*, because the energy must necessarily be distributed more or less at random over the $y-x$ nucleons, thus again giving a *continuous* spectrum extending up to $2x$ atomic units ([3] p. 33). After some time the neutrons and antineutrons produced by these unlike collisions will, furthermore, decay, being transformed into protons + negatons and negative protons + positons, respectively. Due to the Lorentz transformation mentioned above these particles will again have *continuously* distributed energies extending up to some 10^9 e.v.

We may thus conclude that KLEIN's *hypothesis does not lead to a band structure of the primary radiation*, which on his hypothesis consists of electrons (perhaps photons) together with both positive and negative protons having continuously distributed energies of the order of magnitude of some 10^9 e.v. (the maximum energy at any rate not exceeding the rest energy of Si^{28}, i. e. 26×10^9 e.v.). Furthermore, this primary radiation will obviously consist of practically the same number of positons and negatons as well as of positive and negative protons. *Apart from the electrons (perhaps photons)*, which particles must necessarily, as far as we can see, constitute a non-negligible part of the primary radiation, KLEIN's *hypothesis just leads to the same result regarding the primary component of cosmic radiation as our analysis of all the experimental data on the behaviour of the radiation in the atmosphere of the earth.* The crucial point for KLEIN's hypothesis is thus, whether the experiment of SCHEIN, JESSE and WOLLAN[1] is compatible with the existence of a certain electron component in the primary radiation or not. We note, however, that primary photons will *not* be measured in this experimental arrangement and perhaps, therefore, we have to assume the photon rather than the meson annihilation (case (a) above, p. 36). On the other hand, it is impossible at the present state of quantum theory to evaluate quantitatively the cross sections for the various processes in question and thus to estimate the fraction of the primary radiation, which

[1] SCHEIN, JESSE and WOLLAN (1941 a).

according to KLEIN's hypothesis must be electrons (perhaps photons). Roughly one would expect the fraction originating from the collisions between like nuclei to be of the order of magnitude $10\,^0/_0$, because the most frequent collision leading to electrons is the He-He process,[1] the relative frequency of which is of the order of magnitude $10 \times 10 = 100$, which is just $10\,^0/_0$ of the relative frequency of the most frequent collision leading to nucleons, viz. the H-He process, the relative frequency of which is of the order of magnitude $100 \times 10 = 1000$. Hereto must, certainly, be added those electrons originating from the radioactive decay of the neutrons and the antineutrons, but as the energy hereby liberated is only of the order 10^6 e.v., these electrons will in our coordinate system practically move with the same velocity as the neutrons, i.e. their energy will only amount to the fraction $\frac{m}{M}$ of that of the nucleons. Consequently these electrons may be entirely neglected.

Another crucial point for KLEIN's hypothesis, if it is to explain *all* the primary radiation, is, as stated by himself, whether it is reconcilable with the existence of the large AUGER showers, representing a total energy of the order of magnitude of 10^{15} e.v. at sea level, which energy is by several powers of 10 beyond the upper limit represented by the rest energy of Si^{28}, viz. 26×10^9 e.v. We have already above (p. 31) discussed KLEIN's suggestion for solving this problem, and his rough quantitative analysis does not seem to be unreasonable. This point cannot, however, be decided at present; it must be left for future investigations.

Summarizing, we may say that only further experimental investigations can at all decide on the truth of KLEIN's hypothesis. We can only say at present that *it seems at any rate very*

[1] We note that also the most frequent collision between like nuclei, the H-H process, may in fact lead to electrons with energies above the lower limit $1{\cdot}4 \times 10^9$ e.v. caused by the blocking effect of the sun. Although a two-photon annihilation can only lead at most to the energy $0{\cdot}9 \times 10^9$ e.v., and the same applies to the electrons resulting from a two-meson annihilation, an annihilation process of 3 or more mesons may lead to electrons of energies of the order of magnitude of 2 atomic units $= 1{\cdot}8 \times 10^9$ e.v. As this is, however, only the case if one of the mesons gets practically the whole energy and the same applies to its decay electron, we suppose such a process to be of negligible frequency in spite of the fact that the relative frequency of the H-H collision is of the order of magnitude $100 \times 100 = 10\,000$.

promising, since it is a conspicuous fact that the energies of the primary cosmic radiation lie essentially within the region of the annihilation energies of the lighter nuclei known to exist in interstellar space ([1] p. 36). Whether *all* the primary cosmic radiation can be explained in this way or we have to explain some part of it by other processes it is premature to decide at the moment.

Summary.

In this paper we discuss the three main problems of present cosmic ray physics, the origin of the radiation, the composition of the primary component, and the genesis of the various components observed in the atmosphere, at sea level and at great depths. In part 1 we review all the experimental data bearing upon these problems. In part 2 we discuss the three possible hypotheses regarding the primary radiation which involve only particles known at present: (I) the electron hypothesis, (II) the proton hypothesis, and (III) the combined electron-proton hypothesis. It proves that the present total experimental evidence cannot be reconciled with any of these hypotheses. For this negative result the crucial arguments are the experiments of JOHNSON and BARRY, of SCHEIN, JESSE and WOLLAN, the latitude effect of the soft component at great altitude and, finally, the neutrality argument of SWANN, which is necessary for the propagation of a charged radiation in interstellar space. There is thus indirect evidence of the existence of a new hitherto unknown particle in the primary cosmic radiation. In part 3 we discuss the hypothesis, put forward by the author and by KLEIN, that these new particles are negative protons. It is shown that the results of this hypothesis, together with plausible assumptions regarding the genesis of the soft and the hard components, seem to fit extremely well with all the experimental data. Finally, we discuss in part 4 a related hypothesis of KLEIN, that cosmic rays are produced by the annihilation of ordinary and reversed matter consisting of negative protons, antineutrons and positons.

In the discussion it is emphasized that the present experimental material is still rather incomplete. Especially we need more know-

ledge of the latitude and the east-west effects of the hard and the soft components *separately*, and the dependence of these effects on altitude, latitude and zenith angle, together with the transition from SCHEIN, JESSE and WOLLAN's curve to that of PFOTZER. Only such new experiments can decide whether the purely tentative hypotheses, on the existence of negative protons as well as on the cosmic radiation being produced by annihilation processes, contain part of the truth or perhaps even the whole truth of the genesis of cosmic rays.

Institute of Theoretical Physics,
University of Copenhagen.

List of references.

Alfvén 1938, Phys. Rev. **54**, 97.
— 1939 a, Phys. Rev. **55**, 425.
— 1939 b, Nature **143**, 435.
Arley 1938, Proc. Roy. Soc. A, **168**, 519.
— 1940, Fys. Tidsskr. **38**. 74.
— 1943, Stochastic Processes and Cosmic Radiation, Copenhagen (dissertation).
— 1944, Physica (This paper had been printed in the autumn 1944, but the printing office was destroyed during the liberation of Holland. It is now in print again and will appear in the autumn 1945.)
— and Eriksen 1940, D. Kgl. Danske Vidensk. Selskab, Mat.-fys. Medd. **XVII**, no. 11.
— and Heitler 1938, Nature **142**, 158.
Auger and Leprince-Ringuet 1934, Nature **133**, 138 (also in Int. Conf. Nucl. Phys. **1**, 88, 1934).
— Maze and Grivet-Meyer 1938, C. r. Acad. Sci. Paris **206**, 1721.
— — Ehrenfest and Fréon 1939, J. Physique et Radium **1**, 39.
Bethe 1936, Rev. Mod. Phys. **8**, 82.
Blau and Wambacher 1937, Nature **140**, 585.
Bowen, Millikan and Neher 1938, Phys. Rev. **53**, 855.
Braddick 1939, Cosmic Rays and Mesotrons, London.
Carmichael and Dymond 1937, Nature **141**, 910.
Christy and Kusaka 1941, Phys. Rev. **59**, 414.
Compton and Turner 1937 a, Phys. Rev. **51**, 1005.
— — 1937 b, Phys. Rev. **52**, 799.
Cosyns 1936, Nature **137**, 616.
Euler and Heisenberg 1938, Erg. d. exakt. Naturwiss. **17**, 1.
Fussell 1936, Phys. Rev. **51**, 1005.
Fünfer 1937, Naturwiss. **25**, 235.
— 1938, Zs. Phys. **111**, 351.
Heisenberg 1937, Ber. Sächs. Akad. Abh. math. phys. Kl. **89**, 369.
— 1943, Vorträge über kosmische Strahlung, herausg. v., Berlin.
Heitler 1937 a, Proc. Roy. Soc. A, **161**, 261.
— 1937 b, Nature **140**, 235.
— 1938, Progress in Physics, **V**, 361.
Herzog and Bostick 1941, Phys. Rev. **59**, 122.
Jánossy and Ingleby 1940, Nature **145**, 511.
— — 1941, Nature **147**, 56.
— and Lovell 1938, Nature **142**, 716.

JESSE and GILL 1939, Phys. Rev. **55**, 414.
— WOLLAN and SCHEIN 1941, Phys. Rev. **59**, 930.
JOHNSON 1934, Phys. Rev. **45**, 569.
— 1935 a, Phys. Rev. **47**, 318.
— 1935 b, Phys. Rev. **48**, 287.
— 1938, Rev. Mod. Phys. **10**, 193.
— 1939 a, Rev. Mod. Phys. **11**, 208.
— 1939 b, Phys. Rev. **56**, 226.
— 1939 c, J. Franklin Inst. **227**, 37.
— and BARRY 1939, Phys. Rev. **56**, 219.
— and READ 1937, Phys. Rev. **51**, 557.
JUILFS 1942, Naturwiss. **30**, 584.
KLEIN 1945, Ark. f. Mat. Ast. och Fys. **31**, A no. 14.
KOLHÖRSTER, MATTHES and WEBER 1938, Naturwiss. **26**, 576.
KORFF 1939, Phys. Rev. **56**, 210.
LEMAÎTRE and VALLARTA 1936, Phys. Rev. **50**, 493.
MAASS 1936, Ann. d. Phys. (5) **27**, 507.
MILLIKAN, NEHER and PICKERING 1942, Phys. Rev. **61**, 397.
— — — 1943, Phys. Rev. **63**, 234.
NEHER and PICKERING 1938, Phys. Rev. **53**, 111.
NERESON 1942, Phys. Rev. **61**, 111.
PFOTZER 1936, Zs. Phys. **102**, 23.
PICKERING 1936, Phys. Rev. **49**, 945.
RASETTI 1941, Phys. Rev. **60**, 198.
ROSSI and JÁNOSSY 1939, Rev. Mod. Phys. **11**, 279.
— and REGENER 1940, Phys. Rev. **58**, 837.
SCHEIN and GILL 1939, Rev. Mod. Phys. **11**, 267.
— JESSE and WOLLAN 1939, Phys. Rev. **56**, 613.
— — — 1940, Phys. Rev. **57**, 847.
— — — 1941 a, Phys. Rev. **59**, 615.
— — — 1941 b, Phys. Rev. **59**, 930.
— WOLLAN and GROETZINGER 1940, Phys. Rev. **58**, 1027.
SCHOPPER 1939, Phys. Z. **40**, 22.
STETTER and WAMBACHER 1939, Phys. Z. **40**, 702.
SWANN 1933, Phys. Rev. **44**, 124.
— 1941, Phys. Rev. **60**, 470.
TOMONAGA and ARAKI 1940, Phys. Rev. **58**, 90.
TRUMPY 1943, D. Kgl. Danske Vidensk. Selskab, Mat.-fys. Medd. **XX**, no. 6.

Indleveret til Selskabet den 11. Juni 1945.
Færdig fra Trykkeriet den 27. September 1945.

DET KGL. DANSKE VIDENSKABERNES SELSKAB
MATEMATISK-FYSISKE MEDDELELSER, BIND XXIII, NR. 8

DEDICATED TO PROFESSOR NIELS BOHR ON THE OCCASION OF HIS 60TH BIRTHDAY

IONIZATION MEASUREMENTS ON SINGLE RECOIL PARTICLES FROM Po, ThC, AND ThC′

BY

B. S. MADSEN

KØBENHAVN
I KOMMISSION HOS EJNAR MUNKSGAARD
1945

CONTENTS.

Printed in Denmark.
Bianco Lunos Bogtrykkeri A/S

REPRINTED 1948 TUTEIN OG KOCH

The first determinations of the energy in α-recoil were performed by MAKOWER and RUSS (1) and by EVANS and MAKOWER (2); the values found are in good agreement with those calculated from the mass ratio. WERTENSTEIN (3) has examined the ionization of the recoil atoms; in contradistinction to the specific ionization curve of the α-particles, the specific ionization curve of the recoil particles shows a uniform decrease along the track and, for the ratio $\frac{E_R}{E_\alpha}$ in air, where E_R and E_α are the energy loss per pair of ions of the recoil particle and the α-particle, respectively, WERTENSTEIN found a value between 2 and 8. By means of ionization chamber measurements, GERTHSEN and GRIMM (4) found $\frac{E_R}{E_\alpha}$ in air to be almost one. WERTENSTEIN used RaC, while GERTHSEN and GRIMM applied ThC′ to their measurements.

In the present paper, an experiment will be described which gives $\frac{E_R}{E_\alpha}$ in argon with a small (5 %) admixture of air.

I. Method.

In view of the small amount of ions produced by the recoil particles, the measurements were carried out with a proportional counter, *i. e.* a Geiger-Müller counter for which the working potential was chosen somewhat smaller than the potential used for actual counting. Ions produced by a primary ionization in the counter will give rise to a secondary ionization due to collision and, in this way, an amplification is obtained which is effective only for the ions and not for induced electrical disturbances. In the combination of a proportional counter with a valve amplifier,

the background of electrical noise can be reduced to a higher degree than in an ordinary ionization chamber in connection with a valve amplifier. This method of ionization measurements was suggested by RUTHERFORD and GEIGER (5).

WERNER (6) has shown that ions produced by irradiation of the inner side of the proportional counter wall with ultraviolet light are amplified proportionally; he further pointed out the relation between the proportional counter and the G.-M. counting tube. GEIGER (7) too has found a proportional amplification; α-rays from ThC-C′ were sent into the counter perpendicular to and directed against the wire. When particles hit the wire, the impulses produced were precisely half as great as those which originated from particles having passed through the whole diameter. This shows that the specific ionization can be regarded as a constant on the part of the α-particle track inside the counter. The experiment gives, however, no information about the amplification as a function of the locality where the primary ions are formed.

In the present experiments, the counter voltage was taken from a high tension rectifying supply giving 2800 volts d.c. 1260 volts were laid over a filter consisting of resistances and condensors. The remaining 1540 volts were stabilized by means of 11 small neon lamps. This high tension supply, which in this Institute is much used in connection with G.-M. counters, appeared to give sufficiently constant voltage. In all measurements, the voltage over the counter was chosen so that a variation of 1.5 volts caused a variation in the amplification of about 10 %. Under these conditions it was possible to obtain distinct maxima when the number of α-particle impulses was plotted against their magnitude (cf. the example in Fig. 2) and the measurements could be reproduced even after several hours.

The voltage impulses from the proportional counter were amplified further by a resistance capacity coupled valve amplifier containing two stages and a power-stage operating a mechanical oscillograph. The impulses were registered on a slip of electrocardiograph paper. Simultaneously, the amplified impulses could be observed on a cathode ray oscillograph. By means of potentiometers in the anode resistances, the total amplification could be varied within wide limits. The proportionality of the amplifier

was checked by means of artificial impulses. At the highest amplification used the artificial impulses after the amplification showed a variation in size of $\pm$ 1.5 %.

Specific ionization curves for α-particles in air have been published by HENDERSON (8) and by JENTSCHKE (9). HENDERSON gives the position on the α-ray track by measuring the distance from the α-source; JENTSCHKE, on the other hand, measures the distance from the end point of the track of the single α-ray. As it would be expected from this difference in method, JENTSCHKE's curve shows for great residual ranges relatively higher values (up to 5 %) than HENDERSON's curve. In the following experiments, the conditions were similar to those of HENDERSON and, therefore, HENDERSON's curve was taken as a basis of the comparative measurements. The number of ions per mm. produced by α-particles in argon as a function of the range can be obtained in a simple way from HENDERSON's measurements in air, since, according to GIBSON and GARDINER (10), the stopping power of argon relative to that of air as well as the energy loss per pair of ions is almost constant over the whole length of the range.

The number of ions produced in a fraction of the α-particle track was determined by the present author in arbitrary units (denoted as "Henderson units" in Table 3) by measuring the corresponding area under the ionizing curve. As it will be mentioned later, the measurements on ThC-C' α-particles were found to be in complete agreement with the values which should be expected from the Henderson curve.

II. The Proportional Counter as a Measuring Instrument.

As the multiplication of the ions in the proportional counter takes place in the vicinity of the wire, it is to be expected that the amplification of the primary amount of ions is nearly independent of the locality where the ions are formed. This was examined by means of a proportional counter constructed as shown in Fig. 1. The tube was chosen so long that the variations of the electrical field at the ends did not cause essential irregularities. The counter was closed by two ebonite discs, through one of which four glass tubes were introduced at different distances from the axis. In each glass tube two diaphragms with circular

apertures 0.5 mm. in diameter were mounted at a distance of 50 mm. Over the exterior diaphragms thin mica foils (1.3 mg./cm.^{2}) were placed. All joints were sealed with picein. The counter wire, a platinum wire 0.15 mm. in diameter, was introduced through tapered glass tubes. Grounded guard rings screened it against creeping currents.

The counter was filled with argon with an admixture of 5 % air. Pure argon appeared to be inexpedient. Even small con-

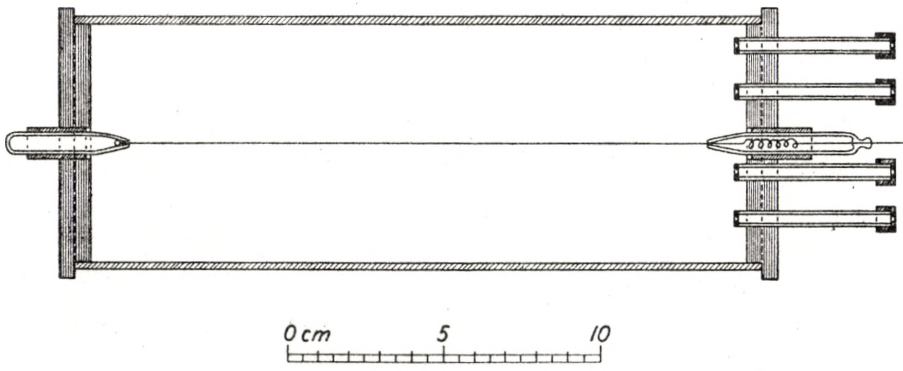

Fig. 1.

taminations influenced greatly the mobility of the ions and, hence, the amplification yielded by the proportional counter, and materials such as ebonite and picein will for a long time give off gases. When air was added to the filling gas the proportional counter worked unchanged for several weeks.

A ThC-C′ preparation was alternately placed in front of the four mica windows, the distance from the window being kept constant. When the α-particles from ThC and ThC′ passed through the whole length of the counter, statistics were produced like that in Fig. 2. Table 1 gives the mean impulse sizes relative to the four distances of the α-beam from the axis. The values

Table 1.

Distance from the axis (mm.)		9.0	16.5	24.0	31.5
Deflections (mm.)	ThC′	26.5	26.6	26.1	25.5
	ThC	42.4	42.4	42.0	41.2

show a slight decrease with increasing distance, a decrease just exceeding the experimental error. This is possibly due to the unavoidable variations in the electrical field at the ends of the counter. Within the distances used in the following experiments the amplification can at any rate be regarded as a constant.

By placing the α-preparation at different distances from the

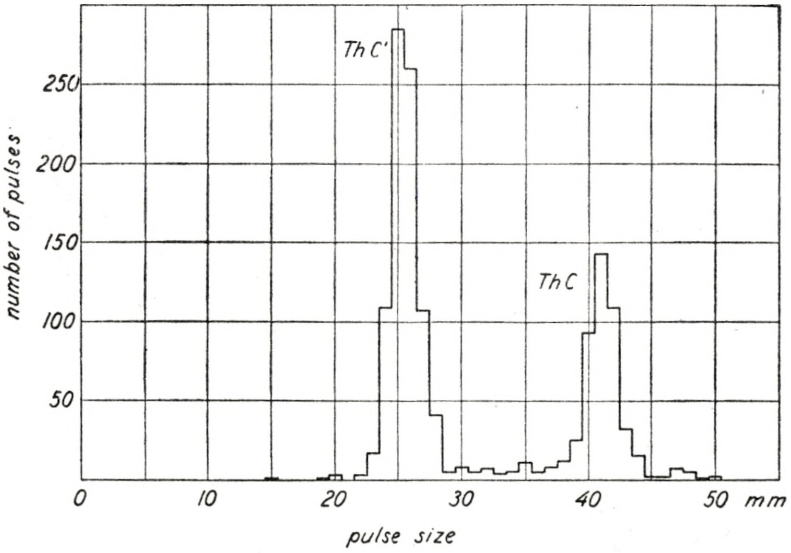

Fig. 2. Size distribution of α-particle impulses from ThC and ThC' (3 inch counter).

axis, it was each time found that the ratio between the deflections from the ThC α-particles and the ThC' α-particles agrees with the ratio expected from the Henderson curve within 2 %.

The amplification of the ions along the counter wire was investigated in the counter shown in Fig. 3. The counting tube, 1 inch in diameter, had a rectangular aperture, 1 mm. × 50 mm., covered by a mica foil, 1.2 mg./cm.^{2}. The counter wire, a platinum wire 0.15 mm. in diameter, was covered by steel tubes, 0.8 mm. in diameter, except for a portion of 34 mm. in the middle of the wire. The ends of the steel tubes were carefully rounded. From a ThC-C' preparation a narrow beam of α-rays was sent into the counter at right angles to the wire. The preparation could be moved parallel to the counter axis and the position was read with an accuracy of $^1/_{20}$ mm.

The α-particles were sent into the counter partly diametrically, partly along a secant. The two cross-sections and the cor-

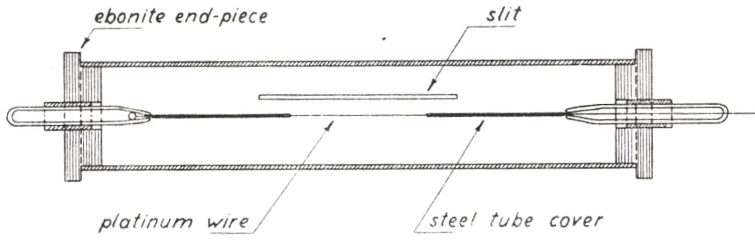

Fig. 3.

responding curves giving the variation of the amplification are shown in Fig. 4. The open and the full circles correspond to the arrangements I and II, respectively. From curve I the average amplification is 63 % of the maximum amplification.

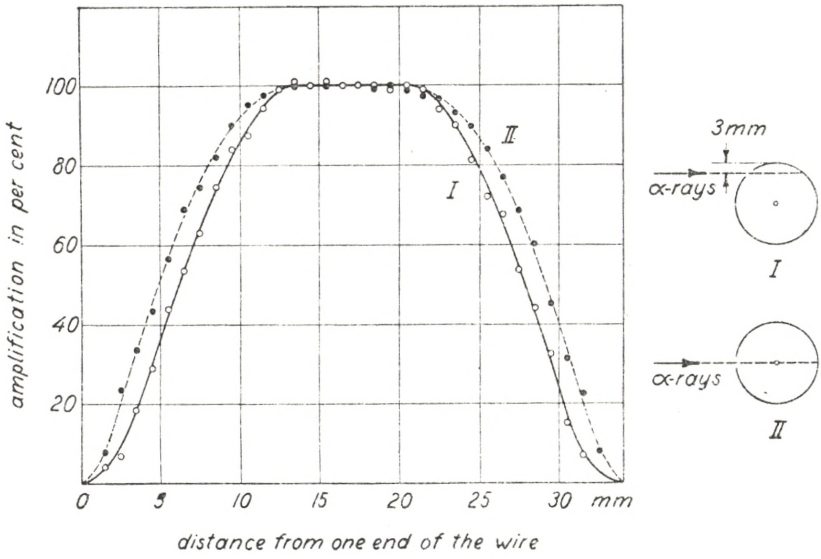

Fig. 4. Variation of the amplification along the counter wire (1 inch counter).

III. Recoil Particle Ionization Measurements.

The ionization of the recoil particles was measured by a coincidence arrangement consisting of a proportional counter and two sealed G.-M. counters enclosed in a T-shaped glass vessel

closed by brass flanges. The arrangement is shown in Fig. 5. The proportional counter was made from a 1 inch brass tube, and a platinum wire, 0.15 mm. in diameter, was placed along its axis. As, in the counter shown in Fig. 3, the wire was covered by two steel tubes, 0.8 mm. in diameter, with the exception of 34 mm. in the middle. The α-particles used for comparison left the Po-α preparation as a narrow beam; subsequently, they

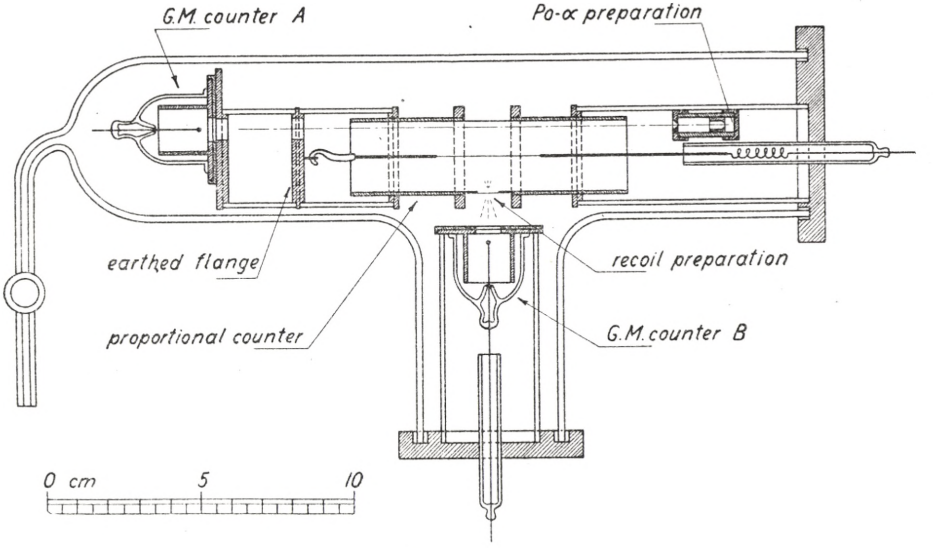

Fig. 5.

passed the proportional counter at a small distance from the wall, finally entering the G.-M. counter A through a thin mica window. In the middle of the tube, a 15 mm. piece was turned down to a wall thickness of 0.1 mm., where a hole, 5 mm. in diameter, was drilled; over the hole, a mica foil was bent which carried the source emitting the recoil particles. The mica foil was made conducting, so that the electrical field in the proportional counter was kept completely undisturbed. The α-particles from the "recoil source" could penetrate the mica foil and enter the G.-M. counter B. The windows of both G.-M. counters weighed 1.4 mg./cm.^{2}.

The recoil source was made as follows. A half-transparent layer of platinum mixed with tungsten was evaporated on a mica foil, 1.2 mg./cm.^{2}; over this, a considerably thicker silver ring was evaporated to insure a conducting connection with the counting

tube. From an activated platinum wire, the radioactive deposit was evaporated on the platinum layer in a spot, 1.5 mm. in diameter. For making ThC-C′ preparations, the platinum wire was exposed to Th-Em and rinsed by heating *in vacuo* to 250° C. Activation with polonium was performed by electrolysis in a solution containing pure polonium. DONAT and PHILLIPS (11) made ThB preparations by evaporation and found that only

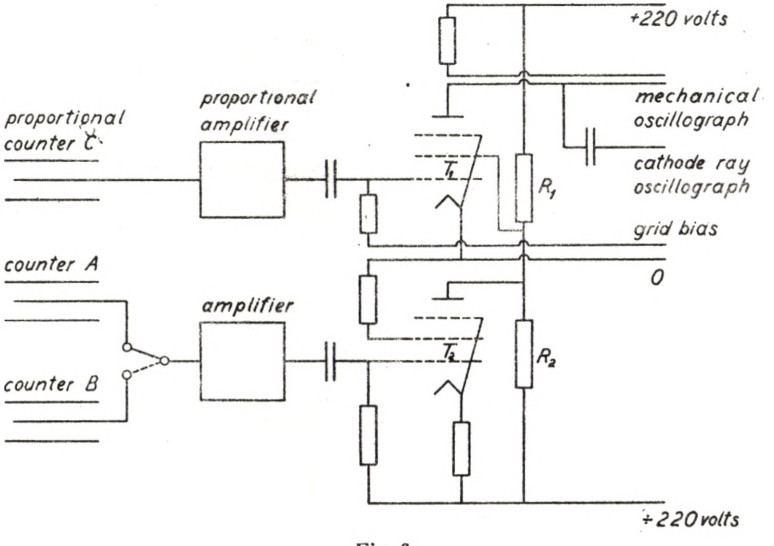

Fig. 6.

2—6 % of the ThC atoms, produced by β-ejection from ThB, would leave the layer due to their recoil energy.

By means of a small change in the circuit, the proportional amplifier was adapted to amplify only such impulses from the proportional counter which coincided with impulses from a G.-M. counter. The diagram is shown in Fig. 6. In the normal state, tube T_2 is open, and the screen grid potential of tube T_1 is so much negative that the tube is completely blocked. An impulse from one of the G.-M. counters will block T_2, and the screen grid of T_1 gets is working potential determined by the resistances R_1—R_2; subsequently, T_1 gives a proportional amplification to an impulse from the counter C. When T_2 is again opened, T_1 is blocked. Fig. 7a shows the course of potential on the anode of T_1 during a coincidence; the figure is taken from a cathode ray

oscillograph. Fig. 7b shows the deflections of the mechanical oscillograph registered on photographic paper. The voltage variations on the screen grid of T_1 are made so swift that they appear only weakly on the registering slip; the slow deflections due to the proportional counter, however, stand out distinctly. The zero line is indicated by impulses from a G.-M. counter, which are not followed by impulses from the proportional counter. The

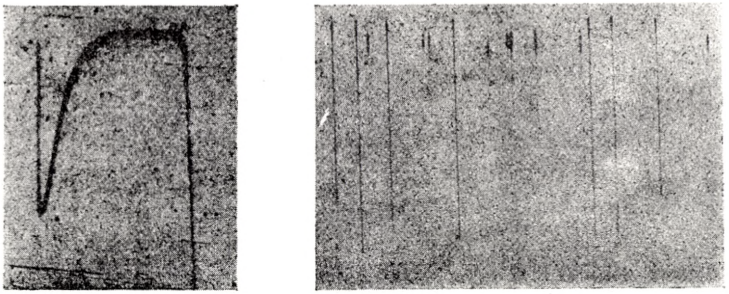

a *b*

Fig. 7.

impulses are partly due to a γ-ray source placed in the vicinity of the apparatus.

The coincidence arrangement picks out for measurement only those recoil particles which start within the cone determined by the active spot and the aperture of counter B. These recoil particles start at approximately right angles to the layer, and there is but little risk of missing branches on the track as those indicated by AKIYAMA (12) and JOLIOT (13).

In order to make direct comparisons between α-particle and recoil particle impulses possible, the coincidence arrangement was used in both cases and the G.-M. counters A and B (Figs. 5 and 6) were switched on alternately.

The measurements were carried out with recoil particles from polonium at counter pressures of 7.4 cm. and 9.2 cm. Hg and with recoil particles from ThC and ThC′ at a pressure of 9.2 cm. Hg. The distribution curves obtained are shown in Figs. 8 and 9. The width of the maxima of the recoil distribution curves was found to be a constant (about 20 %) on all curves taken; experiments with evaporated aluminium instead of the W-Pt mixture as a support of the radioactive source yielded distribution curves

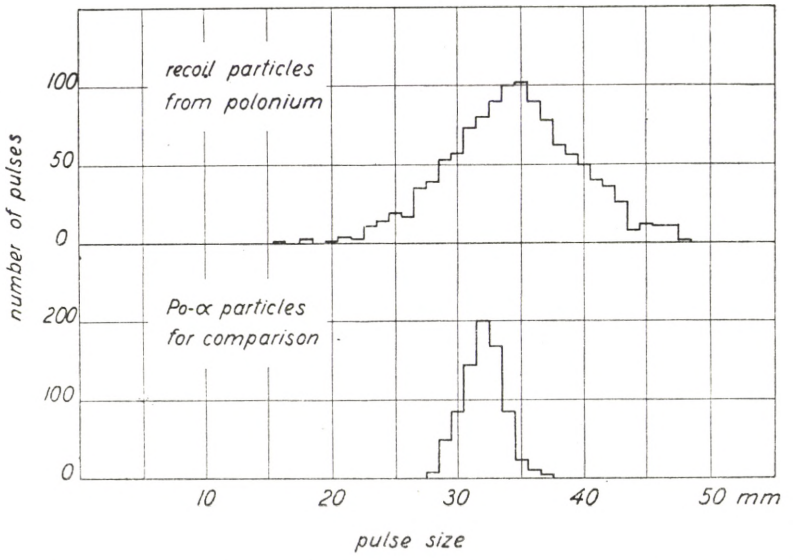

Fig. 8. Impulse size statistics taken at a pressure of 7.4 cm. Hg (argon + 5 % air). The ratio amplification of the recoil particles to that of the α-particles is 9.8 : 1.

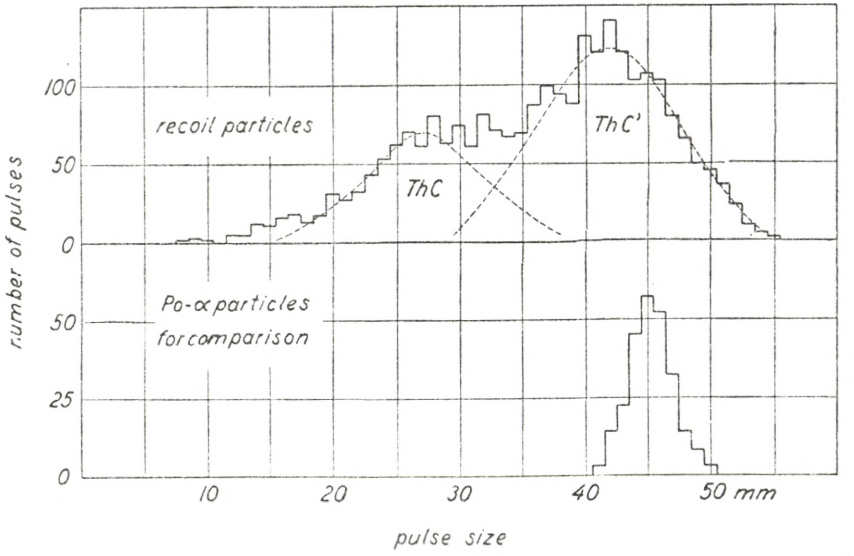

Fig. 9. Impulse size statistics taken at a pressure of 9.2 mm. Hg (argon + 5 % air). The ratio amplification of the recoil particles to that of the α-particles is 5.0 : 1.

Table 2.

Particles	Pressure cm. Hg	Positions of the maxima mm.		Ratio of amplifications
		Recoil particles	Po α-particles	
Po recoil	7.4	34.5	32.0	9.8 : 1
	9.2	34.6	39.0	9.8 : 1
ThC recoil	9.2	27.0	45.4	5.0 : 1
ThC′ recoil	9.2	42.0	45.4	5 0 : 1

of exactly the same shape. Table 2 gives the position of the maxima of the distribution curves of the recoil particles and the α-particles used for comparison. Table 3 presents the ionization in "Henderson units". In the case of α-particles, they were found as described before; for recoil particles, the figures represent the ionization to be expected if the formation of a pair of ions by a recoil particle would claim the same energy as provided by an α-particle. E. g. for polonium recoil particles the figure 42.2 is obtained by dividing the area under the ionization curve until the residual range of 36.7 mm. (the range of Po α-particles) by

Table 3.

Particles	Pressure cm. Hg	Fraction of track in air at 0° and 760 mm. Hg mm	Energy keV*	Henderson units	$\frac{E_R}{E_\alpha}$	Number of ions
Po-α	7.4	5.5– 8.5	..	134	..	..
	9.2	6.9–10.6	..	171	..	..
Po recoil	7.4	..	104	42.2	4.5 / 4.3 } 4.4	950
	9.2	..				
ThC recoil	9.2	..	118	48.2	3.8	1240
ThC′ recoil	9.2	..	170	68.5	3.4	2000

*) The values are calculated on the basis of the corresponding α-particle energies, taken from LIVINGSTON and BETHE (14).

the mass ratio $\frac{206}{4}$. From these values, the ratio $\frac{E_R}{E_\alpha}$ is calculated, E_R standing for the average energy which is required for a recoil particle to make a pair of ions; E_α stands for the corresponding value for α-particles. The uncertainty of the values of $\frac{E_R}{E_\alpha}$ is estimated to be $\pm 6\,\%$.

Finally, Table 3 gives the mean number of ions produced by the three kinds of recoil particles. In the calculations, E_α is put

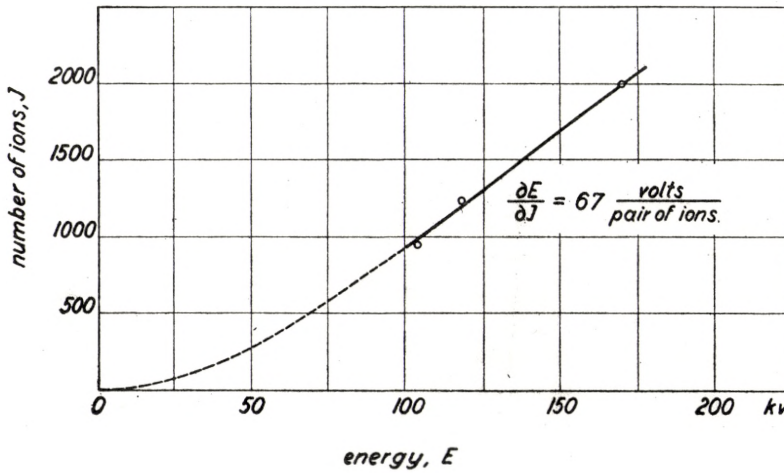

Fig. 10.

equal to 25 volts. In Fig. 10, the total number of ions is plotted against the energies, E, of the recoil particle. From the inclination of the line drawn through these points we get for E between 100 kV. and 170 kV.

$$\frac{\partial E}{\partial I} \approx 67 \text{ volts per pair of ions.}$$

In the vicinity of $E = 0$, $\frac{\partial E}{\partial I}$ will be very great, and the curve must be horizontal. On the other hand, investigations of fission fragments (15) have shown that heavy particles with high energies ionize gases with the same energy per pair of ions as do α-particles; for high energies the curve of Fig. 10 must therefore be expected to continue as a straight line with $\frac{\partial E}{\partial I} = 25$ volts per pair of ions.

Summary.

By means of a proportional counter and a proportional coincidence arrangement the ionization of single recoil atoms from Po, ThC, and ThC′ was measured.

For producing a pair of ions in argon, the recoil particle was found to require on an average 4.4; 3.8; and 3.4 times, respectively, the energy required by the α-particles.

The energy-ionization curve for heavy particles gives within the energy interval 100 kV—170 kV: $\frac{\partial E}{\partial I} = 67$ volts per pair of ions.

The author wishes to express his gratitude to the director of this Institute, Professor NIELS BOHR, for having put the problem. My thanks are further due Professor J. C. JACOBSEN for valuable advice and encouraging interest during the work.

Institute of Theoretical Physics,
University, Copenhagen.

References.

1) MAKOWER and RUSS, Phil. Mag. **20**, 875, 1910.
2) EVANS and MAKOWER, Phil. Mag. **20**, 822, 1910.
3) WERTENSTEIN, Recherches expérimentales sur le recul radioactif. Thèse. Paris 1913.
4) GERTHSEN and GRIMM, ZS. f. Phys. **120**, 476, 1943.
5) RUTHERFORD and GEIGER, Proc. Roy. Soc. London **A 81**, 141, 1908. Phys. Zs. **10**, **1**, 1909.
6) WERNER, ZS. f. Phys. **90**, 384, 1934. ZS. f. Phys. **92**, 705, 1934.
7) GEIGER, Handbuch. d. Phys. **20**, 2, 162.
8) HENDERSON, Phil. Mag. **42**, 538, 1921.
9) JENTSCHKE, Wien. Ber. II a, **144**, 151, 1935.
10) GIBSON and GARDINER, Phys. Rev. **30**, 542, 1927.
11) DONAT and PHILLIPS, ZS. f. Phys. **45**, 512, 1927.
12) AKIYAMA, Japan J. of Phys. **2**, 287, 1924.
13) JOLIOT, Journ. de Phys. (5), **7**, 219, 1934. C. R. **192**, 1105, 1931.
14) LIVINGSTON and BETHE, Rev. of mod. Phys. **9**, 266, 1937.
15) N. O. LASSEN, unpublished.

Indleveret til Selskabet den 24. Juni 1945.
Færdig fra Trykkeriet den 19. September 1945.

DET KGL. DANSKE VIDENSKABERNES SELSKAB
MATEMATISK-FYSISKE MEDDELELSER, BIND XXIII, NR. 9

DEDICATED TO PROFESSOR NIELS BOHR ON THE OCCASION OF HIS 60TH BIRTHDAY

AN APLANATIC ANASTIGMATIC LENS SYSTEM SUITABLE FOR ASTROGRAPH OBJECTIVES

BY

BENGT STRÖMGREN

KØBENHAVN
I KOMMISSION HOS EJNAR MUNKSGAARD
1945

Printed in Denmark.
Bianco Lunos Bogtrykkeri A/S

1. As is well known the ordinary Fraunhofer lens is characterized by a considerable astigmatism and curvature of field. In consequence the usable angular field is rather limited with this type of objective lens.

In the Petzval lens system, consisting of four separate lenses, the astigmatism and curvature of field are much smaller than for the Fraunhofer lens. For the Cooke triplet lens these aberrations are still further reduced.

K. SCHWARZSCHILD[1] in a systematic analysis of lens systems gives the following numerical data. For the Fraunhofer lens the aberration disc is an ellipse the major axis of which is $104'' OG^2$, while the minor axis is $47'' OG^2$. Here O means the aperture ratio expressed with the aperture ratio 1 : 10 as unit, while G is the angular diameter of the field, with 6° as unit. For the Petzval lens the aberration disc is approximately a circle with diameter $12'' O^2G$, while for the Cooke triplet lens it is approximately a circle with diameter $3'' O^2G$.

The objective of the standard Carte du Ciel astrograph is a Fraunhofer lens of 34 cm. aperture and 3.4 m. focal length, corresponding to $O = 1$. The standard field employed is $2° \times 2°$, i. e. $G = 0.47$. The maximum extent of the aberrational disc is thus equal to 23″.

The following data, which refer to the Bruce telescope at Bloemfontein (formerly Arequipa), are typical of an astrograph with a Petzval objective lens, namely, aperture 60 cm., focal length 3.4 m., standard field $7° \times 6°$, i. e. $O = 1.7$, $G = 1.5$. The corresponding maximum extent of the aberrational disc calculated from K. SCHWARZSCHILD's formula given above is about 50″. For a triplet with similar data the result would be about 12″.

In judging these results a number of circumstances should

be observed. With regard to the Fraunhofer lens the effect of the secondary spectrum must be considered. The combined effect of secondary spectrum, astigmatism, and curvature of field is a complicated distribution of light in the focal plane, or rather the plane of the photographic plate, which is close to the focal plane but not necessarily coinciding with it. This light distribution is modified, especially in its central parts, by diffraction, by the influence of atmospheric disturbance (tremor), and by the diffusion of light in the film of the photographic plate. In the case of the fainter stars recorded only the central part of the light distribution affects the photographic plate.

The result is that the images of the fainter stars appear much smaller than one would expect from the calculated effect of astigmatism and curvature of field alone.

Thus the effect of the geometrical aberrations considered is only partly visible in the form of reduced sharpness of the photographic images. A certain unhomogeneity of the field in a photometric respect is produced in addition.

With regard to the Petzval and Cooke triplet lenses the situation is similar. However, the effect of lens aberrations of the fifth and higher orders must be considered here. In a well designed lens these partly balance the third order aberrations.

The curvature of the most heavily curved lens surface of a Fraunhofer lens (apart from the inner surfaces, which need not be considered in this connection since their curvatures are nearly equal, and the refracting indices not very different) is about 1.7 in units of the reciprocal of the focal length. For the Petzval lens the corresponding maximum curvature according to K. Schwarzschild is 2.0, and for the Cooke triplet lens it is about 4.2. This shows that the Petzval type lends itself well to constructions with large aperture ratio, while for the Cooke triplet type the aperture ratio is more restricted. It is, in fact, well-known that the Petzval type is preferable for large aperture and moderate field, while the Cooke triplet type is preferable for moderate aperture and large field.

Finally, it may be mentioned that the triplet lens has the drawback of a secondary spectrum about 1.4 times that of the Fraunhofer lens, while for the Petzval lens the corresponding factor is about 0.9.

In the Fraunhofer objective lens the two component lenses are practically in contact. The Petzval and the Cooke triplet objectives on the other hand are characterized by a relatively wide separation of the component lenses. In the case of the Petzval objective the distance between front and rear lenses is about 0.4 times the focal length *f*. For the Cooke triplet objective the corresponding distance is about 0.25 *f*.

The relative positions of the component lenses of Petzval and triplet objectives must be adjusted to a high degree of accuracy, and this adjustment must be maintained to obtain a

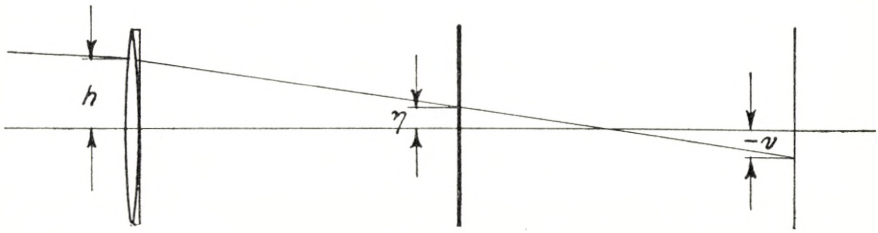

Fig. 1.

satisfactory performance. When the focal length is small, or moderate, this mechanical problem can be solved without great difficulty. For large focal lengths the difficulties, however, would be very great. In fact, astrograph objectives of these types have not up till now been constructed with a focal length of more than about 4 m.

In recent years highly successful constructions of astrograph lens objectives have been added to the Petzval and Cooke types, of which especially the Ross[2] and Sonnefeld[3] quadruplet lens objectives should be mentioned. For the same aperture ratio and field these objectives give a better image quality than the older types. With the latter they share the drawback discussed above of relatively great distance between front and rear lens, and the necessity of very delicate and stable adjustment of the component lenses. Consequently constructions of objectives with a large focal length would meet with the same difficulties as before.

The construction by B. Schmidt[4] of an aplanatic anastigmatic mirror camera constituted an extremely valuable addition to the existing astrograph constructions. When astrographs of

long focal length are considered, however, it is a marked drawback of the Schmidt camera that its total length is twice the focal length.

In view of this situation it was considered useful to examine the possibilities of a lens objective which did not suffer from the drawbacks of excessive mutual distances of the optical components and the corresponding requirement of delicate adjustment of mutual position, nor from the drawback of excessive total length of the camera as a whole. It seemed possible to reach a solution of the problem by considering a lens system,

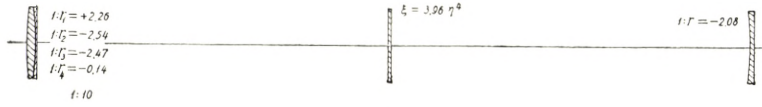

Fig. 2.

the components of which are an achromatic lens pair, a correcting plate of the same type as that used in the Schmidt camera, and a field-flattening lens situated immediately in front of the photographic plate. A lens system, in other words, which results when an achromatic lens pair is corrected with the aid of optical components of the same type as those which convert the spherical mirror into the aplanatic anastigmatic SCHMIDT camera system.

The investigations lead to the lens system illustrated in Fig. 2, consisting of an achromatic lens pair with specified radii, a correcting plate of specified curve situated in the middle between the lens pair and the photographic plate, and a field-flattening lens, also specified, immediately in front of the photographic plate.

It should be emphasized that, although there is a very considerable distance between the various components of the lens system, this is without consequence, since small displacements of the correcting plate and the field-flattening lens have a negligible effect on the quality of the images.

It follows that with the lens system just described the construction of astrographs of a long focal length presents no greater difficulty than the construction of an astrograph with a Fraunhofer objective of the same focal length and aperture.

Since the price of a correcting plate and a field-flattening lens is considerably lower than that of a Fraunhofer objective of the same diameter, the price of the whole lens system should not be much higher than that of a Fraunhofer objective, again of the same aperture and focal length.

The analysis leading to the lens system just described is given in the following paragraphs. The investigations were carried out in 1940—41. Brief summaries were published shortly afterwards, [5] and [6]. In 1941 detailed specifications of an astrograph provided with the lens system shown in Fig. 2, p. 6, were sent to Carl Zeiss, Jena, and an order for such an instrument placed. However, it never became possible for the firm mentioned to construct and deliver the instrument.

2. Let us consider the geometrical third order aberrations of an achromatic lens pair consisting of one crown glass and one flint glass lens, with spherical surfaces, assumed to be infinitely thin and in contact. Rotational symmetry about an optical axis is assumed.

The following notation is adopted, cf. [7]

n_1 Index of refraction of the crown glass lens

n_2 Index of refraction of the flint glass lens

r_1, r_2 Radius of curvature of the front surface of the crown glass, resp. flint glass lens, positive when convex toward the incident rays

r_1', r_2' Radius of curvature of the rear surface of the crown glass, resp. flint glass lens, same sign convention

v Angle of meridional ray incident on the first refracting surface with optical axis, positive when a counterclockwise turn will bring the direction of the incident ray to coincide with that of the optical axis

h Distance of intersection point of incident meridional ray and first refracting surface from the optical axis, positive above the axis

y Distance of intersection point of meridional ray refracted by optical system and focal plane from optical axis, positive above the axis

f Focal length of optical system

A Coefficient of third order spherical aberration
B Coefficient of third order coma
C Coefficient of third order astigmatism
D Coefficient of third order curvature of field
E Coefficient of third order distortion

Consider a meridional ray characterized by h and v (cf. above). The Gaussian image defined by corresponding paraxial rays ($h \to 0$) with angle of incidence v is located in the Gaussian focal plane. Its distance from the optical axis, counted positive above the axis, is denoted by y_0 and is equal to $-f \tan v$. According to the theory of third order, or Seidel aberrations [cf. f. inst. [1] and [8]], the total aberration, i. e. the deviation in the focal plane

$$\Delta = y - y_0 \tag{1}$$

from the Gaussian image, is given by the following expression

$$\Delta = Ah^3 - 3Bh^2v - \frac{1}{2}(C-D)\ hv^2 - Ev^3. \tag{2}$$

We use here the aberrational coefficients A, B, C, D, and E as defined by A. Danjon and A. Couder[9], cf. also [7]. The relations between these coefficients and the coefficients of K. Schwarzschild[1], B_S, F_S, C_S, D_S, and E_S, are as follows,

$$\begin{aligned} A &= -B_S \\ B &= -F_S \\ C &= +2\,C_S \\ D &= -2\,(C_S + D_S) \\ E &= -E_S. \end{aligned}$$

The radii of curvature ϱ_s and ϱ_t of the sagittal and tangential focal plane are, with these definitions,

$$\frac{1}{\varrho_s} = D + C$$

$$\frac{1}{\varrho_t} = D - C.$$

The Petzval radius of curvature ϱ_P is given by

$$\frac{1}{\varrho_P} = 2C + D = -\sum \frac{\varphi}{n}.$$

The radius of curvature of a focal surface is counted positive when the surface is convex towards the incident rays, i. e. the same sign convention is used as for the lens surfaces.

For a lens system consisting of two infinitely thin lenses in contact the Seidel coefficients are given by simple relations [cf. f. inst. [1]]. We introduce

$$\left.\begin{aligned} \varphi_1 &= (n_1 - 1)\left(\frac{1}{r_1} - \frac{1}{r_1'}\right) \\ \varphi_2 &= (n_2 - 1)\left(\frac{1}{r_2} - \frac{1}{r_2'}\right) \end{aligned}\right\} \quad (3)$$

and

$$\left.\begin{aligned} \sigma_1 &= (n_1 - 1)\left(\frac{1}{r_1} + \frac{1}{r_1'}\right) \\ \sigma_2 &= (n_2 - 1)\left(\frac{1}{r_2} + \frac{1}{r_2'}\right), \end{aligned}\right\} \quad (4)$$

further

$$\left.\begin{aligned} \gamma_1 &= \frac{\sigma_1}{\varphi_1} = \frac{\dfrac{1}{r_1} + \dfrac{1}{r_1'}}{\dfrac{1}{r_1} - \dfrac{1}{r_1'}} \\ \gamma_2 &= \frac{\sigma_2}{\varphi_2} = \frac{\dfrac{1}{r_2} + \dfrac{1}{r_2'}}{\dfrac{1}{r_2} - \dfrac{1}{r_2'}}. \end{aligned}\right\} \quad (5)$$

Then with

$$\frac{P_1}{\varphi_1^3} = \frac{n_1^2}{8(n_1-1)^2} + \frac{3n_1+2}{8n_1} - \frac{n_1+1}{2n_1(n_1-1)}\gamma_1 + \frac{n_1+2}{8n_1(n_1-1)^2}\gamma_1^2 \quad (6)$$

and

$$\frac{P_2}{\varphi_2^3} = \frac{n_2^2}{8(n_2-1)^2} + \frac{3n_2+2}{2n_2}\left(\frac{\varphi_1}{\varphi_2} + \frac{1}{2}\right)^2 - \frac{n_2+1}{n_2(n_2-1)}\left(\frac{\varphi_1}{\varphi_2} + \frac{1}{2}\right)\gamma_2 + \\ + \frac{n_2+2}{8n_2(n_2-1)^2}\gamma_2^2 \quad (7)$$

the coefficient A of spherical aberration is found from

$$-A = P_1 + P_2. \tag{8}$$

Similarly with

$$\frac{Q_1}{\varphi_1^2} = -\frac{2n_1+1}{4n_1} + \frac{n_1+1}{4n_1(n_1-1)}\gamma_1 \tag{9}$$

and

$$\frac{Q_2}{\varphi_2^2} = -\frac{2n_2+1}{2n_2}\left(\frac{\varphi_1}{\varphi_2}+\frac{1}{2}\right) + \frac{n_2+1}{4n_2(n_2-1)}\gamma_2 \tag{10}$$

the coefficient B of coma is obtained from

$$-B = Q_1 + Q_2. \tag{11}$$

Further, for the lens system considered, the coefficient C of astigmatism is

$$C = 1, \tag{12}$$

the coefficient D of curvature of field is

$$-D = 2 + \frac{\varphi_1}{n_1} + \frac{\varphi_2}{n_2}, \tag{13}$$

and the coefficient E of distortion is

$$E = 0. \tag{14}$$

Now, for an achromatic lens pair of the kind considered the refractive powers φ_1 and φ_2 of the crown glass and flint glass, respectively, are determined by the focal length of the instrument and the glass dispersions, specified in the customary way by the optical constants ν_1 and ν_2. In fact

$$\left.\begin{aligned}\varphi_1 &= \frac{\nu_1}{\nu_1-\nu_2}\frac{1}{f}\\ \varphi_2 &= -\frac{\nu_2}{\nu_1-\nu_2}\frac{1}{f}.\end{aligned}\right\} \tag{15}$$

When the optical constants of the glass, viz. n_1, n_2, ν_1, and ν_2 are given, the Seidel coefficients A and B can thus be calculated according to equations (6) to (11) as functions of the lens parameters γ_1 and γ_2 [cf. equation (5)], while the Seidel coefficients C, D, and E are calculable constants.

Suppose now that an infinitely thin correcting plate, of refracting index n_3, is inserted between the achromatic lens pair and the focal plane (cf. Fig. 2, p. 6). The front surface of the correcting plate is assumed to be plane, while the equation of the rear surface is supposed to be

$$\xi = g\eta^4. \tag{16}$$

The constant g measures the deformation of the correcting plate.

At the distance η from the optical axis the correcting plate acts as a prism of refracting angle $4\,g\eta^3$. The angular deviation of a ray penetrating the correcting plate at distance y from the optical axis is, therefore, within the accuracy of third order optics equal to $4\,(n_3-1)\,g\eta^3$, or

$$G\eta^3, \tag{17}$$

with

$$G = 4\,(n_3-1)\,g. \tag{18}$$

When g and G are positive, the thickness of the correcting plate increases with the distance from the optical axis. A ray penetrating the correcting plate at a positive distance η from the optical axis, i. e. above the axis will then be deviated by a counterclockwise rotation.

Let us consider a meridional ray specified by v and h (cf. p. 7). This ray penetrates the lens pair at the distance h from the optical axis, and the focal plane at a distance y from the optical axis, which within the accuracy of first order optics is equal to $-vf$ (cf. Fig. 1, p. 5).

We put the unit of length equal to the focal length, so that $f = 1$. The distance from the (infinitely thin) correcting plate to the focal plane is denoted by a. Hence the distance from the achromatic lens pair to the correcting plate is $1-a$.

It is then found that within the accuracy of first order optics the distance η from the optical axis at which the meridional ray specified by v and h penetrates the correcting plate, is given by

$$\eta = h-(1-a)\;(v+h) \tag{19}$$

or

$$\eta = ah-(1-a)\,v. \tag{20}$$

It follows from (17) and (20) that the deviation of the ray considered by the correcting plate is equal to

$$G\,[ah-(1-a)\,v]^3 \tag{21}$$

or

$$Ga^3h^3-3\,Ga^2\,(1-a)\,h^2v+3\,Ga\,(1-a)^2hv^2-G\,(1-a)^3v^3. \tag{22}$$

The deviation causes a shift of position of the point at which the meridional ray considered penetrates the focal plane. The corresponding change Δy of the distance y of the point in question from the optical axis is equal to the angular deviation given by equation (22) multiplied by the distance a from the correcting plate to the focal plane. The quantity Δy has the same sign as the quantity given by (22). Hence

$$\Delta y = Ga^4h^3-3\,Ga^3\,(1-a)\,h^2v+3\,Ga^2\,(1-a)^2hv^2-Ga\,(1-a)^3v^3. \tag{23}$$

It is easily seen that equation (23) is correct within the accuracy of third order optics.

Comparing now equation (23) with equation (2) giving the total aberration in terms of the Seidel coefficients, we find that the insertion of the correcting plate considered gives rise to the following changes of the Seidel coefficients:

$$\left.\begin{aligned} \Delta A &= +Ga^4 \\ \Delta B &= +Ga^3\,(1-a) \\ \Delta\left(\frac{1}{2}C-\frac{1}{2}D\right) &= -3\,Ga^2\,(1-a)^2 \\ \Delta E &= +Ga\,(1-a)^3. \end{aligned}\right\} \tag{24}$$

According to Petzval's theorem [cf. f. inst. [1], [7], [8], or [9]] we have

$$2\,C+D=-\left(\frac{\varphi_1}{n_1}+\frac{\varphi_2}{n_2}\right). \tag{25}$$

The correcting plate gives no contribution to the right-hand side of equation (25), so that

$$\Delta(2\,C+D)=0. \tag{26}$$

Combining this with the third equation (24), we finally get

$$\left.\begin{aligned} \Delta C &= -2\,Ga^2(1-a)^2 \\ \Delta D &= +4\,Ga^2(1-a)^2. \end{aligned}\right\} \tag{27}$$

Returning now to the expressions for the Seidel coefficients of the lens pair alone, we find [cf. equation (12)] that, in order to correct the astigmatism of the lens pair, the position and form of the correcting plate must be chosen in such a way that

$$1 - 2\,Ga^2(1-a)^2 = 0$$

or

$$G = \frac{1}{2\,a^2(1-a)^2}. \tag{28}$$

It then follows from the two first equations (24) that the coefficients A and B of spherical aberration and coma through the introduction of the correcting plate are changed by

$$\left.\begin{aligned} \Delta A &= +\frac{1}{2}\left(\frac{a}{1-a}\right)^2 \\ \text{and} \qquad \Delta B &= +\frac{1}{2}\left(\frac{a}{1-a}\right). \end{aligned}\right\} \tag{29}$$

We can now write down the equations expressing the condition that the introduction of the correcting plate, in addition to annihilating the astigmatism, should also annihilate the spherical aberration and the coma of the lens pair, as given by equations (8) and (11), namely,

$$-(P_1 + P_2) + \frac{1}{2}\left(\frac{a}{1-a}\right)^2 = 0 \tag{30}$$

and

$$-(Q_1 + Q_2) + \frac{1}{2}\left(\frac{a}{1-a}\right) = 0, \tag{31}$$

where P_1, P_2, Q_1, and Q_2 are given by equations (6), (7), (9), and (10).

Considering the quantities n_1, n_2, ν_1, and ν_2 specifying the optical glass of lens pairs as fixed constants of the problem, and remembering that φ_1 and φ_2 are given by equation (15), we

see that (30) and (31) can be regarded as two equations which determine γ_1 and γ_2 [cf. equation (5)] as functions of the parameter a measuring the relative distance of the correcting plate from the focal plane.

When γ_1 and γ_2 are known, σ_1 and σ_2 can be found, since φ_1 and φ_2 are known from equation (15). With the aid of equations (3) and (4) we can then find the radii of the optical surfaces of the lens pair, *viz.* r_1, r_1', r_2, and r_2'.

Equation (28) determines G as a function of the parameter a. Equation (18) then fixes g, n_3 being a specified optical constant. Thus the form of the surfaces of the correcting plate is also determined.

The system consisting of the achromatic lens pair and the correcting plate is free from spherical aberration, coma, and astigmatism. The only remaining third order aberration—apart from distortion, which does not give rise to any blurring of the image—is curvature of field. This can be removed without changing any of the other aberrations by the well-known method of placing an infinitely thin field-flattening lens immediately in front of the focal plane.

The coefficient of curvature of field is [cf. equations (13), (27), and (28)]

$$D = -2 - \frac{\varphi_1}{n_1} - \frac{\varphi_2}{n_2} + 2 = -\left(\frac{\varphi_1}{n_1} + \frac{\varphi_2}{n_2}\right). \tag{32}$$

According to a well-known formula [cf. f. inst. [9]] the refracting power φ_4 of the field-flattening lens (of refracting index n_4) necessary to obtain a flat field. is

$$\varphi_4 = n_4 \cdot D \tag{33}$$

or, according to (32),

$$\varphi_4 = -n_4\left(\frac{\varphi_1}{n_1} + \frac{\varphi_2}{n_2}\right). \tag{34}$$

This result can be obtained immediately from the Petzval condition for the whole system consisting of the achromatic lens pair, the correcting plate, and the field-flattening lens, the refracting power φ_3 of the correction plate being equal to zero, *viz.*

$$\frac{\varphi_1}{n_1} + \frac{\varphi_2}{n_2} + \frac{\varphi_4}{n_4} = 0. \tag{35}$$

The coefficient of distortion of the optical system consisting of the lens pair and the correcting plate is given by equation (14), the last equation (24), and equation (28),

$$E = \frac{1-a}{a}. \tag{36}$$

The field-flattening lens introduces an additional distortion

$$E = \frac{\varphi_4}{2\,n_4} + \frac{\varphi_4^2}{2\,n_4(n_4-1)}. \tag{37}$$

From equation (36) we infer that the distortion introduced by the correcting plate is large if the plate is placed at a small distance from the focal plane.

3. The next step in the analysis consists in an investigation of the equations (30) and (31), to see whether they have real solutions leading to optical systems of practical value, i.e. for which the curvatures of the lens surfaces and the deformation of the correcting plate are not excessive.

Let us consider, first, the case that the crown glass and flint glass of the achromatic lens pair is the schematic typical glass adopted by K. SCHWARZSCHILD, *viz.* crown glass with $n_1 = 1.5$, $\nu_1 = 60$, and flint glass with $n_2 = 1.6$, $\nu_2 = 36$. Equations (15) give for this case, with $f = 1$, $\varphi_1 = +2.5$, and $\varphi_2 = -1.5$. Inserting then numerical values in equations (6), (7), (9), and (10), we find

$$P_1 + P_2 = +13.28 - 26.05\,\gamma_1 + 18.23\,\gamma_1^2 - 10.665\,\gamma_2 - 2.636\,\gamma_2^2 \tag{38}$$

and

$$Q_1 + Q_2 = -0.72 + 5.21\,\gamma_1 + 1.52\,\gamma_2. \tag{39}$$

Equations (30), and (31),

$$P_1 + P_2 - \frac{1}{2}\left(\frac{a}{1-a}\right)^2 = 0 \tag{40}$$

$$Q_1 + Q_2 - \frac{1}{2}\left(\frac{a}{1-a}\right) = 0, \tag{41}$$

can now be solved numerically for any specified value of the parameter a.

The following table gives γ_1 and γ_2 as functions of a. The table further contains the numerical values of the lens curva-

tures r_1, r'_1, r_2, and r'_2 together with the numerical value of G, calculated according to the equations enumerated on p. 14

a	0.2	0.4	0.5	0.6	0.8	Ordinary Fraunhofer lens
γ_1	−0.276	−0.174	−0.096	+0.023	+0.642	
γ_2	+1.502	+1.289	+1.132	+0.888	−0.411	
r_1	+1.81	+2.06	+2.26	+2.56	+4.10	+1.67
r'_1	−3.19	−2.94	−2.74	−2.44	−0.90	−3.33
r_2	−3.13	−2.86	−2.66	−2.36	−1.76	−3.26
r'_2	−0.63	−0.36	−0.16	+0.14	+0.74	−0.76
G	19.53	8.68	8.00	8.68	19.53	
g	9.77	4.34	4.00	4.34	9.77	

The table shows that the curvatures are not excessive, in fact for $a = 0.5$ they are about equal to those of an ordinary Fraunhofer lens, or a Petzval lens, and considerably smaller than those of a Cooke triplet lens. It may be noted that the curvatures of the rear surface of the front lens and the front surface of the rear lens are about equal, as is the case of the ordinary Fraunhofer lens.

In order to judge the amount of deformation of the correcting plate corresponding to a given value of G it is convenient to make a comparison with the correcting plate of a Schmidt camera of equal focal length. The deformation constant g_S of a Schmidt plate is given by [cf. [8]]

$$g_S = \frac{1}{32}\frac{1}{n-1}. \tag{42}$$

Now, according to equation (18)

$$g = \frac{1}{4}\frac{1}{n-1}G.$$

Thus the deformation constant of the correcting plate of the present lens system is $8\,G$ times that of a correction plate of a Schmidt camera of equal focal length. Now, according to equation (28) the ratio $8\,G$ is equal to

$$\frac{4}{a^2(1-a)^2}. \tag{43}$$

Further according to equation (16) the deformation constant varies inversely to the third power of the focal length. This means that the deformation of the correcting plate of the present lens system is equal to that of a Schmidt camera of the same aperture, but with a focal length that is smaller in the ratio of

$$(8\,G)^{\frac{1}{3}} = \left(\frac{4}{a^2\,(1-a)^2}\right)^{\frac{1}{3}} \tag{44}$$

to 1. The correcting plate hence corresponds to that of a Schmidt camera, which has an aperture ratio $(8\,G)^{\frac{1}{3}}$ times greater than that of the lens system considered.

It is seen that G has a minimum for $a = 0.5$, with $G = 8$, and $(8\,G)^{\frac{1}{3}} = 4$. It is thus perfectly practicable to make the correcting plate of a lens system of the type considered for the aperture ratio 1:10, or even 1:5.

It follows from the discussion on p. 21 that it is not desired to construct the lens system in question with a very great aperture ratio. This may be noted in connection with the above discussion regarding the degree of deformation of the correcting plate.

In the following sections we shall give the results of calculations leading to the specification of lens systems with lenses and correcting plate of finite thickness. We shall also state the results of calculations—according to the method of trigonometrical tracing of rays—showing the state of correction of the lens systems in question. All these calculations have been restricted to the case of a correcting plate situated half-way between the achromatic lens pair and the focal plane, i. e. $a = 0.5$.

4. According to the procedure described above it is possible to determine the geometrical parameters of a lens system consisting of an infinitely thin achromatic lens pair, an infinitely thin correcting plate, and an infinitely thin field-flattening lens in such a way that the whole system is achromatic, aplanatic (i. e. $A = 0$, $B = 0$), anastigmatic ($C = 0$), and with a flat field ($D = 0$), in other words so that all third order aberrations (except distortion) vanish.

In order to prepare the actual construction of such an instrument it is necessary to modify the geometrical parameters

in such a way that the lenses and the correcting plate have suitable finite thicknesses, while the lens system still satisfies the two conditions of achromatism together with the conditions $A = 0$, $B = 0$, $C = 0$, and $D = 0$.

Starting with the data obtained for infinitely thin lenses and correcting plate it is possible by a process of systematic small variations of the geometrical parameters to arrive at a lens system satisfying the conditions specified. The process includes a number of numerical determinations of the aberration constants A, B, C, and D by using the method of trigonometrical ray tracing [cf. f. inst. [7]]. The final determination of the state of correction of the resulting lens system is also made by the method of trigonometrical ray tracing.

Such calculations have been carried out by Mr. Erik Lorensen, M. Sc. Altogether four different systems were investigated, two of which were achromatized for the photographic wavelength region, while two were corrected for the photovisual. Below we give a summary of the calculations of one of the photovisual lens systems. It should be noted that this system was designed for use in connection with a curved photographic plate, concave towards the incident rays, i. e. without a field-flattening lens.

Optical constants.

Crown glass, first lens, and correcting plate.

$$n_C = 1.50725,\ n_d = 1.50977,\ n_F = 1.51549,\ n_g = 1.51995,\ n_h = 1.52364$$

Flint glass, second lens.

$$n_C = 1.61504,\ n_d = 1.62004,\ n_F = 1.63210,\ n_g = 1.64206,\ n_h = 1.65068$$

Geometrical data for infinitely thin lenses and plate.

$$\varphi_1 = +2.424,\ \varphi_2 = -1.424,\ f = 1,\ \text{for } d\text{-light}.$$

$$\frac{1}{r_1} = +2.244,\ \frac{1}{r_1'} = -2.512,\ \frac{1}{r_2} = -2.443,\ \frac{1}{r_2'} = -0.146,\ g = 3.92.$$

Geometrical data for final lens system, unit $f = 1$.

Axial thicknesses, crown glass lens 0.011, flint glass lens 0.004, correcting plate 0.005. Axial separation of lenses, 0.0005. Axial separation of rear lens, rear surface, and correcting plate, front surface, 0.4853.

$$\frac{1}{r_1} = +2.258\ 8787,\ \frac{1}{r_1'} = -2.536\ 4387,\ \frac{1}{r_2} = -2.473\ 0643,$$
$$\frac{1}{r_2'} = -0.138\ 7457.\ g = 3.960.$$

Residual aberrations, *d*-light.

Third order aberrations for *d*-light. Spherical aberration 0″.00 O^3, coma 0″.00 O^2G, astigmatism 0″.00 OG^2 (cf. p. 3). Curvature of field $\frac{1}{\varrho_P} = -0.726$.

Aberrations of the fifth and higher orders. Spherical aberration for marginal rays with aperture ratio 1:10, 0″.2. Maximum extent of aberrational image (on Petzval sphere), for *d*-rays with aperture ratio 1:10, and angular diameter of field 5°.7, 2″.0.

Secondary spectrum.

The secondary spectrum is practically equal to the secondary spectrum of an ordinary Fraunhofer lens with the same aperture and focal length. When the photographic plate coincides with the focal sphere of *d*-light (λ = 5876 Å), the aberrational disc due to the secondary spectrum has a diameter of 10″O (unit of aperture ratio O 1:10, cf. p. 3) for *C*-light (λ = 6563 Å), or *F*-light (λ = 4861 Å). Light within the more restricted wave-length range 5400 Å—6300 Å gives rise to an aberrational disc of diameter 3″O. The variation of focal length with wave-length is practically the same as that of the distance between the lens pair and the focus, thus also with the ordinary Fraunhofer lens. This means that with an angular diameter of the field equal to 5°.7, the chromatic elongation of the image in the direction of the center of the field is very small, the maximum extent being 0″.2 for the wave-length range 5400—6300 Å.

Chromatic differences of third and higher order aberrations.

The third order aberrations for *C*-light, and *F*-light, differ very little from those of *d*-light. The same applies to the aber-

rations of fifth and higher order. The effects of these chromatic differences are quite inappreciable in comparison with those of the secondary spectrum.

We give, next, a brief summary of the data describing a lens system differing from the one just described only in its being achromatized for the photographic wave-length region. It has been designed in such a way that the correcting plate is identical with that of the photovisual system, but placed somewhat nearer to the focal plane.

The same glass is used as for the previous system. The axial thicknesses and the axial separation of the lenses are also the same. The axial separation of the rear lens, rear suffface, from the correcting plate, front surface, now, however, is 0.5412. The curvatures of the spherical lens surfaces are

$$\frac{1}{r_1} = +2.123,\ \frac{1}{r_1'} = -2.102,\ \frac{1}{r_2} = -2.084,\ \frac{1}{r_2'} = -0.217.$$

The state of correction is very nearly the same as for the previous system.

Finally we give a brief summary of the data referring to a lens system which includes a field-flattening lens. The data refer to the instrument to be made by Carl Zeiss (cf. p. 7) with 15 cm. aperture, and 1.5 m. focal length, photovisual lens system. The state of correction is practically as good. The maximum extent of total aberration, apart from secondary spectrum is again 2″ for the aperture ratio 1:10 and an angular diameter of field 5°.7. The data of the system are

	C-light	*d*-light	*F*-light
n_1	1.51508	1.51757	1.52318
n_2	1.61598	1.62103	1.63317
n_3	1.51436	1.51684	1.52244
n_4	1.51534	1.51784	1.52344

Axial thicknesses and separations in mm. First lens, 22.0, first to second lens 0.2, second lens 15.0, second lens to correcting plate 714.0, correcting plate 15.0, correcting plate to field-flattening lens 680.0, field-flattening lens 20.0.

Radii of spherical surfaces in mm., $r_1 = +659.4$, $r_1' = -655.1$. $r_2 = -665.3$, $r_2' = -15150.0$. Equation of deformed surface of

correcting plate, $\xi = 1.255 \cdot 10^{-9} \eta^4$, with ξ and η in mm. Radius of front surface of field-flattening lens, -719.7 mm., rear surface plane.

5. It appears from the previous discussion that the lens system considered is suitable for astrographs. If we choose the aperture ratio 1:10, the geometrical aberrations are almost negligible within a field of 5°.7 angular diameter, or within a square field $4°.0 \times 4°.0$. When the correcting plate is given the same diameter as the lens pair, there is no silhouetting. The positions of the correcting plate and the field-flattening lens relative to the lens pair are not critical so that the large separation of the former from the latter is no drawback. It is not necessary that the correcting plate and the field-flattening lens should be perfectly homogeneous with regard to refracting index. In this connection it may be mentioned that, with the aperture ratio and field considered, the maximum angular deviation of a ray produced by the correcting plate is about 200″, giving a deflection in the focal plane equivalent to about 100″.

It should be emphasized that the possibilities of the construction have not been exhausted. It is quite possible that the aberrations of the fifth and higher orders could be reduced by a change of position of the correcting plate and by the introduction of a small curvature of the correcting plate ($\xi = \alpha\eta^2 + g\eta^4$, α small). Thus it might be possible to construct systems of larger aperture ratio and field and yet with the same image quality.

As mentioned on p. 6 the principal application of the lens system is for astrographs with a long focal length, and for such instruments it is not desirable to go much beyond an aperture ratio of 1:10, and a field of $4° \times 4°$. Let us consider a focal length of, say, 8 m. For photographic work it will not be desirable to go beyond an aperture of about 80 cm., since the light loss through the absorption, especially in the achromatic lens pair, will nearly compensate the light gain through the greater aperture, if the latter is further increased. Also, a field of $4° \times 4°$ has the linear extent of 56 cm. × 56 cm., so that it becomes impracticable to cover the whole field with a single plate. Four plates, about 30 cm. × 30 cm. might be used here to cover the field, but it will not in general be desirable to

use a still larger field. Considerations of the conditions necessary for sufficiently exact guiding during exposure lead to a similar conclusion.

6. It is a well-known fact that photographic photometry of faint stars in galactic regions of high star density requires the use of astrographs of a long focal length. With a small focal length the photographic stellar images are not sufficiently separated. This is illustrated by the following considerations.

The magnitude of a star obtained from measurements on a photographic plate is influenced when some other star is situated very close to it. If there is a faint neighbouring star, the magnitude may be influenced though the disturbing star be invisible on the plate. When the disturbing star is very close to the star to be measured, it will be the magnitude corresponding to the combined light that is found from the measurement.

The amount of the disturbance will be a rather complicated function of the magnitude difference and the linear distance between the stars on the photographic plate, and it will depend upon the micro-photometric method used in determining the strength of the photographic image.

Qualitatively it may be said, however, that if the distance between the two stars is less than about 0.05—0.06 mm. there will be a disturbance not much less than that which would result if the stars practically coincided. There will thus be associated with each star to be measured an area of about 0.01 mm.^{2} which must be free from disturbing stars if the photometric magnitude obtained is to be correct. Strictly speaking, the area in question is dependent on the focal length f, in such a way that it increases with f. Within a certain range of f the variation of this area with f is not very pronounced, however, since very small images are not suitable for photometric work. In the following discussion we shall neglect the variation in question.

Let the magnitude of the star to be measured be m. If an accuracy of $0^m.1$ is aimed at, all stars brighter than about $m + 2^m.5$ must be considered as disturbing stars. If an accuracy of $0^m.02$ is wanted, the corresponding limit is about $m + 4^m.5$.

The number of stars per square degree is a known function of the magnitude and the galactic latitude. The following table

has been derived from the tables given by P. J. van Rhijn[10]. It gives the number of stars per square degree, per interval of magnitude 1^m at photographic magnitude m, and galactic latitude b. The values given for 19^m, 20^m, and 21^m are extrapolated.

	$b = 0°$	10°	20°	40°	60°	90°
12^m	90	50	30	17	11	10
13	200	120	80	40	20	20
14	600	300	180	80	40	40
15	1500	800	400	150	80	60
16	3000	1900	900	300	150	100
17	8000	4000	1700	500	300	170
18	17000	8000	3000	800	400	300
19	30000	14000	5000	1200	600	400
20	60000	20000	8000	1700	800	600
21	100000	40000	11000	2000	1000	700

The average number of stars per 0.01 mm.^{2} is given by the expression

$$\frac{A}{30500}\,\frac{1}{f^2}$$

if A is the number of stars per square degree and f the focal length.

The following table gives the average number of stars per 0.01 mm.^{2}, per interval of magnitude 1^m, for focal length 1 m. For other focal lengths the corresponding numbers are obtained by division with the square of the focal length expressed in meters.

	$b = 0°$	10°	20°	40°	60°	90°
12^m	0.003	0.0015	0.0010	0.0005	0.0004	0.0003
13	0.008	0.004	0.003	0.0012	0.0008	0.0007
14	0.02	0.010	0.006	0.002	0.0014	0.0011
15	0.05	0.02	0.013	0.005	0.003	0.002
16	0.11	0.06	0.03	0.009	0.005	0.003
17	0.2	0.13	0.06	0.016	0.008	0.006
18	0.5	0.3	0.10	0.03	0.013	0.010
19	1.0	0.5	0.17	0.04	0.019	0.014
20	1.8	0.8	0.3	0.05	0.03	0.018
21	3	1.2	0.4	0.07	0.03	0.02

Let us consider the case that it is desired to determine photographic magnitudes for stars in a milky-way field, $b = 0°$, of

a magnitude around 16^m. With focal length 1 m. the average number of disturbing stars between magnitude $17^m.5$ and $18^m.5$, would be about 0.5, each star giving rise to a photometric error $0^m.1 - 0^m.2$, and even much greater errors would not be infrequent. To solve the photometric problem in a satisfactory way it will therefore be necessary to use a focal length considerably greater. With $f = 4$ m. the frequency of the errors would, according to the table, be as follows.

$> 0^m.24$	2 per cent.
$0\ .10 - 0^m.24$	3
$0\ .04 - 0\ .10$	7
$0\ .02 - 0\ .04$	11

$m = 16^m$, $b = 0°$, $f = 4$ m.

It depends, of course, upon the particular application in view, whether this is considered satisfactory, or not.

If the object is to determine photographic magnitudes for stars of photographic magnitude 18^m in the milky way ($b = 0°$), it will usually be necessary to increase the focal length still further. Even with $f = 8$ m. the photometric errors of the kind considered are not negligible, as is apparent from the following table of the frequency of errors analogous to the one given above.

$> 0^m.24$	3 per cent.
$0\ .10 - 0^m.24$	3
$0\ .04 - 0\ .10$	5
$0\ .02 - 0\ .04$	8

$m = 18^m$, $b = 0°$, $f = 8$ m.

It should be emphasized that the above estimates are necessarily rather rough. They show, however, that for photometric work on faint stars in the milky way it may be desirable to use astrographs of about 8 m. focal length, or more.

If colour indices are determined by comparison of photographic and photovisual magnitudes obtained from separate plates taken with the same instrument, or instruments of the same focal length, then the error of the colour index due to a disturbing star is proportional to the colour index difference between the two stars, and the resulting colour index is inter-

mediate between that of the two stars. The chance that stars of apparently exceptional colour index are fortuitously produced is thus extremely small.

If, however, the photographic and photovisual magnitudes are obtained from two exposures on the same plate, then the errors due to disturbing stars are uncorrelated for the photographic and photovisual magnitudes. The errors of the colour index, therefore, are not limited as in the case considered above, and fortuitous exceptional colour indices will not be quite rare.

These considerations show that particular caution is indicated when the method of obtaining photographic and photovisual magnitudes from one plate is used, or else when more than one exposure is made on each plate. It will usually be necessary, in such cases, to increase the focal length beyond a value which would otherwise have been satisfactory.

When photometry of faint stars in high galactic latitudes is considered, the situation is quite different on account of the much smaller star density.

The following tables of the frequencies of photometric errors which are valid for $b = 90°$, are analogous to those given on p. 24

$< 0^m.24$	0.07 per cent
0 .10 — $0_m.24$	0.06
0 .04 — 0 .10	0.09
0 .02 — 0 .04	0.11

$m = 16^m$, $b = 90°$, $f = 4$ m.

$0^m.24$	0.06 per cent.
0 .10 — $0^m.24$	0.03
0 .04 — 0 .10	0.03
0 .02 — 0 .04	0.04

$m = 18^m$, $b = 90°$, $f = 8$ m.

Here the errors are quite negligible. In fact, since the star density is between 50 and 200 times smaller than in the milky way, focal lengths of about 0.5 m., respectively 1 m., would have given results comparable to, or slightly better than those obtained in the milky way with 4 m., respectively 8 m., focal length.

Now, the limiting magnitude, which is reached when the exposure time is extended to the limit set by the sky-background [cf. (11)], is a function of the focal length. In order to reach the limiting magnitudes 16^m, or 18^m, the focal length must be chosen somewhat greater than 0.5 m., respectively 1 m. This means that, in regions of high galactic latitude, conditions for reducing the photometric errors due to disturbing stars are automatically fulfilled.

If the focal length is chosen equal to 2– 3 m., methods involving double or multiple exposure on one plate may safely be used here. With one-exposure methods investigations can safely be extended to intermediate galactic latitudes.

7. Astrographs intended for photometric and spectroscopic Durchmusterung work may be classified as follows. The most powerful instruments are the large reflectors, but it may sometimes be felt that their field is too small. The Ross correctors [cf. (12)] are a great improvement in this respect, but even their extended field may sometimes be considered too small. The Schmidt cameras fulfil every requirement with respect to aperture and field, but because of the fact that the total length of the construction is twice the focal length, the focal length is somewhat restricted. When faint stars are concerned, this type of astrograph is therefore better suited for work in high and intermediate galactic latitudes than in low ones. Astrographs with triplet, or quadruplet, lenses have applications in much the same field as the Schmidt camera. According to the particular problem in view, a choice will be made between mirror and lens objective. The lens system investigated in the present paper has optical properties similar to those of the triplet and quadruplet constructions, but contrary to the latter it is suitable also for instruments of a great focal length.

References.

(1) K. Schwarzschild, Untersuchungen zur geometrischen Optik I–III, Astr. Mitt. Göttingen, 9.–11. Teil, 1905.
(2) F. E. Ross, Journ. Opt. Soc. America **5**, 123, 1921.
(3) Sonnefeld, cf. Hdb. d. Aph. I, p. 142, 1933.
(4) B. Schmidt, Central-Zeitung für Optik und Mechanik **52**, Heft 2, 1931, Mitt. Hamb. Sternwarte Bergedorf **7**, Nr. 36, 1932.
(5) Vierteljahrschr. der Astr. Ges. **76**, 111, 1941; **77**, 168, 1942.
(6) Oversigt over det Kgl. Danske Videnskabernes Selskabs Virksomhed Juni 1940–Maj 1941, København 1941, p. 50.
(7) B. Strömgren, Optical Sine-Tables giving seven-figure values of $x - \sin x$ with arguments x and $\sin x$. Geodætisk Instituts Skrifter, 3. Række Bind V, København 1945.
(8) B. Strömgren, Vierteljahrschr. der Astr. Ges. **70**, 65, 1935.
(9) A. Danjon et A. Couder, Lunettes et Télescopes, Paris 1935.
(10) P. J. van Rhijn, Publ. Groningen No. 43, 1929.
(11) F. E. Ross, Ap. J. 88, 548, 1938.
(12) F. E. Ross, Ap. J. **77**, 243, 1933; **81**, 156, 1935.

Indleveret til Selskabet den 25. Juni 1945.
Færdig fra Trykkeriet den 21. September 1945.

DET KGL. DANSKE VIDENSKABERNES SELSKAB
MATEMATISK-FYSISKE MEDDELELSER, BIND XXIII, NR. 10

DEDICATED TO PROFESSOR NIELS BOHR ON THE OCCASION OF HIS 60TH BIRTHDAY

NOTE ON THE PERMEABILITY OF RED BLOOD CORPUSCLES TO POTASSIUM

BY

HILDE LEVI

KØBENHAVN
I KOMMISSION HOS EJNAR MUNKSGAARD
1945

Printed in Denmark.
Bianco Lunos Bogtrykkeri A/S

The change in permeability of red blood corpuscles under the action of certain substances which affect the cell surface has been the subject of a number of investigations described earlier (1). It was found that very dilute solutions of bee venom cause a swelling of the cells or even hemolysis, and it was assumed that these changes in the cell surface are accompanied by a change in permeability both to anions and cations.

It was the aim of the above mentioned studies and of those to be described in the following to measure these changes in permeability with the aid of radioactive indicators. Radio-phosphorus and radio-potassium were applied as indicators, and the measurements were performed mainly on human blood. The experimental technique when using potassium as an indicator is somewhat different from the usual technique developed for phosphorus, mainly in view of the short half-life period of potassium (12.4 h) and, furthermore, owing to the fact that it involves some difficulty to precipitate potassium quantitatively within a reasonable time.

Since a comparative evaluation of permeability measurements claims a detailed knowledge of the prevailing experimental conditions, the following account will include a rather detailed description of the experimental procedure.

Radio-potassium.

The preparations of artificially radioactive potassium applied here were most kindly put at our disposal by the Nobel Institute for Physics, Stockholm. The author takes the opportunity to express her most sincere thanks to the director of this Institute, Prof. M. SIEGBAHN, and to Dr. H. ATTERLING for their great

readiness and the trouble in providing us with especially strong preparations.

Due to the experimental conditions during bombardment of the potassium sample the latter always contained some radio-phosphorus (c. 5 $^0/_0$ of the initial activity) and mostly even radio-sodium. It was therefore necessary to subject the preparation to a chemical purification which had to be quantitative and—in view of the 12.4 h period—had to be carried through as quickly as possible. Moreover, when developing a suitable method of purification it had to be taken into consideration that neither the precipitate nor possible excess precipitants contained substances which might be injurious to living cells[1].

The radioactive preparation of KCl (20—40 mgm.) in aqueous solution obtained by deuteron bombardment of KOH in the Stockholm cyclotron was in the first approximation freed from ^{32}P by adding a given quantity of ordinary sodium phosphate which was precipitated with $CaCl_2$ at pH 8 as hydroxyl apatite. Although this precipitation occurred in 50 $^0/_0$ alcohol, only 98 $^0/_0$ of the phosphate were removed. This proved to be insufficient in view of the strong P-activity present and its comparatively slow decay. For a further purification which moreover aimed at a separation of the radio-potassium from traces of radio-sodium, the filtrate after the phosphate precipitation was evaporated on the water bath to c. 1 ml. and transferred to a platinum crucible. After addition of a slight excess of (10 $^0/_0$) perchloric acid plus an equal quantity of 96 $^0/_0$ alcohol and evaporation, the crystalline potassium perchlorate was washed repeatedly with a few ml. of 1 $^0/_0$ perchloric acid in alcohol and the supernatant liquid was removed with a pipette. The precipitate was then dried in the crucible, a c. twentyfold quantity of ammonium chloride was added, and the mixture was evaporated over a Bunsen burner. Generally, the latter manipulation was repeated once. The resulting KCl was dissolved in distilled water.

Decay measurements over 6—8 half-life periods on samples of this initial labelled KCl showed no residual phosphorus activity worth mentioning. The strength of the preparations available for our experiments was of the order of magnitude

[1] The author wishes to express her best thanks to Magister Th. Rosenberg for valuable advice concerning the purification of the potassium samples.

of $50 \cdot 10^6$ impulses per minute, measured on a Geiger counter of the Copenhagen type (2), corresponding to c. 0.5 milliCurie. The ^{32}P impurities still present were at least below 0.1 %. Control measurements and experiments which will be described elsewhere (3) indicated that the KCl preparations even were practically free from radio-sodium.

Measurement of the Distribution Coefficient.

Experimental. When labelled potassium is added to blood *in vivo*, a fairly rapid exchange with the potassium present in the organs and the muscles takes place. HEVESY (4) has shown that labelled K injected intravenously into a rabbit disappears from the plasma at a high rate, entering mainly the tissue cells. A marked activation of the corpuscles can only be obtained after repeatedly introducing labelled K into the organism.

The present experiments on human blood corpuscles *in vitro* showed that the rate of penetration of potassium ions through the membrane of red cells is of the same order of magnitude as that of phosphate ions (cf. also (5)). The experimental procedure for the determination of the distribution coefficient was as follows.

The blood was drawn from healthy persons by venous puncture (without special regard to the preceding diet). Either citrate or heparin was employed as anticoagulant (cf. below). Immediately after drawing, the blood was cooled in ice-water. A quantity of c. 30 ml. was then transferred to an Erlenmeyer flask containing labelled KCl and was shaken in a water thermostat at 37° C. At intervals, c. 3 ml. blood were removed with a pipette and centrifuged in ice-cooled centrifuge tubes of known weight. After separation from the plasma the corpuscles were washed twice with physiological NaCl-solution and centrifuged sharply. After weighing, the tubes containing the washed corpuscles or the plasma were placed into a glycerine bath at 110° C until most of the water had boiled off, and the samples were subsequently dried to constant weight at 120° C. Their wet weight and their dry weight were thus determined. Finally, the dried substance was ground in a mortar and a quantity of each sample was weighed into a small aluminium dish for activity measurements.

The activity of the samples was measured by means of a Geiger counter arrangement as described earlier (2), and the activities determined repeatedly at any time were calculated back to a given time on the basis of the exact formula for the decay with a period of 12.4 h. In this way, samples could be remeasured and accuracy considerations could be taken into account for each step involved in the whole procedure.

Results. The distribution coefficient for potassium, viz. the quotient

$$\frac{\text{activity per g corpuscles}}{\text{activity per g plasma}}$$

in human blood has been measured over a period of 3 h. The curves obtained are represented in Fig. 1. Curve A was found on freshly drawn citrate blood and with a small quantity of labelled K of a very high specific activity. It appears from the curve that a distribution coefficient 1 is reached already after 100 min. of shaking at 37°, and after 3 h of shaking the quotient assumes a value 2.5. Obviously, this does not mean equilibrium or complete exchange between the potassium of the plasma and that of the corpuscles, since the potassium content of the corpuscles is almost 20 times that of the plasma. However, it appears impossible to obtain complete exchange during *in vitro* experiments as the state of the blood after some hours of shaking by no means can be regarded as physiological. When radio-phosphorus is applied in an analogous way a distribution coefficient 1 is reached in the course of c. 2 h. (cf. 1.).

The experiment exhibited in curve A was repeated with the same potassium preparation 48 h later, however, in view of the decay of the potassium activity c. 15 times the quantity of KCl had to be employed. Moreover, the preparation contained some excess $CaCl_2$ after a repeated phosphate precipitation. The distribution coefficient measured is represented in curve B, and the difference between curves A and B is very marked.

In view of these results it is very tempting to assume that either the presence of Ca or the increased amount of K present, or a combination of both factors might strongly affect the permeability of blood corpuscles to potassium ions under the conditions prevailing in these experiments. An attempt was therefore made

to clear up this question by measuring the distribution coefficient in the presence of various amounts of Ca. Experiments with varying concentrations of potassium had to be delayed to a later date (cf. the conclusive remark on p. 8). As the application of sodium citrate as an anticoagulant involved the removal of Ca

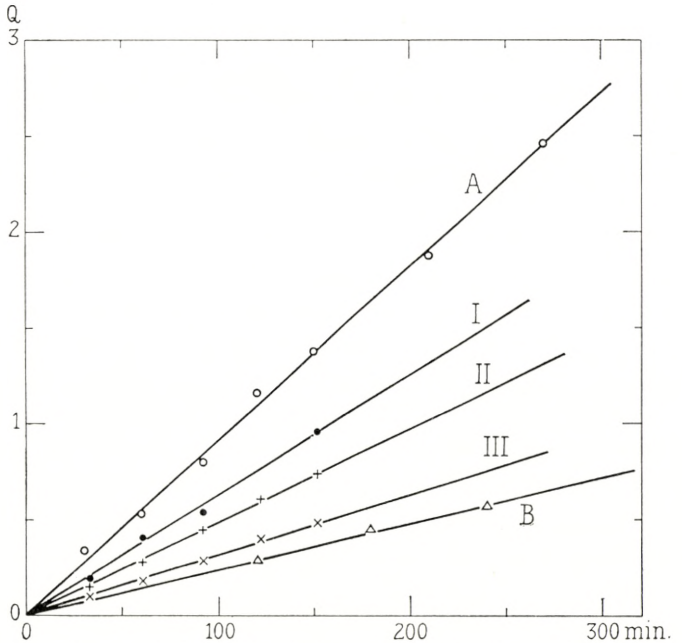

Fig. 1. Distribution coefficient of labelled potassium in human blood corpuscles.
ordinates: $\frac{\text{activity per g corpuscles}}{\text{activity per g plasma}}$
abscissae: time in min.

from the blood, citrate blood was considered to represent the Ca-content zero, while heparin blood was taken to represent blood of the ordinary calcium content. Finally, to 25 ml. heparin blood of the same subject 11 mgm. $CaCl_2$ were added and all three samples were shaken with the same quantity of radio-potassium in the manner described above. The curves I, II, and III illustrate the dependence of the permeability to K upon the amount of Ca present in the blood. The permeability of red cells to potassium ions *in vitro* is markedly reduced in the presence of increasing amounts of calcium.

It was moreover studied at what rate the labelled K atoms

which entered the blood corpuscles leave the cell and re-enter the plasma. For this purpose total blood was shaken for 2 h with labelled KCl just as described above, the corpuscles were centrifuged off, washed twice with physiological NaCl-solution and then resuspended in inactive plasma. Subsequently, the blood was shaken in a thermostat at 37° and samples were taken at intervals during a period of 2 h. The activity then found in the plasma originates from labelled K which left the activated corpuscles. In the course of 2 h, 5 % of the corpuscle activity had entered the inactive plasma. Corresponding measurements with radio-phosphorus showed that 2—3 % of the corpuscle activity had permeated into the plasma in the course of 2 h.

The present investigations were carried out at the Wenner-Gren Institute for Experimental Biology, Stockholm. Due to the end of the war in Europe my work at this institute had to be discontinued; however, it is planned to resume these problems and to complete the experiments in Copenhagen as soon as possible.

The author wishes to express her deepest gratitude to Professor J. Runnström for the hospitality granted at the Wenner-Gren Institute since October 1943, for the excellent working conditions, and for his living interest in this work.

My thanks are furthermore due phil. lic. M. Malm for her readiness to put the counter arrangements at my disposal and for numerous stimulating discussions.

References.

1) H. Levi, Arkiv f. Kemi, Min. och Geol. Stockholm 1945, in print.
2) H. Levi, Acta Physiol. Scand. **2**, 311, 1941.
3) M. Malm, Arkiv f. Zool. Stockholm 1945, in print.
4) G. Hevesy and L. Hahn, D. Kgl. D. Vid. Selsk. Biol. Medd. XVI, 1, 1941. L. A. Hahn, G. Ch. Hevesy and O. H. Rebbe, Biochem. J. **33**, 1549, 1939.
5) R. B. Dean, T. R. Noonan, L. Haege and W. O. Fenn, J. gen. Physiol. **24**, 353, 1941.

Indleveret til Selskabet den 30. Juni 1945.
Færdig fra Trykkeriet den 21. September 1945.

DET KGL. DANSKE VIDENSKABERNES SELSKAB
MATEMATISK-FYSISKE MEDDELELSER, BIND XXIII, NR.11.

DEDICATED TO PROFESSOR NIELS BOHR ON THE OCCASION OF HIS 60TH BIRTHDAY

ON THE THEORY OF β-DECAY II

BY

STEFAN ROZENTAL

KØBENHAVN
I KOMMISSION HOS EJNAR MUNKSGAARD
1945

Printed in Denmark.
Bianco Lunos Bogtrykkeri A/S
REPRINTED 1948 TUTEIN OG KOCH

Introduction.

Among the experimental tests of a theory of nuclear forces one of the most important is the comparison of its results concerning the process of β-decay with experimental evidence. From the assumptions on which a theory of nuclear forces is based, it should be possible not only to derive the magnitude and the general character of these forces, but also to calculate the lifetime of β-radioactive elements and to predict the shape of the energy distribution curve of the β-rays emitted. A theory based on the assumption of a nuclear meson field must furthermore yield a value of the lifetime of a free meson, which agrees with the value of the lifetime of mesons in cosmic radiation.

Various types of a meson theory of nuclear forces have been developed, but, so far, none of them has proved to be satisfactory in all respects. Particularly, the scattering of fast neutrons by protons is a phenomenon for which the experimental results seem to be very difficult to bring into harmony with the theoretical expectation. One type of a meson theory has been put forward by MØLLER and ROSENFELD [1] who regard the meson field as a superposition of two components, one of which is described by a vector and the other by a pseudoscalar wave-function. Against this theory (in the following denoted as the MR-theory) the objection has been raised that the results concerning the character of the scattering of fast neutrons by protons are in disagreement with known experiments. In fact, it follows from the theory that a beam of fast neutrons will be scattered in such a way that the intensity in the direction anti-parallel to the incident beam is larger (about 1.5 times) than the intensity in the direction perpendicular to it, the angles being measured in a system of reference where the centre of gravity of the two colliding particles is at rest. The experiments, on the contrary, seem to indicate that the ratio of

the intensities anti-parallel and perpendicular to the neutron beam is smaller than unity. Two remarks should be made in this connection. First, the accuracy of the measurements is so far not sufficient to allow a decisive statement. Even the experiments of CHAMPION and POWELL [2], who use the powerful photographic method, are not accurate enough. It is possible, however, that an improvement in the geometrical arrangement will lead to conclusive results. Second, as pointed out by HULTHÉN [3], the discrepancy in question, if real, will appear in every consistent meson theory of nuclear forces and not in the MR-theory, only.

Owing to the progress in the experimental technique during the last years, a very extensive and well-founded knowledge of the shape of different β-ray spectra could be gathered. In contrast to earlier investigations, the recent measurements seem to indicate [4] that, in the case of the so-called allowed transitions, the spectra coincide—at any rate for not too small energies of the electron emitted—with the curve given by the original formula of FERMI [5]. In the region of lower energies, a certain deviation from the Fermi law has been found. Whether the β-spectrum really differs from the pure Fermi distribution law and is given by another formula as, for example, the generalized Fermi law [13], which also follows from the present investigation, is difficult to decide with certainty. In the case of positron emitters, this latter law leads to a curve which differs from the pure Fermi law only little and in the same direction as the experimentally found spectra, and the elements examined were obviously all positron emitters. On the other hand, the deviation may be due to the scattering of the β-rays from the support, an effect which, if sufficiently large, also would explain the deviation from an original distribution given by the pure Fermi law. If it is true that the β-spectrum is given by a generalized Fermi formula, the deviation from the pure Fermi law would be more pronounced in the case of electron emitters which are not found among the light nuclei so far investigated. All these considerations show that it may be of some value to examine what kind of law for the β-decay follows from the MR-theory.

In an earlier paper ([6], in the following quoted as I), the theory of β-decay was developed for light nuclei from the point of view of the MR-theory of the nuclear meson field. The calculations resulted in a formula for the disintegration probability

which besides terms of the Fermi type includes terms differing from them. Whether such terms really are of significance for the shape of the spectrum or not depends on the relative magnitude of the coefficients. Since the number of constants involved in these coefficients is very large, the discussion of all possibilities is rather troublesome, and the formula would become still more complicated in the case of heavier radioactive elements. It is possible, however, to reduce the number of independent constants and to determine their values, and the final formula for the energy distribution becomes easy to survey.

The notations used in the present paper are the same as in I.

Determination of the Constants.

The method applied to the derivation of the decay probability of heavy nuclei is similar to that used in I. The starting point is a Hamiltonian describing a system of heavy particles (nucleons), light particles (electrons, neutrinos), and the meson field (vector and pseudoscalar). With this expression for the Hamiltonian the probability is derived for a process in which a neutron is transformed into a proton at the same time as a neutrino in a negative energy state disappears and an electron in a positive energy state is created. This probability (per unit time) is given by the formula

$$P(E_s) = \frac{2\pi}{\hbar}\,\delta(W + E_\sigma - E_s)\,|(n, s\,|\,H_\beta\,|\,n_0, \sigma)\,|^2, \qquad (1)$$

where H_β is the part of the Hamiltonian responsible for the β-emission, n_0 and n denote the initial and the final states of the nucleus, and σ and s the states of the neutrino and the electron, respectively. The energies of the electron and the neutrino are denoted by E_s and E_σ, while $W = E_{n_0} - E_n$ is the total energy released in the β-process. The expression H_β is built up of wave-functions and contains a number of universal constants. Thus, the constants g_1 and g_2 govern the strength of the coupling between the nucleons and the vector meson field, while the interaction between the nucleons and the pseudoscalar part of the meson field depends on the value of the constants f_1 and f_2. Similarly, the constants $\breve{g}_1$, $\breve{g}_2$ and $\breve{f}_1$, $\breve{f}_2$ appear in the terms

which describe the interaction between the light particles and the vector and the pseudoscalar meson field, respectively. All these constants have the dimensions of electric charge.

Furthermore, the expression H_β contains four constants of a character deviating from that of the f's and g's. The Hamiltonian of the nuclear system is not defined in a unique way by the demand of relativistic invariance. In fact, we can write down four expressions (I, formula 10) which are relativistically invariant and which, therefore, can be added to the Hamiltonian provided with the constant factors η, η', η'', η''', respectively. According as such a coefficient is put equal to 1 or 0, the corresponding term will or will not appear in the Hamiltonian.

One of the main points of the MR-theory is in the expression for the nuclear force to make disappear terms with a singularity of dipole type. The singular terms originating from the vector and the pseudoscalar meson field, respectively, become equal with opposite sign, and cancel each other, if

$$f_2^2 = g_2^2 .$$

A more effective reduction in the number of constants involved can be achieved by following MØLLER [7], who has developed a formalism in which the vector and the pseudoscalar parts of the meson field are united into one five-dimensional scheme. The constants connected with the two kinds of fields are, then, no longer independent and have to satisfy the following relations:

$$\left.\begin{aligned} f_1 &= g_1 \\ f_2 &= -g_2 \\ \check{f}_1 &= \check{g}_1 \\ \check{f}_2 &= -\check{g}_2 . \end{aligned}\right\} \quad (2)$$

Moreover, if this formalism is adopted, it will be quite natural to demand that the four terms provided with the factors η, η', η'' and η''' and added to the Hamiltonian should be invariant with respect to the group of rotations in the whole five-dimensional space in question. From this assumption we get as a necessary condition

$$\left.\begin{aligned} \eta &= \eta'' \\ \eta' &= \eta''' . \end{aligned}\right\} \quad (3)$$

In this way, the number of constants is reduced from twelve to six. The values of the universal constants g_1, g_2, $\breve{g}_1$, $\breve{g}_2$ can now be fixed by using some experimentally known properties of atomic nuclei and mesons.

As regards the two constants g_1, they and g_2 are found from the value of the binding energy of the deuteron and the range of the nuclear force. We have approximately

$$\frac{g_1^2}{4\pi\hbar c} = \frac{1}{35}. \qquad \frac{g_2^2}{4\pi\hbar c} = \frac{1}{15}. \tag{4}$$

As regards the values of the constants $\breve{g}_1$ and $\breve{g}_2$ we have, as already mentioned, to consider the connection between the β-decay of light elements and the radioactive properties of cosmic ray mesons. In the meson theory the β-disintegration is imagined to take place in two steps. In the first step, a meson is virtually created under the transition of a nucleon from the neutron to the proton state. In the second step, the meson is annihilated into an electron and an antineutrino. The probability of the second step, for which the decay constant of the meson is a direct measure, is an essential part of the probability of the whole complex process of β-decay.

Thus, the constants $\breve{g}_1$ and $\breve{g}_2$ appear both in the expression found in I for the decay constant λ_{rad} of a light β-radioactive nucleus (the transition being an allowed one) and in the decay constant of a free meson. According as the meson is of vector or of pseudoscalar type, we get for the decay probability the following formulae [8, 9]:

$$\lambda_V = \frac{M_m c^2}{4\pi\hbar}\,\frac{1}{\hbar c}\left(\frac{2}{3}\,\breve{g}_1^2 + \frac{1}{3}\,\breve{g}_2^2\right) \tag{5a}$$

$$\lambda_{PS} = \frac{M_m c^2}{4\pi\hbar}\,\frac{1}{\hbar c}\left(\breve{g}_1 - \frac{\mu}{M_m}\,\breve{g}_2\right)^2 \tag{5b}$$

where M_m and μ are the masses of the meson and of the electron, respectively. No agreement between the lifetimes of light β-radioactive nuclei and the lifetime of a meson can be obtained, if we consider vector mesons, only. For every possible choice of $\breve{g}_1$ and $\breve{g}_2$ compatible with the empirical values of λ_{rad}, the cal-

culated lifetime of the vector meson turns out to be about 1000 times smaller than the measured one which is of the order of magnitude of 2×10^{-6} sec. [10]. As soon as we assume, however, that the cosmic ray mesons are of the pseudoscalar type with the decay constant (5b). the discrepancy disappears [11], if only

$$\breve{g}_1^2 \ll \breve{g}_2^2. \tag{6}$$

The ratio between $\breve{g}_1$ and $\breve{g}_2$ has to be chosen of the order of magnitude of 0.02—0.05. From this assumption it follows that the vector mesons created simultaneously with the pseudoscalar mesons in the upper layers of the atmosphere will, due to their very short lifetime, disintegrate before they can reach the surface of the earth and, consequently, only pseudoscalar mesons will be found in our laboratories where the measurements are performed.

If the condition (6) is fulfilled, we get, from the disintegration formula in I, an energy distribution which, for $\eta = 1$ follows the curve given by the Fermi function

$$F(E) = E \sqrt{E^2 - 1}\ (W - E)^2 \tag{7}$$

and for $\eta = 0$ the curve

$$\Phi(E) = F(E)\left(1 \pm \frac{1}{E}\right), \tag{8}$$

where the upper sign refers to the emission of positrons and the lower to the emission of electrons. Actually, we have

$$P(E)\,dE = \frac{2}{\pi^3}\left(\frac{\mu}{M_m}\right)^4 \left(\frac{\mu c^2}{\hbar}\right) F(E)\left(1 \pm \frac{(1-\eta)^2}{E}\right) \frac{g_2^2\,\breve{g}_2^2}{(\hbar c)^2}\, 2\,|M|^2\,dE. \tag{9}$$

Here, $|M|^2$ is a matrix element depending on the wave-functions of the nucleons. It is independent of the value of η', but is different according as the constant η has the value 0 or 1. The empirical selection rules seem to indicate that the first of these matrix elements should be preferred, since it is of the proper spin-dependent type [12]. It will, therefore, be appropriate to put the constant η equal to 0.

It should be mentioned here that the spectrum given by the function (8) is the same as that which, as pointed out by FIERZ [13], follows from the most general Fermi theory. For positrons, the shape of the spectrum differs from the pure Fermi distribution (7) only in the region of lower energies (cf. I, Fig. 1), but it is difficult to say whether the deviation from the distribution (7) found experimentally (all light elements for which the transition is allowed are positron emitters) is of the type given by the generalized Fermi function (8).

Derivation of the Disintegration Formula.

The formula for the decay probability derived in I applies to elements with a small nuclear charge Z fulfilling the condition

$$Z\alpha \ll 1, \tag{10}$$

where α is the fine structure constant

$$\alpha = \frac{e^2}{\hbar c} = \frac{1}{137}.$$

The simplifications carried out in the preceding Section now allow to extend the calculation to heavier elements for which the condition (10) is not satisfied.

The method used in this case is similar to that adopted in I, where all details of the calculations can be found.

We start with the expression for the Hamiltonian and go on with the evaluation of the quantity (1). It must be noticed that, despite the relation (6), it is not allowed in the Hamiltonian to cancel all terms with $\breve{g}_1$. Although, in the final formula, the terms with the coefficient $\breve{g}_1$ or $\breve{g}_1^2$ generally are small compared with terms with $\breve{g}_2^2$, they may in some cases play a decisive part, when the other terms happen to vanish due to selection rules.

In order to find the matrix element in (1) belonging to the transition of the nucleus from the initial stage n_0 to the final state n, we insert the wave-functions of the light particles. The neutrino is not affected by the charge of the nucleus and can therefore be described by means af a plane wave while, for the electrons, exact solutions of the wave equation have to be applied.

The expressions involving such wave-functions are integrals extended over the volume of the nucleus. Since we may assume that the radial part of the electron wave-function $\varphi_s(x)$ (x stands for all spatial coordinates, and s denotes the electron state) does not vary appreciably inside the nucleus, we can replace the radial part of the wave-function by its value at the boundary of the nucleus, a value which in its turn is nearly equal to the value—taken in the same point—of an exact solution of the wave equation for a Coulomb field.

After the summation over all states of the neutrino belonging to the energy E_σ, we get the formula

$$P(E)\,dE = \frac{2\pi}{\hbar}\,\frac{1}{(hc)^3}\,(W-E)^2\,dE\sum_s U, \tag{11}$$

where the terms U are composed of the electron wave-functions and the Dirac spin operators. The summation is extended over all electron states with the energy E_s. The four-component wave-functions in the Coulomb field can be used in the shape given by Rose [14], who denotes the radial parts of the two first and the two last components by $f_\varkappa$ and $g_\varkappa$, respectively, where $\varkappa$ is a quantity connected with the total angular momentum number. The functions $f_\varkappa$ and $g_\varkappa$ are given by the formula

$$\left\{\begin{matrix} f_\varkappa \\ g_\varkappa \end{matrix}\right\} = \frac{\sqrt{1 \mp E}\,(2pr)^{\gamma-1}\sqrt{p}\,e^{\pi\frac{\alpha ZE}{p}}\left|\Gamma\left(\gamma + i\frac{\alpha ZE}{p}\right)\right|}{\sqrt{\pi}\,\Gamma(2\gamma+1)}\times \left\{\begin{matrix} \\ \\ \end{matrix}\right.$$

$$\times\left\{e^{-ipr}\sqrt{-\left((\varkappa - i\frac{\alpha Z}{p}\right)\left(\gamma + i\frac{\alpha ZE}{p}\right)}\cdot\right. \tag{12}$$

$$\left.\left. F\left(\gamma+1+i\frac{\alpha ZE}{p}, 2\gamma+1; 2ipr\right) \mp c.\,c.\right\}\right\}.$$

Here. p is the momentum of the electron, F is the confluent hypergeometric function, Γ is the gamma function, and

$$\gamma = \sqrt{\varkappa^2 - \alpha^2 Z^2}.$$

All quantities are expressed in atomic units. With these notations the sum in (11) transforms into a sum $\sum_\varkappa V$ of terms, each of which is a function of the $f_\varkappa$, $g_\varkappa$, and the unit vector

$$\vec{n} = \frac{\vec{x}}{|\vec{x}|}.$$

Generally, it is unnecessary to extend the summation over all $\varkappa$. The functions $f_\varkappa$ and $g_\varkappa$ are taken at the boundary of the nucleus: $r = r_{\text{nucl}} \ll 1$. From (12) it is seen that the values of $f_\varkappa$ and $g_\varkappa$ for r_{nucl} decrease very rapidly with increasing $|\varkappa|$. In most cases, we can confine ourselves to the terms with $\varkappa = \pm 1$, but in some terms V, particularly in those which involve derivatives of the wave function, it is necessary to take also terms with $|\varkappa| = 2$ into consideration.

Discussion of the Decay Formula.

The final formula giving the probability $P(E)\,dE$ per unit time for the emission of an electron with the energy (expressed in units μc^2) between E and $E + dE$ consists of a number of terms. The most important terms are the "Fermi terms", *i. e.* terms which in the limit of light nuclei would give a pure or generalized Fermi distribution. Other terms containing an extra factor $\sqrt{E^2 - 1}$ or $(E^2 - 1)$ are in addition multiplied by $\frac{\mu}{M_m} \approx \frac{1}{200}$ or $\left(\frac{\mu}{M_m}\right)^2 \approx \frac{1}{40000}$ and may, therefore, be cancelled. The "Fermi terms" can be classified according as the constant factor is $\breve{g}_2^2$, $\breve{g}_1\breve{g}_2$ or $\breve{g}_1^2$. Mostly, only terms with the large coefficient $\breve{g}_2^2$ have to be retained, the others being small owing to the relation (6). One of such terms with $\breve{g}_2^2$ is

$$\frac{g_2^2\,\breve{g}_2^2}{(\hbar c)^2}\, 4\,\omega_2\,(B, B)\,(f_{+1})^2. \tag{13}$$

Here, $\omega_2\,(B, B)$ (cf. I, formula 42) is a matrix element of the Gamow-Teller type [12]:

$$\omega_2\,(B, B) = \iint \vec{B}\,(x')\,\vec{B}^*\,(x)\,dx'\,dx, \tag{14}$$

where

$$\vec{B} = \sum_{i=1}^{N} \int \psi_n^*\, Q^{(i)}\, \vec{\sigma}^{(i)}\, \psi_{n_0} dx^{(i)} \cdots dx^{(i-1)}\, dx^{(i+1)} \cdots dx^{(N)}$$

is an integral over the wave-functions Ψ' of the nucleus in the initial and final states, $Q^{(i)}$ is an operator transforming the i'th nucleon from the neutron state into a proton state, N is the number of the nucleons in the nucleus, and $\vec{\sigma}^{(i)}$ is the Pauli spin operator to the i'th nucleon.

The most important case is that of an allowed transition, *i. e.* a process for which the matrix element (14) attains its maximum value

$$\omega_2(BB) = \iint (B_x^* B_x + B_y^* B_y + B_z^* B_z)\, dx'\, dx \approx 3.$$

In this case, the result is quite independent of the value of η'. All terms with $\breve{g}_1^2$ and $\breve{g}_1\breve{g}_2$ are small and can be cancelled. The remaining terms are the same for $\eta' = 0$ and $\eta' = 1$. In the limit of small Z, *i. e.* when condition (10) is satisfied, and for that part of the β-spectrum where

$$\frac{\alpha ZE}{p} \ll 1,$$

we get, as it was to be expected, the formula (9) with $\eta = 0$. Actually, it is seen from (12), when expanding in series, that f_{-1} is, for $Z\alpha \ll 1$ small of the order of magnitude of $r_{\text{nucl}} \ll 1$ as compared with f_{+1}, and the other terms with g_2^2, *viz.*

$$\frac{g_2^2 \breve{g}_2}{(\hbar c)^2} 4 (f_{-1})^2 \omega_{10}(B, B), \tag{15}$$

where

$$\left.\begin{aligned} \omega_{10}(B, B) = \iint \{ &(\vec{B}(x')\vec{B}^*(x))(\vec{n}(x)\cdot\vec{n}(x')) \\ &+ (\vec{B}(x')\vec{n}(x'))(\vec{n}(x)\vec{B}^*(x)) \\ &+ (\vec{B}(x')\vec{n}(x))(\vec{n}(x')\vec{B}^*(x))\} dx'\, dx \end{aligned}\right\} \tag{16}$$

are negligible, so that (13) is the only remaining term. We get a β-spectrum of a generalized Fermi type described by the function (8).

With increasing Z we get a deviation from the Fermi distribution and the energy distribution is now characterized by a function

$$F(E)\ C(E, Z)$$

which is found in substituting the proper function f_{+1} into (13). The correctional factor C becomes, of course, equal to 1 for small Z. Moreover, with increasing Z the function f_{-1} remains small as compared with f_{+1} only in the region where $\frac{\alpha Z}{p} E \ll 1$, *i. e.* for sufficiently great energies. This means that, if only ω_{10} does not vanish, the correction introduced by the term (15) is not negligible and makes itself perceptible in a part of the β-spectrum which lies below a certain electron energy, this limit energy becoming higher and higher with increasing nuclear charge Z.

In the case of a forbidden transition, *i. e.* when $\omega_2 (B, B)$ vanishes, the situation is changed. The term (13) disappears, and if ω_{10} is also equal to 0, other terms with the coefficient $\breve{g}_1 \breve{g}_2$ and with other matrix elements will now be responsible for the general character of the β-spectrum. In contrast to the case of allowed transitions, there is now a difference between the formulae for $\eta' = 0$ and $\eta' = 1$. In the disintegration formula we have terms of pure Fermi type and of the type $F(E)(E^2-1)$ (cf. I, Fig. 2). The decay constant, which is simply the integral over $P(E)$ from $E = 1$ to $E = W$, is now smaller and, consequently, the lifetime is longer than in the case of an allowed transition with the same maximum energy W, since the constant coefficient $\breve{g}_1 \breve{g}_2$ in $P(E)$ is smaller than the coefficient $\breve{g}_2^2$ appearing in the decay formula for allowed transitions. Also the selection rules for the transition are now given by the differing form of the matrix elements appearing in the disintegration formula.

Summary.

A theory of β-decay for elements with high nuclear charges is developed on the lines of the special meson theory proposed by Møller and Rosenfeld. The values of the universal constants involved have been determined from the requirement of a consistent qualitative description of the nuclear forces, the β-process and the disintegration of the meson. The discussion of the disintegration formula indicates that, for an allowed transition, the spectrum is represented by the generalized Fermi formula. For a forbidden transition also terms of other type can occur

The author wishes to express his deep gratitude to Professor NIELS BOHR for his kind interest in this work. Professor BOHR's highly stimulating discussions and neverfailing help have been of the utmost significance to me during my stay at the Institute of Theoretical Physics, Copenhagen. The present investigation has been made possible through a stipend from the Rask-Ørsted Foundation to whom the writer is greatly indebted.

Due to war circumstances, part of the investigation had to be carried out in Sweden. The author cordially thanks Professor OSKAR KLEIN for the excellent working conditions and the hospitality offered to him at the Institute of Mechanics and Mathematical Physics, University of Stockholm. Also to the Nobel Foundation, Stockholm, he is much obliged for a grant.

References.

1. C. Møller and L. Rosenfeld, D. Kgl. Danske Vidensk. Selskab, Mat.-fys. Medd. **XVII**, Nr. 8, 1940.
2. F. C. Champion and C. F. Powell, Proc. Roy. Soc. (A) **183**, 64, 1944.
3. L. Hulthén, Private communication.
4. Cf. for instance, K. Siegbahn, Arkiv f. Mat. Fys. Astr. **30 A**, No. 20, 1944.
5. E. Fermi, ZS. f. Phys. **88**, 161, 1934.
6. S. Rozental, D. Kgl. Danske Vidensk: Selskab, Mat.-fys. Medd. **XVIII**, Nr. 7, 1941.
7. C. Møller, D. Kgl. Danske Vidensk. Selskab, Mat.-fys. Medd. **XVIII**, Nr. 6, 1941.
8. H. Yukawa, S. Sakata, M. Kobayashi and M. Taketani, Proc. Phys.-Math. Soc. Japan **20**, 720, 1938.
9. T. S. Chang, D. Kgl. Danske Vidensk. Selskab, Mat.-fys. Medd. **XIX**, Nr. 10, 1942.
10. F. Rasetti, Phys. Rev. **60**, 198, 1941.
11. S. Rozental, Phys. Rev. **60**, 612, 1941.
12. G. Gamow and E. Teller, Phys. Rev. **49**, 895, 1936.
13. M. Fierz, ZS. f. Phys. **104**, 553, 1937.
14. M. E. Rose, Phys. Rev. **51**, 484, 1937.

Indleveret til Selskabet den 6. August 1945.
Færdig fra Trykkeriet den 26. September 1945.

DET KGL. DANSKE VIDENSKABERNES SELSKAB
MATEMATISK-FYSISKE MEDDELELSER, BIND XXIII, NR. 12

DEDICATED TO PROFESSOR NIELS BOHR ON THE OCCASION OF HIS 60TH BIRTHDAY

ON THE RECOIL OF THE NUCLEUS IN BETA-DECAY

BY

J. C. JACOBSEN AND O. KOFOED-HANSEN

KØBENHAVN
I KOMMISSION HOS EJNAR MUNKSGAARD
1945

Printed in Denmark
Bianco Lunos Bogtrykkeri

Introduction.

It has long been known that in a β-transformation the energies of individual β-particles vary over a wide range (1), from zero to a well defined upper limit (2) characteristic of the element in question. Experiments performed by ELLIS and WOOSTER (3) and by MEITNER and ORTHMANN (4) showed that the observed variation in energy of the β-particles cannot be ascribed to any secondary process outside the nucleus. Since both the mother and the daughter substances must be assumed to have a definite energy content, which is the same for the individual atoms, the difference in energy between the individual β-particles apparently shows a lack in conservation of energy in a β-transformation. PAULI then suggested that in a β-transformation two particles are emitted and that the available energy, which may be identified with the upper limit of energy for the β-particles, is shared between them. The new particle, *i. e.* the neutrino, must have a small rest mass and zero charge. With the help of a number of additional assumptions, FERMI (5) developed a theory which in a general way accounted for the experimental results including the energy distribution of the β-particles and the empirical relation between lifetime and transformation energy.

The direct experimental evidence for the emission of neutrinos is entirely negative (6), (7), no indication having been obtained of any ionization which could be attributed to such particles in their passage through matter. Hence, the only possibility remaining is to look for an effect on the emitting nucleus itself. The question here is, whether the recoil of the nucleus in a β-transformation corresponds to the momentum gained from the β-particle alone or to the resultant momentum of the β-particle

and the neutrino. Considerable experimental difficulties may here be expected in view of the smallness of the recoil energy.

In experiments on the β-recoil from ThB, DONAT and PHILIPP (8) found an efficiency amounting to a few per cent of that obtained in α-recoil. This low efficiency, which may reasonably be attributed to spurious surface effects, may illustrate the difficulties which are to be expected from an attempt to determine the recoil energy. If only a few per cent of the recoil atoms were able to leave the surface, a quantitative determination of the energy of the individual recoil atoms, if it could be carried out, would probably be of minor interest.

LEIPUNSKI (9) was the first to make an attempt to measure the recoil energy in a β-transformation. He determined the number of recoil atoms from ^{11}C which were able to pass through a retarding electric field, thus supposing that they were charged. Without exact knowledge of the experimental conditions it is difficult to decide whether this has been the case. It should generally be expected that the recoil atoms leave the surface as neutral atoms if the radioactive material rests on the surface of a metal. The same applies to LEIPUNSKI's experiments where a negative ion of ^{11}B was formed by the emission of the β-particle.

The disturbing influence of surface effects was avoided by CRANE and HALPERN (10) who worked with ^{38}Cl in a cloud chamber. They observed that frequently a cluster of droplets was formed at the beginning of a track, a phenomenon which they ascribed to ionization and dissociation of the gas in the chamber by the recoil atom. In similar experiments with ^{32}P, where the maximum energy of the β-particles is much smaller than for ^{38}Cl, no such clusters could be found. A direct determination of the recoil energy from the number of droplets was difficult, since the energy expanded per droplet is not known with certainty and may probably be considerably smaller than the energy expanded per ion by fast particles. CRANE and HALPERN interpreted their results as an indication of the existence of a neutrino. The main support for this interpretation was the observation that clusters of many droplets at low energy of the β-particles were found just as frequently as at high energy; this

would not have been the case if only the β-particle was emitted, conservation of momentum being assumed.

ALVAREZ, HELMHOLTZ and WRIGHT (11) exposed *in vacuo* a clean surface to a vacuum distilled layer of cadmium with period 6.7 hours formed by the Ag (d, 2n) Cd reaction. On this clean surface the daughter substance formed by K-capture from the cadmium was found. The passage of the active silver from one surface to another was ascribed either to a recoil following K capture (emission of an X-ray or a neutrino) or to a change in the surface binding of the atom during K capture.

Experimental Method.

For a quantitative determination of the recoil energy the active element should be a gas at a pressure which is so low that the mean free path is large compared to the dimensions of the vessel. Then the recoil atoms must necessarily be charged before their collision with the walls of the vessel, and the recoil energy can be determined by a retarding electric field. If the daughter substance formed in the transformation is radioactive, the number of recoil atoms passing through the retarding field can be simply determined.

In Table I, the active isotopes of krypton and xenon which are formed by the fission of uranium or otherwise are listed as far as they have been identified at present (12), (13), (14). Some constants in the table were redetermined in this work. As it results also from the table, GLASOE and STEIGMAN (15) have found that the active deposit from the gases consists entirely of ^{88}Rb, if a sample of uranium is left for about 3 hours after irradiation with neutrons before the inert gases formed by fission are driven off. The figures in Table I further show that, if the inert gases are collected about 5 minutes after a short irradiation, the active deposit collected during the next 5 minutes will mainly consist of ^{89}Rb. In this case, the separation is not as complete as with ^{88}Rb, since both ^{88}Rb and ^{138}Cs will be present to some extent. Unfortunately, the decay constants of ^{88}Rb and ^{89}Rb are nearly identical, so that a determination of the amount of ^{89}Rb

Table 1.

$$^{81}\mathrm{Kr} \xrightarrow[34.5\ \mathrm{h.}]{0.4\ \mathrm{MeV}} \mathrm{Br}$$

$$^{82}\mathrm{Kr} \xrightarrow[113\ \mathrm{m.}]{\gamma = 0.5\ \mathrm{MeV}} \mathrm{Kr}$$

$$^{85}\mathrm{Kr} \xrightarrow[4.6\ \mathrm{h.}]{0.8\ \mathrm{MeV}} \mathrm{Rb}$$

$$^{87}\mathrm{Kr} \xrightarrow[75\ \mathrm{m.}]{4\ \mathrm{MeV}} \mathrm{Rb}$$

$$^{88}\mathrm{Kr} \xrightarrow[2.7\ \mathrm{h.}]{2.4\ \mathrm{MeV}} \mathrm{Rb} \xrightarrow[17.8\ \mathrm{m.}]{5\ \mathrm{MeV}} \mathrm{Sr}$$

$$^{89}\mathrm{Kr} \xrightarrow[\sim 3\ \mathrm{m.}]{4.5\ \mathrm{MeV}} \mathrm{Rb} \xrightarrow[15.4\ \mathrm{m.}]{3.8\ \mathrm{MeV}} \mathrm{Sr} \xrightarrow[55\ \mathrm{d.}]{1.5\ \mathrm{MeV}} \mathrm{Y}$$

. . . . . .

$$^{133}\mathrm{Xe} \xrightarrow[5\ \mathrm{d.}]{0.3\ \mathrm{MeV}} \mathrm{Cs}$$

$$^{135}_{135}\mathrm{Xe} \xrightarrow[9.4\ \mathrm{h.}]{10\ \mathrm{m.}} \mathrm{Cs} \xrightarrow{?}$$

$$^{137}\mathrm{Xe} \xrightarrow[3.8\ \mathrm{m.}]{4\ \mathrm{MeV}} \mathrm{Cs}\ ?$$

$$^{138}\mathrm{Xe} \xrightarrow[18\ \mathrm{m.}]{?} \mathrm{Cs} \xrightarrow[33\ \mathrm{m.}]{?} \mathrm{Ba}$$

$$^{139}\mathrm{Xe} \xrightarrow[45\ \mathrm{s.}]{?} \mathrm{Cs} \xrightarrow[7\ \mathrm{m.}]{?} \mathrm{Ba} \xrightarrow[87\ \mathrm{m.}]{1\ \mathrm{MeV}} \mathrm{La.}$$

present can only be performed if the amount of ^{89}Sr (half period = 55 days) can be measured; this, however, can only be done with fairly strong sources. For these reasons, it was decided to work with ^{88}Kr, although a few experiments have also been made with ^{89}Kr.

The experimental method is schematically demonstrated in Fig. 1. A metal box with one end consisting of a wire gauze was placed in a vessel containing the inert gases obtained from uranium fission. Two metal plates, I and II, which were placed at equal distances from the wire gauze and the opposite end of the box, were kept at a positive potential relative to the box. After

the inert gases had been kept in the apparatus for a suitable time, the amount of active deposit collected on I and II was measured. The difference between these activities was due to recoil atoms starting from the interior of the box and having sufficient energy to surmount the potential difference between the box and the plates. When the potential difference between the box and the plates was varied in separate experiments, the energy distribution of the recoil atoms could be determined.

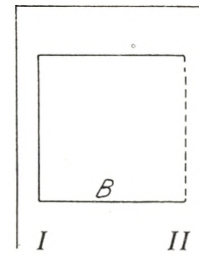

Fig. 1.

By this method the energy of a β-particle cannot be determined simultaneously with that of the corresponding recoil atom; it is possible only to compare the energy distribution of the recoil atoms with that of the β-particles. The limitations of the method will be discussed later in connection with the results.

The main part of the apparatus (Fig. 2) was a rectangular box B_1 made of sheet copper, one side of the box being closed by a brass wire gauze. The box was divided into a number of smaller partitions by means of cross-walls, the purpose of which was to limit the free paths of the recoil atoms and thus to reduce the influence of the residual gases in the apparatus. The box with the wire gauze was placed, electrically insulated, inside a second box B_2 also made of sheet copper. The active deposit from the inert gases was collected on aluminium foils, F_1 and F_2, attached to the inner sides of B_2. For measurements of the activity of the deposit the aluminium foils were removed from the apparatus and wrapped around a cylindrical counter.

The difference between the activities of the aluminium foils, which determines the number of recoil atoms with energy higher than the potential difference between the outer and the inner box, was of course proportional to the total amount of inert gas present in the apparatus. For the comparison of different experiments, this latter quantity which varied somewhat from one experiment to another, had to be determined in some arbitrary unit. For this purpose the arrangement in the lower part of Fig. 2 was used.

A circular brass disc D was placed in the bottom wall of a

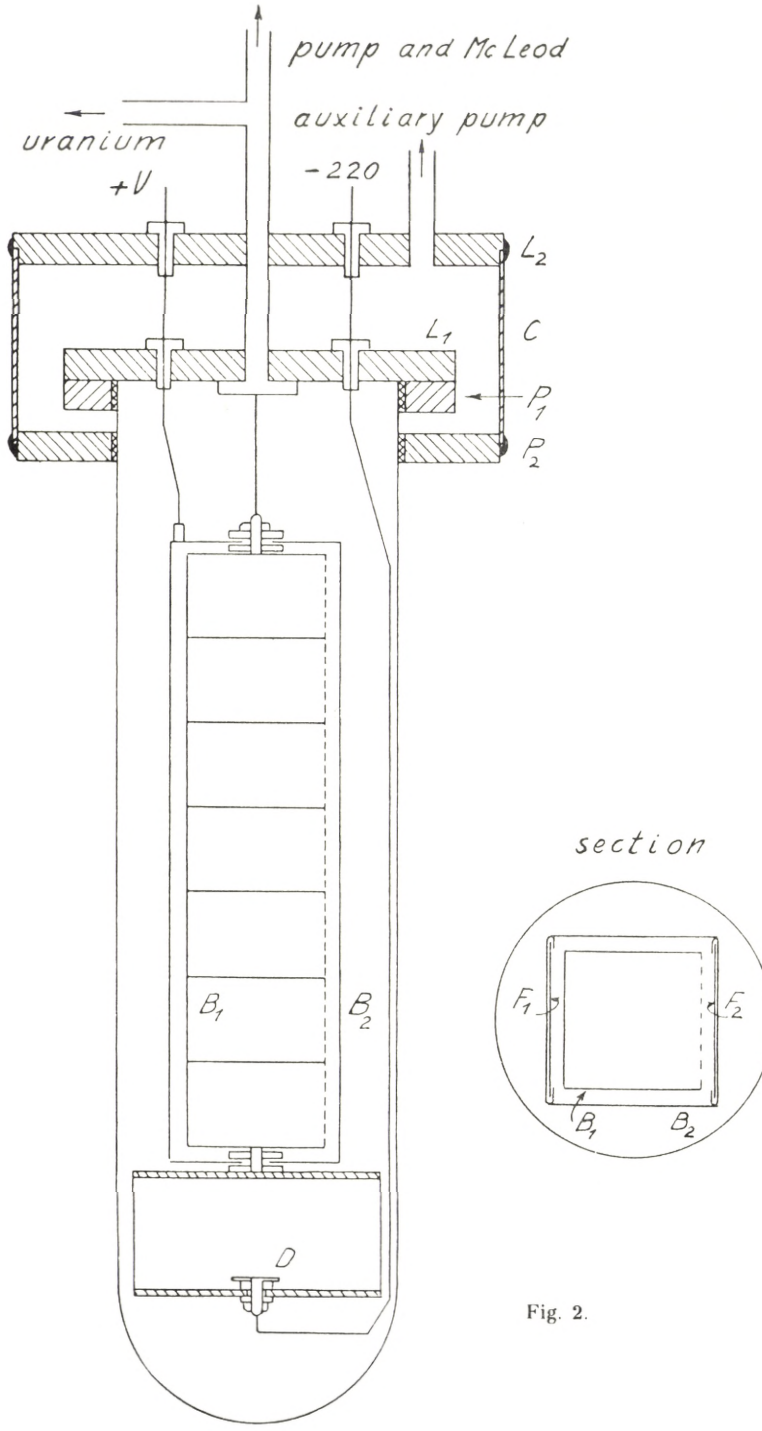
pump and McLeod
auxiliary pump
uranium
+V
-220
L_2
L_1
C
P_1
P_2
B_1
B_2
D
section
F_1
F_2
B_1
B_2

Fig. 2.

brass cylinder, electrically insulated and kept at a potential of —220 volts relative to the cylinder. The activity of the disc, determined under standard conditions, was used as a measure of the total amount of ^{88}Kr present. The constancy of the counters used was checked before and after each measurement by irradiation with a γ-ray source placed in a standard position.

The metal parts of the apparatus were housed in a pyrex tube, diameter 8 cm. and length 30 cm., provided with brass flange and lid. The wires leading to the different parts of the apparatus were brought in through insulating plugs in the lid. It was found that the wax joints gave rise to a slight increase in pressure of about 10^{-4} mm. per hour. In order to eliminate this, an arrangement with a double lid was used (Fig. 2). Two brass flanges, P_1 and P_2, were waxed to the pyrex tube with sealing wax, the inner lid, L_1, rested directly on P_1. Connection between P_2 and the outer lid L_2 was made by a brass cylinder C fitting loosely around P_2, the joints being tightened by Apiezon Q. The tube leading to the pump, was hard soldered through both L_1 and L_2; the space between L_1 and L_2 was connected to a separate pump. To dismount the apparatus after air had been let in, it was only necessary to remove C. With this arrangement, the rise in pressure during an experiment, which usually lasted about 45 minutes, was less than 10^{-5} mm. The uranium was placed in a glass bulb which was connected to the main part of the apparatus by a long glass tube, so that the uranium could be brought in between the coils of the cyclotron magnet. In the glass tube a U-tube and a stopcock H were placed. The apparatus was evacuated by a single-stage mercury diffusion pump and an oil pump. The pressure was read on a McLeod gauge.

The uranium was used in an emanating form obtained by precipitating a mixture of $UO_2(NO_3)_2$ and $FeCl_3$ with ammonia; after washing, the precipitate was dried at room temperature and powdered. In the state in which the uranium was used in the experiments, it gave off large amounts of water vapour and other gases when placed under vacuum. When the pyrex tube containing the main part of the apparatus was cooled in liquid air, most of these gases were condensed, a residual pressure of about 10^{-4} to 10^{-3} mm. remaining. As far as could be determined, this

residual pressure was proportional to the number of neutrons used in the irradiation, the other conditions being constant. This observation indicates that the gases causing the residual pressure were produced by decomposition of the uranium precipitate by neutrons and thus gives some idea of the chemical nature of these gases, which is of interest in connection with a discussion of the possibilities of the recoil atoms losing energy during their passage through the apparatus. The condensation of the gases actually was carried out in two steps, the U-tube being cooled in solid carbon dioxide and the pyrex tube in liquid air. The gases passing through the U-tube, in which mainly the water vapour was condensed, had a pressure of roughly 0.1 mm. which, as mentioned above, was reduced to 10^{-4} to 10^{-3} mm. by cooling the pyrex tube in liquid air. When the condensation was made in one step, cooling also the U-tube in liquid air, it was found that a considerable part of the krypton gas was retained by the gases condensed on the walls of the U-tube, the activities obtained being much larger after condensation in two steps.

The general course of an experiment was as follows. After the apparatus had been assembled and evacuated, the uranium was irradiated with neutrons from the cyclotron for 15 to 30 minutes. About 3 hours after the irradiation, Dewar beakers with solid carbon dioxide and liquid air were placed around the U-tube and the pyrex tube containing the main part of the apparatus, and the stopcock H was opened. The copper box B_2, inside which the active deposit from the krypton gas was collected, was closed on all sides except for a hole in the bottom, so that the gaseous mixture before entering B_2 had to pass along the wall of the pyrex tube. On a single occasion, the pressure inside the box was further controlled, while the gases were let in, by placing a hot wire gauge consisting of a 4 μ platinum wire, length 3 cm., inside the box. The wire was placed as one arm in a Wheatstone bridge, and the changes in resistance were recorded by a galvanometer during the admission of the gases. No increase in pressure beyond 10^{-3} mm. could be observed.

The stopcock H was left open for about 1 minute and the apparatus was then left to itself for 30 minutes. Subsequently, the gaseous mixture was removed by the pump before air was let in, the voltage difference between B_1 and B_2 being maintained.

The pumping had to be performed rather thoroughly, because the deposit collected with air in the apparatus was distributed in a way completely different from that obtained at low pressure. A number of experiments were actually wasted before the importance of this precaution was realized.

The amount of ^{88}Rb on the aluminium foils was determined by wrapping the foils around cylindrical counters and counting

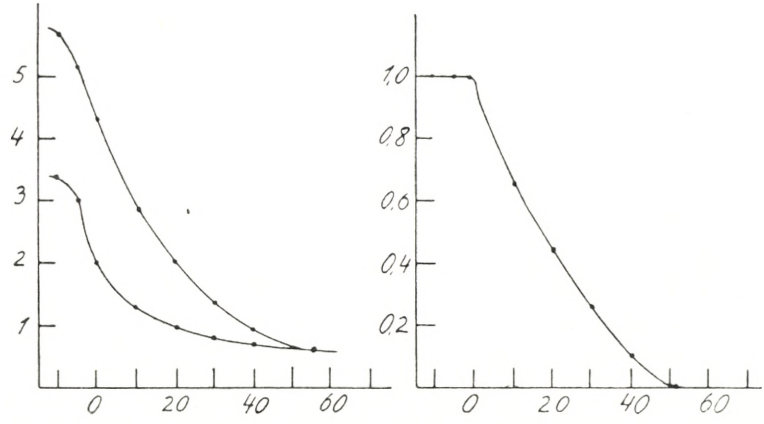

Fig. 3 a. Fig. 3 b.

Abscissa: retarding potential X in volts. Ordinate: Fig. 3a, activities of collecting foils. Fig. 3b, fraction of recoil atoms with energy greater than X.

for 36 minutes. The activity of the brass disc D was measured simultaneously by a third counter. In Fig. 3a are shown the amounts of ^{88}Rb on the aluminium foils, referred to a standard activity of D, as a function of the voltage. The total number of counts in each experiment was about 1000 times the figures given as ordinate, so that the statistical errors are fairly small. Other measurements with higher voltages showed that up to 900 volts the activities of the foils were equal and decreased steadily with increasing voltage.

Fig. 3b shows the difference between the curves in Fig. 3a, the difference at zero voltage being taken as unity. This, then, shows the fraction of the total number of recoil atoms starting from the interior of the copper box and having sufficient energy to surmount the potential difference in question.

From Fig. 3a the upper limit of the energy of the recoil atoms from ^{88}Kr is found to be 51.5 ± 2 eV. Before this result can be discussed in relation to the β- and γ-rays emitted from ^{88}Kr, a number of possible sources of error must be taken into consideration.

Experimental Errors.

The upper limit of energy of the recoil atoms can be determined rather accurately; a further result would be the distribution of energy for the recoil atoms, obtained by differentiating the curve in Fig. 3b. Due to an instrumental error, which will now be discussed, the measured energy distribution must be subjected to a considerable correction.

Suppose a positively charged particle starts from a point within a homogeneous electric field between two parallel electrodes with kinetic energy E in a direction making an angle θ with the direction of the field. The path of the particle will be a parabola, and it is easily shown that, if the particle is just able to reach the positive electrode, the potential difference between its starting point and the positive electrode will be $X = E \cos^2\theta$. If N particles start from a point within the electric field in all directions, the number of particles starting in directions making angles between θ and $\theta + d\theta$ with the direction of the electric field is $N \sin\theta d\theta$. If the energy is determined by variation of the field, as is the case in the present experiment, then, since $dX = -2E \sin\theta \cos\theta d\theta$, an apparent energy distribution will be found, in which the number of particles with energy between limits X and $X + dX$ is

$$N(X)\,dX = \frac{N}{2}\,\frac{1}{\sqrt{EX}}\,dX \qquad \text{(Fig. 4, curve I).}$$

In the experimental arrangement the space inside B_1 may to a good approximation be considered field – free (cf. later), so that the present considerations apply to the passage of the recoil atoms through the field between the wire gauze and the aluminium foil. If the recoil atoms are regarded as being divided into homo-

geneous groups with energy E, where E lies between O and a maximum value, then in the measured energy distribution each of these groups will be spread out into a band of energies ranging from O to E, as shown in Fig. 4. It results from this that in the measured energy distribution the number of recoil atoms with small energies has been much exaggerated.

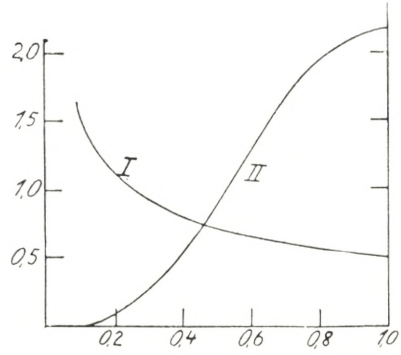

Fig. 4.

The distribution curve I in Fig. 4 is changed considerably when the geometry of the apparatus is taken into account. Fig. 5, which is a two-dimensional representation of the main part of the apparatus, shows that recoil atoms starting in a direction which makes an angle θ with the direction of the electric field can only be emitted from part of the space inside B_1 if they are to reach the collecting foil. The passage of the recoil atoms through the wire gauze acts in the same direction because the free opening of the wire gauze decreases to zero when θ approaches $\frac{\pi}{2}$. As a result, the measured energy distribution for a homogeneous group of recoil atoms cannot be represented by curve I in Fig. 4, but is more correctly represented by curve II. The lower part of this curve is fixed by the finite thickness of the wires of the gauze, the free opening of the gauze actually becoming zero for an angle θ somewhat less than $\frac{\pi}{2}$. A further estimate of the shape of the curve was obtained from a rough determination of that part of the space inside B_1 from where recoil atoms can be emitted, forming an angle θ with the direction of the electric field.

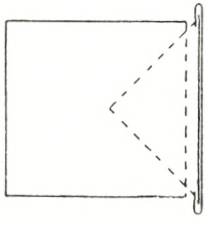
Fig. 5.

An accurate determination of the distribution to be expected is rendered extremely difficult by the irregularities of the electric field at the edges of the copper box. Even if the distribution was known accurately, a correction of the results shown in Fig. 3b could hardly be carried out unambiguously. The only method

would be to assume a suitable energy distribution for the recoil atoms and to compare the resulting corrected distribution with the experimental results. In the light of a later discussion it may, however, be unnecessary to perform the correction in question. For the moment, it suffices to state that

1) the upper limit for the energy of the recoil atoms is unaffected,
2) the true energy distribution of the recoil atoms should be represented by a curve which, in Fig. 3b, would lie everywhere above the measured points.

In comparison with the correction which has been discussed, other possible sources of error are of minor importance. Among these, the influence of the gas in the apparatus should primarily be considered. As mentioned above, during the collection of ^{88}Rb the pressure was 10^{-3} to 10^{-4} mm., measured with a McLeod gauge. The gases were probably formed by decomposition of the uranium hydroxide by neutrons and may thus be expected to have small molecular weights (hydrogen, oxygen, etc.), while no heavy molecules were present. In a determination of the density of the gas, it must be taken into account that the pressure was measured at room temperature while the pyrex tube with the main part of the apparatus was cooled in liquid air. As is well known, a difference in temperature between two communicating vessels is equivalent to a difference in the number of molecules per cc. in the ratio of the square root of the absolute temperature. A measurement of the temperature of the copper box by a thermojunction showed that the cooling of the copper box took place so slowly that in the experiments its temperature probably never has been below 0° C. This difference from the temperature of the McLeod gauge is so small that the influence on the density of the gas can be neglected.

The energy losses which occur when ions of the alkaline metals pass through gases have been studied by various observers. It has been generally found that inelastic collisions are rare; thus, only energy losses due to elastic collisions need to be considered. To determine the loss of energy in a collision between a recoil atom and a molecule of the gas, let M and V be the mass and the velocity of the recoil atom and m the mass of the

molecule, which is supposed to be at rest before the collision. The centre of gravity of the system moves with the velocity $\frac{M}{M+m} \cdot V$; relative to the centre of gravity the two molecules move with velocities $\frac{m}{M+m} \cdot V$ and $\frac{M}{M+m} \cdot V$. In Fig. 6, which represents the two molecules at the moment of impact, let these latter quantities be given by AB and DE; after the impact, the velocities relative to the centre of gravity will be BC and EF. If A'B is the velocity of the centre of gravity, the velocity of M after the impact is A'C, or

$$\overline{A'C}^2 = V_1^2 = \left[\frac{M^2+m^2}{(M+m)^2} - \frac{2\,Mm}{(M+m)^2}\cos 2\varphi\right] \cdot V^2.$$

The probability that φ is within limits $d\varphi$ is proportional to $\sin 2\varphi\, d\varphi$, and the mean value of V_1^2 is

$$V_1^2 = \frac{\int V_1^2 \sin 2\varphi\, d\varphi}{\int \sin 2\varphi\, d\varphi} = \frac{M^2+m^2}{(M+m)^2} \cdot V^2.$$

Finally, the mean value for the loss of energy is

$$\frac{1}{2} M (V^2 - V_1^2) = \frac{1}{2} MV^2 \cdot \frac{2\,Mm}{(M+m)^2}$$

or half that occurring in a head-on collision. For a rubidium ion colliding with a molecule of oxygen the mean loss of energy is thus 26 %.

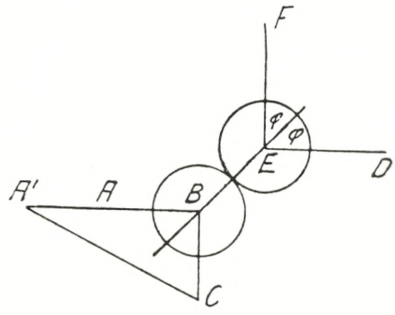

Fig. 6.

The evidence as regards the number of collisions suffered by alkaline ions during their passage through gases is somewhat conflicting. SCHMIDT (17) has determined the mean free path for K^+ ions with energies 25 and 200 volts in a large number of gases. For the gases which come into consideration here, SCHMIDT found values for the mean free path ranging from 8 cm. to 24 cm. referred to a pressure of 10^{-3} mm. In similar experiments,

DURBIN (18) found values which generally were about twice as large. If x is the mean distance traversed by a recoil atom in the apparatus, and λ is the mean free path, the probability that a recoil atom will traverse the distance x without collision is $e^{-\frac{x}{\lambda}}$. With $x = 2$ cm., which roughly is the mean distance traversed by a recoil atom before it collides with a wall, and $\lambda \sim 20$ cm., this is about 0.9, *i. e.* 10 % of the recoil atoms would lose energy due to the residual gas in the apparatus. Considering the somewhat discordant evidence concerning the value of the mean free path, and since the chemical composition of the gaseous mixture in question is practically unknown, the figures found for the energy loss can only be taken as a rough approximation. The effect of an energy loss of this order of magnitude would be to shift slightly downwards the curve in Fig. 3b; this effect, however, would probably be only just detectable. The result of these considerations is in good agreement with the experience gained from our experiments. Measurements with the same retarding potential and with pressures ranging between 10^{-3} and 10^{-4} mm. actually gave always the same results.

A further effect to be considered is the collision of the recoil atoms with the metal walls of the apparatus. Up to now it has been assumed that the rubidium atoms always remain attached to the wall after the first impact. If this was not the case, the atoms which leave the wall would probably be neutral and thus would give rise to a more or less uniform distribution of ^{88}Rb over the walls. Such an effect, if present, might change the observed energy distribution of the recoil atoms, especially near the upper limit of energy.

In the experiments, it was found that the activity of the foils continued to decrease with increasing retarding potentials up to 900 volts, the activities of the two foils being equal. This shows clearly that the contribution due to neutral recoil atoms is insignificant.

It should further be mentioned here that a very similar result was obtained by COMPTON and his co-workers (13) for the accomodation coefficient of ions. From purely classical conceptions, COMPTON concluded that, if an ion with mass M collides with a wall built up from atoms with masses m, the ion will always

remain attached to the wall, if $M > m$. In COMPTON's experiments, the ions had energies of the order of 100 volts and, accordingly, his results should apply directly to the present case. It is somewhat uncertain how low the energy of the ion can be before the forces between the atoms of the wall come into play. Recoil atoms with an energy of the order of 1 Volt may probably be present, in which case the accomodation coefficient may be below 1. However this may be, the fact that the activities of the collecting foils continued to decrease with increasing retarding potential shows definitely that the number of neutral recoil atoms must have been small.

In obtaining the energy distribution in Fig. 3b as the difference between the activities of the two collecting foils, it was supposed that the space inside the copper box was field-free. In order to test this assumption more closely, a model of the apparatus was made in 6-fold enlargement and the field inside the box was mapped out by a small flame connected to an electrometer. Inside the wire gauze, in front of one of the openings, the potential was about 2 % of the potential of the collecting electrode, and decreased nearly linearly with the distance from the gauze. This means that the potential difference between the collecting foil and the interior of the box is slightly smaller than that between the foil and the wire gauze or, in other words, that the observed energy limit of the recoil atoms is somewhat too high. The correction is, however, so small that it hardly needs consider ation.

β- and γ-rays from ^{88}Kr.

The upper limit of energy for the β-particles from ^{88}Kr has been determined by WEIL (19) to 2.3 MeV. by an expansion chamber in a magnetic field. The β-spectrum was found as the difference between the spectrum obtained from ^{88}Kr in equilibrium with ^{88}Rb and that obtained from ^{88}Rb alone. In his note, WEIL does not state how he has eliminated the β-particles from ^{87}Kr (T = 75 min.), which probably have been present, and the β-particles from ^{85}Kr (T = 4.6 hours) which certainly have been present in his experiments. To remove any doubt as to which of the krypton isotopes the upper limit of 2.3 MeV. belongs,

WEIL's determination was checked by absorption measurements. The result obtained for ^{88}Kr was 2.4 MeV. and is thus in good agreement with WEIL's value. Since the measurements, however, were complicated by the presence of both ^{85}Kr, ^{87}Kr and ^{88}Rb, the work will be considered in greater detail.

An approximate determination of the relative amounts of ^{85}Kr, ^{87}Kr and ^{88}Kr present in the gaseous mixture from uranium can be obtained from FLAMMERSFELD's (20) results for the amounts of different mass numbers formed in the fission process, on the supposition that the total amount of the mass numbers 85, 87 and 88 formed during the fission process has been transformed into isotopes of krypton at the time when the measurements were made. This must be approximately the case, since all the isobars with nuclear charges smaller than 36 have short periods. With this assumption, FLAMMERSFELD's figures give for the relative activities of ^{85}Kr, ^{87}Kr and ^{88}Kr after a short irradiation the ratio 0.39 : 1.9 : 1.0. If the gaseous mixture is left for 15 hours, the ratio is changed into $1{,}9 : 2{,}0 \cdot 10^{-2} : 1{,}0$, so that now the mixture contains mainly ^{85}Kr and ^{88}Kr. As ^{85}Kr has an upper energy limit of 0.8 MeV., its β-particles can be absorbed completely by 0.3 g./cm.^{2} of aluminium. The activity due to ^{88}Rb, the daughter substance from ^{88}Kr which has a very penetrating β-radiation, was determined by observations of the growth in activity of ^{88}Kr freed from Rb.

The arrangement used for the irradiation of the uranium was similar to that employed in the main experiment, except that the gases were removed from the uranium by a Toepler pump and stored over mercury in a glass crucible. A U-tube in the pump line was cooled by solid CO_2 to remove water vapour. The gases were pumped off immediately after the irradiation and left in the glass crucible for 15 hours. Subsequently, the gases were transferred to a cylindrical brass cell with a thin aluminium window, which was placed below a counter. A cotton plug in the connecting tube served to retain any rubidium which might be carried along together with the gas. With an aluminium absorber of suitable thickness ($>$ 0.3 g./cm.^{2}) placed above the cell, the rise in activity due to the formation of ^{88}Rb was followed, the measurements being continued for about 1 hour. From this rise, the activity at the moment when the gas was let into the

cell could be determined. The thickness of the absorber being more than 0.3 g./cm.^{2}, this initial activity was due to ^{88}Kr alone. The measurements were performed with a number of different absorbers, different experiments being compared by measuring the activity of ^{88}Kr + ^{88}Rb in equilibrium through a standard absorber.

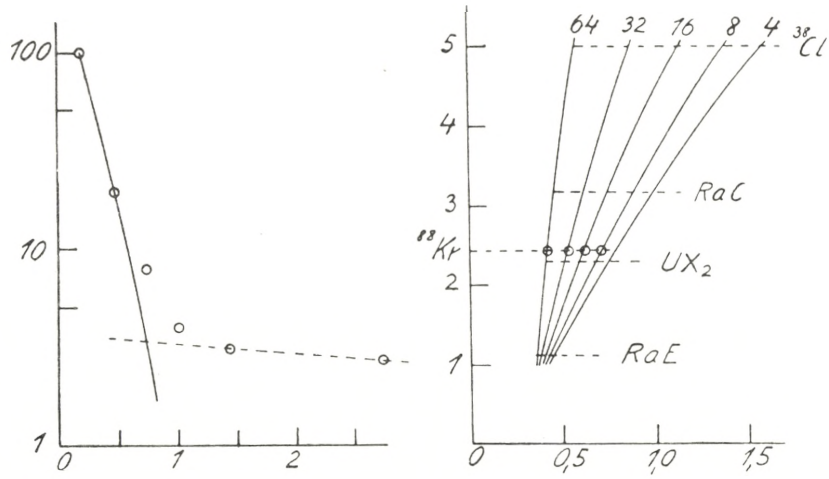

Fig. 7 a. Fig. 7 b.

Abscissa: thickness of absorber in g Al per cm^2. Ordinate: Fig. 7a number of β-particles from ^{88}Kr, Fig. 7b upper limit of energy in MeV.

The results are shown in Fig. 7 a, where the activity of ^{88}Kr measured through an aluminium absorber, thickness 0.3 g./cm.^{2}, has been put equal to 100. The absorption curve for the β-particles (full curve) was obtained by subtracting the γ-ray activity (dotted line) from the measured activities. The measurements show that the range of the β-particles in aluminium is about 1.1 g./cm.^{2}, but the existence of a γ-radiation makes an exact determination of the range difficult. Therefore, an attempt was made to obtain the range by means of an interpolation method.

For this purpose, absorption curves for the β-particles from ^{38}Cl, RaC, UX_2, and RaE were measured, using the same arrangement as with ^{88}Kr. The activity measured through an aluminium absorber, thickness 0.3 g./cm.^{2}, was taken as unity. In Fig. 7 b the curves marked 64, 32, etc. were obtained by deter-

mining for each element mentioned the thickness of absorber which gave an activity of 0.64, 0.32, etc. The points for ^{88}Kr were found in the same way from the absorption curve in Fig. 7 a. These points lie on a horizontal line, giving for the upper limit of energy the value of 2.43 MeV. It is doubtful, however, whether the result is as accurate as might appear from the number of figures which can be read from the curves. Although the method consists in an interpolation between absorption curves for elements for which the upper limit of energy has been fairly well determined, the difference in shape of the β-spectra due to the emission of γ-rays might probably affect the result. On the other hand, the smoothness of the curves in Fig. 7 b indicates that the complexity of the β-spectra cannot be of great influence, probably because the absorbers used transmit only the high-energy part of the β-spectra, for which the shape remains almost unaffected by the presence of a γ-radiation. For the later discussion, the upper limit of energy will be taken as 2.4 MeV; the agreement with WEIL's result is satisfactory.

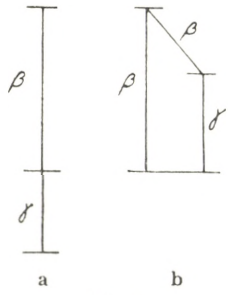

Fig. 8.

An investigation of the γ-rays from ^{88}Kr is complicated by the presence of ^{87}Kr and ^{88}Rb which both emit γ-rays. As already shown in connection with the measurements of the β-spectrum, the influence of ^{87}Kr could be sufficiently eliminated by performing the measurements on sources which had been left for about 15 hours after the irradiation. The relative amount of ^{85}Kr actually increases at the same time, but fortunately, this element does not emit any or at least only a weak γ-radiation.

The main problem to be considered in relation to the energy of the recoil atoms is whether the emission of a β-particle with energy 2.4 MeV. leads to the ground state of ^{88}Rb, in which case the level scheme might be represented as in Fig. 8 b or, if it is followed by a γ-radiation, as in Fig. 8 a. A distinction between these possibilities can be obtained by a determination of the number of β-γ-coincidences. If the β-spectrum is simple (level scheme Fig. 8 a), the number of coincidences per β-particle is independent of the energy of the β-particle and will thus remain constant when absorbers are placed in the path of the β-particle

while, for a complex β-spectrum, the number of β-γ-coincidences under the same circumstances will decrease.

In the measurements on γ-rays, the cell which had been used for the absorption measurements was placed between two counters. One of the counters recorded the β-particles, the other the γ-radiation. The β-counter was provided with a thin mica window, the γ-counter was screened by 2 mm. of lead; aluminium absorbers could be placed between the cell and the β-counter.

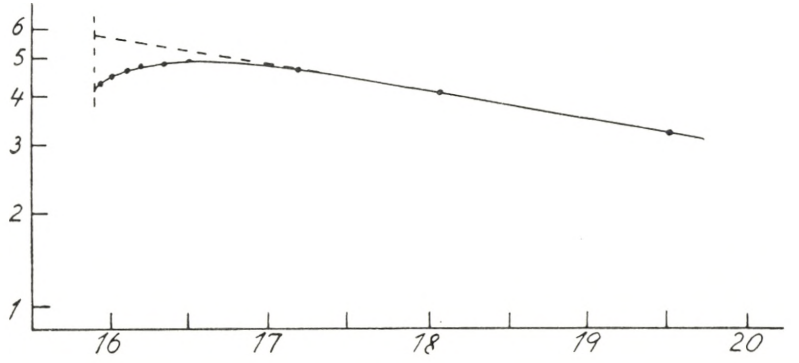

Fig. 9.

Abscissa: time in hours after irradiation. Ordinate: number of β-particles from $^{85}Kr + {}^{88}Kr + {}^{88}Rb$.

The counters were connected to a Rossi stage to record β-γ-coincidences.

As in the experiments described previously, the number of β-particles increased for about an hour due to the formation of ^{88}Rb, and then decreased (Fig. 9). In the present case, the rise in β-activity was relatively small since, at the beginning of the experiment, the β-activity was due both to ^{88}Kr and ^{85}Kr. The γ-activity remains nearly constant for about 30 minutes, then decreasing with a period of 2.7 hours. From the particular shape of the decay curve, the relative intensities of the γ-rays from ^{88}Kr and ^{88}Rb can be determined approximately. This, however, is of minor interest for the present problem, since the number of β-particles and β-γ-coincidences due to ^{88}Rb alone can be determined directly. The amount of ^{88}Rb present was determined as the difference between the number of counts obtained by extrapolating the decay curve for the gaseous mixture in equilibrium

with ^{88}Rb backwards to the moment when the mixture was let into the cell, and the number of counts from the gas alone (Fig. 9).

The counting of β-γ-coincidences was commenced when the gas was let into the cell and was continued for about 4 hours. It was to be expected that, due to the γ-rays from ^{88}Rb, an increase in the number of coincidences would occur together with the growth of ^{88}Rb. A quantitative determination of the increase was, however, difficult in view of the small number of coincidences which could be obtained with the sources available. The number of coincidences from ^{88}Rb alone was determined in a separate experiment, in which the same cell as had been used in the main experiment was activated with ^{88}Rb, the gaseous mixture being removed before the measurements were made. Some uncertainty still remains concerning the correction for the presence of ^{88}Rb, since indications were found that the location of ^{88}Rb on the inner wall of the cell was not the same in different experiments.

Table 2, which refers to the same experiment as Fig. 9, gives the number of counts per minute obtained with a source of ^{85}Kr + ^{88}Kr + ^{88}Rb in equilibrium and the correction in the number of β-γ-coincidences due to ^{88}Rb. The amount of ^{88}Rb (1400 counts per minute, without absorber) was found from the decay curve in Fig. 9.

Table 2.

Absorber	^{85}Kr + ^{88}Kr + ^{88}Rb			^{88}Rb	Difference
	β	γ	β-γ-coinc.	β-γ-coinc.	
0 g./cm² Al.....	5600	32	1.4 ± 0.2	0.33 ± 0.1	1.1
100 —	2380	32	0.41 ± 0.06	0.22 ± 0.06	0.2
200 —	1450	32	0.05 ± 0.05	0.09 ± 0.05	~0

The figures in the last column of Table 2 show that the number of β-γ-coincidences decreases rapidly with increasing absorber thickness and has practically disappeared with an absorber of 0.2 g./cm.². The reduction in the number of β-particles from ^{88}Kr due to this absorber is unknown, since the absorption could only be determined for absorbers with thicknesses greater

than 0.3 g./cm.²Al. If, however, the β-spectrum of ^{88}Kr was elementary (level scheme of the type in Fig. 8a), about 40 per cent of the β-particles would be transmitted through an absorber of 0.2 g./cm.². This is quite incompatible with the observed decrease in the number of coincidences. It may thus be concluded that the transformation, in which a β-particle with energy 2.4 MeV. is emitted, leads to the ground state of ^{88}Rb.

This result is supported by more indirect evidence. Actually, a transformation energy of 2.4 MeV. for ^{88}Kr, which has an even number of protons and an even number of neutrons, is surprisingly high. From the formulae given by BOHR and WHEELER (18) for the energy content in nuclei a value of about 1.5 MeV. ensues, depending somewhat on the choice of the constants. Hence, the conclusion is obtained that the emission of γ-rays from ^{88}Kr does not change the upper limit of energy of the recoil atoms; the energy distribution is, however, changed in the direction of an increasing number of recoil atoms with small energies due to the complexity of the β-spectrum. This evidence cannot be traced further, since the details of the level scheme in Fig. 8 have not been determined. A detailed knowledge of the level scheme would, however, not be of much interest so long as the correction for the change in energy distribution due to the passage of the recoil atoms in oblique directions through the retarding field cannot be evaluated quantitatively.

Discussion.

If a β-particle with kinetic energy E_β is emitted from a nucleus with mass M, the recoil energy X is determined from

$$X_\beta \cdot 2\,Mc^2 = E_\beta^2 + E_\beta \cdot 2\,mc^2,$$

or, with M = 88,

$$X_\beta = 6.10\ E_\beta^2 + 6.24\,E_{\beta_1} \quad \ldots\ldots \qquad (1)$$

where X_β is expressed in eV, and E_β in MeV. For a neutrino with zero rest mass and kinetic energy E_ν, the recoil energy is

$$X_\nu = 6.10 \cdot E_\nu^{\,2} \quad \ldots\ldots \qquad (2)$$

in the same units as in (1). For $E_\beta = 2.4$ MeV., (1) gives $X_\beta = 50$ eV. in close agreement with the measured value. This shows that, if a neutrino is emitted together with a β-particle of maximum energy, the kinetic energy of the neutrino must be small, or that, apart from the rest mass of the electron and the neutrino, the energy release in a β-transformation is determined by the upper limit of energy of the β-spectrum.

This has usually been assumed. The experimental evidence, however, which has mainly been derived from the branch products of the radioactive series, is rather conflicting, especially in regard of the energy emitted in the form of γ-rays (25), (26).

In view of the estimated errors in the measurements of the recoil energy and of the upper limit of energy of the β-spectrum, the largest possible difference between the measured value of X_β and that obtained from (1) may be fixed at $\Delta X = 2$ eV.; this value sets a limit to the energy of a neutrino emitted together with a β-particle with the maximum energy. If p, p_β, and p_ν are the momenta of the recoil atom, the β-particle, and the neutrino, respectively, then $p = p_\beta + p_\nu$, if the electron and the neutrino are emitted in the same direction. This point, however, will be discussed later. Since $p^2 = 2MX$, we have

$$2\,Mc^2X = \left[\sqrt{E_\beta^2 + 2\,mc^2\,E_\beta} + E_\nu\right]^2, \text{ or approximately}$$

$$X = 6\,(E_\beta + E_\beta^2) + 6\,E_\nu^2 + 12\,E_\nu\sqrt{E_\beta + E_\beta^2}$$

with the same units as in (1), and finally

$$\Delta X = 6\,E_\nu^2 + 12\,E_\nu\sqrt{E_\beta + E_\beta^2} \sim 6\,E_\nu^2 + 34\,E_\nu.$$

For $\Delta X = 2$ eV., this gives $E_\nu \sim 0.06$ MeV.

The agreement between the measured and the calculated values of the recoil energy actually is much better than assumed here. The value for X_β found from (1), corresponding to $E_\beta = 2.43$ MeV., is 51.2 eV., while the measured value is 51.5 eV. In view of the errors to be expected, it appears appropriate to consider such a close agreement fortuitous.

The evidence for or against the emission of a neutrino must be obtained from the energy distribution of the recoil atoms. If

no neutrino is emitted, the energy distribution of the recoil atoms is simply obtained from the β-spectrum. The Fermi distribution is given by

$$W(p)dp = \text{const. } p^2 \left[\sqrt{m^2c^2 + p_m^2} - \sqrt{m^2c^2 + p^2}\right]^2 dp, \quad (3)$$

where $W(p)dp$ is the number of β-particles with momentum between limits dp, and p_m is the upper limit of p. With the kinetic energy E_β as independent variable, the expression changes into

$$W(E_\beta)\,dE_\beta = \text{const.} \cdot (E_\beta + mc^2)(E_{\beta m} - E_\beta)^2 \sqrt{E_\beta^2 + 2mc^2 E_\beta}\, dE_\beta, \quad (4)$$

where $E_{\beta m}$ is the upper limit of E_β. If momentum is conserved during the emission of the β-particle, and no neutrino is emitted, we have $p^2 = 2MX$, and the energy distribution of the recoil atoms is given by

$$W(X_\beta)\,dx_\beta = \text{const.} \sqrt{X_\beta}\left[\sqrt{m^2c^2 + 2MX_{\beta m}} - \sqrt{m^2c^2 + 2MX_\beta}\right]^2 dX_\beta, \quad (5)$$

where $X_{\beta m}$ is the upper limit of X_β.

The constant is determined by the condition $\int W(X_\beta)\,dX_\beta = 1$. To compare the distribution given by (5) with the experimental results, a curve showing $W(X_\beta)$ as a function of X_β was constructed (Fig. 10). From this differential distribution the probability that a recoil atom has an energy greater than X_β or $\int W(X_\beta)\,dX_\beta$ was obtained by numerical integration. The result is shown in Fig. 11, curve III, where curve I is the experimentally determined energy distribution from Fig. 3b. As shown previously, the curve representing the true energy distribution, if it could be determined, would lie everywhere above the measured points. The result is thus clearly that the number of recoil atoms with energies near the upper limit is much larger than can be accounted for by recoil from the β-particles alone.

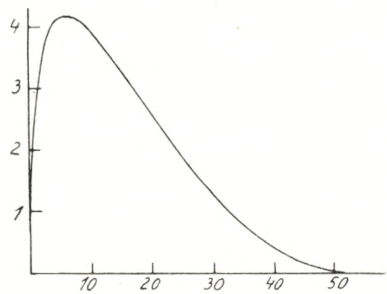

Fig. 10.
Abscissa: recoil energy X in eV.
Ordinate: number of recoil atoms with energy between limits dX.

It has here been assumed that the β-spectrum is simple. According to the level scheme in Fig. 8, the transformation energy can be emitted either in a single β-transformation or it can be divided between a β- and a γ-ray. In the latter case, no further experimental evidence is available at present, but the

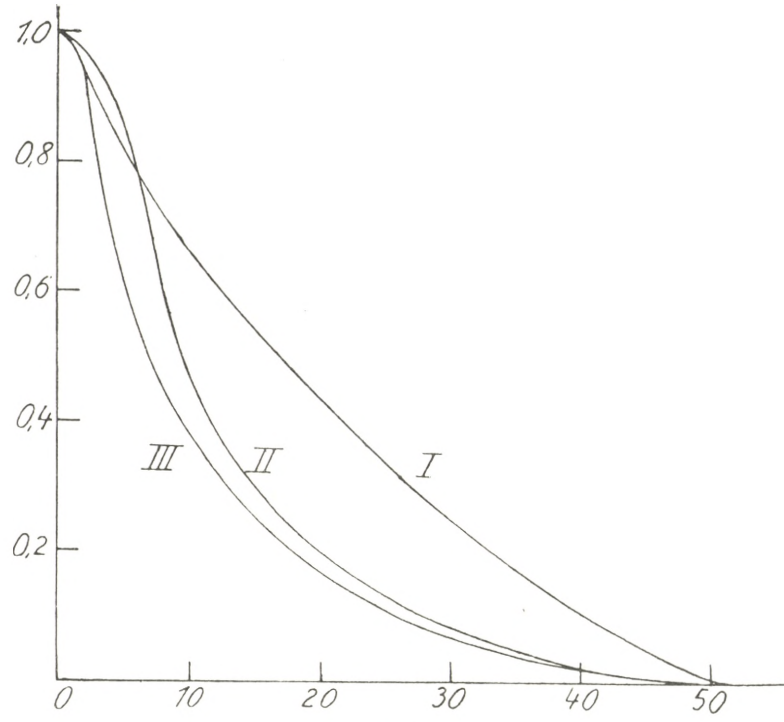

Fig. 11.
Abscissa: recoil energy X in eV. Ordinate: fraction of recoil atoms with energy greater than X.

only possibility which must be taken into account with respect to the recoil energy is that in which the γ-ray energy is emitted in a single quantum.

If p_β and p_γ denote the momenta due to the emission of the β- and the γ-ray separately, the total momentum is given by

$$p^2 = p_\beta^2 + p_\gamma^2 - 2\, p_\beta p_\gamma \cos\varphi,$$

where φ is the angle between the directions of p_β and p_γ, or

$$X = X_\beta + X_\gamma - 2\sqrt{X_\beta X_\gamma}\cos\varphi, \qquad (6)$$

where

$$p^2 = 2\,MX,\ p_\beta^2 = 2\,MX_\beta,\ p_\gamma^2 = 2\,MX_\gamma = \left(\frac{E_\gamma}{c}\right)^2.$$

Assuming for p_β the Fermi distribution, the probability that X_β is within the limits of dX_β is given by (5). If there is no correlation between the directions of p_β and p_γ, the number of recoil atoms for which φ is within limits $d\varphi$ is proportional to $\sin\varphi\,d\varphi$, so that the combined probability that X_β is within the limits dX_β and φ within the limits $d\varphi$ is given by

$$W(X_\beta, \varphi)\,dX_\beta d\varphi = \text{const.}\ W(X_\beta)\,dX_\beta \sin\varphi d\varphi.$$

Introducing here $\sin\varphi\,d\varphi = \dfrac{dX}{2\sqrt{X_\beta X_\gamma}}$ from (6), we obtain

$$W(X, X_\beta)\,dX dX_\beta = \text{const}\ W(X_\beta)\,dX_\beta \frac{dX}{\sqrt{X_\beta \cdot X_\gamma}}. \qquad (7)$$

When X is constant, X_β must be within the limits g_1 and g_2 determined from (5) by putting $\cos\varphi = \pm 1$,

$$g_1 = X + X_\gamma - 2\sqrt{XX_\gamma} \geqq 0$$

$$g_2 = X + X_\gamma + 2\sqrt{XX_\gamma} \leqq X_{m\beta}.$$

The energy distribution for the recoil atoms is now given by

$$W(X)\,dX = \text{const.} \cdot \int_{g_1}^{g_2} \frac{W(X_\beta)}{\sqrt{X_\beta \cdot X_\gamma}}\,dX_\beta \cdot dX \qquad (8)$$

together with the condition $\int_0^{X_m} W(X)\,dX = 1$, where

$X_m = X_{\beta m} + X_\gamma + 2\sqrt{X_{\beta m} \cdot X_\gamma}$ is the upper limit of X.

For a numerical test, some arbitrary assumption must be made regarding the way in which the energy is divided between the β-and the γ-radiation. The figures in Table 3 indicate that for various possible combinations of β- and γ-ray energy the upper limit of energy for the recoil atoms varies but slightly.

Table 3.

β	γ	X_m
0.4 MeV.	2.0 MeV.	46.3 eV.
1.0 —	1.4 —	48.5 —
2.0 —	0.4 —	51.1 —

The energy distribution for the case in which the β-energy is 1.0 MeV. has been calculated from (7) by the same procedure as that used previously. Primarily, a curve showing W(X) as a function of X was constructed; from this differential distribution the probability that a recoil atom has an energy greater than X was found by numerical integration. The result appears from Fig. 11, curve II. The difference between this curve and the distribution corresponding to a simple β-spectrum is small, especially as regards the number of recoil atoms with energy near the upper limit. A combination of the distribution in Fig. 11, II and Fig. 11, III in the (unknown) branching ratio of the level scheme (Fig. 8b) would again give very nearly the same result.

It has here been assumed that no correlation exists between the directions of p_β and p_γ. According to HAMILTON (22), however, a correlation occurs for light nuclei and high energies in the case of forbidden transitions. For the Fermi interaction, HAMILTON gives the angular distribution of the γ-ray as $W(\theta) = 1 - \frac{9}{13}\cos^2\theta$, or that the γ-ray is mainly emitted in a direction perpendicular to that of the β-particle. It is doubtful whether HAMILTON's result applies to the γ-rays from ^{88}Kr. If it does, the change in the energy distribution for the recoil atoms will be in the direction of a smaller number of recoil atoms with energies near the upper limit.

To sum up, we may now conclude that in the experimentally determined energy distribution the number of recoil atoms with energies near the upper limit is much larger than can be accounted for by the momentum due to the emission of β- and γ-rays.

When the emission of a neutrino is assumed, the calculated energy distribution of the recoil atoms is changed; to obtain a comparison with the experimental results, additional assumptions

must be made about the rest mass of the neutrino and about the angular distribution of the neutrino relative to the direction of the electron (22). For a qualitative discussion of the matter, the following possibilities for the angular distribution may be considered:

1) The electron and the neutrino always emitted in the same direction.

2) The angular distribution $1 + \frac{v}{c} \cos \varphi$.

3) The angular distribution $1 - \frac{v}{c} \cos \varphi$.

4) The electron and the neutrino always emitted in opposite directions.

In 2) and 3), v is the velocity of the β-particle and φ the angle between the β-particle and the neutrino. The rest mass of the neutrino will be assumed to be equal to zero. Although a rest mass different from zero might probably come into consideration, the accuracy of the experimental results is hardly sufficient to justify such a detailed discussion, especially because the recoil energy is mainly determined by the energy distribution just mentioned. As an example, the energy distribution will now be calculated with the angular distribution $1 + \frac{v}{c} \cos \varphi$.

If p_β and p_ν are the momenta due to the emission of the β-particle and the neutrino separately, then

$$p^2 = p_\beta^2 + p_\nu^2 + 2\, p_\beta\, p_\nu \cos \varphi, \quad \text{or}$$

$$2\, Mc^2 \cdot X = E_\beta^2 + 2\, mc^2\, E_\beta + E_\nu^2 + 2\, E_\nu \sqrt{E_\beta^2 + 2\, mc^2}\, E_\beta \cos \varphi,$$

where E_β is the energy of the β-particle and E_ν that of the neutrino. Putting $E_\nu = E_m - E_\beta$, we get

$$\left.\begin{aligned} X = \frac{1}{2\, Mc^2} \Big(& E_\beta^2 + 2\, E_\beta\, mc^2 + (E_m - E_\beta)^2 + 2\,(E_m - E_\beta) \\ & \sqrt{E_\beta^2 + 2\, E_\beta\, mc^2} \cos \varphi \Big) = A\,(E_\beta) + B\,(E_\beta) \cos \varphi. \end{aligned}\right\} \quad (9)$$

For a fixed value of E_β, the number of recoil atoms for which φ is within the limits of $d\varphi$ is proportional to

$$W(\varphi)\,d\varphi = \sin\varphi\left(1+\frac{v}{c}\cos\varphi\right)d\varphi = \sin\varphi\,\frac{\sqrt{E_\beta^2+2E_\beta mc^2}}{E_\beta+mc^2}\cos\varphi\,d\varphi;$$

the combined probability that E_β is within limits dE_β and φ within limits $d\varphi$ is

$$W(E_\beta)\,dE_\beta \cdot W(\varphi)\,d\varphi,$$

where $W(E_\beta)$ is given by (4). Introducing here $\cos\varphi = \frac{X-A}{B}$ and $dX = -B\sin\varphi\,d\varphi$, the expression can be transformed into

$$W(E_\beta, X)\,dE_\beta\,dX = \text{const}\cdot[(E_{\beta m}-E_\beta)(E_\beta+mc^2)+Mc^2X$$

$$-\frac{1}{2}(E_\beta^2+2E_\beta mc^2+(E_{\beta m}-E)_\beta^2)]\,dE_\beta\,dX,$$

where $W(E_\beta\ X)\,dE_\beta\,dX$ is the number of recoil atoms with energies between limits dX originating from the emission of β-particles with energies between limits dE_β. The total number of recoil atoms with energies within limits dX is now obtained by integrating over the region of $\mathfrak{E}_\beta$, which contributes to the recoil energy X, ór

$$W(X)\,dX = \text{const}\cdot\int_{g_1}^{g_2} W(E,X)\,dX\,x\,d\,E,$$

where g_1 and g_2 are determined from (9) as the values of E_β corresponding to $\cos\varphi = \pm 1$.

Fig. 12 shows W(X) as a function of X. By a numerical integration of this differential distribution, the probability that a recoil atom has an energy greater than X was found. The result is shown in Fig. 13, curve III, where curve I is the experimentally determined distribution. It is apparent that agreement is obtained with the experimental results insofar as the calculated curve is now above the measured points. The same result would of course be obtained if it was assumed that the neutrino is always emitted in the same direction as

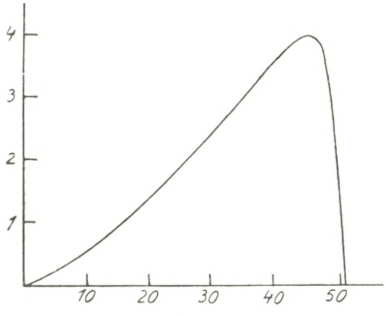

Fig. 12.
Abscissa: recoil energy X in eV.
Ordinate: number of recoil atoms with energy between limits dX.

the β-particle since, in the latter case, the number of recoil atoms with energies near the upper limit would be still larger.

A similar calculation made under the assumption that the angular distribution is $1 - \frac{v}{c}\cos\varphi$ gives the result in Fig. 13,

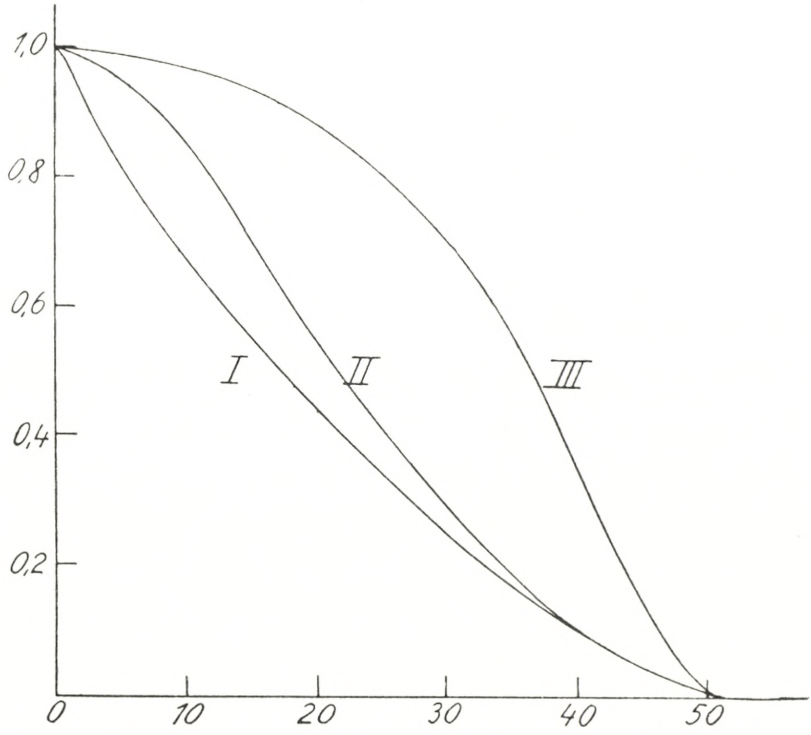

Fig. 13.

Abscissa: recoil energy X in eV. Ordinate: fraction of recoil atoms with energy greater than X.

curve II. It is seen that the energy distribution of the recoil atoms is shifted in favour of smaller energies and that, for energies near the upper limit, the calculated curve now is slightly below the measured points.

To account in a qualitative way for the experimental results, it seems thus necessary to assume that the neutrino is emitted mainly in the same direction as the β-particle. A further comparison, aiming at the distinction between the angular distributions

quoted as (1) and (2), would claim a higher accuracy of the experimental results than has been obtained here. For an improvement of the experimental results it would primarily be necessary to correct for the shift in the energy distribution due to the passage of the recoil atoms in oblique directions through the retarding field, *i. e.* to obtain an exact determination of the curve in Fig. 5, II. This correction which is inherent in the use of a gas as a radioactive source, can be evaluated if the apparatus is changed in such a way as to eliminate irregularities of the retarding field. A further complication is that caused by the emission of γ-rays; here serious difficulties in obtaining quantitative results are to be expected. In fact, a complete level scheme has hardly been established for any γ-ray transition and, in the present case, the matter is further complicated by the circumstance that ^{88}Rb cannot be obtained free from other radioactive elements.

As mentioned previously, a few experiments have been made with ^{89}Kr, the procedure being the same as with ^{88}Kr, except for the changes which were made necessary by the difference in period. The upper limit of energy for the β-particles was found to be 4.5 MeV., using the same method as for ^{88}Kr. The determinations of the recoil energy are as yet incomplete; the results show that the upper limit of energy is considerably higher than for ^{88}Kr.

After the completion of the work, a paper by J. S. Allen (24) came into our possession. This author has worked on ^{7}Be which by a special evaporation process was deposited in a very thin layer on platinum. Allen was able to observe recoil atoms with an energy of about 40 eV. and he attributed these atoms to the emission of neutrinos in the transformation

$$\begin{cases} {}^{7}\mathrm{Be} + e_k \rightarrow {}^{7}\mathrm{Li} + \nu + 0.85 \text{ MeV.} \\ \text{or} \\ \begin{cases} {}^{7}\mathrm{Be} + e_k \rightarrow ({}^{7}\mathrm{Li})^{x} + \nu + 0.40 \text{ MeV.} \\ ({}^{7}\mathrm{Li})^{x} \rightarrow {}^{7}\mathrm{Li} + \gamma + 0.45 \text{ MeV.} \end{cases} \end{cases}$$

Allen's method is more direct than that used in the present work, since no β-particles are emitted from ^{7}Be, but at the same time the difficulties caused by surface effects are obvious. If the value of 0.85 MeV. for the energy difference between ^{7}Be and ^{7}Li is accepted as correct, an unexplained discrepancy of about 25 % remains between the calculated and the observed recoil

energies. In the interpretation of ALLEN's results, an uncertainty which, however, may not be serious is caused by the emission of γ-rays from ^{7}Li. An attempt was made to demonstrate the emission of γ-recoil atoms by a coincidence method; it failed, however, which is somewhat surprising, since about one-tenth of the total number of disintegrations should be accompanied by the emission of γ-rays.

The experiments were performed at the Institute of Theoretical Physics, Copenhagen. Our thanks are due professor NIELS BOHR for the facilities kindly placed at our disposal, Mr. N. O. LASSEN for his help in the work with the cyclotron, and Mr. B. MADSEN for the construction of the counters.

Summary.

The upper limit of energy for the recoil atoms from ^{88}Kr has been determined to 51.5 ± 2 eV. in close agreement with the value to be expected from the upper limit of energy of 2.4 MeV. for the β-particles. From the energy distribution of the recoil atoms it is concluded that a neutrino is emitted and that the neutrino probably is emitted mainly in the same direction as the β-particle.

Institute of Theoretical Physics.
University. Copenhagen.

References.

1. Chadwick, Verh. d. D. Phys. Ges. **16**, 383, 1914.
2. Gurney, Proc. Roy. Soc. **109**, 540, 1925.
3. Ellis and Wooster, Proc. Roy. Soc. **117**, 109, 1927.
4. Meitner and Orthmann, Zs. f. Phys. **60**, 143, 1930.
5. Fermi, Zs. f. Phys. **88**, 161, 1934.
6. Chadwick and Lea, Proc. Cam. Phil. Soc. **30**, 59, 1934.
7. Nahmias, Proc. Cam. Phil. Soc. **31**, 99, 1935.
8. Donat and Philipp, Zs. f. Phys. **45**, 512. 1927.
9. Leipunski, Proc. Cam. Phil. Soc. **32**, 301, 1936.
10. Crane and Halpern, Phys. Rev. **56**, 232, 1939. Cf. also Wertenstein Phys. Rev. **54**, 306, 1938.
11. Alvarez, Helmholtz and Wright, Phys. Rev. **60**, 160, 1941.
12. Born and Seelmann Eggebert, Naturwiss. **31**, 86, 1943.
13. Born and Seelmann Eggebert, Naturwiss. **31**, 201, 1943.
14. Seelmann Eggebert, Naturwiss. **31**, 491, 1943.
15. Glasoe and Steigman, Phys. Rev. **58**, 1, 1940.
16. Comptom and Lamar, Phys. Rev. **44**, 339, 1933.
17. Schmidt, Ann. d. Phys. **21**, 241, 1934.
18. Durbin, Phys. Rev. **30**, 844, 1927. Cf. also Handb. d. Phys., vol. 22_2, p. 296.
19. Weil, Phys. Rev. **60**, 167, 1941.
20. Flammersfeld, Jensen and Gentner, Zs. f. Phys. **120**, 450, 1943.
21. Bohr and Wheeler, Phys. Rev. **56**, 426, 1939.
22. Hamilton, Phys. Rev. **60**, 168, 1941.
23. Bloch and Møller, Nature **136**, 911, 1935.
24. Allen, Phys. Rev. **61**, 293. 1942.
25. Mattauch and Flügge, Kernphysikalische Tabellen, p. 74.
26. Rutherford, Chadwick and Ellis, Radiations from radioactive Substances, p. 501.

Indleveret til Selskabet den 24. Juli 1945.
Færdig fra Trykkeriet den 21. September 1945.

DET KGL. DANSKE VIDENSKABERNES SELSKAB
MATEMATISK-FYSISKE MEDDELELSER, BIND XXIII, NR. 13

DEDICATED TO PROFESSOR NIELS BOHR ON THE OCCASION OF HIS 60TH BIRTHDAY

NON-CENTRAL COUPLING IN THE MIXED MESON THEORY OF NUCLEAR FORCES

BY

L. ROSENFELD

KØBENHAVN
I KOMMISSION HOS EJNAR MUNKSGAARD
1945

REPRINTED BY
TUTEIN & KOCH
1949
Printed in Denmark
Bianco Lunos Bogtrykkeri A/S

The discovery by RABI and his collaborators [1] of the electric quadrupole moment of the deuteron has brought to light the existence in the law of interaction between a pair of nucleons of a term of non-central coupling, as a result of which the ground state of the deuteron is not a pure ^3S state, but contains also a D component. In fact, if the interaction is assumed to be independent of the charges (proton or neutron states) of the nucleons, it follows from general considerations of invariance of the interaction operator with respect to linear transformations of space [2] that for the two body system the only type of non-central coupling to be taken into consideration involves a spin dependence of the "axial dipole" form*

$$D^{(12)} \equiv \left(\vec{\sigma}^{(1)}\vec{x}_0\right)\left(\vec{\sigma}^{(2)}\vec{x}_0\right) - \frac{1}{3}\left(\vec{\sigma}^{(1)}\vec{\sigma}^{(2)}\right) \tag{1}$$

* The following notations are used: To the i'th nucleon of the system considered correspond space coordinates $\vec{x}^{(i)}$ with conjugate momenta (multiplied by c) $\vec{p}^{(i)}$, spin coordinates $\vec{\sigma}^{(i)}$, isotopic coordinates $\boldsymbol{\tau}^{(i)}$, and coordinates discriminating the "large" and "small" components of the wave-functions $\varphi_l^{(i)}$ $(l = 1, 2, 3)$. The $\vec{\sigma}^{(i)}$, $\varphi_l^{(i)}$ are taken in the usual Dirac representation (except for the sign of the φ's). Relative space coordinates and momenta of the pair $(i\ k)$ will be defined as

$$\vec{x}^{(ik)} = \vec{x}^{(i)} - \vec{x}^{(k)}, \qquad \vec{p}^{(ik)} = \frac{1}{2}\left(\vec{p}^{(i)} - \vec{p}^{(k)}\right);$$

further

$$\left|\vec{x}^{(ik)}\right| = r^{(ik)}, \qquad \vec{x}_0^{(ik)} = \vec{x}^{(ik)}/r^{(ik)};$$

if there is only one pair, the index $^{(12)}$ will be dropped. Summations over i, k must always be understood to exclude $i = k$.

The meson potential is represented by

$$\varphi(r) = e^{-\kappa r}/4\pi r;$$

the quantity κ, which is a measure for the inverse of the range of the potential, is connected with the meson mass M_m by the relation

$$\kappa = M_m c/\hbar.$$

The mass of the nucleon (neglecting the difference between proton and neutron mass) is denoted by M.

which just provides the desired mixing of $^3S_1$ with $^3D_1$ states. As it is well known, several forms of meson field theories of nuclear forces include such a term of non-central interaction even in the approximation in which only static effects are retained. However, this non-central interaction is introduced through the operator

$$S^{(12)} = -\frac{1}{K^2}\left(\vec{\sigma}^{(1)}\mathrm{grad}^{(1)}\right)\left(\vec{\sigma}^{(2)}\mathrm{grad}^{(2)}\right)\varphi(r) \tag{2}$$

which can be decomposed into

$$\left.\begin{aligned} S^{(12)} &= \frac{1}{3}V_{\sigma}^{(12)} + V_{D}^{(12)} - \frac{1}{3}C_{\sigma}^{(12)} \\ V_{\sigma}^{(12)} &= \vec{\sigma}^{(1)}\vec{\sigma}^{(2)}\varphi(r) \\ V_{D}^{(12)} &= D^{(12)}F(r),\quad F(r) = \left(1 + \frac{3}{Kr} + \frac{3}{K^2r^2}\right)\varphi(r) \\ C_{\sigma}^{(12)} &= \frac{3}{4\pi K^2}\lim_{\vec{\xi}\to 0}\int \delta\left(\vec{x} - \vec{\xi}\right)\left(\vec{\sigma}^{(1)}\vec{\xi}_0\right)\left(\vec{\sigma}^{(2)}\vec{\xi}_0\right)d\Omega,\quad \left(\vec{\xi}_0 = \vec{\xi}/|\vec{\xi}|\right), \end{aligned}\right\} \tag{3}$$

i. e. it involves, besides a central spin-spin coupling $V_{\sigma}^{(12)}$ and an axial dipole coupling $V_{D}^{(12)}$, an additional term of "contact" interaction, the presence of which was first emphasized by BELINFANTE [3]. Even the distance dependence $F(r)$ of the axial dipole coupling, having a pole of the third order at the origin, would by itself cause the eigenvalue equation of the energy of the system to break down, and the same may be said of the still more singular contact interaction. A law of nuclear force of the form $S^{(12)}$ can therefore not lead, as it stands, to any well-defined result. It has been attempted [4] to avoid this inconvenience by arbitrarily "cutting off" the singularity, i. e. by replacing in $V_{D}^{(12)}$ the distance dependence $F(r)$ by some constant for distances smaller than a certain critical value r_0, and further ignoring the contact term $C_{\sigma}^{(12)}$. But, apart from its arbitrariness, such a procedure would not seem [5] to be consistent, because the non-static interactions arising from the precession of the spin and isotopic variables under the influence of the static forces should, on this theory, be expected to become of an order of magnitude comparable to that of the static forces themselves. Another way out of the difficulty has therefore been put forward [5]. It consists in

adopting a combination of two suitable types of meson fields, generated by the nucleons with such relative intensities that their respective contributions of the $S^{(12)}$ form to the static interaction just compensate each other. The mixing of states with different orbital momenta, revealed by the occurrence of the electric quadrupole moment of the deuteron, is then brought about by smaller coupling terms depending on the velocities of the nucleons.

The "mixed" meson theory contrasts with the "cut-off" theory also in another important respect, viz. as regards the assumed charges of the meson fields. As is well known, two possible choices of these charges are formally compatible with the charge-independence property of the nuclear forces: either are the meson fields neutral, or they enter into a definite, so-called symmetrical combination of both neutral and (positively and negatively) charged ones. Now, the cut-off theory yields the right sign and magnitude of the deuteron quadrupole moment only in its neutral form. This is certainly a very unsatisfactory feature of the cut-off theory, for it is hard to see by which physical arguments any neutral meson theory could be justified: since, namely, such a theory cannot have any point of contact with the evidence from cosmic ray mesons or β-radioactivity, the special distance dependence of the nuclear interaction to which it leads is nothing else than an arbitrarily assumed one, distinguished from any other only by its unhandiness. Worse still, a law of interaction independent of the isotopic variables of the nucleons, such as implied by a neutral meson theory, cannot be reconciled with the saturation properties of this interaction as exhibited in heavy nuclei. Indeed, if one assumes that the non-central forces give a large contribution to the total interaction (as is the case in the cut-off theory), it is doubtful [6] whether any saturation can at all be obtained. And, under the alternative assumption that the main part of the interaction can be represented by a central, charge-independent potential, one finds that the saturation requirements fix the dependence of this potential on the isotopic variables to a factor of the form $A + B\boldsymbol{\tau}^{(1)}\boldsymbol{\tau}^{(2)}$, with $A \ll B$: to a sufficient approximation, therefore, these requirements are fulfilled just by a symmetrical theory, characterized by a dependence on the $\boldsymbol{\tau}$'s of the type

$$T^{(12)} \equiv \tau^{(1)}\tau^{(2)}. \tag{4}$$

For these reasons, the symmetrical form of the mixed theory has been adopted and only this form, which involves a combination of pseudoscalar and vector meson fields, has so far been discussed, although a neutral type of mixed theory can formally be just as well set up by means of the dual combination of fields (scalar and pseudovector).

It could be shown, then, that the above-mentioned velocity-dependent coupling of the symmetrical mixed theory was able to yield the right sign and order of magnitude of the deuteron quadrupole moment, provided that the parameters expressing the intensities of the meson field sources were appropriately connected by simple relations [5, 7]. There subsisted, however, a flaw in this derivation, inasmuch as the same coupling apparently gave rise to a very large perturbation of the energy of the ground state. It was even contended by FERRETTI [8] that we would actually here have to do with an essential divergence of the theory. The main purpose of the present note is to show how a closer analysis of the velocity-dependent coupling leads to a simple solution of the difficulty just mentioned, at the same time clearing up the physical meaning, hitherto rather obscure, of the coupling in question: in the two-nucleon case, this coupling effectively reduces to just an axial dipole interaction, in agreement with expectation on general invariance grounds.

The symmetrical mixed theory is, however, confronted with a much more serious difficulty in connexion with the recent Italian experiments [9] on the angular distribution of fast neutrons (of about 12–14 MeV energy) scattered by protons. The considerable asymmetry found in this angular distribution is namely in complete disagreement, as regards sign as well as absolute value, with the predictions of the symmetrical theory [10]. On the other hand, it has been pointed out that the asymmetry would agree in sign—and roughly, in order of magnitude—with the value deduced from the neutral cut-off theory [10]. In view of the serious objections against the latter theory, enumerated above, it would be rash to attribute much weight to this coincidence; it rather seems that, if the results of the Italian experiments are confirmed on further investigation, a

much more radical departure from current theories of nuclear interaction would be required than a mere adoption of some form of neutral meson theory. Nevertheless, it might be of some interest, for the sake of information, to ascertain the kind of velocity-dependent coupling to which the mixed neutral meson theory gives rise: this discussion, carried out in the last section of the present paper, leads to the rather surprising result that in the two-nucleon case there is no velocity-dependent coupling between states of different orbital momenta. This form of meson theory is thus utterly unable to account for the deuteron quadrupole moment.

§ 1. Nuclear Forces on Symmetrical Mixed Theory.

The symmetrical mixed theory starts from the following expressions of the source densities of the meson fields in terms of the nucleon variables:

Vector field,

vector density
$$\begin{cases} \vec{M} = g_1 \vec{m}, & \vec{m} = \sum_i \tau^{(i)} \varrho_1^{(i)} \vec{\sigma}^{(i)} \delta\left(\vec{x} - \vec{x}^{(i)}\right) \\ N = g_1 n, & n = \sum_i \tau^{(i)} \delta\left(\vec{x} - \vec{x}^{(i)}\right) \end{cases}$$

tensor density*
$$\begin{cases} \vec{S} \approx \frac{g_2}{K} \vec{s}, & \vec{s} = \sum_i \tau^{(i)} \vec{\sigma}^{(i)} \delta\left(\vec{x} - \vec{x}^{(i)}\right) \\ \vec{T} = \frac{g_2}{K} \vec{t}, & \vec{t} = -\sum_i \tau^{(i)} \varrho_2^{(i)} \vec{\sigma}^{(i)} \delta\left(\vec{x} - \vec{x}^{(i)}\right). \end{cases}$$

Pseudoscalar field,

pseudoscalar density $\quad R = f_1 r, \quad r = \sum_i \tau^{(i)} \varrho_2^{(i)} \delta\left(\vec{x} - \vec{x}^{(i)}\right)$

pseudovector density
$$\begin{cases} \vec{P} = \frac{f_2}{K} \vec{s}, \\ Q = \frac{f_2}{K} q, \quad q = \sum_i \tau^{(i)} \varrho_1^{(i)} \delta\left(\vec{x} - \vec{x}^{(i)}\right). \end{cases}$$

* The formula for $\vec{S}$ is correct only to the first order in the nucleon velocities, a factor $\varrho_3^{(i)}$ having been replaced by 1 in $\vec{s}$.

In terms of these density functions and intensity parameters g's and f's, the static interaction potential may be written in the form·

$$\left.\begin{aligned} V &= g_1^2\, V_{g_1} + g_2^2\, V_{g_2} + f_2^2\, V_{f_2} \\ V_{g_1} &\equiv \frac{1}{2}\int \boldsymbol{n}\left(\vec{x}\right) \boldsymbol{n}\left(\vec{x}'\right) \varphi\left(\left|\vec{x}-\vec{x}'\right|\right) dvdv' \\ V_{g_2} &\equiv -\frac{1}{2\,\kappa^2}\int \left[\vec{\boldsymbol{s}}\left(\vec{x}'\right) \wedge \operatorname{grad}' \varphi\right] \operatorname{rot} \vec{\boldsymbol{s}}\left(\vec{x}\right) dvdv' + \frac{1}{2\,\kappa^2}\int \vec{\boldsymbol{s}}^{\,2}\, dv \\ V_{f_2} &\equiv \frac{1}{2\,\kappa^2}\int \left[\vec{\boldsymbol{s}}\left(\vec{x}'\right) \cdot \operatorname{grad}' \varphi\right] \operatorname{div} \vec{\boldsymbol{s}}\left(\vec{x}\right) dvdv'. \end{aligned}\right\} \tag{5}$$

After insertion of the above expressions of the source densities, the V's defined in (5) are easily reduced to

$$\left.\begin{aligned} V_{g_1} &= \frac{1}{2}\sum_{i,k} T^{(ik)}\, \varphi\left(r^{(ik)}\right) \\ V_{g_2} &= \frac{1}{2}\sum_{i,k} T^{(ik)}\left[V_\sigma^{(ik)} - S^{(ik)}\right] \\ V_{f_2} &= \frac{1}{2}\sum_{i,k} T^{(ik)}\, S^{(ik)}; \end{aligned}\right\} \tag{6}$$

in these formulae, use has been made of the notations (2), (3), and (4). By comparing the last expressions of V_{g_2} and V_{f_2}, it becomes obvious that the non-central interactions $S^{(ik)}$ can be suppressed by simply assuming

$$g_2^2 = f_2^2. \tag{7}$$

We are then left with a purely central potential; in particular, the spin-spin coupling $V_\sigma^{(12)}$ is entirely responsible for the separation of the ^3S and ^1S states of the deuteron.

Besides the static potential (5), the theory yields, to the first order of approximation in the nucleon velocities, a non-static coupling

$$\begin{aligned} W = \frac{g_1 g_2}{\kappa}\int \left\{\boldsymbol{n}\left(\vec{x}'\right) \vec{\boldsymbol{t}}\left(\vec{x}\right) \operatorname{grad} \varphi + \left[\vec{\boldsymbol{s}}\left(\vec{x}'\right) \wedge \operatorname{grad}' \varphi\right] \vec{\boldsymbol{m}}\left(\vec{x}\right)\right\} dvdv' \\ + \frac{f_1 f_2}{\kappa}\int \vec{\boldsymbol{s}}\left(\vec{x}'\right) \boldsymbol{r}\left(\vec{x}\right) \operatorname{grad} \varphi\, dvdv'. \end{aligned} \tag{8}$$

We shall now analyze this formula by replacing the velocity-dependent factors $\vec{t}$, $\vec{m}$, $\vec{r}$ by their approximate expressions resulting from a transformation analogous to the well-known Gordon decomposition of the current density in the Dirac electron theory. This transformation eliminates the variables $\varrho_1^{(i)}$, $\varrho_2^{(i)}$ and brings out explicitly the dependence on the momenta. It yields*

$$\left.\begin{aligned}
\vec{m} &= \sum_i \tau^{(i)} \overline{\frac{\vec{p}^{(i)}}{Mc^2}\,\delta\left(\vec{x}-\vec{x}^{(i)}\right)} + \frac{\hbar}{2\,Mc}\,\mathrm{rot}\,\vec{s} - \frac{\hbar}{2\,Mc}\frac{d\vec{t}}{cdt} \\
\vec{t} &= \sum_i \tau^{(i)}\vec{\sigma}^{(i)} \wedge \overline{\frac{\vec{p}^{(i)}}{Mc^2}\,\delta\left(\vec{x}-\vec{x}^{(i)}\right)} + \frac{\hbar}{2\,Mc}\,\mathrm{grad}\,\boldsymbol{n} + \frac{\hbar}{2\,Mc}\frac{d\vec{m}}{cdt} \\
r &= -\frac{\hbar}{2\,Mc}\,\mathrm{div}\,\vec{s} - \frac{\hbar}{2\,Mc}\frac{dq}{cdt} \\
q &= \sum_i \tau^{(i)}\vec{\sigma}^{(i)}\overline{\frac{\vec{p}^{(i)}}{Mc}\,\delta\left(\vec{x}-\vec{x}^{(i)}\right)} + \frac{\hbar}{2\,Mc}\frac{d\vec{r}}{cdt};
\end{aligned}\right\} \quad (9)$$

the terms containing time derivatives are of higher order in the velocities and must here consistently be neglected. The terms in $\vec{m}$ and $\vec{t}$ explicitly depending on the momenta give rise, when inserted in (8), to an interaction

$$\left.\begin{aligned}
W_{\text{sp.-orb.}} &= -\frac{2\,g_1 g_2}{\varkappa}\cdot\frac{1}{Mc^2}\cdot\frac{1}{2}\sum_{i,k} T^{(ik)}\,\frac{\varphi'\left(r^{(ik)}\right)}{r^{(ik)}}\cdot \\
&\qquad \left(\vec{\sigma}^{(i)}+\vec{\sigma}^{(k)}\right)\left(\vec{x}^{(ik)}\wedge\vec{p}^{(ik)}\right) \\
&= \frac{2\,g_1 g_2}{\hbar c}\,\frac{M_m}{M}\cdot\frac{1}{2}\sum_{i,k} T^{(ik}{}'\left(\frac{1}{\varkappa r^{(ik)}}+\frac{1}{\varkappa^2 r^{(ik)^2}}\right)\varphi\left(r^{(ik)}\right) \\
&\qquad \left(\vec{\sigma}^{(i)}+\vec{\sigma}^{(k)}\right)\left(\vec{x}^{(ik)}\wedge\vec{p}^{(ik)}\right)
\end{aligned}\right\} \quad (10)$$

of the usual "spin-orbit" type, involving, for each pair of nucleons, the scalar product of total spin and relative orbital momentum. The remaining terms of (9), though not explicitly containing the momenta, are nevertheless of the first order in

* In the derivation of these formulae, a convenient algebraic method, indicated in *l. c.* [11], § 5, has been followed. The bars mean that the underlying expressions have to be symmetrized. The time derivatives refer, strictly speaking, to a system of free nucleons.

the velocities on account of the factor $\hbar/2Mc$; they yield contributions to W of the same structure as the static potentials, apart from certain contact interactions of the form

$$C_0 = \frac{1}{2\varkappa^2}\int \boldsymbol{n}^2\, dv = \frac{1}{2\varkappa^2}\sum_{i,k} T^{(ik)}\,\delta\left(\vec{x}^{(ik)}\right) \tag{11}$$

and

$$\left.\begin{aligned} C_\sigma &= \frac{1}{2\varkappa^2}\int \vec{\boldsymbol{s}}^2\, dv = \frac{1}{2}\sum_{i,k} T^{(ik)} C_\sigma^{(ik)} \\ C_\sigma^{(ik)} &= \frac{1}{\varkappa^2}\vec{\sigma}^{(i)}\vec{\sigma}^{(k)}\,\delta\left(\vec{x}^{(ik)}\right). \end{aligned}\right\} \tag{12}$$

Indeed ,a comparison with (5) shows, after a partial integration and application of the equation $\Delta\varphi - \varkappa^2\varphi = -\delta\left(\vec{x}-\vec{x}'\right)$, that these contributions reduce to

$$-g_1 g_2 \frac{M_m}{M}\left[V_{g_1} - C_0 + V_{g_2} - C_\sigma\right] + f_1 f_2 \frac{M_m}{M} V_{f_2}. \tag{13}$$

Summing up, and transforming (13) by means of (6) and (3), we finally get

$$\left.\begin{aligned} W = &-g_1 g_2 \frac{M_m}{M}\left(V_{g_1} - C_0\right) \\ &- \frac{2}{3} g_1 g_2 - f_1 f_2 \frac{M_m}{M}\frac{1}{2}\sum_{i,k} T^{(ik)} V_\sigma^{(ik)} \\ &+ \frac{M_m}{M}\frac{1}{2}\sum_{i,k} T^{(ik)}\left\{g_1 g_2\, C_\sigma^{(ik)} - \frac{g_1 g_2}{3} + f_1 f_2\, C_{\bar{\sigma}}^{(ik)}\right\} \\ &+ (g_1 g_2 + f_1 f_2)\frac{M_m}{M}\frac{1}{2}\sum_{i,k} T^{(ik)} V_D^{(ik)} + W_{\text{sp.-orb.}}; \end{aligned}\right\} \tag{14}$$

the three first lines represent central and contact interactions, while the last one contains non-central couplings of axial dipole and spin-orbit types.

§ 2. The Deuteron Problem on Symmetrical Mixed Theory.

In the case of the two-nucleon system, we can think the wave-functions expanded in series of eigenfunctions of the

energy corresponding to static central forces which are characterized by definite values of the orbital angular momentum. All matrixelements of the contact interaction operators between such stationary states vanish on account of the radial dependence of the eigenfunctions, except for the diagonal elements pertaining to S states. For the calculation of these matrix elements, the operator $C_{\bar{\sigma}}^{(12)}$ is clearly equivalent to $C_{\sigma}^{(12)}$, so that the non-static coupling (14) takes the somewhat simpler form

$$W = \frac{M_m}{M} T^{(12)} \left\{ \begin{array}{l} -g_1 g_2 \varphi(r) - \frac{2 g_1 g_2 - f_1 f_2}{3} V_{\sigma}^{(12)} \\ + g_1 g_2 \frac{\delta(\vec{x})}{\kappa^2} + \frac{2 g_1 g_2 - f_1 f_2}{3} C_{\sigma}^{(12)} \\ + (g_1 g_2 + f_1 f_2) V_D^{(12)} \end{array} \right\} + W_{\text{sp.-orb.}} \quad (15)$$

In this operator, the only term bringing about a mixing of states with different orbital momenta is the last but one, the axial dipole coupling. In particular, the spin-orbit coupling in this case is diagonal with respect to orbital momentum.

By setting up the four-component wave-equations of the deuteron, including the operator W given by (8), FERRETTI [8] came to the conclusion that there was no regular solution for S states. The same conclusion can be reached without this complicated procedure by considering the transformed operator (15): this presents in fact the same kind of singularities as the static operator $S^{(12)}$. However, the non-static operator is smaller than the static one by a factor of about M_m/M, representing the order of magnitude of the ratio of the velocities of the nucleons to the velocity of light: it is therefore in keeping with the general rules for the interpretation of the formalism of mixed theory [5] to treat it as a perturbation and to retain as significant only the effects which can be derived in an unambiguous way by application of the perturbation method. From this point of view, the contact terms, as already stated, do not offer any difficulty of convergence; and the same is true for the terms in r^{-3} contained in the axial dipole as well as the spin-orbit couplings, the situation being here entirely analogous to that in the atomic

theory of fine and hyperfine structures. The apparent divergence of the expectation value of r^{-3} in S states is namely due solely to the neglect of a relativistic correction factor $\left(1+\frac{\varepsilon - V}{Mc^2}\right)^{-2}$ (ε being the *un*relativistic eigenvalue of the energy): the potential energy V becoming infinite at the origin, this factor is indeed sufficient to secure the convergence of the expectation value in question*. When account is taken of this circumstance, it is immediately clear that both the spin-orbit coupling and the diagonal elements of $V_D^{(12)}$ for S states vanish.

At this point, however, arises the difficulty mentioned in the introduction: if we determine the energy of the ground state, in the initial approximation, by the static central forces alone, and compute the correction due to the non-static coupling by the usual perturbation method, we find indeed a very large contribution** from the central and contact terms of W. Furthermore, as noted by FERRETTI [8], the corresponding perturbation of the eigenfunction is even represented by a diverging series. On closer examination, it is found that the interactions mainly responsible for this situation are the contact ones. But it now becomes clear how to remedy these defects. In the first place, contact interactions can always be eliminated by addition of suitably chosen invariants to the Hamiltonian of the system. So the term

$$-g_1 g_2 \frac{M_m}{M} C_0 = \frac{g_1 g_2}{2\kappa^2} \frac{M_m}{M} \int \boldsymbol{n}^2 \, dv$$

disappears if the invariant

$$\frac{g_1 g_2}{2\kappa^2} \frac{M_m}{M} \int \left(\vec{\boldsymbol{m}}^2 - \boldsymbol{n}^2\right) dv$$

is added: it is then replaced by an interaction of the same type, but of higher order in the nucleon velocities, which must therefore be discarded according to the general rules for the interpretation of the formalism of mixed theory [5]. Similarly, the

* Cf. H. BETHE, Hdb. d. Phys. XXIV/1, p. 307, 385–386; W. PAULI, *ibid.* p. 237, equ. (89).

** I wish here to emphasize that a substantially correct statement of the reason for this abnormally large energy perturbation is already contained in SERPE's thesis [12], in which the decomposition (9) of the field sources was applied to the general interaction between nucleons and free mesons. However, SERPE did not follow up the matter.

term in C_G can be reduced to higher order in the velocities by addition of the invariant $\int (\vec{s}^2 - \vec{t}^2)\, dv$ with a suitable coefficient. As regards the central interactions, on the other hand, they can simply be reckoned with those which determine the initial approximation; the central potential in that approximation thus becomes, on taking account of (7),

$$V_0 = \left(g_1^2 - \frac{M_m}{M} g_1 g_2\right) V_{g_1} + \left(g_2^2 - \frac{M_m}{M} \cdot \frac{2\, g_1 g_2 - f_1 f_2}{3}\right) \frac{1}{2} \sum_{i,k} T^{(ik)} V_G^{(ik)}. \quad (16)$$

The remaining non-static interaction is then

$$W_{\text{eff}} = \frac{M_m}{M} (g_1 g_2 + f_1 f_2) \frac{1}{2} \sum_{i,k} T^{(ik)} V_D^{(ik)} + W_{\text{sp.-orb.}}. \quad (17)$$

In the deuteron case, this interaction gives rise to a perturbation of the energy of the ground state which is of the second order only and may be neglected. There is, however, a first order perturbation of the eigenfunction of this state, resulting in an admixture of ${}^3D_1$-states and a corresponding quadrupole moment.

Although working with a non-central coupling of exactly the same type, viz. axial dipole coupling, the cut-off theory presents a quite different picture: the non-central coupling appears with a coefficient as large as that of the central interaction and can therefore not be treated as a perturbation. It gives rise to a large contribution to the energy of the ground state, sensitively depending on the cut-off radius r_0. All the same, the admixture of D state to the eigenfunction of the ground state is small (as required to explain the small quadrupole moment), the cut-off so to say compensating here the largeness of the coefficient of the axial dipole term. The mixed theory is unquestionably much simpler, and also more natural inasmuch as it deduces a small effect by means of a perturbation calculation and not by a device involving a considerable departure from the simple representation of nuclear forces by a central potential.

The intensity constants g_2, g_2 are primarily determined, in the mixed theory, by the binding energy of the ground state of the deuteron and the energy of the virtual ${}^1S$ state, which together fix the numerical coefficients of the central potential V_0; the inclusion in (16) of the non-static central interactions implies only relatively small modifications of the resulting values of

these costants. In particular, even when account is taken of the relation (7), which further fixed $|f_2|$, the sign and magnitude of the calculated quadrupole moment, which is proportional to $g_1 g_2 + f_1 f_2$, can still be adjusted to fit observation. As a matter of fact, the experimental value of the quadrupole moment can be used together with the other evidence just mentioned to determine the four parameters g and f. One has the system of equations

$$\left.\begin{aligned} g_1^2 - \frac{M_m}{M} g_1 g_2 &= \alpha \\ g_2^2 - \frac{1}{3}\frac{M_m}{M}(2 g_1 g_2 - f_1 f_2) &= \beta \\ g_1 g_2 + f_1 f_2 &= \gamma \\ g_2^2 &= f_2^2, \end{aligned}\right\} \qquad (18)$$

α, β, γ, being given positive numerical quantities (of the dimensions of energy times length) of comparable orders of magnitude. It is easy to see that this system yields two essentially distinct solutions*, according to the sign assumed for the product $g_1 g_2$.

The mixed theory can in this respect admittedly be blamed for a wealth of adjustable parameters affording it an unfair amount of self-protection. A not unattractive possibility of restricting the number of independent source constants is suggested by the preceding discussion. If one would assume that

$$2 g_1 g_2 - f_1 f_2 = 0, \qquad (19)$$

the contact interaction C_σ would be completely eliminated as well as the additional spin-spin interaction, so that the value of g_2^2 would directly be fixed by the coefficient β of the zero-approximation central potential. Then, the absolute value, though not the sign, of the electric quadrupole moment would be predicted by the theory. It remains to be seen, however, whether this predicted value would not come out a little too small to fit observation: an estimate by HULTHÉN [7] would namely rather seem to suggest the relation $g_1 g_2 - f_1 f_2 = 0$.

* There subsists, of course, an arbitrariness in the signs corresponding to the invariance of the equations (18) for simultaneous change of sign of g_1 and g_2, or f_1 and f_2, or both pairs. But this arbitrariness is of no physical significance.

§ 3. Velocity-dependent Coupling on Neutral Mixed Theory.*

On the neutral mixed theory, the source densities of the meson fields are as follows:

Scalar field,

scalar density** $\approx f_1' n$

vector density $\frac{1}{\kappa} f_2' \vec{m}, \quad \frac{1}{\kappa} f_2' n;$

Pseudovector field,

pseudovector density $g_1' \vec{s}, \quad g_1' q$

pseudotensor density** $\frac{1}{\kappa} g_2' \vec{t}, \approx \frac{1}{\kappa} g_2' \vec{s};$

the functions n, $\vec{m}$, $\vec{s}$, $\vec{t}$, q are the same as those denoted by the same letters in the symmetrical theory, except that the factors $\tau^{(i)}$ are to be cancelled. The resulting static interaction may be written, in our notations,

$$V = -\frac{1}{2} \sum_{i,k} \{ f_1'^2 \varphi(r^{(ik)}) + g_1'^2 V_\sigma^{(ik)} - (g_1'^2 - g_2'^2) S^{(ik)} \}, \qquad (20)$$

the last term disappearing if one puts

$$g_1'^2 = g_2'^2. \qquad (21)$$

The non-static coupling in this case takes the form

$$\left.\begin{aligned} W = &-\frac{f_1' f_2'}{\kappa} \int n(\vec{x}') \vec{m}(\vec{x}) \operatorname{grad} \varphi \, dv dv' \\ &+ \frac{g_1' g_2'}{\kappa} \int \{ q(\vec{x}') \vec{s}(\vec{x}') \operatorname{grad} \varphi + \vec{t}(\vec{x}') [\vec{s}(\vec{x}) \wedge \operatorname{grad} \varphi] \} dv dv'; \end{aligned}\right\} \qquad (22)$$

After insertion of the expressions (9) (without the τ's) for $\vec{m}$, $\vec{t}$ and q, it is immediately apparent that the terms not explicitly involving the momenta yield vanishing contributions. The scalar part thus reduces to

$$W_{\text{scal}} = -\frac{2 f_1' f_2'}{\kappa^2} \frac{M_m}{M} \frac{1}{2} \sum_{i,k} \overrightarrow{\frac{p^{(i)}}{\hbar c}} \operatorname{grad}^{(i)} \varphi(r^{(ik)}), \qquad (23)$$

* *Note added in proof.* After completion of the present paper i have been informed that the results of this Section have been obtained indepedently by Bengt Holmberg in a paper published in Kungl. Fysiografiska Sällskapets Förhandlingar, Lund, **14**, No. 22, 1944.

** The factors $\varrho_3^{(i)}$ have here been replaced by 1.

while the pseudovector part may successively be written:

$$\left.\begin{aligned} W_{\text{ps. vect.}} &= \frac{2\,g_1' g_2'}{\kappa^2}\frac{M_m}{M}\frac{1}{2}\sum_{i,k}\left\{\overline{\left(\vec{\sigma}^{(i)}\frac{\vec{p}^{(i)}}{\hbar c}\right)\left(\vec{\sigma}^{(k)}\,\mathrm{grad}^{(k)}\,\varphi\,(r^{(ik)})\right)}\right. \\ &\quad \left.+\overline{\left(\vec{\sigma}^{(i)}\wedge\frac{\vec{p}^{(i)}}{\hbar c}\right)\left(\vec{\sigma}^{(k)}\wedge\mathrm{grad}^{(k)}\,\varphi\,(r^{(ik)})\right)}\right\} \\ &= \frac{2\,g_1' g_2'}{\kappa^2}\frac{M_m}{M}\frac{1}{2}\sum_{i,k}\left\{\left(\vec{\sigma}^{(i)}\wedge\vec{\sigma}^{(k)}\right)\overline{\left(\frac{\vec{p}^{(i)}}{\hbar c}\wedge\mathrm{grad}^{(k)}\,\varphi\right)}\right. \\ &\quad \left.-\left(\vec{\sigma}^{(i)}\vec{\sigma}^{(k)}\right)\overline{\frac{\vec{p}^{(i)}}{\hbar c}\,\mathrm{grad}^{(i)}\,\varphi}\right\}. \end{aligned}\right\} \tag{24}$$

These expressions are not at all of a form which would be expected on general invariance considerations for first order velocity-dependent interactions, but, from this point of view, rather belong to the second order types [as may be seen by replacing grad φ by $\frac{i}{\hbar c}\left(\vec{p}\,\varphi-\varphi\vec{p}\right)$].

It is clear that a coupling of the form (23) will not give rise to any mixing of states with different orbital momenta. Indeed, the operator* W_{scal} commutes with that of the total orbital momentum $\sum_i \vec{x}^{(i)}\wedge\vec{p}^{(i)}$. The same applies to the last term of (24), while the first term, which has the general form

$$\frac{2\,g_1' g_2'}{\kappa^2}\frac{M_m}{M}\frac{1}{2}\sum_{i,k}\frac{\varphi'\,(r^{(ik)})}{r^{(ik)}}\left(\vec{\sigma}^{(i)}\wedge\vec{\sigma}^{(k)}\right)\left[\vec{x}^{(ik)}\wedge\frac{1}{2}\left(\vec{p}^{(i)}+\vec{p}^{(k)}\right)\right],$$

vanishes for any two-nucleon system whose center of gravity is at rest. There is thus in the neutral theory no alternative to the cut-off procedure to explain the quadrupole moment of the deuteron.

* In the two-nucleon case, the operator W_{scal} may be written

$$W_{\text{scal}} = -\frac{2\,f_1' f_2'}{\kappa}\frac{M_m}{M}\overline{\frac{\vec{p}}{\hbar c}\,\vec{x}\,\frac{\varphi'\,(r)}{r}};$$

a more familiar form is obtained by going over to a representation in terms of quantized amplitudes ψ, $\psi^\dagger$: the energy density then becomes

$$\psi^\dagger W_{\text{scal}}\,\psi = \frac{2\,f_1' f_2'}{\kappa^2}\frac{M_m}{M}\left\{\frac{1}{2\,i}\,\mathrm{div}\,[\psi^\dagger\,\mathrm{grad}\,\varphi\cdot\psi]-\frac{1}{2\,i}\,(\mathrm{grad}\,\psi^\dagger\cdot\psi-\psi^\dagger\,\mathrm{grad}\,\psi)\,\mathrm{grad}\,\varphi\right\}.$$

References.

1. J. KELLOGG, I. RABI, N. RAMSEY and J. ZACHARIAS, Phys. Rev. **57**, 677, 1940.
2. E. WIGNER, Phys. Rev. **51**, 106, 1937.
3. F. BELINFANTE, Theory of Heavy Quanta, Leiden thesis 1939, p. 88.
4. H. BETHE, Phys. Rev. **57**, 390, 1940.
5. C. MØLLER and L. ROSENFELD, D. Kgl. Danske Vidensk. Selskab, Mat.-fys. Medd. **17**, No. 8, 1940.
6. Cf. E. WIGNER and L. EISENBUD, Phys. Rev. **56**, 214, 1939.
   H. BETHE, Phys. Rev. **57**, 260, 1940 (end of § 5, p. 270).
7. L. HULTHÉN, Arkiv för Mat., Astron. och Fysik **29 A**, No. 33, 1943.
8. B. FERRETTI, Nuovo Cimento **1**, 229, 1943.
9. E. AMALDI, D. BOCCIARELLI, B. FERRETTI and G. TRABACCHI, Naturwiss. **48**, 39, 1942.
10. B. FERRETTI, Ricerca scient. **12**, 843, 993, 1941.
    B. FERRETTI, Nuovo Cimento **1**, 25, 1943.
    L. HULTHÉN, Arkiv för Mat., Astron. och Fysik **29 A**, No. 33, 1943.
    L. HULTHÉN, Arkiv för Mat., Astron. och Fysik **30 A**, No. 9, 1943.
    A. PAIS, D. Kgl. Danske Vidensk. Selskab, Mat.-fys. Medd. **22**, No. 17, 1943.
11. C. MØLLER and L. ROSENFELD, D. Kgl. Danske Vidensk. Selskab, Mat.-fys. Medd. **20**, No. 12, 1943.
12. J. SERPE, Mém. Soc. Roy. Sc. Liège (in–4°) **1**, 251, 1943.

Indleveret til Selskabet den 13. Juli 1945.
Færdig fra Trykkeriet den 27. September 1945.

DET KGL. DANSKE VIDENSKABERNES SELSKAB
MATEMATISK-FYSISKE MEDDELELSER, BIND XXIII, NR. 14

DEDICATED TO PROFESSOR NIELS BOHR ON THE OCCASION OF HIS 60TH BIRTHDAY

OM ET KOMPLEMENTARITETSFORHOLD VED SPREDNINGSEKSPERIMENTER

AV

HARALD WERGELAND
OSLO

KØBENHAVN
I KOMMISSION HOS EJNAR MUNKSGAARD
1945

Printed in Denmark.
Bianco Lunos Bogtrykkeri A/S

Enskjønt det særlig var eksistensen av de atomfysiske systemers stasjonære tilstander og utforskningen av disse, som ledet til kvanteteoriens nåværende stadium, har også de ikke-stasjonære fenomener, som man f. eks. har å gjøre med ved spredning av partikler eller bølger, like fra første stund stått i forgrunnen for interessen.

Man behøver bare å tenke på Bohrs bremsningsformel allerede fra 1913, fra kvantefysikkens »Mykenske tid«, som stadig finner en så utstrakt anvendelse, med eller uten de i almindelighet små korreksjoner som bølgemekanikken og relativitetsteorien forlanger.

Andre store fremskritt på dette område, som umiddelbart faller i tankene, er Møllers relativistiske støtformel og Bohrs tydning av Ramsauereffekten, som fikk sitt matematiske belegg i teorien for elektronbølgenes diffraksjon i atomfelter ved Faxén og Holtsmark.

Når man bortser fra de ennå uløste problemer som knytter seg til energirike støtprosesser i den kosmiske stråling, danner kvantemekanikkens spredningsteori et særlig vakkert avsluttet hele; hensikten i det følgende er å anvende den på et skjematisk lite eksempel, som på atter en ny måte turde belyse det paradoksale i en samtidig anvendelse av to anskuelige billeder som gjensidig utelukker hverandre, eller rettere: står i det eiendommelige reciprocitetsforhold som er karakteristisk for kvanteteorien, og som nå er alminnelig kjent under begrepet komplementaritet.

For å gjøre det matematiske så enkelt som mulig vil vi betrakte spredningen av en homogen partikkelstråle på en stiv

kule. Regningen kan da gjennomføres explicit og leder til forholdsvis enkle uttrykk.

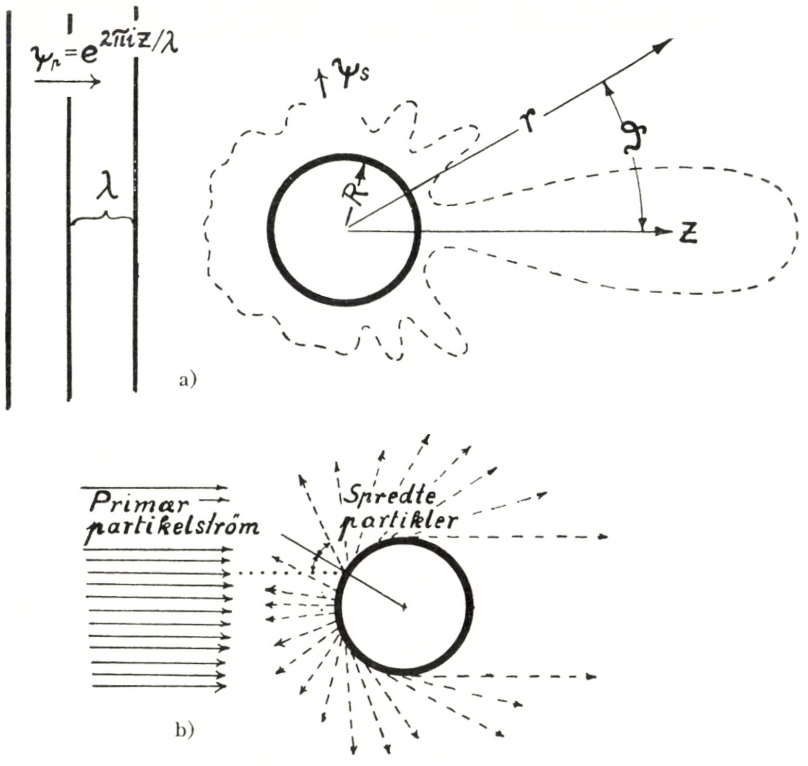

Fig. 1. Spredning på en stiv kule, a) bølgemekanisk, b) punktmekanisk.

Etter bølgemekanikken kan den primære partikelstrøm fremstilles ved en plan monokromatisk De Broglie-bølge,

$$\psi_p = e^{2\pi i z/\lambda},$$

hvis bølgelengde λ er gitt på kjent måte av partiklenes masse og hastighet.

Den matematiske oppgave som skal løses er å bestemme en sekundær bølge ψ_s således at hele feltet, $\psi = \psi_p + \psi_s$, tilfredsstiller SCHRØDINGERS bølgeligning og randbetingelsene:

$$\psi(\vartheta) = \psi(\vartheta + 2n\pi) \quad ; \; n = 1, 2, 3, \ldots \tag{1}$$

$$\psi \quad = 0 \qquad\qquad ; \; r = R \tag{2}$$

$$\psi \quad \to f(\vartheta) \cdot \frac{e^{2\pi i r/\lambda}}{r} \quad ; \; r \to \infty. \tag{3}$$

Det vil si:

1) Feltet skal være en éntydig funksjon av polarvinkelen ϑ (fig. 1a).
2) Amplituden skal til enhver tid være 0 på kulens overflate. Det svarer til at overflaten fremstilles ved en uendelig høy potensialbarrière, hvilket kan oppfattes som en definisjon på absolutt stivhet.
3) Den tredje betingelse som angår bølgefeltets forløp i stor avstand fra spredningscentret, utelukker innløpende sekundærbølger. Sådanne kan nemlig ikke tillates fordi en fysisk meningsfull løsning av problemet ikke kan fremstille noen innstråling fra uendeligheten utover den som er inneholdt i primærbølgen.

Den asymptotiske løsning for store r har formen:

$$\psi_\infty = \psi_p + \frac{e^{ikr}}{kr} \cdot \sum_{l=0}^{\infty} a_l P_l(\cos\vartheta); \quad \begin{matrix} P_l = \text{Legendre polynom}, \\ k = 2\pi/\lambda, \end{matrix} \tag{4}$$

hvorav intensitets-fordelingen i tilstrekkelig store avstander kan beregnes når koeffisientene a_l er kjent. Disse må egentlig bestemmes av den eksakte løsning ved hjelp av randbetingelsen (2) etter en metode som går tilbake på Lord RAYLEIGH og som består i å utvikle primærbølgen i en tilsvarende rekke etter kulefunksjonene P_l.

I det foreliggende tilfelle hvor spredningen er elastisk, kan imidlertid en viktig egenskap ved sekundærbølgens utviklingskoeffisienter a_l avledes allerede av materialbalansen.

Danner man nemlig massestrømmen $\vec{S}$ ved å sette inn (4) i den velkjente bølgemekaniske formel,

$$\vec{S} = \frac{h}{4\pi i}(\psi \operatorname{grad} \psi^* - \psi^* \operatorname{grad} \psi), \tag{5}$$

og integrerer over en lukket flate som omslutter den spredende kule, så må resultatet være lik 0, ettersom partikler hverken oppstår eller forsvinner innenfor det betraktede volum.

Det gir ligningen:

$$\sum_{l=0}^{\infty} \left\{ \frac{2}{2l+1} |a_l|^2 + i(a_l - a_l^*) \right\} = 0. \tag{6}$$

Da koeffisientene a_l er funksjoner av bølgelengden λ og kulens radius R, må denne ligning være oppfylt identisk. Hvis man altså skriver de komplekse koeffisienter a_l på formen $|a_l| \exp(i\eta_l)$, må vi for alle indices l ha:

$$|a_l| = (2l+1) \sin \eta_l. \tag{7}$$

Den fysiske betydning av størrelsene η_l er faseforskjellen mellom ut- og innløpende kulebølger i uendeligheten. Disse »faser« er de fundamentale størrelser i ethvert spredningsproblem; er de gitt, så er også bøyningsfiguren entydig bestemt.

Ved hjelp av (7) kan altså det asymptotiske uttrykk for sekundærbølgen skrives på formen:

$$\psi_{s,\infty} = \frac{e^{ikr}}{kr} \sum_{l=0}^{\infty} (2l+1) \sin \eta_l \cdot e^{i\eta_l} \cdot P_l(\cos \vartheta). \tag{8}$$

Denne del av feltet kalles i alminnelighet den spredte bølge, men det må bemerkes at en slik avspaltning av sekundærbølgen fra det fullstendige felt er en rent matematisk operasjon, som i visse situasjoner virker kunstig, således for eksempel ved geometrisk skygge.

Det synes ganske unaturlig å si at kulen sprеder noe inn i skyggen, men i virkeligheten har jo »den spredte bølge« i ovennevnte matematiske betydning en stor amplitude just i dette område — nemlig like stor som primærbølgen — og motsatt fase, således at de tilsammen opphever hverandre.

For å skille primær- og sekundærbølge er det videre nødvendig å innføre en skjerm, men på grunn av bøyning på kantene formår ingen skjerm å separere ut primærbølgen for alle vinkler.

Det er bare i retninger tilstrekkelig langt fra den primære bølgenormal at den spredte bølge har en enkel eksperimentell betydning. I nærheten av primærretningen er det bare mulig å måle intensiteten av det totale interferensfelt.

La oss imidlertid opprettholde definisjonen ovenfor og beregne strømtettheten av sekundærbølgen alene, ved innsetning av (8) i (5). Integrasjon over alle vinkler og divisjon med primærintensiteten gir den velkjente formel for det totale elastiske spredningstverrsnitt:

$$Q = \frac{4\pi}{k^2} \sum_{l=0}^{\infty} (2l+1) \sin^2 \eta_l. \tag{9}$$

Beregningen av spredningstverrsnittet som funksjon av bølgelengden efter (9) er i alminnelighet meget besværlig på grunn av rekkens konvergensforhold.

I området $0 < l < kR$ antar fasene alle mulige verdier, men for $l > kR$ er de små av størrelsesorden $(kR/l)^l$. For å få en god tilnærmelse er det derfor nødvendig å ta med ca. kR ledd i rekken.

Men i to grensetilfeller: a) for meget lange bølgelengder og b) for meget korte bølgelengder — det vil si lange eller korte i forhold til kulens dimensjoner — kan man uten nøyere kjennskap til fasene slutte seg til spredningsfunksjonens alminnelige forløp.

Det er det siste grensetilfelle som vesentlig interesserer i denne sammenheng. Som en brukbar tilnærmelse kan vi her sette alle faser $\eta_l = 0$ for $l > kR$, og skrive

$$\left.\begin{aligned} Q &= \frac{4\pi}{k^2} \sum_{l=0}^{[kR]} (2l+1) \sin^2 \eta_l \\ &= \frac{2\pi}{k^2} \left\{ \sum_{l=0}^{[kR]} (2l+1) - \sum_{l=0}^{[kR]} (2l+1) \cos 2\eta_l \right\}. \end{aligned}\right\} \tag{10}$$

Fordi fasene oscillerer på en uregelmessig måte vil den siste sum i klammeren være av mindre størrelsesorden enn den første, i grensen kan vi anta at den vokser langsommere enn kvadratisk med kR, således at vi får $Q \sim 2\pi R^2$ eller det dobbelte av kulens tverrsnitt, $Q_0 = \pi R^2$.

Resonnementet kan begrunnes nøyere ved å anslå de ledd som er kastet bort. Det viser seg at den viktigste korreksjon er av størrelsesorden $(kR)^{4/3}$. Det elastiske spredningstverrsnitt nærmer seg altså kvotientasymptotisk til 2 ganger det geometriske tverrsnitt:

$$\lim_{\lambda \to 0} Q/Q_0 = 2. \tag{11}$$

Denne grenseverdi 2 som visstnok først blev bemerket av Massey og Mohr*, synes ganske forbløffende, for grenseprosessen, $\lambda \to 0$, er jo matematisk likeverdig med $h \to 0$, eller overgang til punktmekanikken. Ved uendelig korte bølgelengder har man geometrisk stråleutbredelse, og man kunde tenke at spredningen skulde være nøyaktig lik den flux som kulens skygge skjærer ut av den primære partikkelstrøm; det vil si en relativ spredning $Q/Q_0 = 1$, og forøvrig — etter den enkle refleksjonslov — med konstant intensitet i alle retninger.

Paradoxet henger sammen med den konvensjonelle definisjon av spredt stråling. Hvis vi tenker oss en lukket flate lagt om spredningscentret, så nær at den faller innenfor området med geometrisk skygge, så har vi nå regnet som om en stråle med primærbølgens fulle intensitet passerte gjennom kulens skyggebillede på flaten.

Men urimelighetene kan omgåes ved en mere kritisk anvendelse av den geometriske strålekonstruksjon. I virkeligheten blev det fremholdt allerede av Rayleigh (1871) i forbindelse med hans optiske undersøkelser, at retningen av en begrenset stråle er prinsipielt ubestemt på grunn av den uundgåelige diffraksjon i de begrensende blender.

I kvanteteorien er jo dette forhold velkjent. Strålekonstruksjonen og bølgebegrepene kan ikke anvendes samtidig utover visse grenser som er gitt ved en uskarphetsrelasjon.

* Proc. Roy. Soc. A **141**, 434, 1933.

Det kritiske område er i vårt tilfelle en kegle,

$$\vartheta \lesssim \frac{1}{kR}, \tag{12}$$

hvis åpningsvinkel ganske visst stadig avtar med bølgelengden, men som allikevel alltid vil gjøre begrepet geometrisk skygge ugyldig i tilstrekkelig stor avstand fra det spredende objekt.

Nå kan man vise at dette snevre område omkring primærretningen omfatter en tett strålebundt som bærer just halvparten av den spredte energi. Hvis altså den kritiske kegle blev utelatt ved integrasjonen (9), vilde den resterende spredning anta den verdi som er forenlig med rettlinjet stråleutbredelse.

For å se det er det fordelaktig å spalte opp sekundærbølgen (8) i to deler:

$$_{s,\infty} = \underbrace{\frac{e^{ikr}}{ikr} \cdot \sum_{l=0}^{[kR]} \left(l+\frac{1}{2}\right) P_l(\cos\vartheta)}_{\psi_s'} - \underbrace{\frac{e^{ikr}}{ikr} \cdot \sum_{l=0}^{[kR]} \left(l+\frac{1}{2}\right) e^{2i\eta_l} \cdot P_l(\cos\vartheta)}_{\psi_s''} . \tag{13}$$

Vi vil først studere den ved små vinkler, $\vartheta \sim 1/kR$. Faktorene $P_l(\cos\vartheta)$ vil da meget nær være konstante lik 1, og ved et resonnement analogt til (10) (11) sidene 7 og 8 kan man slutte at den første sum ψ_s' er dominant, idet leddene i den annen sum ψ_s'' i stor utstrekning opphever hverandre.

Ved hjelp av kulefunksjonenes egenskaper kan summasjonen utføres, og man får som tilnærmelsesformel for små vinkler,

$$\psi_s' \approx (kR)^2 \cdot \left[\frac{J_1(2\,kR\sin\vartheta/2)}{2\,kR\sin\vartheta/2}\right] \cdot \frac{e^{ikr}}{ikr} \tag{14}$$

hvor J = Besselfunksjon av 1. art.

Faktoren i hakeparentesen har et skarpt maksimum for $\vartheta = 0$, dens alminnelige forløp fremgår av fig. 2. Det tilsvarende strømuttrykk gir ved integrasjon over den lille kegle $\vartheta \leq 1/kR$, en flux $\approx \pi R^2 \cdot h/\lambda$, eller tilnærmet like meget som kulens tverrsnitt skjærer ut av primærstrålen.

Subtraksjon av dette bidrag vilde følgelig redusere spredningen til en halvpart, som nevnt ovenfor. Men den åpningsvinkel

$\vartheta \sim 1/kR$ som skal utelukkes er selvsagt bare gitt med hensyn til størrelsesorden.

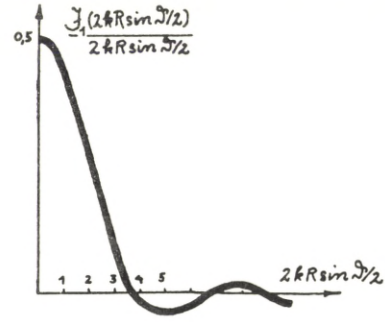

Fig. 2.

Idet vi vender tilbake til uttrykket (13) for sekundærbølgen, må vi huske at det er bare for meget små vinkler at den siste sum ψ_s'' kan neglisjeres. Når variasjonen av funksjonene, $P_l(\cos\vartheta)$, og fasene, η_l, tas nøyere i betraktning, viser det seg at de forskjellige kulefunksjonskomponenter summerer seg opp til en bølge med tilnærmelsesvis konstant amplitude,

$$|\psi_s''| \approx \frac{R}{2r} \tag{15}$$

for alle vinkler.

Hertil svarer en kulesymmetrisk spredning med en total intensitet lik den primærflux som treffer kulen, altså nettopp hvad man vil vente etter det klassiske billede av en partikkelstrøm som spredes ved elastiske støt mot en kule.

Derimot har den første sum i (13), ψ_s', ingen partikkelstrøm som punktmekanisk motstykke; som vi nå skal se, fremstiller denne del av sekundærbølgen i det vesentlige skyggen:

Ved benyttelse av de eksakte bølgefunksjoners egenskaper finner man etter forskjellige omformninger at forholdet mellom primærbølgens og sekundærbølgens amplitude, ved små vinkler, tilnærmet kan skrives*:

$$\frac{\psi_s}{\psi_p} \approx -(kR)^2 \cdot \left[\frac{J_1(2\,kR\sin\vartheta/2)}{2\,kR\sin\vartheta/2}\right] \cdot 2\sin^2\vartheta/2 \int_{2\,kr\sin^2\vartheta/2}^{\infty} \frac{e^{i\tau}}{\tau}\,d\tau\,. \tag{16}$$

* Formelen gjelder ikke i kulens umiddelbare nærhet.

Hakeparentesen er den intensitetsfunksjon vi allerede har støtt på i (14). Den har en bemerkelsesverdig optisk analogi, nemlig i det Fraunhoferske bøyningsbillede av en cirkulær blende.

Den siste faktor med integralet spiller en lignende rolle som Cornuspiralen ved Fresnelske diffraksjonsfenomener, man overser den best ved å skrive:

$$\int_{\tau}^{\infty} \frac{e^{i\tau}}{\tau} d\tau = x + iy \tag{17}$$

og velge x, y som rettvinklede koordinater. Den kurve som er gitt ved parameterfremstillingen:

$$x(\tau) = \int_{\tau}^{\infty} \frac{\cos \tau}{\tau} d\tau, \quad y(\tau) = \int_{\tau}^{\infty} \frac{\sin \tau}{\tau} d\tau, \tag{18}$$

er en spiral som antydet i fig. 3. Man vil legge merke til at kurvens vinkelkoeffisient, dy/dx, i ethvert punkt simpelthen er lik parameterverdien τ.

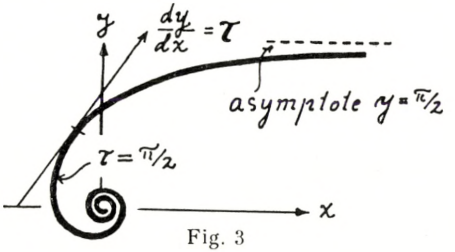

Fig. 3

Uten å gå nøyere inn på den numeriske diskusjon av formelen (16) kan vi nå i grove trekk fiksere skyggegrensen. Skyggevirkning har vi åpenbart i de områder hvor forholdet ψ_s/ψ_p er negativt reelt og i absolutt verdi ≈ 1, idet primær- og sekundærbølge da tilnærmet opphever hverandre.

For at der skal være en merkbar utslukning av primærbølgen, må to betingelser være oppfylt:

For det første må intensitetsfaktoren i hakeparentesen (16) være stor, det vil si dens argument må ligge vel innenfor det første sekundærmaksimum.

Dernest må faktoren $x + iy$ ha en relativt liten imaginær del. Parameteren τ må altså ikke være så stor at man når inn i spiralens vindinger som svarer til de små intensitetsvariasjoner

utenfor skyggen. Som en grense for dette område kan man velge $\tau \approx \pi/2$, den kan naturligvis ikke fastlegges skarpt. (Ved $\tau \approx \pi/2$ har man i virkeligheten allerede igjen en liten forsterkning av primærbølgen, da x jo her er negativ.)

Etter disse to betingelser kan man definere skyggegrensen ved

$$\left.\begin{aligned} 2\,kR \sin \vartheta/2 &\approx \pi \\ 2\,kr \sin^2 \vartheta/2 &\approx \pi/2 \end{aligned}\right\} \qquad (19)$$

eller

$$\sin \vartheta/2 \approx \frac{R}{2\,r},$$

hvilket etter forutsetningen, små vinkler, stemmer med den geometriske skyggekonstruksjon.

Da intensiteten av sekundærbølgen avtar (omtrent som $(kr)^{-2}$), vil skyggen naturligvis intet sted være absolutt men gradvis utviskes med voksende avstand fra kulen, hvor kort enn bølgelengden måtte være.

Summary.

The scattering of particles by a rigid sphere is discussed with particular reference to a curious result enunciated by Massey and Mohr:

With increasing velocity the scattering cross section does not, as might be conjectured, tend to the projected area of the sphere; but to *twice* this value.

The interpretation of the paradox lies in the essential indeterminateness of the primary direction. It can be shown that the scattered intensity consists of two parts, both carrying the same current. One part represents a spherical wave of uniform intensity in all directions, the other is confined to a narrow region around the primary direction. The latter part is intimately connected with the shadow.

Indleveret til Selskabet den 1. August 1945.
Færdig fra Trykkeriet den 21. September 1945.